UCRL-16050

University of California

Ernest O. Lawrence Radiation Laboratory

STUDIES OF ATOMIC HYDROGEN AT LOW PRESSURES

Berkeley, California

DISCLAIMER

UCRL-16050
UC-4 Chemistry
TID-4500 (39th Ed.)

UNIVERSITY OF CALIFORNIA

Lawrence Radiation Laboratory
Berkeley, California

AEC Contract No. W-7405-eng-48

STUDIES OF ATOMIC HYDROGEN AT LOW PRESSURES

Peter R. Rony

April 20, 1965

Printed in USA. Price $6.00. Available from the Clearinghouse for Federal Scientific and Technical Information, National Bureau of Standards, U. S. Department of Commerce, Springfield, Virginia.

STUDIES OF ATOMIC HYDROGEN AT LOW PRESSURES

Contents

STUDIES OF ATOMIC HYDROGEN AT LOW PRESSURES

Peter R. Rony

Lawrence Radiation Laboratory
University of California
Berkeley, California

April 20, 1965

ABSTRACT

A variety of subjects concerning the gas- and surface-phase kinetics of atomic hydrogen at low pressures is considered. The theoretical description of diffusion and flow tubes is extended to the following situations: (a) the discharge zone is of finite length, (b) the discharge-zone walls are inactive catalytically, (c) the end-plate sink is composed of two or more catalytic materials, and (d) the atom-recombination coefficients on the discharge- and reactor-zone walls differ in magnitude. The dimensionless groups characterizing the rate processes within the system are systematized, and practical examples illustrating the use of the theoretical solutions are given.

After a description of a simple water-cooled Wrede-Harteck gauge capable of detecting atom concentrations of less than 0.06% at 75 mtorr, it is experimentally shown that the device may not be absolute, is sensitive to the presence of H_2O and HCl, is susceptible to thermal effusion problems, and cannot discriminate between atomic hydrogen or atomic oxygen.

The presence of small amounts of H_2O does not influence the yield of atomic hydrogen from a microwave or electrodeless discharge at 75 mtorr. This result is independent of the measurement technique, the source of hydrogen, the source of water, and the discharge power.

Small amounts of O_2 stoichiometrically increase the yield of atomic hydrogen from the low-pressure discharge by a ratio of at least two atoms of hydrogen per molecule of oxygen. Molecular nitrogen has a similar but a smaller effect.

A cyclotron-resonant microwave discharge is a convenient method for producing an electrical discharge in the low-pressure system with a microwave power as low as 250 mW. The intensity of the Balmer lines or color of low-pressure hydrogen discharges is not a reliable qualitative indication of the atomic-hydrogen yield.

The location of an active catalytic probe affects the atom-concentration level throughout a diffusion tube or flow tube at low pressures. Studies with Teflon or copper probes indicate that both have recombination coefficients below 10^{-3}.

In order for an isothermal calorimeter to be used for the measurement of absolute atom concentrations in a low-pressure system, (a) most of the atoms produced must recombine on the calorimeter, (b) both the diffusive and convective flux of atoms must be known, (c) the presence of the atoms must not alter the rate of heat loss from the calorimeter, and (d) the thermal-accommodation coefficient of the recombination energy must be equal to unity.

I. INTRODUCTION

Studies to determine the feasibility of purifying liquid metals by reacting atomic hydrogen with the residual oxides, carbides, and nitrides present brought up the interesting question: What is the rate of recombination of atomic hydrogen on a liquid metal? Since no data nor predictions about this rate were found in the literature, I started a project to determine whether there would be any difference in the recombination coefficient of atomic hydrogen on liquid and solid gallium or liquid and solid mercury at their respective melting points. I felt that such measurements, being of a fairly critical nature, might yield intriguing results on the relative importance of reaction sites and the electronic factor in this particular heterogeneous catalytic reaction—one of the simplest known.

The low-pressure diffusion-tube technique, first applied by Smith[1] and subsequently used by Wise and co-workers,[2-14] Linnett and co-workers,[15-29] Tsu and Boudart,[30-33] and others,[34-42] I chose as the method to measure the recombination coefficients of hydrogen atoms on the mercury and gallium surfaces.

The mathematical theory of the diffusion tube I rederived and extended considerably. As a result of these calculations, I chose an atom-concentration measuring device—the Wrede-Harteck gauge[43-51]—in preference to an atom-flux measuring device—the thermocouple probe or isothermal calorimeter.[30,39] The use of ESR or a mass spectrometer was not considered since such instruments were not readily available to me.

After a sensitive and stable Wrede-Harteck gauge had been successfully constructed and operated, measurements were first made to demonstrate the validity of the derived equations for the operation of the diffusion tube. During these measurements, serious difficulties appeared—the atom-concentration level produced by an electrical discharge did not remain constant, but instead decayed at a relatively rapid rate while the discharge was still on. This problem was so serious that it clearly made my attempts to perform any type of kinetic studies impossible.

Thus, I undertook a side project to discover the reason for this decay and eliminate it. As the "well-known" effect of water and other gaseous impurities in enhancing the atom yield from a low-pressure hydrogen discharge appeared to be the most probable explanation of the atom-concentration decay,[52-81] I initiated a study to determine quantitatively the effect of small quantities of oxygen, nitrogen, water, and hydrochloric acid on the hydrogen-atom yield from the discharge.

The experiments were critical, requiring a measurement to determine the presence or absence of a predicted effect or behavior. Rather than perform one experiment to extremely high precision and accuracy, I made many experiments involving different effects and different types of behavior in order to emphasize the single interpretation of the results which was completely consistent with all of the observations. The results for water—it had no effect on the atom yield from a low-pressure hydrogen discharge—disagreed with 45 years of experience accumulated by others on the subject.

This conflicting observation for the effect of water is responsible for the unusual length of this report. Since the observation may be controversial, I felt it was better to provide a plethora rather than a dearth of information substantiating it. The experiments with water and oxygen are described in Sec. V, which can be read independently of the rest of the report.

Section II describes the experimental equipment, gases, parameters, and procedure, and is useful only to those interested in repeating the experiments or checking on the caliber of the measurements.

Section III describes the design, construction, and operation of a Wrede-Harteck gauge, and is useful mainly to those interested in duplicating the technique. The Wrede-Harteck gauge that I developed reliably measured relative atom concentrations. As an absolute device, it may have been as much as 50% low.

Section IV develops, summarizes, and extends the mathematical theory for low-pressure flow and diffusion tubes in the absence of gas-phase reactions. The derivations for the fourteen cases considered are

individually brief. The newly derived equations are Eqs. (IV-90), (IV-96), (IV-110), (IV-134), (IV-151), and (IV-157), and (IV-162). Section IV.E provides a convenient summary of the physical meaning of the dimensionless groups used.

Section VI describes the Wood-Wise-Tsu-Boudart controversy about the effect of a catalytic probe on the atom-concentration profile in a low-pressure diffusion tube and then gives my own opinions and experiments on the subject.[4,12,30,32]

Notation used in Secs. III through VI are listed in Sec. VII.

II. EXPERIMENTAL APPARATUS AND PROCEDURE

A. Apparatus for Measuring Experimental Parameters

1. Pressure

The total pressure inside the vacuum system was measured either with (a) a McLeod gauge (Consolidated Vacuum Corporation Model GM-100A) having a 100-mtorr nonlinear scale and linear 1.00- and 10.0-torr scales, (b) a thermocouple vacuum gauge (NRC Equipment Corporation Type 501) having a useful operating range of 2 to 200 mtorr, or (c) a VG-1A/2 ionization gauge having a useful pressure range of 10^{-3} to 10^{-7} torr.

An identical McLeod gauge was calibrated at the Laboratory by Gerald P. Pfaff, who thoroughly tested the gauge and found that the agreement between the measured and the corrected company scales was better than 0.5%.[82] I therefore assumed that all measurements with my McLeod gauge were as good as 1% (at best) or 2% (at worst) and used it with full confidence for all micromanometer calibrations and total-pressure measurements in the diffusion-tube or flow-tube systems. Because the McLeod gauge was situated about 100 cm downstream from the WHG, the measured pressure for typical gas velocities used in the flow-tube experiments was corrected about 1.5%. The micromanometers were calibrated with the liquid nitrogen trap alternately filled with ice water or liquid nitrogen to minimize the possible errors associated with trap pumping. The calibration measurements are described in greater detail elsewhere.[83]

The uncalibrated thermocouple gauge was used for all experiments when the pressure measurement needed was only approximate. This was the case for all preliminary experiments and those for which only relative atom-concentration measurements were made at some general pressure level, usually in the range 70 to 110 mtorr. Estimated corrections were made for behavior differences of the gauge in air and in pure hydrogen.

The uncalibrated ionization gauge was used only to detect leaks or the extent of outgassing when the system was pumped down with the diffusion pump.

2. Temperature

The most important thermal problem was that of drifts of thermal origin in the signal from the Wrede-Harteck gauge. The heat of recombination of atoms on the WHG catalytic surface or the heating of the main gas stream by the discharge made the gauge susceptible to thermal-effusion effects.

These thermal-effusion effects were eliminated by the construction of a special water-cooled WHG attachment and by operating the discharge intermittently, at low power levels, and far away from the WHG whenever possible. An air blast was directed at the 14-mm o.d. quartz or 41-mm o.d. Pyrex discharge region whenever microwave cavities were used. I also constructed a special Pyrex reaction tube that permitted liquid cooling of both the discharge and the measurement zones (described in Sec. II.B.2).

A recirculating system using Aroclor 1248,[84] a somewhat viscous and messy chlorinated biphenyl kindly supplied by Professor Charles R. Wilke, was provided for the special Pyrex tube mentioned above. Von Hippel[85] gives an extensive list of other fluids that have low power factors at microwave frequencies. The perfect fluid for this experiment would have a low power factor, low dielectric constant, and low vapor pressure, and would be inexpensive, nontoxic, and nonflammable.

The glassware surrounding the thermocouple probe was cooled with the same tap water used for the Wrede-Harteck gauges.

The ambient temperature of the air-conditioned and thermostatically controlled room, 23° to 25.5°C, varied slowly in any eight-hour interval. All of the equipment supplied some local heat, which was monitored by an uncalibrated 50°C immersion thermometer hung on the rack near a WHG.

3. Atom Concentration

The atom concentration was measured with either (a) a Wrede-Harteck gauge, (b) a thermocouple probe, or (c) a thermometer probe. The design, construction, and operation of the WHG is described in detail in Sec. III.

The thermocouple probe, a device for measuring relative concentration of atoms, consisted of a long length of No. 30 iron-constantan thermocouple wire with one junction soft-soldered and coated with epoxy, and the other junction soft-soldered to a piece of silver foil with a cross-sectional area of about 4 cm^2. The remaining exposed thermocouple wires were also covered with epoxy. Both junctions were mounted inside the vacuum system in a specially constructed water-cooled glass unit, the vacuum-to-atmosphere seal being made with epoxy and Glyptal lacquer (Fig. 1).

The thermometer probe, another device for measuring relative concentration of atoms was a 360° C nonimmersion thermometer whose bulb end was first abraded and then coated with either $AgNO_3$ or electroplated nickel. The thermometer was centered and moved by means of two magnetically controlled Teflon spacers (Fig. 2). The graduations on the stem served to fix the location of the tip when measured externally with a cathetometer.

A qualitative indication of the hydrogen-atom concentration in the system was the color of the microwave discharge in the 14-mm o.d. quatrz-tube; this discharge varied from whitish pink for pure hydrogen (very few atoms) to a beautiful crimson for a 20:1 hydrogen-oxygen mixture (many atoms). Estimations of atom concentrations intermediate between these two extremes frequently were unreliable and difficult to make. The hydrogen α- and β-Balmer lines were always present (as shown by a small hand spectroscope) and were never used for even a qualitative indication of the atomic-hydrogen concentration.

4. Flow Rate

The most accurate flowmeters were small mercury plugs that moved at a constant timed rate inside a capillary tube of known cross-sectional area. The flowmeter (Figs. 3 and 4) was patterned after those of Ehlers[86] and Chavet,[87] and conveniently measured flow rates to a reproducibility of better than 1% in the range 0.01 to 0.5 cm^3 STP/sec. A plunger operated by a small magnet external to the flowmeter forced a small amount of mercury through a capillary tip (to minimize the quantity of mercury in

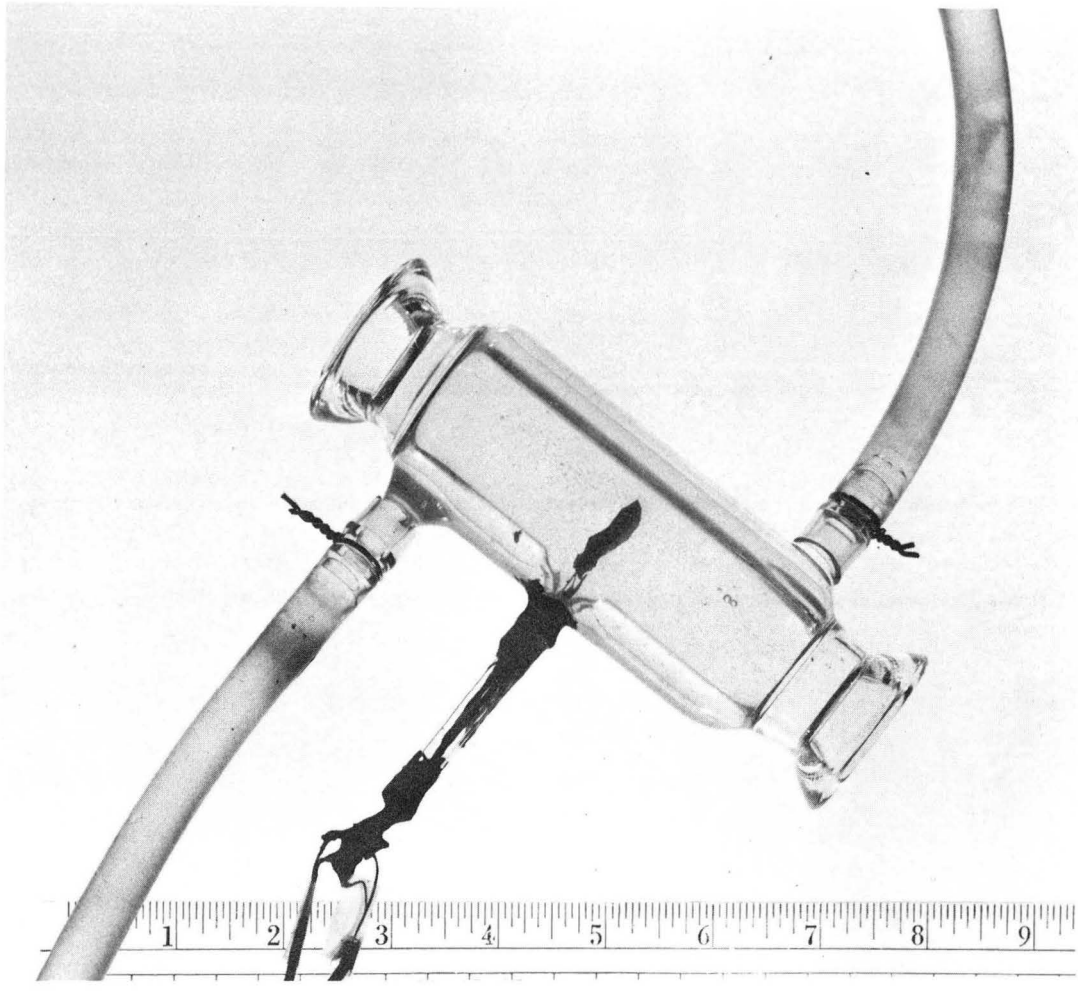

ZN-4922

Fig. 1. Photograph of water-cooled-glass thermocouple assembly. Pyrex O-ring joints (No. 25) are used.

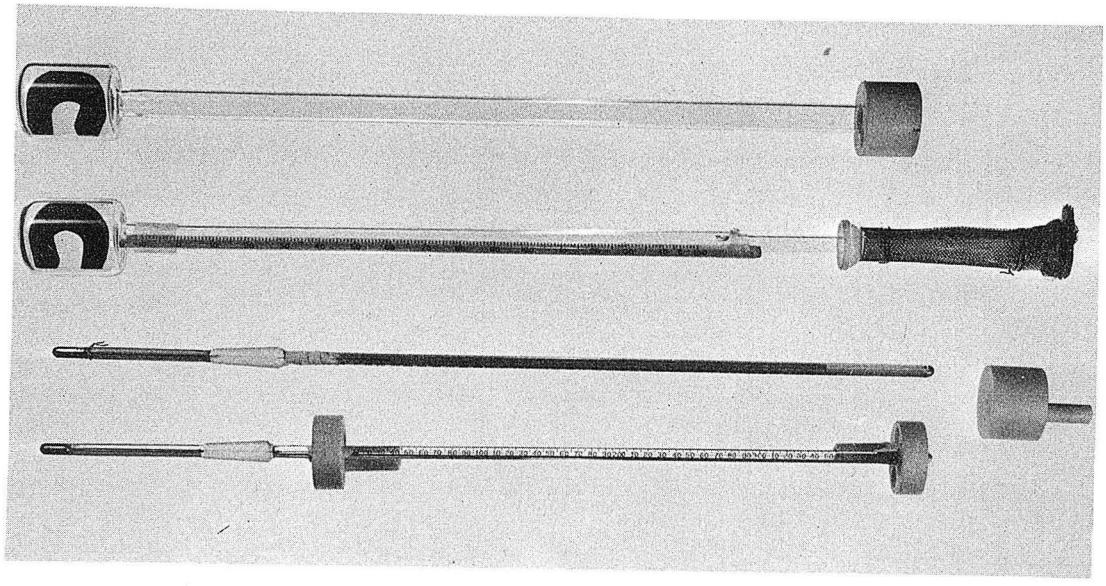

ZN-4923

Fig. 2. Photograph of movable probes. From top to bottom they are (a) a magnetically moved glass-tube and Teflon-sleeve assembly to hold metal or glass disks, (b) a magnetically moved glass-tube assembly to hold a probe containing platinum mesh and nickel-plated copper mesh, (c) a 360°C thermometer with an electroplated nickel end, (d) a magnetically moved 360°C thermometer with an $AgNO_3$-coated, and (e) a magnetically moved Teflon plug (on lower right-hand side).

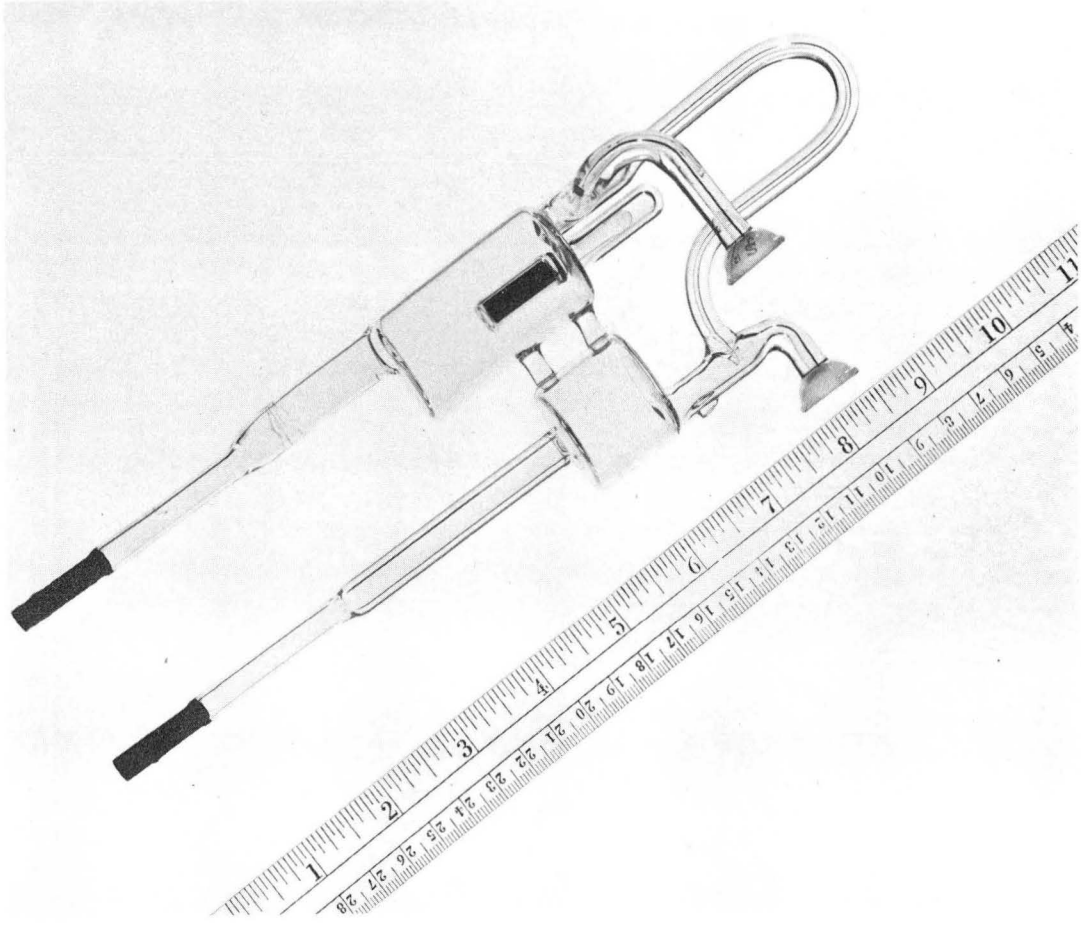

ZN-4916

Fig. 3. Close-up photograph of mercury-plug flowmeter showing details of the capillary tip, magnetic plunger, U-shaped tube, and inlet and outlet chambers.

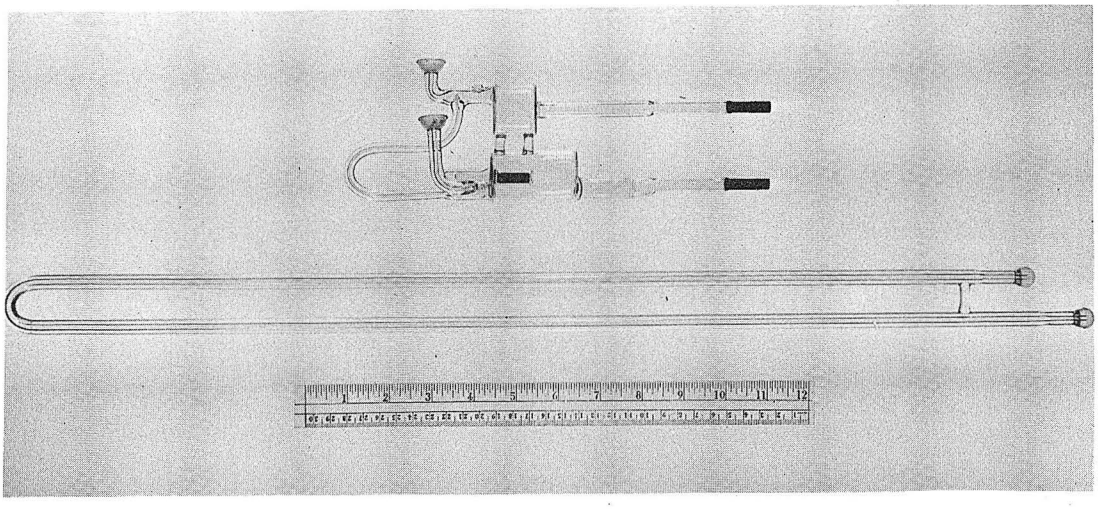

ZN-4921

Fig. 4. Photograph of the complete mercury-plug flowmeter showing the relative sizes of the mercury-housing part and the 3-mm i. d. capillary tube.

the drop) into a small-bore heavy-walled capillary tube of cross-sectional area 0.058_4 cm^2 (as determined from the weight of a mercury column of known length) and length 60 cm. The mercury traveled around the capillary tube, up the slight incline, and back into the mercury pool, maintaining the mercury level in the U-shaped tube. By means of an additional mercury pool, the level was adjusted in the U-shaped tube pool. The rate of travel of the drop in the calibrated portion of the capillary tube was measured with a stopwatch and meter stick. With hydrogen gas, operation of the flowmeter became a problem only when the glass or mercury was or became dirty, because the dirt caused the mercury drops to move somewhat erratically through the capillary tube. The use of ball joints facilitated cleaning (with chromate cleaning solution) of the glassware. A simple calibrated bellows vacuum-pressure gauge (U. S. Gauge) monitored the inlet pressure of the gas to the vacuum system.

Two other rotameters (Fischer and Porter, Model 10A-2735-4001), which monitored cylinder hydrogen either pure or bubbled through water, each consisted of a case, glass flowmeter, sapphire float, and brass inlet fittings.

These rotameters were useless for measuring flow rates of 0.1 cm^3 STP/sec, the nominal flow rate used for most of the experiments. However, when flow-rate measurement was not critical, the low end of the graduated flowmeter scale did facilitate the setting of the desired pressure level within the vacuum system. The rotameter case leaked. For some experiments, a slight air leak into the water bubbler was actually an asset, so the rotameter cases were used without change for the duration of the experiments. When "pure" cylinder hydrogen was desired, thorough flushing of the rotameter was necessary.

The impurity-gas (O_2, N_2, H_2O, or HCl) flow rate was measured by means of the rate of pressure drop in a chamber of known volume, consisting of a 500-cm^3 glass bulb, glass and copper tubing, and one side of a micromanometer (Decker Corporation Model 306-2A, full scale 1.87 torr). The gases were transferred directly from small cylinders into individual 500-cm^3 glass storage bulbs, and then individually as

desired from the storage bulb to the previously evacuated chamber of known volume (44 cm^3 or 537 cm^3)(Fig. 5). This system was somewhat inoperable with water or HCl, since both were adsorbed or condensed inside the micromanometer and gave spurious readings.

5. Impurity Concentration

The mole fraction impurity within the gaseous system, computed from the ratio of the impurity- and hydrogen-gas flow rates of the pure gases was calculated from the known volume (44 cm^3, for example), the rate of decrease of pressure as measured by the Decker micromanometer (15 mtorr/sec, for example), and the flow rate of the hydrogen gas (0.08 cm^3 STP/sec, for example):

$$x_{Imp} = \frac{(44\ cm^3)(15\ mtorr/sec)}{(0.08\ cm^3/sec)(760{,}000\ mtorr)} = 0.011$$

The mole fractions were determined in this manner to better than 3% accuracy.

6. Gas Velocity

The average velocity of the gas stream in the main reaction tube was calculated from the measured value of the flow rates, the pressure in the vacuum system (76 mtorr, for example), and the cross-sectional area of the reaction tube (10.7 cm^2):

$$V_{av} = (1.011)\ \frac{(0.08\ cm^3/sec)(760{,}000\ mtorr)}{(10.7\ cm^2)(76\ mtorr)} = 75\ cm/sec\ .$$

It never exceeded 100 cm/sec in the main reaction tube.

7. Linear Measurements

Most lengths were measured with an uncalibrated meter stick (such as hydrogen-gas flowmeter, length of reaction-tube sections, distance between WGH port holes) or a metal ruler (movable-probe ratchet assembly). Thicknesses were measured with a micrometer or vernier caliper.

ZN-4918

Fig. 5. Photograph of the gas-handling system, including the gas-storage bulbs, the known-volume bulb (V_o), and the hydrogen purifier, reservoir, and flowmeter.

8. Time

Time was either measured with a stopwatch or determined directly from the recorder-chart (one large box = 3-1/3 minutes).

B. Other Equipment

1. Gases

All gases used were from commercial sources. Liquid Carbonic Company 99.99+% hydrogen (N_2 < 3 ppm, O_2 < 3 ppm, H_2O < 1 ppm, hydrocarbons < 0.5 ppm, dew point -105°F) was used directly, passed through a water bubbler, or purified with a hydrogen purifier (Englehard Model HPD-0-50D). Small cylinders of oxygen, nitrogen, or HCl were used for the impurity gases (any contaminants in these gases appeared as second-order effects in the final experiments), which were transferred to and stored in individual gas-storage bulbs of 500-cm^3 volume (Fig. 5). The discharge work and atom-concentration measurements verified the general purity of the cylinder hydrogen.

2. Reaction Tubes

The composite-glass assembly (whether whole or in parts), consisting of a discharge zone and a reactor zone, is called the reaction tube throughout this paper. The definition of these two zones is schematically shown in Fig. 6 [λ is defined by Eq. (IV-45)].

The first tube consisted of a 54-cm discharge zone and a jacketed 88-cm reactor zone with two WHG ports (described in Sec. III) and a 1-1/2-in. glass-pipe end for the movable-probe assemblies (Figs 7(a) and 8).

The second tube was quite similar, except that the entire tube was jacketed, there was only one WHG port, and the reactor section was longer—102 cm [Fig. 7(b)].

The third reaction tube was completely different, consisting of several segments coupled with No. 25 O-ring joints and Viton O-rings. The two end segments had one WHG port each, but the middle segment consisted of the jacketed glass-thermocouple assembly shown previously (Figs. 1, 9, and 10). The large-diameter segment containing the 2-in.

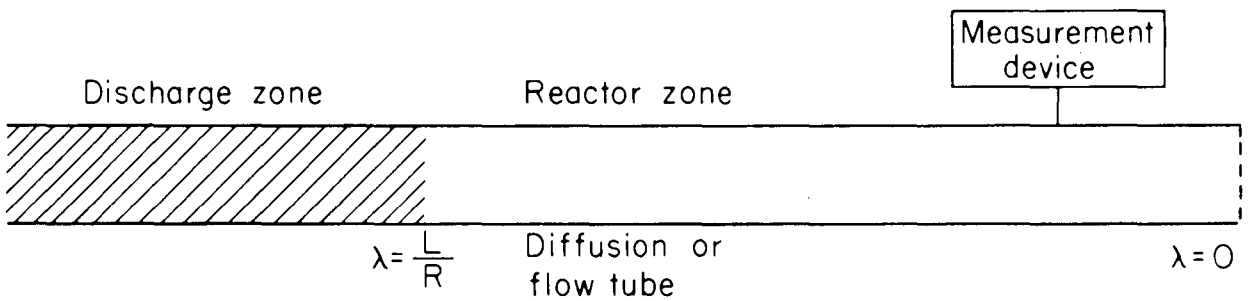

MU-35708

Fig. 6. Schematic drawing of a typical "reaction tube," showing the location of the discharge zone, the reactor zone, and the discharge-zone boundary (at $\lambda = L/R$).

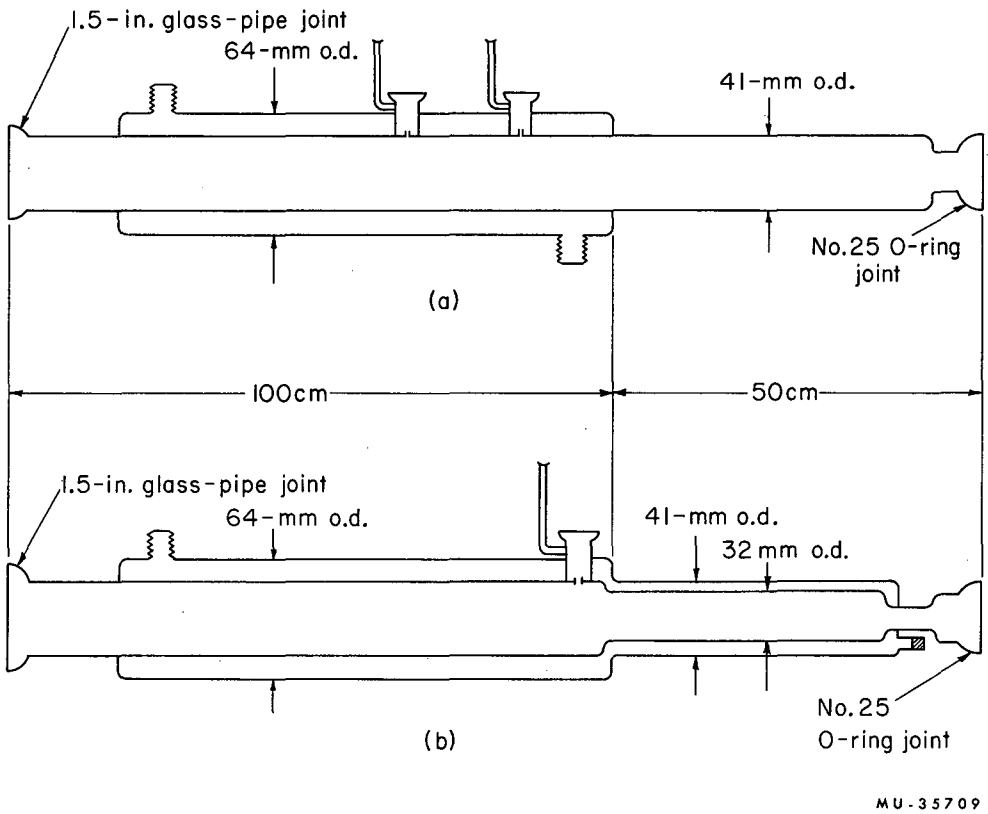

Fig. 7. Schematic drawings of (a) reaction tube No. 1, and (b) reaction tube No. 2.

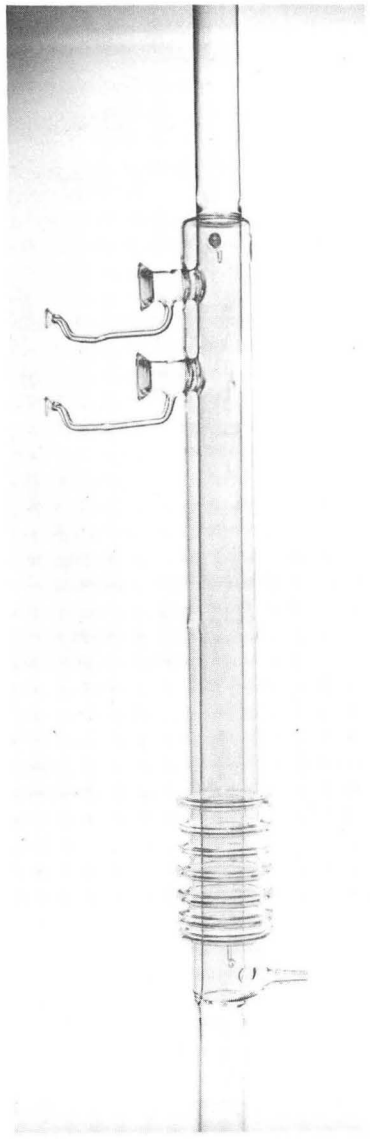

ZN-4917

Fig. 8. Photograph of central portion of reaction tube No. 1 showing the water-cooled reactor zone, part of the discharge zone, and two Wrede-Harteck gauge ports.

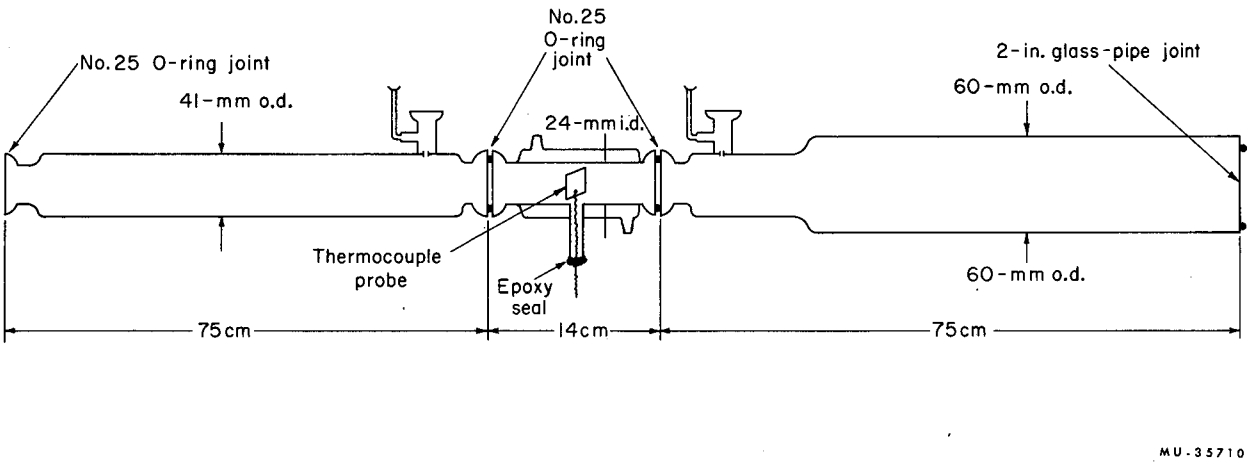

Fig. 9. Schematic drawing of reaction tube No. 3, which is composed of three segments: (a) a 75-cm discharge-zone tube containing a WHG port, (b) a 75-cm buffer-zone tube containing a WHG port, and (c) an intermediate part (of variable length) which could be the 14-cm thermocouple assembly or a glass tube internally vapor plated with a metal.

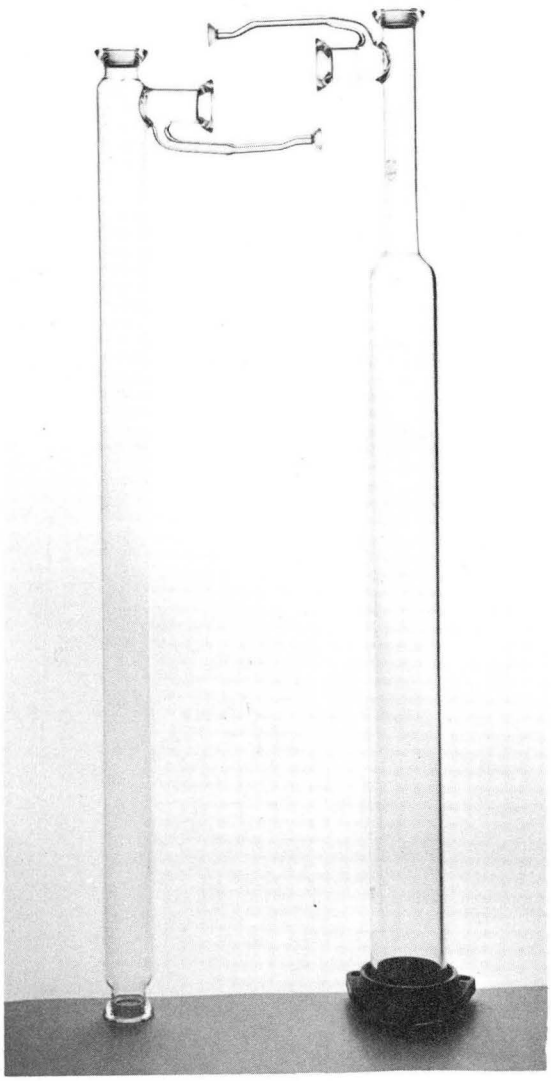

ZN-4919

Fig. 10. Photograph of reaction tube No. 3 showing the 75-cm discharge-zone tube (on the left-hand side) and the 75-cm buffer-zone tube.

glass-pipe end was previously used without the WHG port as a buffer zone to minimize gas-flow fluctuations when reaction tubes No. 1 and No. 2 were used as diffusion tubes. Even with the WHG port, it still served in this capacity.

Initially I planned to coat the inside of all of the reaction tubes with Teflon (DuPont Clear Finish 852-201) according to the instructions given by Berg and Kleppner.[88] My early experiments made such a procedure unnecessary, so I refrained from doing this to avoid introducing an additional experimental parameter.

Other glassware consisted of a glass-pipe joint-size reducer, (used when reaction tubes No. 1 and No. 2 were set up as flow tubes), a water bubbler (Fig. 11), a quartz discharge tube of 14-mm outer diameter (not shown, but used with the small microwave cavity), and a discharge tube also containing a 45-foot long coil of copper tubing internally electroplated with nickel (used as a converter of oxygen to water, see Fig. 12).

3. Movable Probes

By means of several types of movable probes, I determined the effect of a "catalytic probe" on the atom-concentration distribution in a diffusion tube:

a. A magnetically moved Teflon plug (Fig. 13),
b. A magnetically moved 360°C thermometer with the end coated with $AgNO_3$ (Fig. 2),
c. A magnetically moved glass-tube and Teflon-sleeve assembly to hold metal or glass disks (Fig. 2),
d. A long glass tube for internally heating a metal resistance wire (Fig. 14),
e. A long glass tube (not shown) for holding a thermometer, a probe containing platinum mesh and nickel-plated copper mesh, or a nickel-plated copper plug (Fig. 13),
f. A long water-cooled glass-tube and Teflon-sleeve assembly to hold metal or glass disks (Fig. 14).

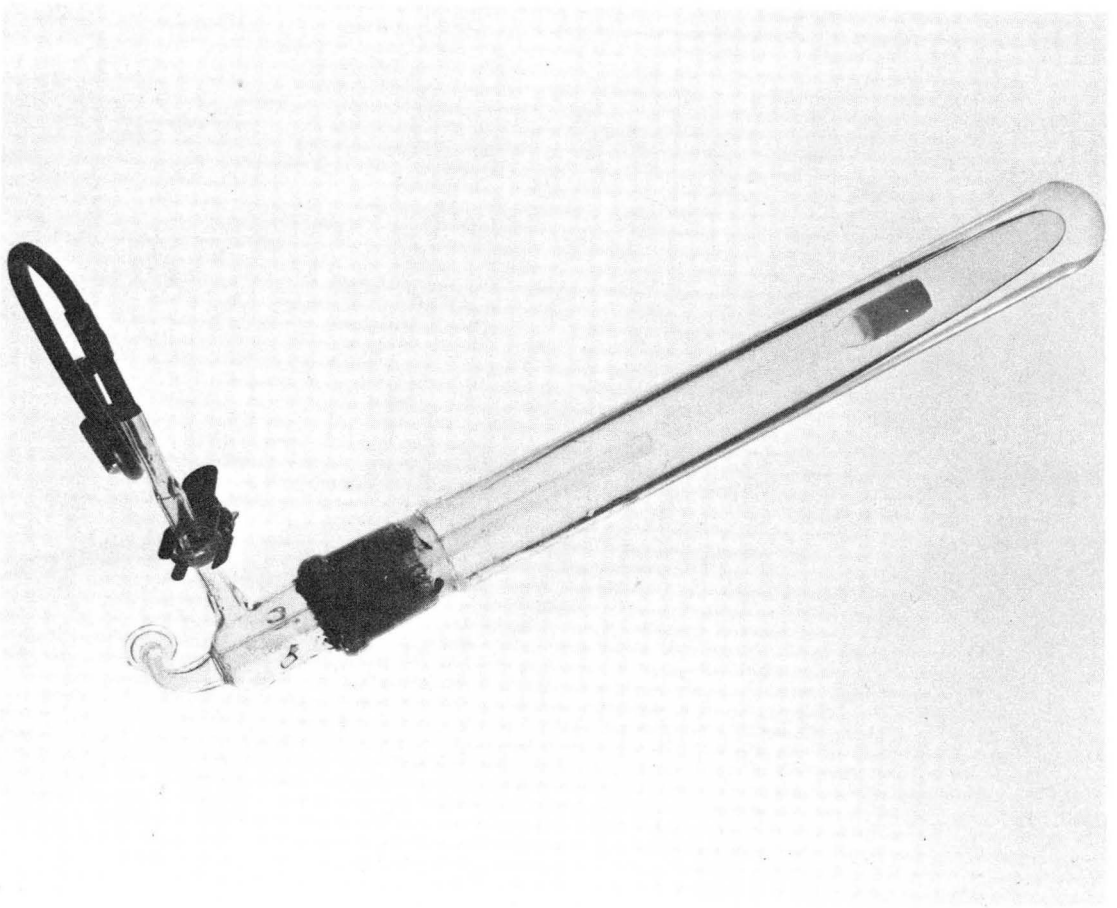

ZN-4914

Fig. 11. Photograph of the water bubbler, which was leak tight.

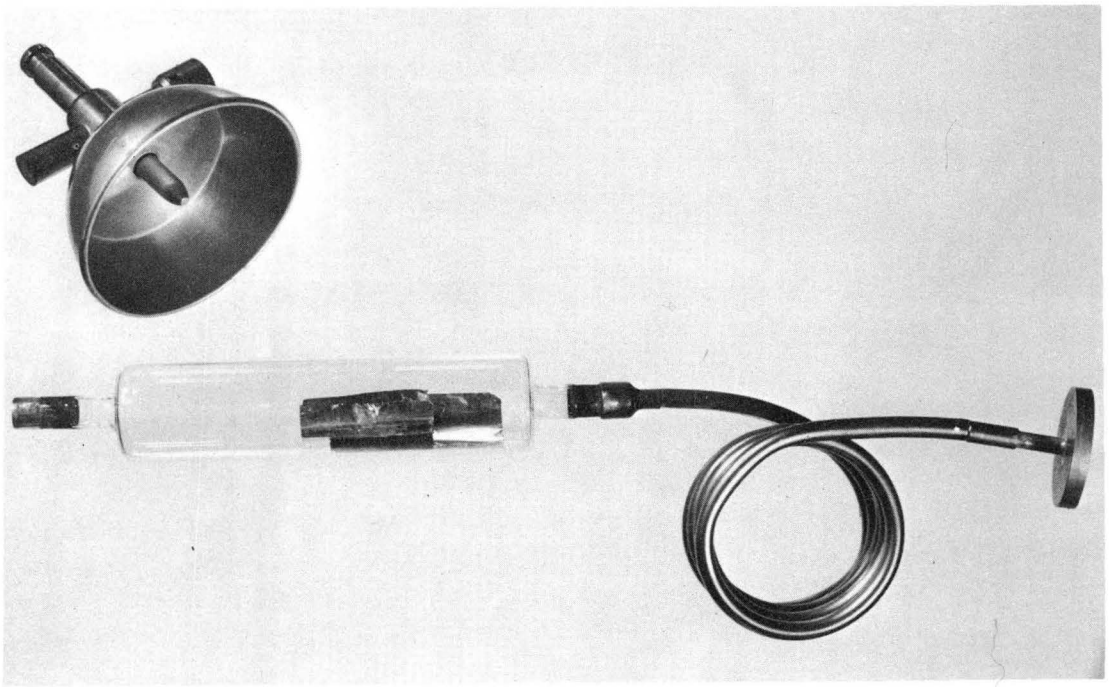

ZN-4935

Fig. 12. Photograph of (a) the Burdick Type A reflector, which was used with (b) the oxygen-to-water converter consisting of a 40-mm o. d. 15-cm long glass tube and 8-mm o. d. 45-foot long copper tubing internally electroplated with nickel.

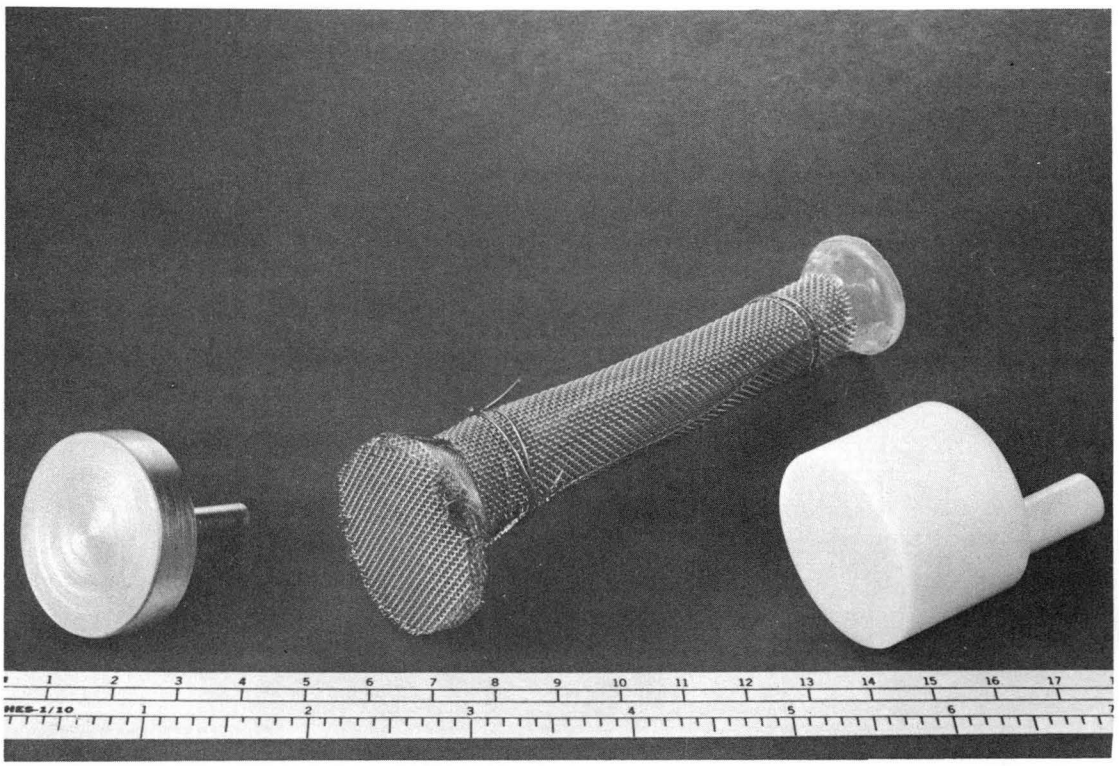

ZN-4931

Fig. 13. Photograph of movable probes: (a) a nickel-plated copper plug (on left), (b) a Teflon plug with magnetic stirring rod (on right), and (c) a probe containing platinum mesh (not visible) and nickel-plated copper mesh to provide a large amount of catalytic surface area.

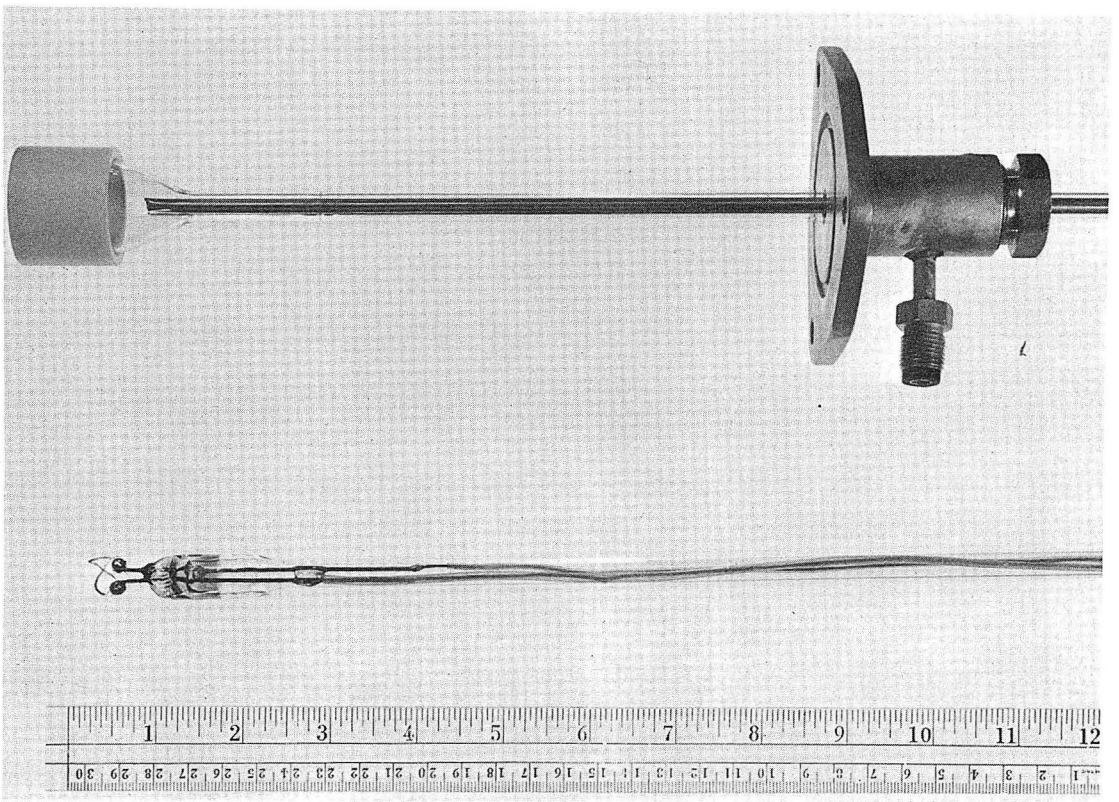

ZN-4934

Fig. 14. Photograph of movable probes used with Wilson-seal and ratchet assembly: (a) a long water-cooled glass-tube and Teflon-sleeve assembly to hold metal or glass disks (top), and (b) a long glass tube for internally heating a metal resistance wire.

The latter three pieces and a Wilson-seal-and-ratchet assembly were used when an accurate position of the probes was desired (Fig. 15). Leaks in the Wilson seal were minimized by vacuum pumping on the middle-gasket chamber and by introducing motion slowly. The magnetically moved probes introduced fewer pressure perturbations into the system but were occasionally hard to move and were inferior to the ratchet assmbly for determining the probe position accurately.

The disks were of copper, platinum vapor plated on copper, and silver nitrate deposited on glass. Each had a 2.9-cm diameter and fitted tightly into the Teflon probe or sleeve assembly.

4. Discharges

The discharges were excited by either a 100-watt 2.45-GHz diathermy machine (Burdick Company) or a specially designed "Radio-Frequency Light Power Supply" consisting of an oscillator, modulator, and power amplifier. The latter unit, operating at 50 MHz with a rated maximum power level of 500 watts, was chosen only because it was available. The entire unit has been schematically described in Engineering Drawings 5V1354, 5V1364, and 3Z5232A of the Lawrence Radiation Laboratory, Berkeley, California. The pi network along with the output L-C circuit used for producing the discharge is shown in Fig. 16. No attempts were ever made to optimize the setting of the tunable capacitor, C_t, which (along with the eight-turn 40-mm inner-diameter coil) was housed inside a well-shielded iron and copper-mesh enclosure through which the reaction tube passed (Fig. 17).

Two cavities were used with the Burdick diathermy unit: (a) a large-diameter cavity (43-mm i.d.) described by Zelikoff, Wykoff, Aschenbrand, and Loomis;[89] and (b) a small-diameter cavity (15-mm i.d.), recently described by Fehsenfield, Evenson, and Broida.[90] The small cavity was kindly loaned for the later stages of this work by Dr. John G. Conway. Figure B20 is a photograph of these two cavities (see also cavity 5 in reference 90). They were used with the large-diameter (38-mm inner diameter) Pyrex reaction tubes and small-diameter (14-mm outer diameter) quartz discharge tube described previously. Burdick reflector "A" was used for the oxygen-to-water converter (Fig. 12).

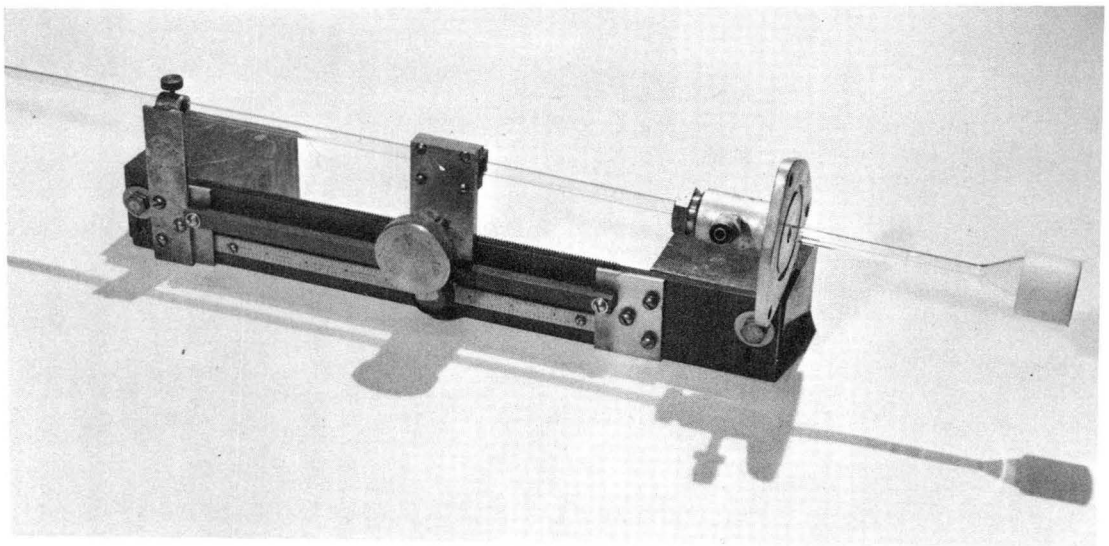

ZN-4928

Fig. 15. Photograph of Wilson-seal and ratchet assembly.

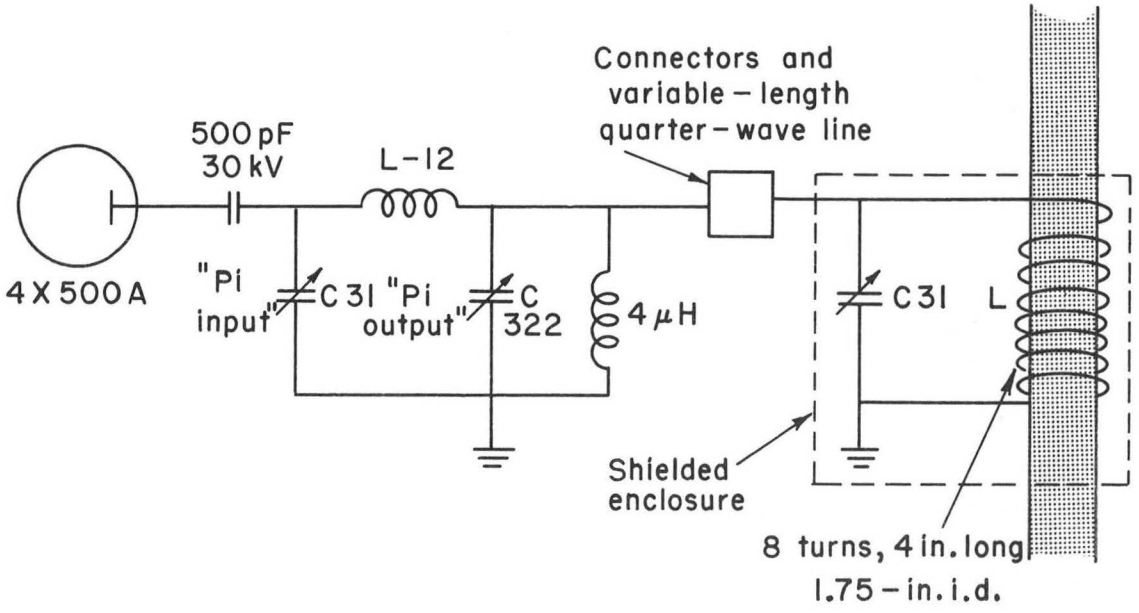

MU-35711

Fig. 16. Schematic diagram of pi network of 50-MHz oscillator and output LC circuit; L has eight turns of 1/4-in. o.d. copper tubing, is 4 in. long, and has an i.d. of 1.75 in.

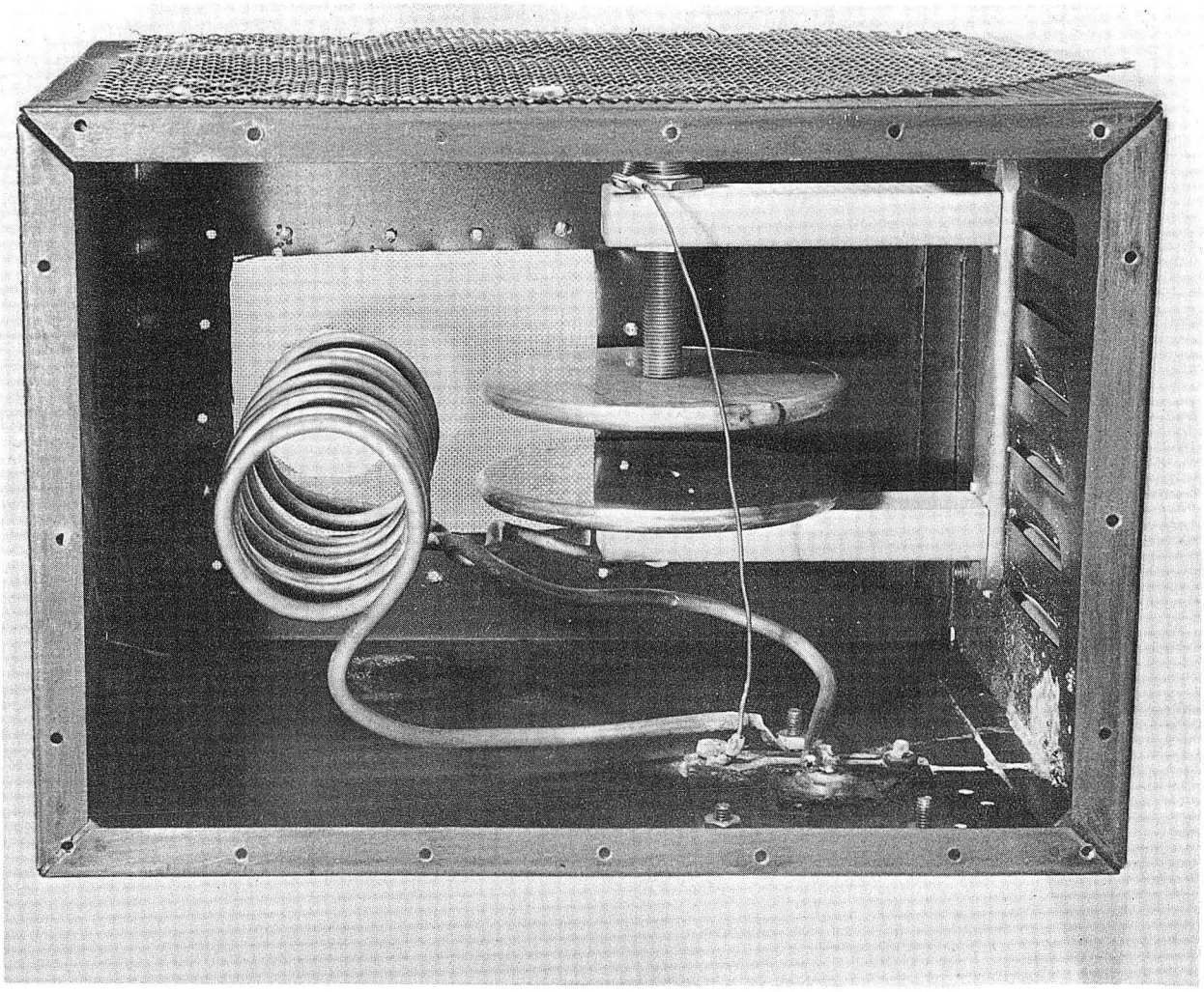

ZN-4933

Fig. 17. Photograph of output LC circuit and shielded enclosure.

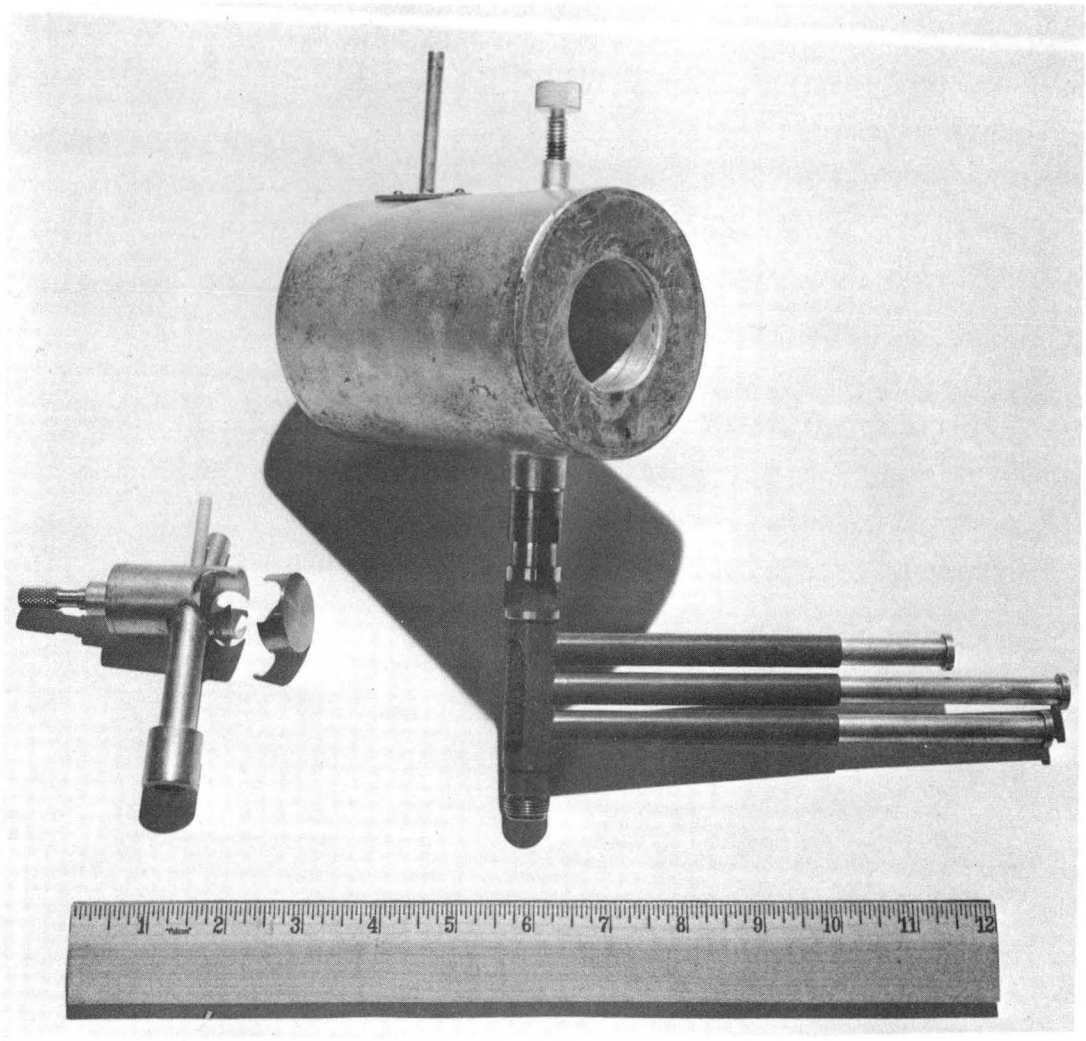

ZN-4927

Fig. 18. Photograph of small-diameter and large-diameter microwave cavities and triple-stub tuner.

Throughout most of the work, the microwave power was simply passed through a triple-stub tuner (Fig. 18) which minimized the amount of power reflected back to the magnetron. The percent-power dial on the front of the diathermy console was used as a relative measure of the amount of energy being transmitted to the discharge.

After most of the experiments were over, measurements were made to determine the typical standing-wave ratios for the operation of both cavities in the presence of a low-pressure hydrogen discharge. These measurements demonstrated that the percent reflected power for most of the atom experiments was quite high and probably exceeded 70%.

Occasionally the Burdick diathermy unit pulsed and became erratic. These pulsations either disappeared naturally after a few days of inactivity, or else were minimized by a Sola line voltage regulator that reduced the voltage levels within the diathermy unit. This action also produced much finer control of the power at low power levels (<30 watts).

Neither the large-diameter cavity nor the reflector could produce or maintain a stable hydrogen discharge in pure hydrogen at a pressure level of about 75 mtorr, a fact previously noted.[64,65] The work of Brown, Buchsbaum, Ward, Gordon, and others at the MIT Laboratory of Electronics furnished a beautiful solution to the problem: the use of a cyclotron-resonant microwave discharge.[91-94]

Instead of using an electromagnet, I tried with considerable success a large magnetron magnet producing an inhomogeneous magnetic field (maximum field strength, 1400 G). It was loaned through the kindness of Vincent J. Honey (Fig. 19). The field inhomogeneity made the discharge insensitive to frequency changes, simple to start, and easy to maintain. A Tesla coil was rarely necessary to start the discharge, which could be maintained at a Burdick dial settings as low as 2%. The microwave discharge at these low power levels was maintained by several hundred milliwatts or less. I typically used dial settings of 5 to 20% and occasionally tried 100% settings for curiosity. This type of microwave discharge does not appear to be widely appreciated by physical chemists working with gas-discharge systems.

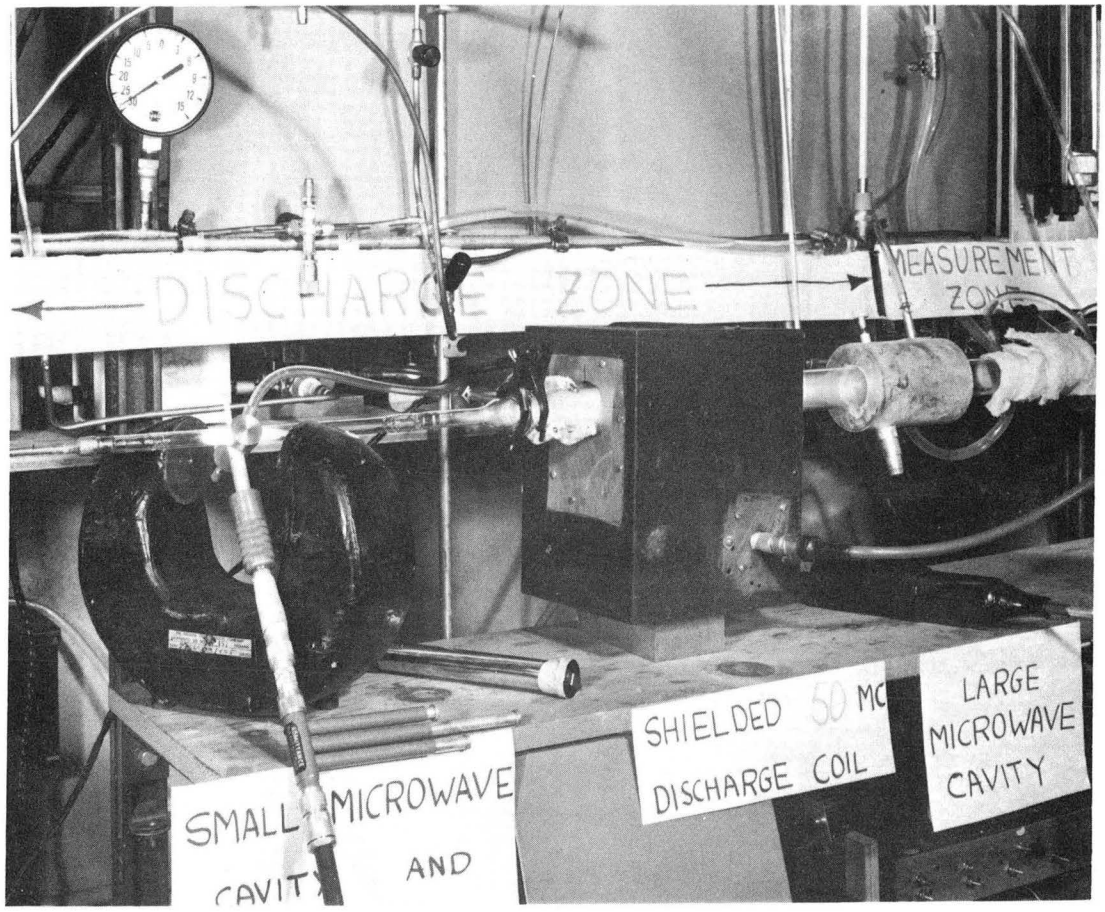

ZN-4925

Fig. 19. Photograph of the reaction-tube No. 3 discharge zone and the small-diameter microwave cavity and magnetron magnet (on left), the shielded 50-MHz output LC circuit (center), and the large-diameter microwave cavity (right).

5. Pumps and Traps

An air-cooled diffusion pump (Consolidated Vacuum Corporation Model V-21, using Dow Corning 704 silicone oil) backed by a mechanical vacuum pump (Duo-Seal Model 1400) thoroughly evacuated and outgassed the reaction system (Fig. 20). In the absence of leaks, the system pressure, as measured just above the diffusion-pump liquid-nitrogen trap, was between 1 and 5 μtorr. The entire system was frequently checked for leaks by means of a large flow of helium and a helium leak detector.

The system was not bakeable. The glassware was washed and rinsed in succession with detergent solution, distilled water, dilute nitric acid, distilled water, and acetone, and then dried prior to installation. A large ball valve and large-diameter flexible copper tubing between the diffusion pump and the system increased the effective pumping speed.

During the year of operation the diffusion pump broke down only twice, but thoroughly ruined the silicone oil in the process. Each time, this pump was cleaned and reused with no adverse effects.

When the gases were introduced for an experiment, the diffusion pump was shut off and a Kinney KC-5 pump used instead. A large-diameter liquid-nitrogen trap filled with corrugated copper sheeting minimized pump backstreaming or the contamination of the pump oil with water (Fig. 20). Oil in the mechanical pump was periodically changed.

A third mechanical pump (another Duo-Seal 1400) was used as a multipurpose pump wherever the system required it (i.e., the Wilson seal or the Decker gauge).

The exhausts from all mechanical pumps were passed through a copper tube to a hood vented on top of the building.

6. Needle and Other Valves

Needle valves were used primarily to monitor the flow rates of the pure hydrogen or the impurity gases. The best valve found for the job was a metering valve (Nupro Type B-2SD Double Pattern) which had two needles, one for coarse and one for fine control of the gas flow.[95] The needles can stick due to excessive tightening. Specification that

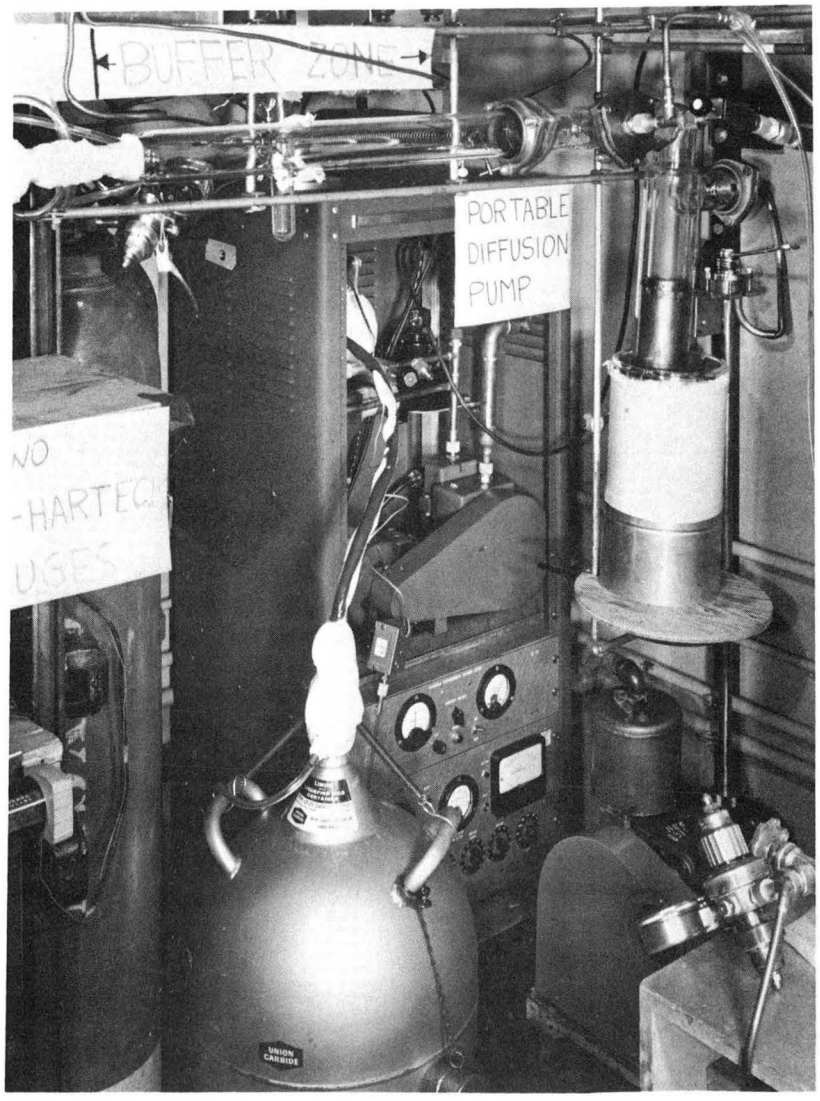

ZN-4920

Fig. 20. Photograph of the portable diffusion pump, large-diameter liquid nitrogen trap with corrugated copper sheet (upper right corner), Kinney KC-5 mechanical pump (lower right corner), and buffer-zone tube.

the valve is to be used for vacuum work should be made at the time of ordering, since the valves are primarily made for flow metering at 1-atm pressure. In practice, two Hoke valves in series and parallel with the Nupro valve provided easy evacuation around the needle valve and total control over any slight leaks.

Small helium-leak-tested valves (Hoke) were used throughout the vacuum system wherever necessary. A valve (Granville-Phillips Ultra-High Vacuum Valve, Type C) controlled the effective pumping speed of the Kinney KC-5 vacuum pump. Medical-oxygen brass-needle valves controlled the addition of cylinder hydrogen through the Fischer and Porter flowmeters into the vacuum system.

7. Miscellaneous Tubing and Connections

In addition to the previously mentioned equipment and glassware, a glass-pipe cross, Viton O-rings, Kovar glass-to-metal joints, copper tubing to minimize breakage, LRL fittings and flat O-rings, flexible copper tubing, Tygon tubing (for the cooling water), an 8-liter glass reservoir for the very pure palladium-diffused hydrogen, and other hardware completed the gas-handling and vacuum system.

8. Recorders

Two recorders (Speedomax Type G, Model S, 60000 Series), one with two inputs, monitored and recorded the following electronic signals:

a. Wrede-Harteck gauge No. 1 (atom concentration),
b. Wrede-Harteck gauge No. 2 (atom concentration),
c. Decker Corporation 306-2A micromanometer (for impurity gas flow rate),
d. Thermocouple probe (relative atom concentration).

The chart speeds on the two recorders were nearly matched (one inch = 3 1/3 minutes). The signals from the Wrede-Harteck gauges or the Decker micromanometer were passed directly to the recorder with or without the aid of a resistance divider. The thermocouple signal was first amplified by a Kintel Model 111BF amplifier, passed through an RC filter, and then to the recorder.

As the response times of all of the electronic measurements were slow, the recorders showed to excellent advantage the instantaneous level of the signals and provided a permanent record of the data. This permanent record was extremely valuable, as previous recorder-chart readings were repeatedly scanned for subtle effects, confirmatory behavior, or illustration of phenomena. The instantaneous tracings provided transient data that could easily have been missed if the recorders were not used.

C. Overall Apparatus

1. Preliminary Apparatus

The preliminary experiments determined whether the Wrede-Harteck gauge responded correctly to the presence of atoms. The apparatus, shown schematically in Fig. 21, is generally self explanatory. The glass joints were silicone-greased ball joints rather than O-ring joints. The large-diameter microwave cavity; a Lamers-Rony homemade micromanometer,[83] operated open loop; the magnetically moved platinum-and-nickel-mesh probe (Fig. 13); two leaky Fischer and Porter rotameters; an uncalibrated thermocouple pressure gauge; and cylinder hydrogen were all used for the measurements.

The system worked fine. The data obtained, though somewhat crude, were confirmed in more elaborate experiments performed later.

2. Diffusion-Tube Apparatus

The diffusion-tube apparatus was used to determine the effect of various catalytic and noncatalytic probes on the atom-concentration distribution within the diffusion tube. The apparatus consisted of the Decker-Lamers-Rony differential micromanometer (Figs. 22 and 23),[83] either the water-cooled or non-water-cooled WHG attachment, reaction tube No. 1 or No. 2, magnetically or ratchet-moved catalytic probes, the buffer-zone tube, the portable diffusion-pump unit, a Kinney KC-5 pump and Granville-Phillips valve, the Engelhard palladium hydrogen purifier, the CVC McLeod gauge, the large liquid-nitrogen trap with corrugated copper, and other miscellaneous valves and fittings (Fig. 24).

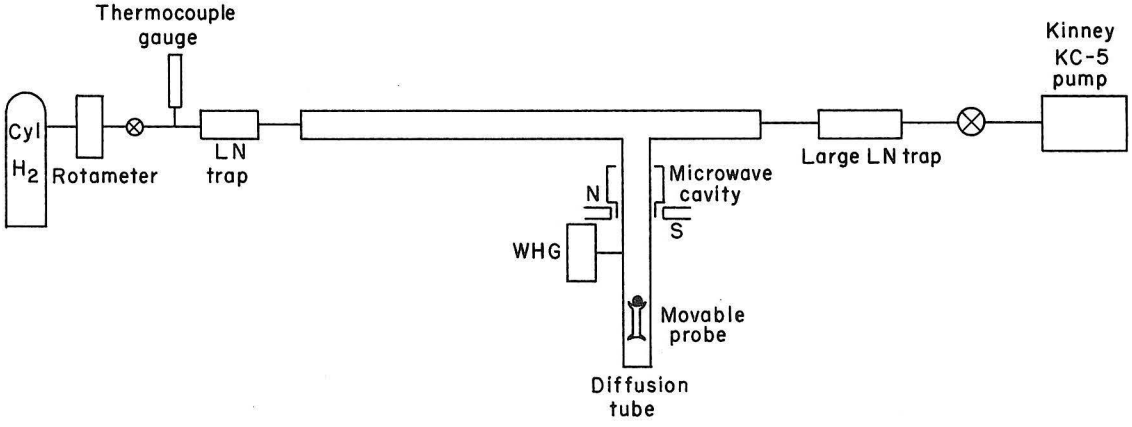

Fig. 21. Schematic drawing of preliminary apparatus. The rotameter leaked.

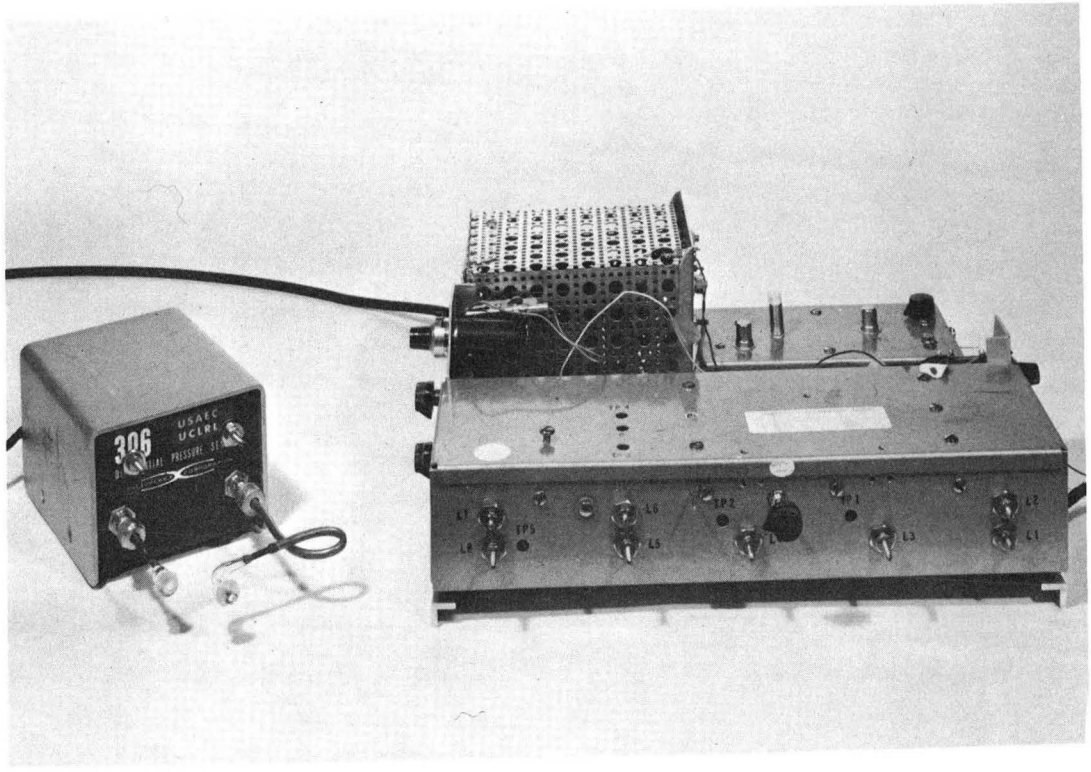

ZN-4932

Fig. 22. Photograph of the complete Decker-Lamers-Rony differential micromanometer showing the modified Decker pressure transducer (on left) and the Laboratory-designed electronics. This unit had a short-term stability of 1 μtorr and a long-term stability of 30 μtorr/hour at a total pressure of 1 μtorr. The pressure transducer was calibrated electrostatically to an accuracy of ± 2% in the pressure range 0.2 to 35 mtorr (see Ref. 83).

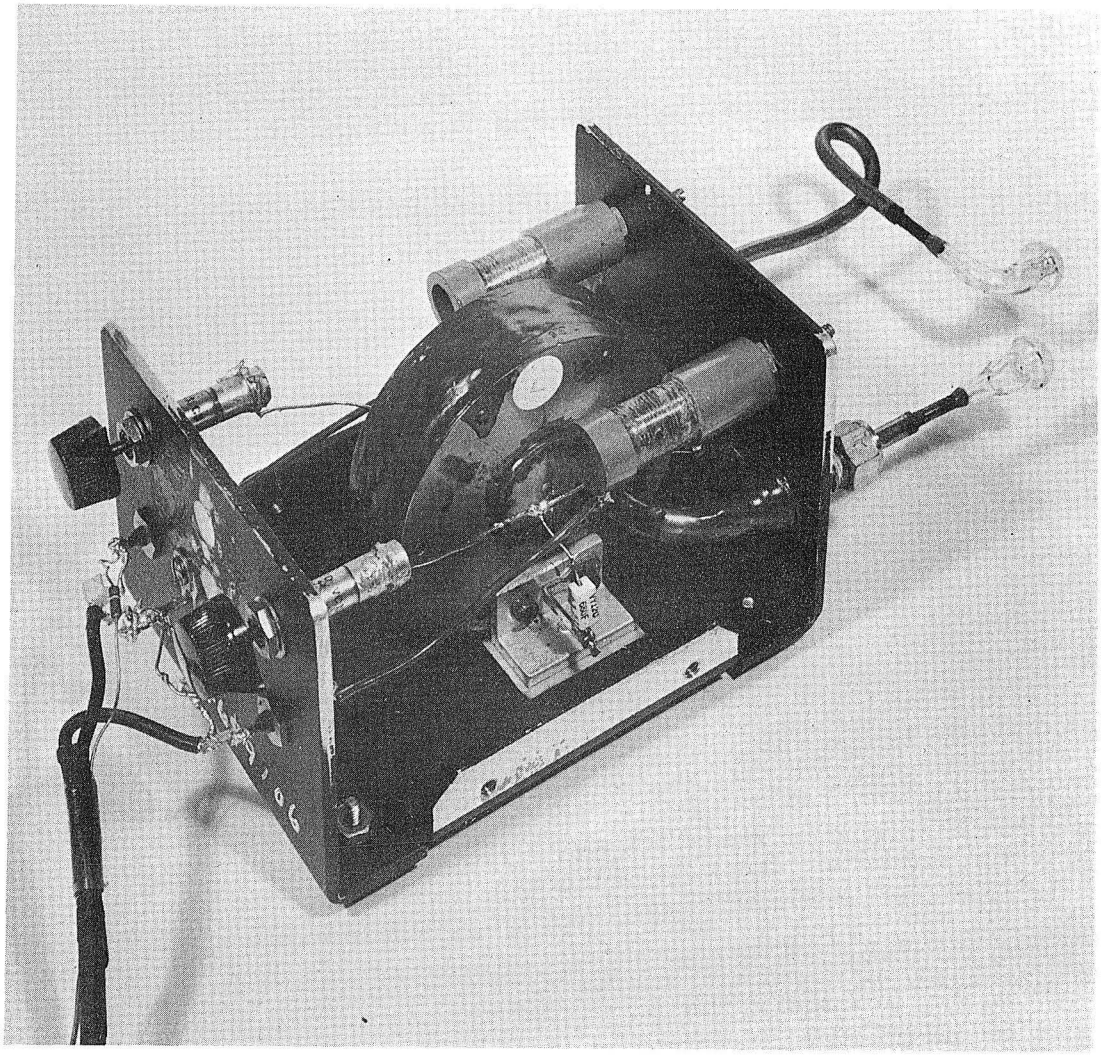

ZN-4930

Fig. 23. Close-up photograph of modified Decker 306-2A pressure sensor. The ionization transducer has been replaced by a tuned capacitance bridge. The residual volume of the connecting stainless-steel tubing and glass ball joints can be considerably decreased.

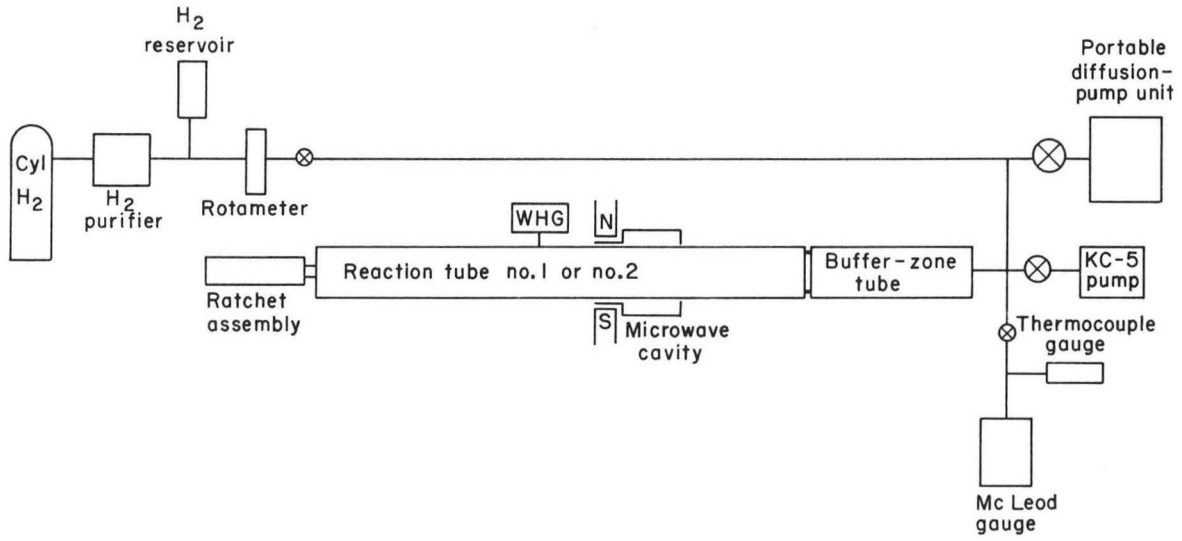

Fig. 24. Schematic drawing of diffusion-tube apparatus. The rotameter leaked, so that the "purified" hydrogen was in fact contaminated with an unknown amount of air.

The apparatus both performed the task required and verified the perturbing effect of highly catalytic probes on the atom-concentration level very close to the discharge region, as predicted by Tsu and Boudart.[30,32]

3. Flow-Tube Apparatus

The flow-tube apparatus was used to determine the effect of various gaseous impurities on the production of atomic hydrogen from a low-pressure gaseous discharge. This apparatus was very similar to the diffusion-tube apparatus described above, but had several notable differences: no movable probes were used, the hydrogen and impurity gas flowmeters described in Sec. A.4 were needed to monitor the amount of impurity in the gas, and either reaction tube No. 1 or No. 3 was used for the experiments.

At one time or other, the apparatus also employed the quartz-glass discharge tube, the small microwave cavity, the 50-Mc/sec oscillator, the water bubbler, cylinder hydrogen, the same leaky Fischer and Porter rotameters, an additional Decker-Lamers-Rony differential micromanometer (DLR) and associated water-cooled WHG attachment, the thermocouple probe for measuring relative atom concentrations, the Kintel Model 111BF amplifier, and the Decker 306-2A micromanometer (Figs. 1, 25 to 29).

Despite repeated attempts with this apparatus, the effect of water in enhancing the atomic-hydrogen yield from a low-pressure electrical discharge could not be demonstrated.

Both the flow- and the diffusion-tube systems were deliberately made sturdy, flexible, and as non breakable as possible. I felt free to open the system to an atmospheric pressure of air or helium, make the necessary changes, and then reevacuate over night. Although the system was never baked, the glasware was cleaned for several hours occasionally by a hydrogen or nitrogen discharge. Despite repeated vacuum-to-atmosphere cycles, all experiments were prefectly reproducible.

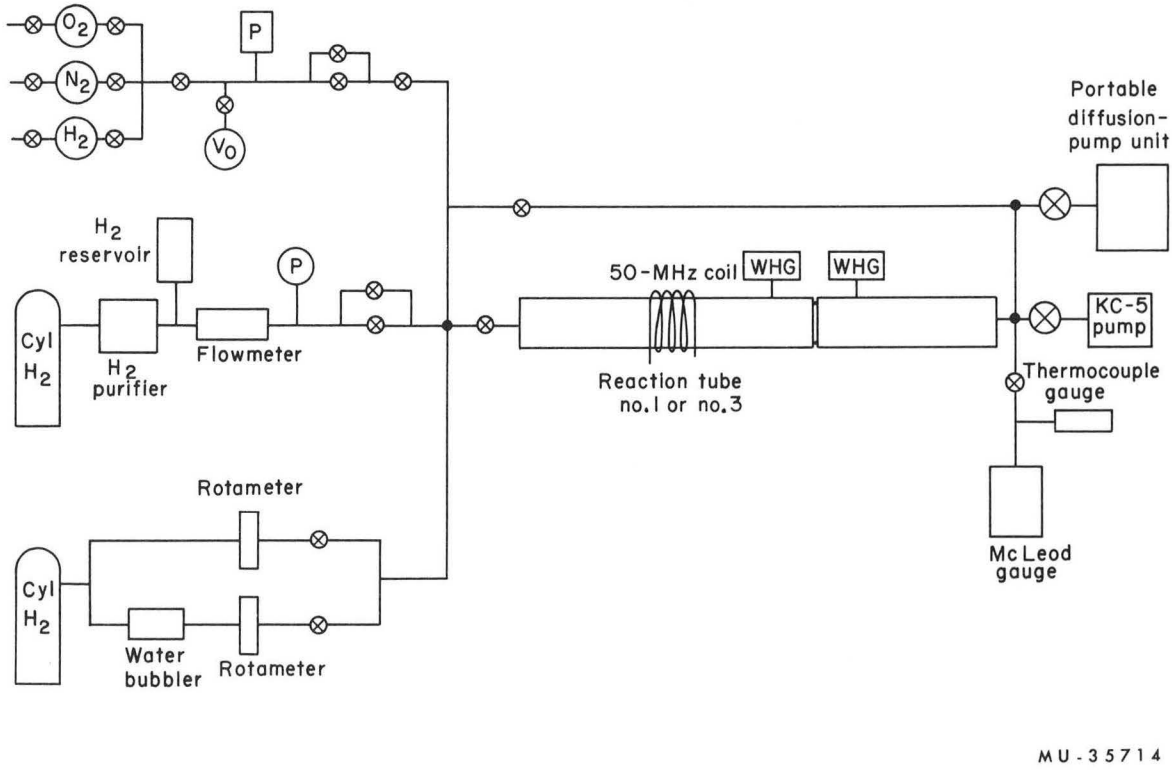

Fig. 25. Schematic drawing of flow-tube apparatus. Either the small-diameter or large-diameter microwave cavities could be operated independently of the 50-MHz discharge. Both rotameters leaked.

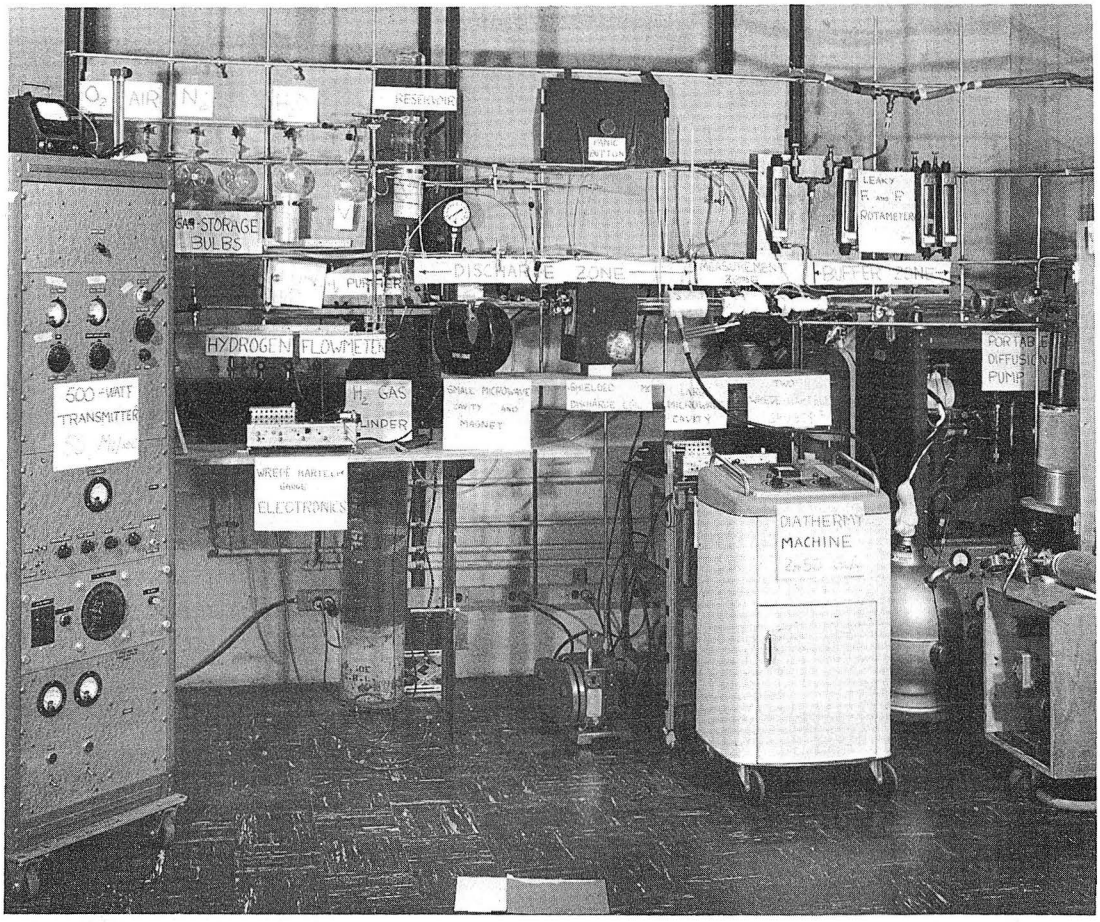

ZN-4926

Fig. 26. Photograph of the overall flow-tube apparatus showing the 50-MHz oscillator and the 2.45-GHz diathermy machine.

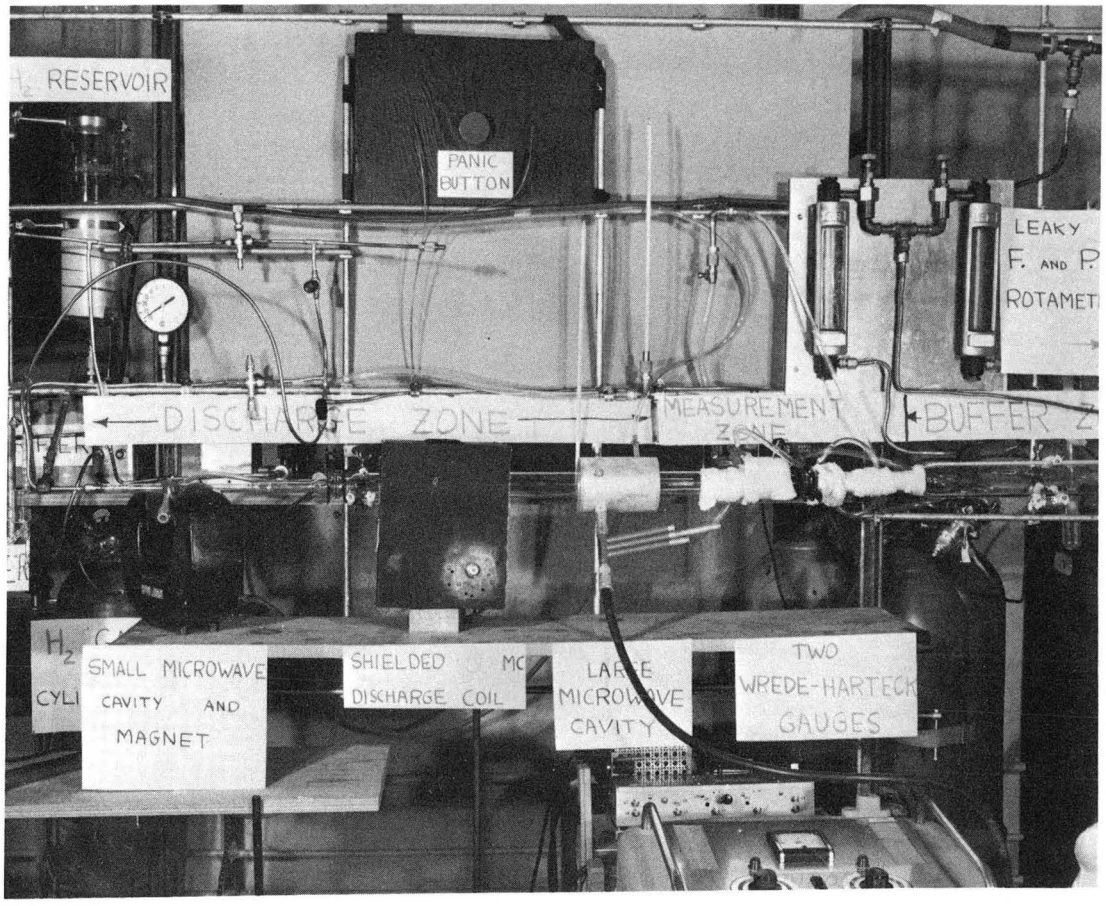

ZN-4936

Fig. 27. Photograph of the central part of the flow-tube apparatus.

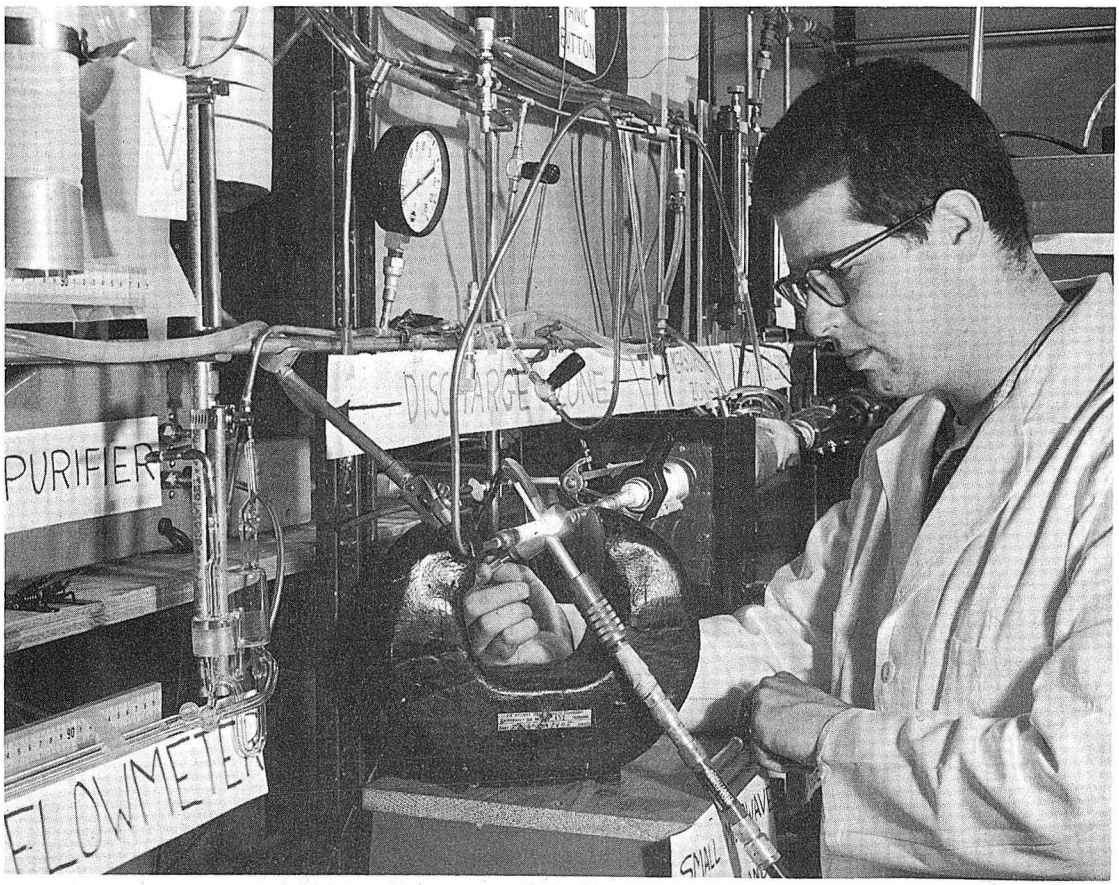

ZN-4960

Fig. 28. Photograph showing author tuning small-diameter microwave cavity.

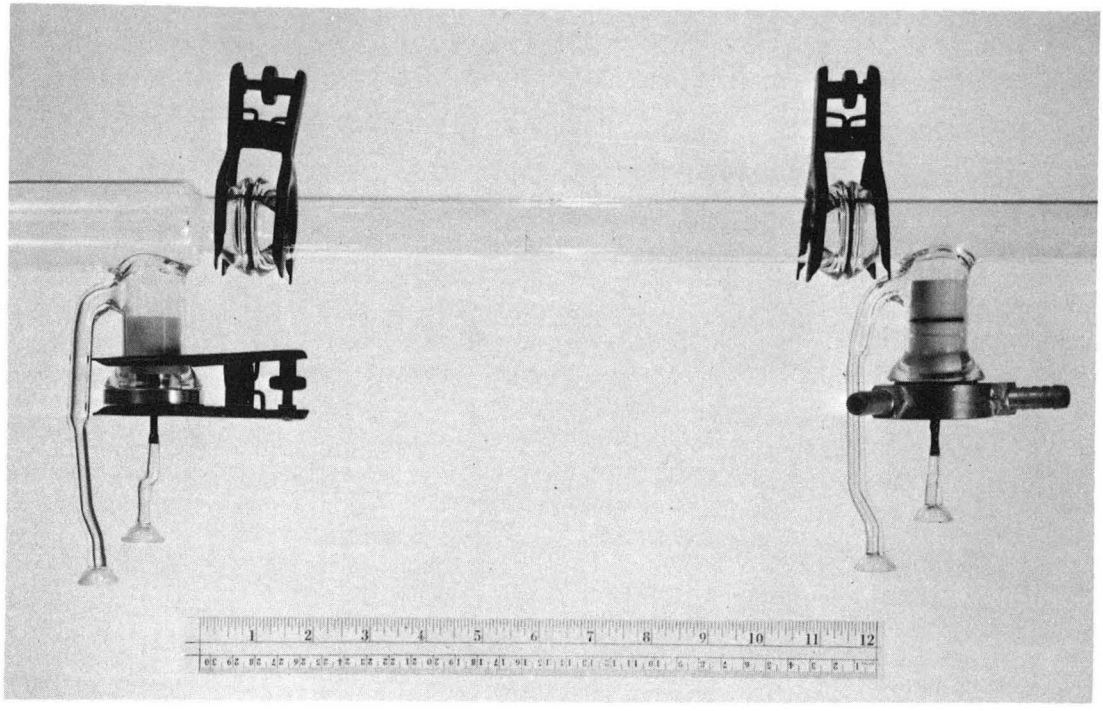

ZN-4965

Fig. 29. Close-up photograph of the central portion of reaction tube No. 3 showing the (a) non-water-cooled WHG fitting (located in the left WHG port), (b) water-cooled WHG fitting (located in the right WHG port), and (c) an intermediate glass section constructed to determine the recombination coefficient of atomic hydrogen on metals (vapor plated on the inside of the glass tube).

D. Experimental Procedure

The experimental procedure for the diffusion-tube or flow-tube experiments was essentially the same: the Wrede-Harteck gauge or gauges and possibly the thermocouple probe were turned on and their signals individually monitored on one of the three signal channels present in the two Speedomax recorders running at identical chart speeds. The behavior of the signal(s) was observed while definite changes were made to the system. Figure 30 schematically illustrates the typical response of a WHG and a thermocouple probe operated in a fast-flow tube to the following changes or "perturbations" of the system:

a. Letting gas into the high-vacuum (3 μtorr) system.
b. Adding a little more gas to the system at 70 torr pressure,
c. Turning on the 50-MHz discharge,
d. Turning off the discharge,
e. Turning on the discharge a second time,
f. Turning off the discharge,
g. Adding a little impurity gas,
h. Turning on the discharge to the same power level previously used,
i. Turning off the discharge,
j. Stopping the input of impurity gas,
k. Stopping the input of the main gas.

The regions between some of the points a to k also illustrate some of the features consistently seen in the experiments:

Before a: low noise level and long-term drift in the high-vacuum system; c to d and e to f: decay in the measured atom concentration when the discharge is operated continuously;

f to g: drift in the baseline during normal operation.

With the diffusion-tube experiments, the primary variable was the location of the catalytic probe. With the flow-tube experiments, the primary variable was the impurity concentration in the flowing gas stream. A discussion of the above gauge responses as well as others is given in Sec. V of this report.

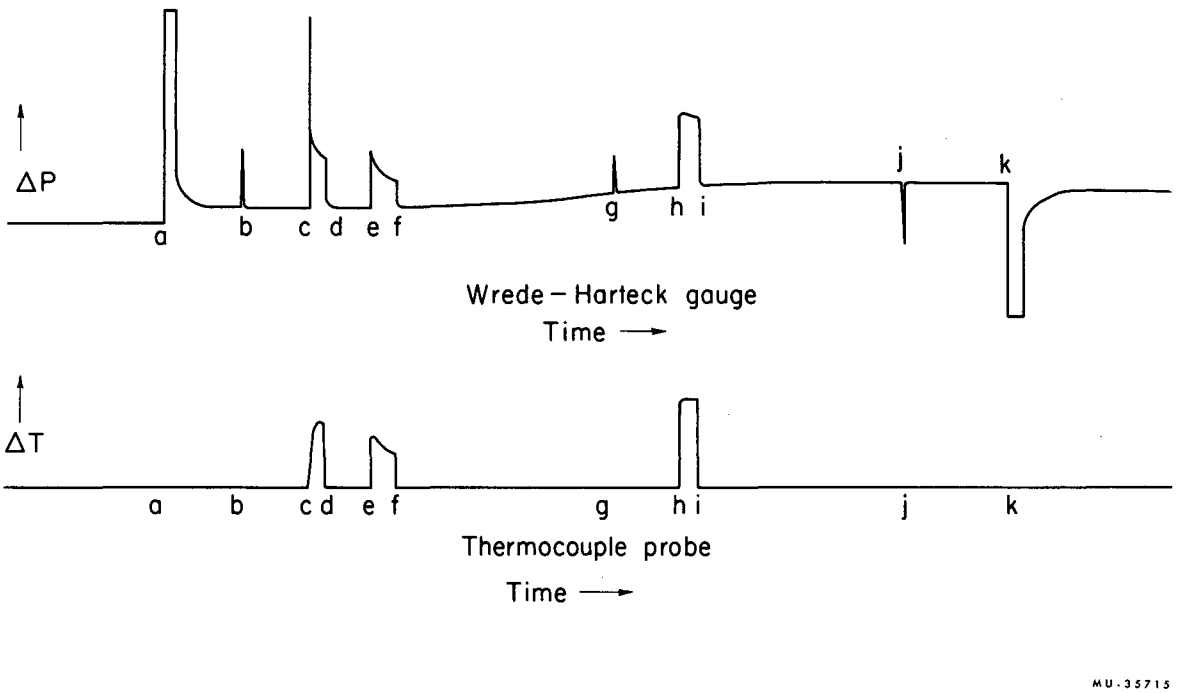

Fig. 30. Schematic diagram showing the output signals of a Wrede-Harteck gauge and a thermocouple probe resulting from various perturbations in the flow system.

III. DESIGN, CONSTRUCTION, AND OPERATION OF A WREDE-HARTECK GAUGE (WHG)

A. Introduction

In this section are described the design, construction, operation, and testing of two similar Wrede-Harteck gauges (abbreviated as WHG throughout the report).

Recently, Cambel[96] has commented on the disuse into which the WHG method has now fallen, whereas Kaufman[38] has pointed out that, even though the gauge has been in use since its discovery in 1928,[43-51] an experimental re-examination of its operation is still necessary to resolve some fundamental questions. Unfortunately, the purpose of the overall work was not to thoroughly characterize the WHG, but instead to study the gas- and surface-phase kinetics of hydrogen atoms in a low-pressure system. As a consequence of this research, however, a few new experimental tests were made to determine the applicability of the WHG for the measurement of hydrogen-atom concentrations. These experiments were not thorough nor are they the final word on the subject.

After a brief comparison of the WHG with other devices of measurement (Sec. III.B) and summary of the theory of the WHG (Sec. III.C), a description of the experimental unit and the results from experimental tests are first given (Secs. III.D and E) and then discussed (Sec. III.F).

B. Comparison with Other Methods of Measurement

Cambel,[96] Kaufman,[38] Jennings,[97] Steacie,[98] Ingram,[99] Minkoff,[100] and others have already discussed the relative merits of the various techniques for determining atom concentrations in a gaseous low-pressure system. In the interests of brevity, a thorough description is not repeated here.

The various methods can be divided into six categories, according to the nature of the physical quantity measured:

a. Mass: Wrede gauge (direct, absolute, perturbs slightly); Mass spectrometer (direct, relative, perturbs slightly); Pressure in known volume (direct, absolute, perturbs slightly)

b. Paramagnetism: Electron-spin resonance (direct, relative, does not perturb); Nuclear magnetic resonance (direct, relative, does not perturb); Gross paramagnetism (direct, relative, perturbs slightly)

c. Spectroscopic: Visible and uv emission (indirect, relative, does not perturb); Visible and uv absorption (indirect, relative, perturbs slightly)

d. Optical: Surface recombination luminescence (indirect, relative, perturbs)

e. Thermal: Catalytic probe (indirect, relative, perturbs greatly); Isothermal calorimeter (indirect, relative, perturbs greatly); Thermal conductivity (indirect, relative, perturbs greatly)

f. Chemical: Chemiluminescent titration (indirect, relative, perturbs); Mirror deposition or removal (indirect, relative, perturbs); Chemical titration (indirect, relative, perturbs) Inorganic solid reduction (indirect, relative, perturbs)

These classifications are not meant to be rigorous. The comments in parentheses refer to whether the method measures a direct or indirect property of the atoms, whether the technique is relative or absolute (without calibration), and the extent to which the apparatus perturbs the atoms (i.e., removal, activation, or deactivation). Other important non-listed characteristics of the methods are: response time; sensitivity; accuracy; stability; reproducibility; linearity; cost of apparatus; simplicity of construction, use, and mathematical interpretation; sensitivity to the external environment; temperature, concentration, and pressure range of application; and suitability for multiple-point measurements.

The most popular methods at present involve ESR, isothermal calorimeter, and chemiluminescent titration. With the expected advent of tunable lasers, the use of absorption spectroscopy in the visible region will probably become much more common, especially when relative measurements only are needed. Investigators have ignored the WHG in recent years,

a fact which is surprising in view of the increased availability of accurate, sensitive, and stable diaphragm differential micromanometers[83,101] and the very large expense of an ESR spectrometer.

C. Theory of the Wrede-Harteck Gauge

The operation of the WHG is based upon the difference in the rate of effusion of atoms and their parent molecules through a Knudsen hole—a hole whose dimensions are small compared with the mean free path or either the atoms or the molecules. A low-pressure system that takes advantage of this difference to determine the atom concentration consists of: (a) a thin membrane with one or more effusion holes, (b) a metal surface highly catalytic for the recombination of the atoms (Fig. 31) and (c) a differential micromanometer (Figs. 22 and 23). Atoms and molecules in the partly dissociated gas on the left side of the effusion membrane effuse through the membrane to the right chamber where recombination of the atoms on the catalytic surface leaves only molecules to effuse out. Under steady-state conditions, there is no mass flow through the holes in either direction, since there is no atom or molecule sink in the right chamber. As a result of these processes a differential pressure is produced, and measured by the differential micromanometer.

An easier way to understand the operation of the WHG is to consider it as a composite of two transducers, one to convert the atom concentration into a differential pressure, and the other to convert the differential pressure into an electrical signal (Fig. 32). The measurement of the differential pressure can be done as accurately as present techniques allow.[83] The accurate conversion of the atom concentration into a differential pressure is more difficult and requires further study.

According to kinetic theory, the molar flux of atoms or molecules striking the hole area is given by

$$R = \frac{c\bar{v}}{4} \text{ species/cm}^2\text{-sec} \qquad \text{(III-1)}$$

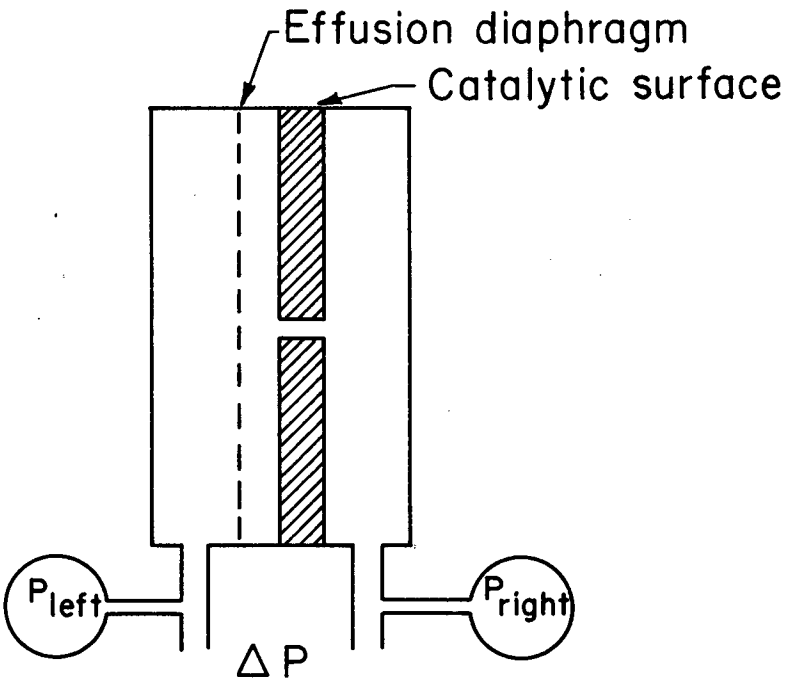

MU-35716

Fig. 31. Schematic drawing of a Wrede-Harteck gauge atom-concentration-to-pressure transducer. The catalytic surface is on the right-hand side of the effusion diaphragm.

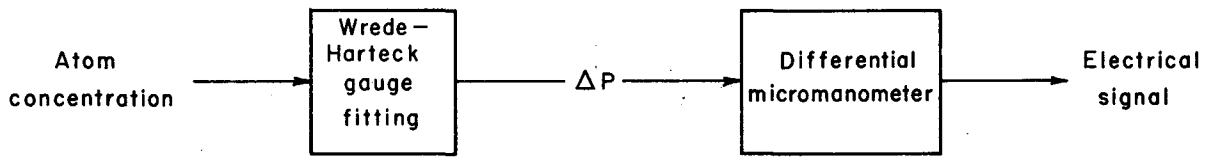

MU-35717

Fig. 32. Schematic diagram of the Wrede-Harteck gauge as a composite transducer.

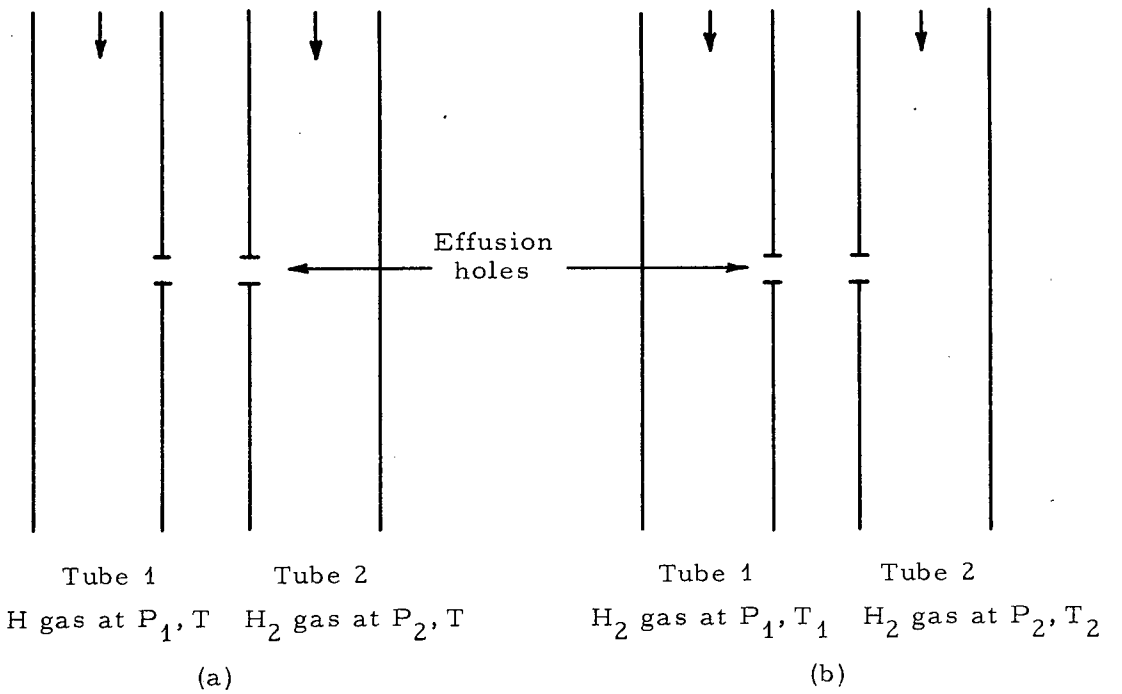

Fig. 33. Schematic drawing flow tubes (each with an effusion hole) used to demonstrate the principles of a Wrede-Harteck gauge: (a) isothermal system, and (b) non-isothermal system.

where c is the species concentration in species/cm^3 and $\bar{v}$ is the average velocity of the species,

$$\bar{v} = \left[\frac{8kT}{\pi m}\right]^{1/2} , \qquad \text{(III-2)}$$

k is the Boltzmann constant, and m is the mass of the species. The average velocities of H, H_2, O, O_2, N, N_2, OH, and H_2O at 298°K are given in Table I. The species concentration is obtained from the Loschmidt number, $2.687 \cdot 10^{19}$ species/cm^3 at STP,

$$c = 9.656 \cdot 10^{18} \frac{P(mm)}{T(^oK)} \quad \text{species/cm}^3 . \qquad \text{(III-3)}$$

As an example, the species concentrations at pressures of 0.1 and 1 torr and 298°K are $3.240 \cdot 10^{15}$ and $3.240 \cdot 10^{16}$ species/cm^3, respectively.[102]

When there are both atoms and molecules of hydrogen on the left side but molecules only on the right side of the effusion diaphragm, the no-mass-flow condition can be stated as

$$\left.\frac{m_1 c_1 \bar{v}_1}{4}\right|_L + \left.\frac{m_2 c_2 \bar{v}_2}{4}\right|_L = \left.\frac{m_2 c_2 \bar{v}_2}{4}\right|_R . \qquad \text{(III-4)}$$

This can be simplified by means of Eq. (III-2) and

$$c = \frac{P}{kT} \qquad \text{(III-5)}$$

to

$$P_{1L}\sqrt{\frac{m_1}{T_L}} + P_{2L}\sqrt{\frac{m_2}{T_L}} = P_{2R}\sqrt{\frac{m_2}{T_R}} \qquad \text{(III-6)}$$

or

$$\frac{P_{1L} + \sqrt{2}\, P_{2L}}{\sqrt{T_L}} = \frac{\sqrt{2}\, P_{2R}}{\sqrt{T_R}} \qquad \text{(III-7)}$$

Table I. Average velocity ($\bar{v}$) and mean free path (L_m) for selected atoms and molecules at 298°K.

Species	$\bar{v}$ (10^4 cm/sec)	L_m at 0.1 torr (mm)	L_m at 5 torr (μ)
H	25.0	1.07	21
H_2	17.7	0.93	18
O	6.25	0.99	20
O_2	4.44	0.54	11
N	6.68	0.92	18
N_2	4.75	0.50	10
OH	6.06	--	--
H_2O	5.92	0.34	7

where 1 = atoms, 2 = molecules, L = left-hand side (Fig. 31) and R = right-hand side. For isothermal operation Eq. (III-7) simplifies to the standard formula

$$P_{1L} = \Delta P \frac{\sqrt{2}}{\sqrt{2} - 1} = 3.42\ \Delta P, \qquad \text{(III-8)}$$

where ΔP (the measured differential pressure) $= (P_{1L} + P_{2L}) - P_{2R}$.

The requisite conditions for the practical use of the WHG are:

a. The diameter of the effusion hole(s) must be less than one-tenth the mean free path of the species involved in the measurement;
b. The probability that an atom passes unrecombined from the catalytic chamber back through the effusion diaphragm is small;
c. The response time is reasonable fast (< 1 min);
d. The differential micromanometer is sensitive, accurate, and stable;
e. The operation of the WHG is not subject to unusual environmental conditions.

Condition a. governs the ambient pressure range within which the WHG can be effectively used. Listed in Table I are the approximate mean-free paths at 298°K and 0.1 and 5 torr for H, H_2, O, O_2, N, N_2, and H_2O.[40,102-104] The higher the ambient pressure, the thinner the effusion diaphragm and the smaller the effusion hole must be. Teflon membranes approximately 0.0013-cm thick are commercially available[105] and, with the advent of laser drilling, it certainly seems possible that effusion membranes containing varying numbers of holes of different diameters can be made available commercially at very low cost. An opaque but removable coating on the membrane should facilitate drilling.

Conditions b and a determine whether the WHG can be made to measure the <u>absolute</u> concentration of atoms in a system, and can be written mathematically

$$\gamma A \gg \frac{d^2}{4} N \ , \qquad \text{(III-9)}$$

a formula which states that the probability of an atom's recombining within the chamber is proportional to both the amount of catalytic surface and its efficiency (γ is the recombination coefficient), and is very much greater than the probability of an atom's effusing back through the effusion hole(s). The term N is the number of effusion holes, d is the hole diameter, and A is the catalytic surface area. For A = 1 cm^2, γ = 0.01, N = 10, and d = 0.005 cm (values typical of my WHG's) condition b was

$$0.01 \gg 0.0002 \quad .$$

A relatively fast response time is not as critical as some of the other conditions, but its achievement facilitates measurement and multiplies the used of the WHG. The fastest response time to date, 1 sec, was obtained with the elegant design of Sharpless et al. for detecting nitrogen atoms at a pressure of 1 torr.[51] The mathematical statement of the condition is

$$P_1 = P_o \, e^{-t/\tau} \qquad \text{(III-10)}$$

where τ, the response time, is

$$\tau = \frac{4V_o}{N \frac{d^2}{4} \bar{v}} \qquad \text{(III-11)}$$

The term V_o is the residual volume in the catalytic chamber, $\bar{v}$ is the average velocity of the species, and the other quantities are previously given [Eq. (III-9)]. The key experimental variables are the residual volume V_o, which should be minimized, and the number of holes N, which should perhaps be maximized within the limits of Eq. (III-9). For my WHG's N = 10, d = 0.005 cm, and the residual volume $V_o \approx 10$ cm^3 (crude estimate), which estimate gives a theoretical response time of approximately 8 sec (a value which is within a factor of two of the experimentally observed one). Very little care was taken to drastically minimize this quantity, so the performance of my WHG's was gratifying.

A differential micromanometer isn't a prerequisite for a WHG, but its use definitely minimizes the error associated with one's taking the small difference between two large quantities if two absolute manometers are used (Poole has emphasized this point).[106] I used a specially designed electronics system in conjunction with a commercial capacitive pressure transducer to give readings of good accuracy and sensitivity.[83] The new Barotron (MKS Instruments, Inc.), the best commercial differential micromanometer available today (in my opinion), is an excellent substitute for the one above if time is more important than expense.[101]

The above paragraphs complete the summary of previous work and derivations of the equations characterizing the behavior of the WHG. I now give closer consideration to some other aspects of the use of these equations in practical systems.

I always had some difficulty in developing the proper intuitive "feel" for the effusion process of gases and the operation of the WHG, so I usually used Eq. (III-4) as a partial substitute for physical intuition. One particular example, though, did help to clarify matters somewhat.

Consider Fig. 33(a), which shows two separate flow tubes for pure atomic and pure molecular hydrogen, each containing one effusion hole of identical area. The gas flow in each tube is maintained at equal pressure and temperature. When all other effects are ignored, the mass and molar fluxes of H and H_2 through the holes are [from Eqs. (III-1, III-2, and III-5)]

$$\text{molar flux H} = P_1 \left[\frac{1}{2\pi kTm_1}\right]^{1/2} \qquad \text{(III-12)}$$

$$\text{mass flux H} = P_1 \left[\frac{m_1}{2\pi kT}\right]^{1/2} \qquad \text{(III-13)}$$

$$\text{molar flux } H_2 = P_2 \left[\frac{1}{2\pi kTm_2}\right]^{1/2} \qquad \text{(III-14)}$$

$$\text{mass flux } H_2 = p_2 \left[\frac{m_2}{2\pi kT}\right]^{1/2} \qquad \text{(III-15)}$$

The relative mass and molar flux ratios for $m_2 = 2\,m_1$ and $P_1 = P_2$ are

$$\frac{\text{mass flux H}}{\text{mass flux } H_2} = \frac{1}{\sqrt{2}}$$

$$\frac{\text{molar flux H}}{\text{molar flux H}_2} = \sqrt{2} \quad .$$

The condition for the operation of a WHG, no mass flux, can be simulated here by decreasing the pressure of the molecular hydrogen by a factor of $1/\sqrt{2}$, i.e., $P_2 = P_1/\sqrt{2}$. The new relative mass and molar flux ratios are now

$$\frac{\text{mass flux H}}{\text{mass flux H}_2} = 1$$

$$\frac{\text{molar flux H}}{\text{molar flux H}_2} = 2 \quad ,$$

and the differential pressure, $\Delta P = P_1 - P_2$, between the left and right tubes is

$$\Delta P = (1 - 1/\sqrt{2})\, P_1 = \frac{\sqrt{2} - 1}{\sqrt{2}}\, P_1 \quad , \qquad \text{(III-16)}$$

a formula identical to Eq. (III-8). On the basis of this result, the very first sentence of Sec. III can be restated: The operation of the WHG is based on the difference in the relative mass and molar fluxes of atoms and their parent molecules effusing through a Knudsen hole.

Another similar example effectively illustrates the problem of thermal effusion. Consider the same two flow tubes, but with molecular hydrogen as the flowing gas in each tube. The pressure in both tubes is identical, $P_1 = P_2$, but the temperature in the left tube is twice that of the right, $T_1 = 2\,T_2$ [Fig. 33(b)]. The relative mass flux ratio, which equals the relative molar flux ratio, is

$$\frac{\text{mass flux } H_2 \text{ in 1}}{\text{mass flux } H_2 \text{ in 2}} = \left(\frac{T_2}{T_1}\right)^{1/2} = \frac{1}{\sqrt{2}} \quad .$$

The no-mass-flux condition can be simulated by a decrease of the molecular hydrogen pressure in tube 2 by a factor of $1/\sqrt{2}$: $P_2 = P_1/\sqrt{2}$. Now both the relative-mass and molar-flux ratios are unity

mass flux ratio = molar flux ratio = 1.

The differential pressure $\Delta P = P_1 - P_2$ is the same as before,

$$\Delta P = \frac{\sqrt{2} - 1}{\sqrt{2}} \; P_{1_{H_2}} .$$

Therefore, the response of the WHG is identical when (a) the gas in the tube 1 is either completely dissociated, or (b) at twice the temperature of tube 2 and not dissociated.

For small temperature differences, $\Delta T = T_L - T_R$, $\Delta T/T_R \ll 1$, Eq. (III-7) simplifies from

$$\Delta P = \frac{\sqrt{2} - 1}{\sqrt{2}} P_{1L} + P_{2R} \left[\left(\frac{T_L}{T_R} \right)^{1/2} - 1 \right] \qquad \text{(III-17)}$$

to

$$\Delta P = \frac{\sqrt{2} - 1}{\sqrt{2}} \; P_{1L} + P_{2R} \cdot \frac{\Delta T}{2T_R} \qquad \text{(III-18)}$$

where $(\sqrt{2} - 1)/\sqrt{2} = 3.42$. If it is assumed that the differential pressure ΔP is so small that the total pressure on both sides is about the same, $\approx P_{2R}$

$$\frac{\Delta P}{P} = 3.42 \; \frac{P_{atoms}}{P} + \frac{\Delta T}{T} \qquad \text{(III-19)}$$

where P_{atoms}/P is the mole fraction of atoms in the gas stream. For atom mole fractions of 0.001 and 0.01, the temperature differentials producing identical differential pressures are only $2^{\circ}C$ and $20^{\circ}C$, respectively, at $298^{\circ}K$. Such small temperature differences can be caused by the heat from an electrical discharge or from the recombination of atoms on the catalyst within the WHG. This fact reduces the accuracy of measurements at extremely low atom-concentration levels.

Equation (III-6), simplified for the isothermal case, can also be used as the basis for deriving the behavior of a WHG when more than one type of atom is present in the main gas stream. Consider a system

consisting of H_2, H, O, and H_2O in the main gas stream (left side of Fig. 31) all effusing through the membrane, the H and the O recombining to produce only H_2 or H_2O on the catalytic side of the membrane. In this system two separate mass balances must be made, one for the total hydrogen in the system and another for the total oxygen,

$$P_{HL} + \sqrt{2}\, P_{H_2L} + \frac{2}{3\sqrt{2}} P_{H_2O_L} = \sqrt{2}\, P_{H_2R} + \frac{2}{3\sqrt{2}} P_{H_2O_R} \qquad \text{(III-20)}$$

$$4\, P_{O_L} + \frac{16}{3\sqrt{2}} P_{H_2O_1} = \frac{16}{3\sqrt{2}} P_{H_2O_R} \,. \qquad \text{(III-21)}$$

The correct total mass balance is given by the sum of these equations. Simplifying with the relations, $P_{H_2L} = P_{total_L} - P_{O_L} - P_{H_L} - P_{H_2O_L}$, $P_{H_2R} = P_{total_R} + P_{H_2O_R}$, and $\Delta P = P_{total_L} - P_{total_R}$, I obtained the following surprising result:

$$\Delta P = \frac{\sqrt{2} - 1}{\sqrt{2}} \left(P_{H_L} + P_{O_L} \right) \,. \qquad \text{(III-22)}$$

This result implies that the WHG, when operated with such a system, measures the <u>total</u> atom concentration of the system, and can be generalized even for such radicals as OH and CH_3.

If the notation

(species 1, species 2, species,.../species 1, species 3, species 4,...)

is used to denote the species assumed to exist on either side of the effusion membrane (represented by the slash), with the convention that the catalyst is on the right side of the slash, the following formulas analogous to (III-8) or (III-22) are obtained.

<u>System</u>	<u>Formula</u>
(H, H_2/H_2)	$\Delta P = 0.293\, P_H$
(O, O_2/O_2)	$\Delta P = 0.293\, P_O$

System	Formula
$(N, N_2/N_2)$	$\Delta P = 0.293\ P_N$
$(Cl, Cl_2/Cl)$	$\Delta P = 0.293\ P_{Cl}$
$(Br, Br_2/Br_2)$	$\Delta P = 0.293\ P_{Br}$
$(I, I_2/I_2)$	$\Delta P = 0.293\ P_I$
$(H_2, O, H_2O/H_2, H_2O)$	$\Delta P = 0.293\ P_O$
$(H, H_2, O, H_2O/H_2, H_2O)$	$\Delta P = 0.293\ (P_H + P_O)$
$(OH, H_2, H_2O/H_2, H_2O)$	$\Delta P = 0.144\ P_{OH}$
$(CH_3, CH_4, H_2/CH_4, H_2)$	$\Delta P = 0.151\ P_{CH_3}$
$\left(\frac{H, He, Ne, Ar, Kr}{H_2, He, Ne, Ar, Kr}\right)$	$\Delta P = 0.293\ P_H$
$(H, H_2, O, OH, H_2O/H_2, H_2O)$	$\Delta P = 0.293\ (P_H + P_O) + 0.144\ P_{OH}$
$(N, NH_3, H_2/NH_3, H_2)$	$\Delta P = 0.464\ P_N$
$(Cl, HCl, H_2/HCl, H_2)$	$\Delta P = 0.405\ P_{Cl}$

Except for the simple atom-molecule system and the $(H, H_2, O, H_2O/H_2, H_2O)$ system, which result is fortuitous, most of the systems listed are not too useful. These formulas serve to illustrate that the WHG, even though it is an aboslute measurement device for ideal binary systems, is still generally nonspecific and cannot distinguish among individual atoms or radicals in a complex mixture as can an ESR spectrometer.

During the experiments, one spurious effect was observed. Water and HCL, when added to the gas stream in the absence of a discharge, caused a measurable and sometimes large reading in the WHG which decayed extremely showly once it reached its peak level. When added to a hydrogen gas stream, nonpolar gases such as oxygen or nitrogen failed to exhibit this behavior. This effect may be attributable to a nonequilibrium nonconserving effusion process. Experimental curves illustrating it are shown in Sec. III.D.

D. Design and Construction of the Wrede-Harteck Gauge

After I made several attempts to convert the atom concentration into a pressure differential by means of a WHG fitting, I finally developed a model that worked well in the system. The unit was closely related to the one constructed by Sharpless, Clark, and Young[51] but differed in three important respects: (a) it was mounted external to the differential-micromanometer pressure transducer, (b) it was water cooled, and (c) it had an easily replaceable effusion-hole diaphragm.

Shown in Figs. 34 and 35, it consisted of: a solid copper base with an O-ring groove, an electroplated nickel end, a hole for a Kovar-to-glass joint, and a water-cooled region; a Teflon sleeve; and an effusion membrane of 1/2-mil Teflon.[105] Three to two hundred holes per diaphragm were drilled with a 2-mil bit in a jeweler's drill. When examined under a stereo microscope, the holes were found to be of uniform size and cleanly cut.

The "WHG fitting," as the base-diaphragm-sleeve assembly was called, fitted into a glass "WHG port," shown in Figs. 26 and 36. A Pyrex O-ring joint (No. 25) was used and a 3-mm hole, defined as the "WHG port hole," was made in the glass wall. Two O-ring grooves of different depths were machined into the Teflon sleeve (to minimize the equilibration of pressure between the two sides of the micromanometer). Only one groove, which depended on the variation in the i.d. of the Pyrex joints, was used at a time. In this way, the WHG fittings were very easily interchanged between the various reaction tubes.

A non-water-cooled WHG fitting was made prior to the above water-cooled one. An aluminum base and nickel end piece were used instead of the nickel-electroplated copper base (Fig. 34). The micromanometer signal drifted as a result of the heat liberated by the atoms recombining on the nickel surface, so the unit was soon replaced.

As the WHG worked well, I have no suggestions to improve the design of the fitting and port. If faster response is desired, the necessary changes can be made to the pressure transducer and the Kovar-to-glass fitting to minimize the resuidal volume. I tried making holes with

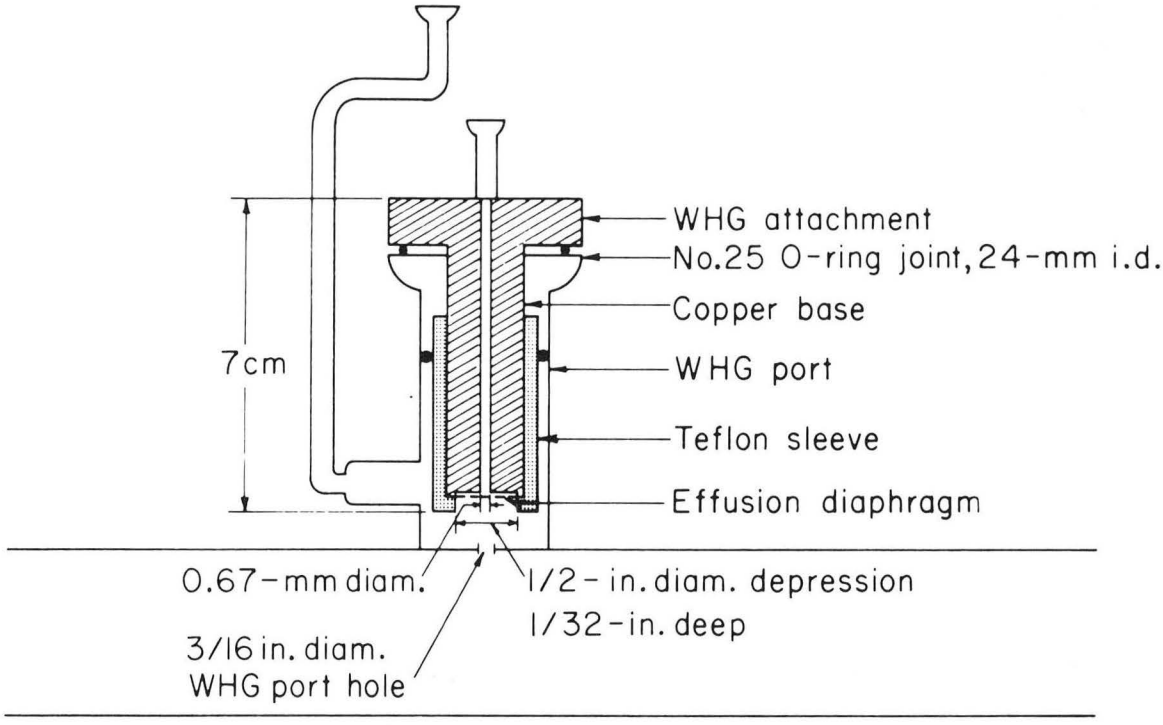

Fig. 34. Schematic drawing of the WHG fitting, the WHG port, and the WHG port hole.

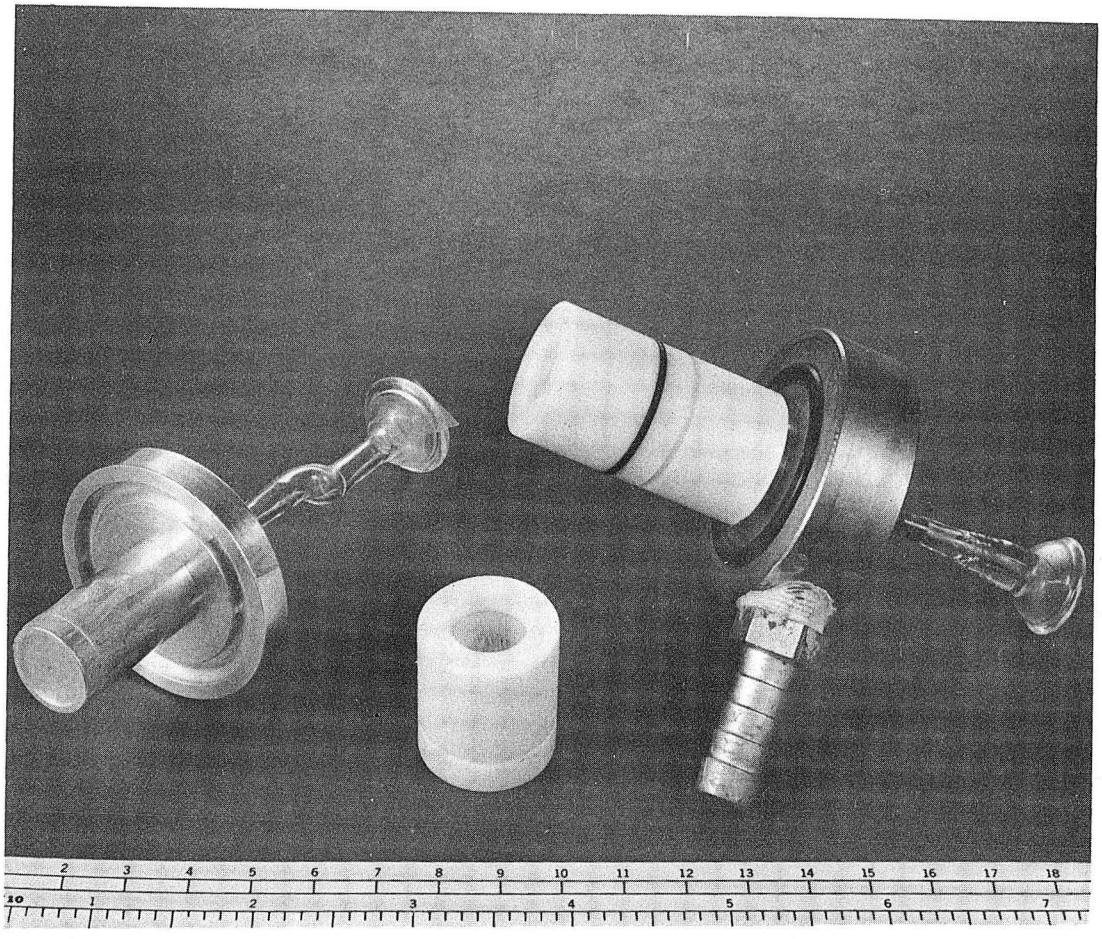

ZN-4929

Fig. 35. Photograph of a disassembled non-water-cooled WHG fitting (left and center) and an assembled water-cooled WHG fitting (right).

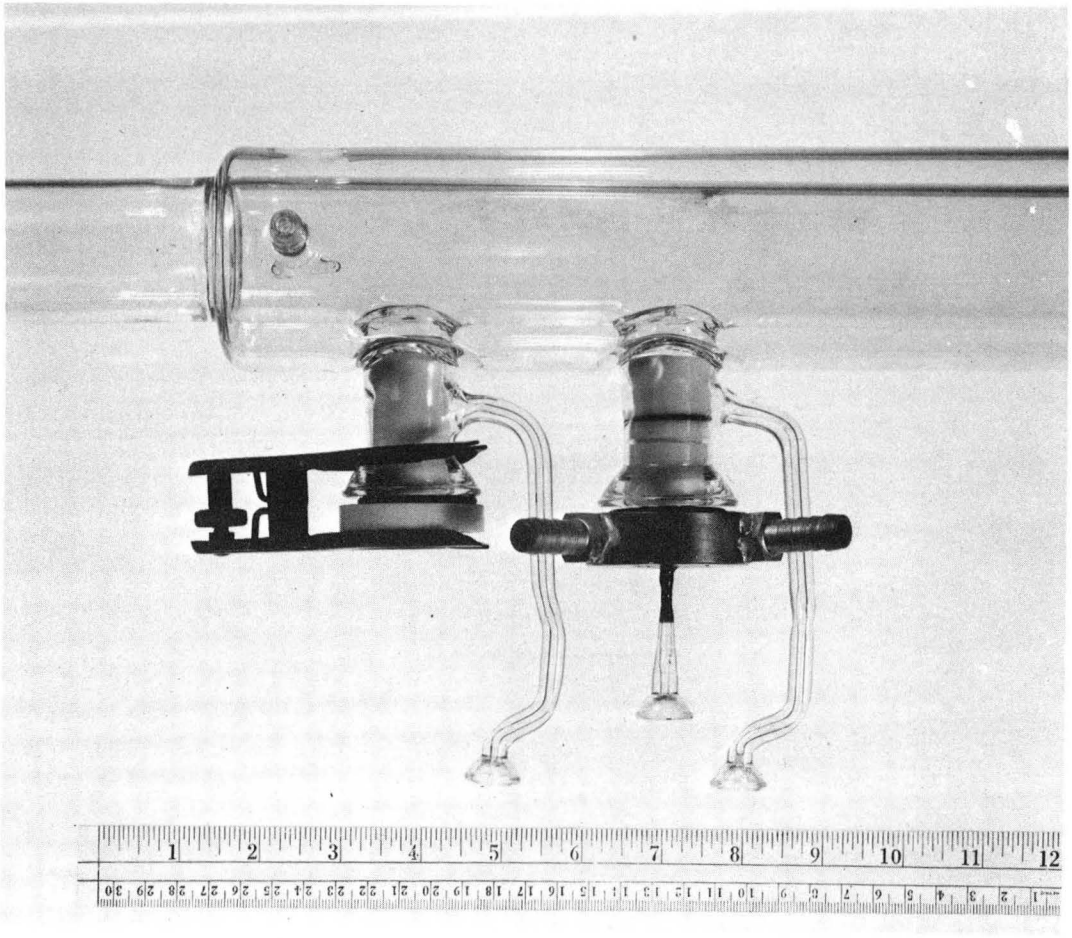

ZN-4915

Fig. 36. Close-up photograph of reactor zone of reaction tube No. 1 showing two WHG ports, a Teflon plug (left), and a water-cooled WHG fitting (right).

a cold or hot electrolytically sharpened tungsten point, an abrasive jet of fine dust particles, and a Tesla coil. The holes produced by the cold tungsten point were acceptable, but the others weren't. As a Q-switched high-intensity laser was not available, I could not determine if its use would provide the best method to conveniently produce many uniform and extremely small holes.

I never tried to use the gauge at any temperatures other than ambient. Though thermal-effusion effects are present at either temperature extreme, the operating limits of the gauge can probably be extende by 100°C in either direction with the proper insulation and thermal regulation.

E. Some tests of the Wrede-Harteck Gauge

During the experiments, the absolute accuracy of the WHG was tested in two ways. In the first test, the temperature of the cooling water was changed at varying rates and the WHG response at a given pressure was determined. Providing that the temperature of the gas on either side of the effusion membrane was known and that thermal accomodation across the membrane was slow, this technique was a convenient method for proving that the WHG could in principle measure the absolute atom concentration in a low-pressure system.

The second test was actually the first of a planned series of measurements on two WHG's in close proximity with varying ratios of hole size and number. This series was not carried out because of a lack of time. In the only test performed, one gauge had a split membrane and exposed nickel surface while the other had an effusion membrane containing ten 2-mil holes.

Tables II and III and Figs. 37 to 41 show the results of these tests. With the thermal measurements, the predicted WHG response calculated from the temperature of the surroundings and of the water stream passing through the WHG was about twice the measured response. Since the temperature of the nickel surface was lower than that of the water stream and some thermal accommodation probably occurred across the effusion membrane, this result was understandable.

Table II. Measured and calculated thermal effusion data.[a]

T (°C)	Calculated P(mtorr)	Measured P(mtorr)
7.8	1.20	0.44
7.0	1.10	0.40
4.0	0.63	0.35
28.7	3.90	2.20
12.0	1.70	0.88
22.1	3.00	1.40
2.5	0.34	0.29
11.8	1.60	0.87
7.8	1.10	0.43
3.6	0.49	0.21
5.8	0.80	0.31
8.8	1.20	0.47
15.1	2.10	0.86
13.7	1.90	0.59
3.0	0.41	0.16
6.3	0.86	0.39
1.4	0.19	0.27
11.4	1.60	0.66
16.3	2.20	1.00
10.3	1.40	0.54
6.0	0.82	0.48

[a]Wrede-Harteck gauge No. 1 with WHG fitting No. 1. DLR micromanometer No. 1, signal attenuation factor = 0.02 and recorder output setting = 3.00 turns. P = 79 mtorr.

Table III. Measured Wrede-Harteck gauge signal ratios.[a]

P(mtorr)	Measured ratio
17	1.20
37	1.20
	1.20
	1.30
52	1.50
	1.50
55	1.40
	1.40
	1.65
230	2.20
	2.30
340	2.30
	2.50
	2.70
590	3.8
	4.0
970	5.7
	6.6

[a]Ratio of response of WHG No. 2 (10-hole effusion diaphragm) to response of WHG No. 1 (split diaphragm, nickel catalytic surface exposed). Small amount of oxygen added to hydrogen gas stream to increase the yield of atoms. Gauges located about 8 cm apart.

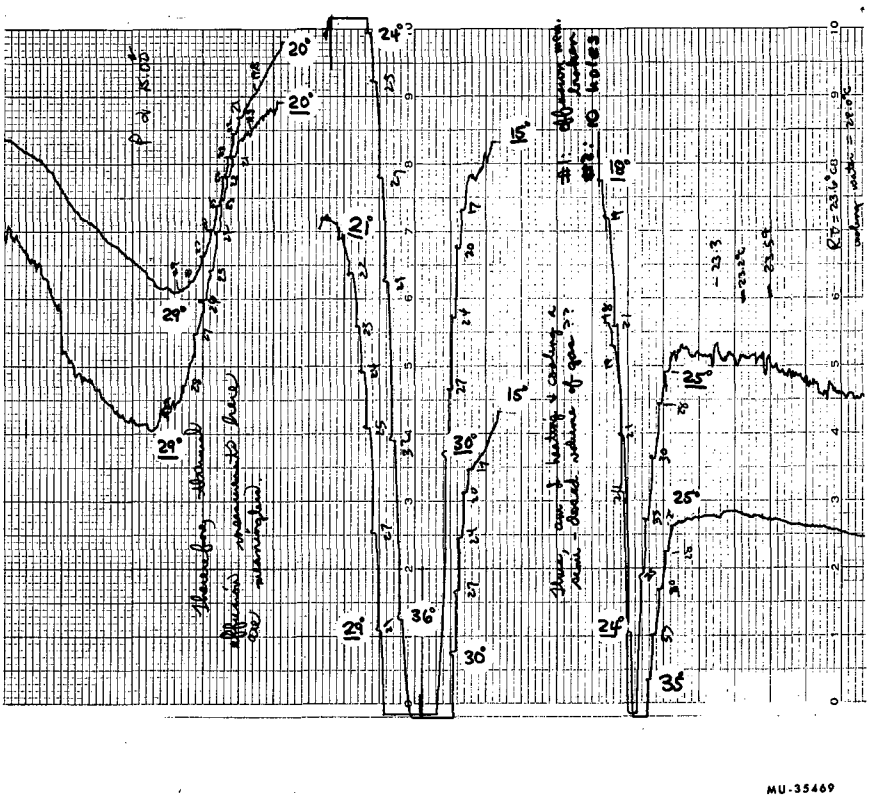

Fig. 37. Response of water-cooled WHG No. 1 (split diaphragm, 0.54 mtorr full scale) and WHG No. 2 (10 holes, 0.50 mtorr full scale) to identical changes (assumed) in the water temperature. These curves demonstrate the disturbing influence of thermal effusion on a WHG. P = 56 mtorr and t = 20 sec/small div (right to left). (March 30, 1965).

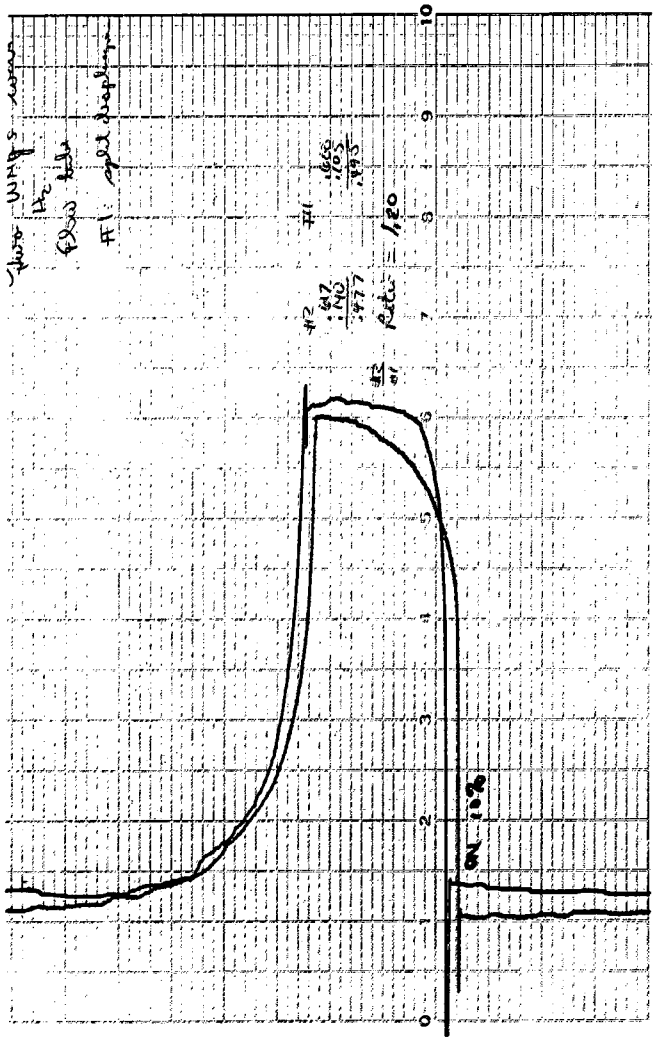

MU-35507

Fig. 38. Response of water-cooled WHG No. 1 (split diaphragm, 0.50 mtorr full scale) and WHG No. 2 (10 holes, 0.62 mtorr full scale) to identical changes (assumed) in atom concentration. The ratio of the gauge responses is 1.20, which indicates that a WHG may not be an absolute device even at low pressures. P = 17 mtorr and t = 20 sec/small div (right to left). (April 2, 1965).

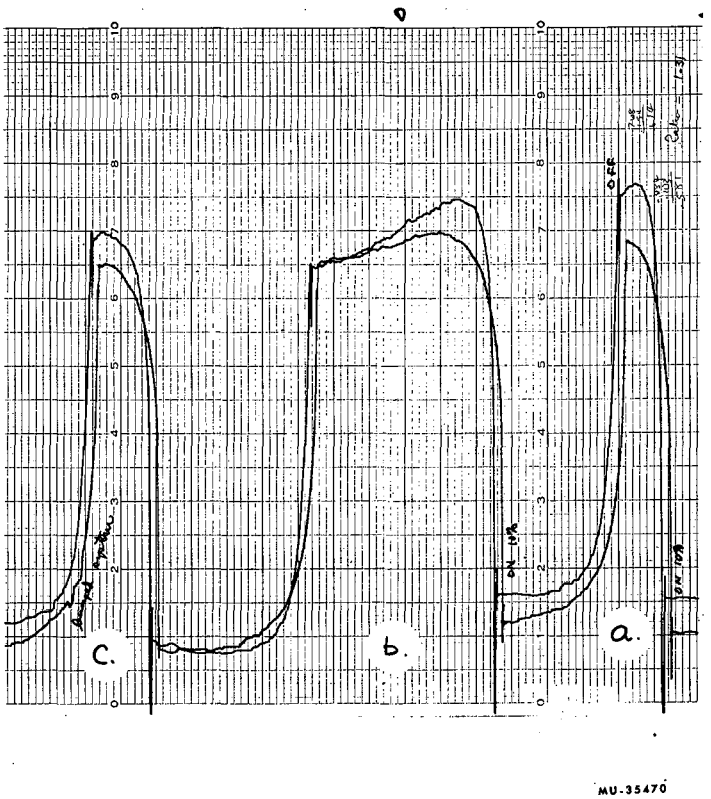

Fig. 39. Response of water-cooled WHG No. 1 (split diaphragm, 0.50 mtorr full scale) and WHG No. 2 (10 holes, 0.62 mtorr full scale) to identical changes (assumed) in atom concentration. The ratio of the gauge responses is (a) 1.30, (b) 1.20, and (c) 1.20, which indicates that a WHG may not be an absolute device even at low pressures. P = 37 mtorr and t = 20 sec/ small div (right to left). (April 2, 1965).

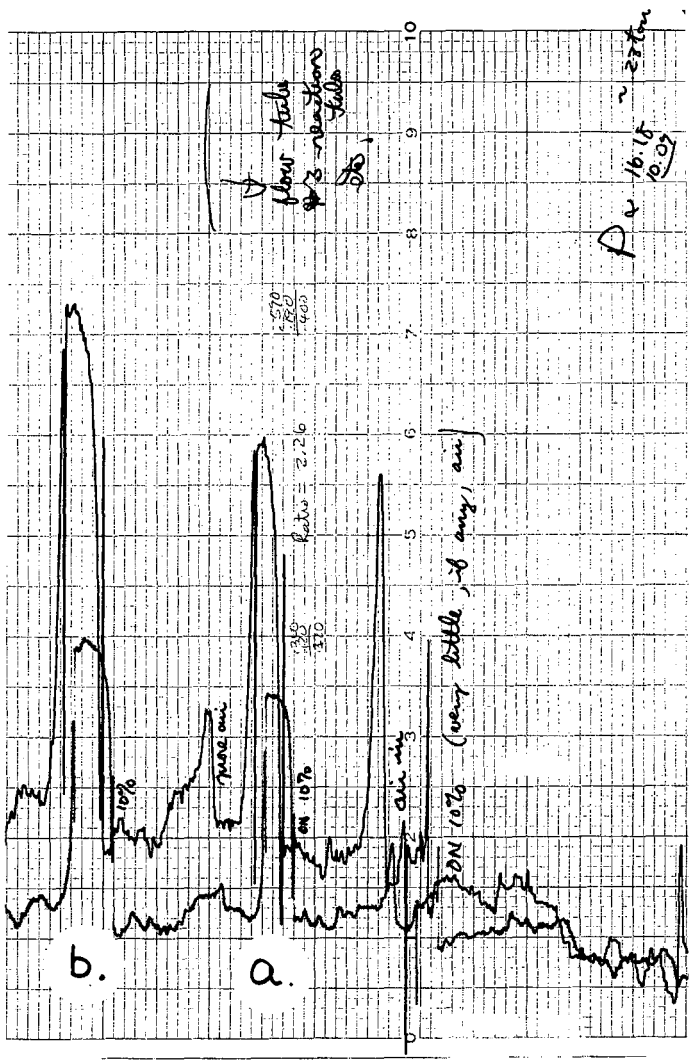

Fig. 40. Response of water-cooled WHG No. 1 (split diaphragm, 0.50 mtorr full scale) and WHG No. 2 (10 holes, 0.62 mtorr full scale) to identical changes (assumed) in atom concentration. The ratio of the gauge responses is (a) 2.30 and (b) 2.20, which indicates that the 0.66-mm effusion hole in WHG No. 1 is too large. P = 230 mtorr and t = 20 sec/small div (right to left). (April 2, 1965).

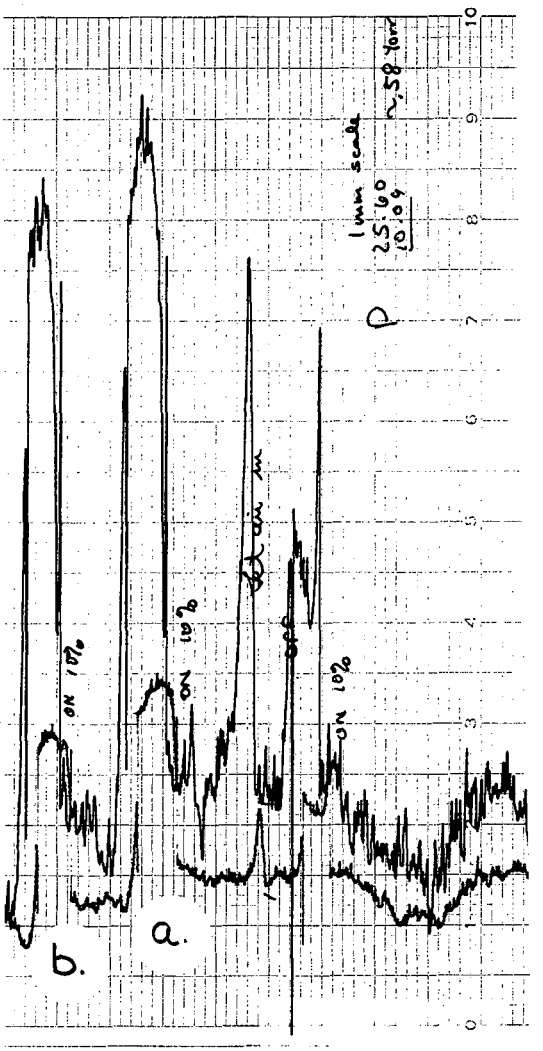

Fig. 41. Response of water-cooled WHG No. 1 (split diaphragm, 0.53 mtorr full scale) and WHG No. 2 (10 holes, 0.63 mtorr full scale) to identical changes (assumed) in atom concentration. The ratio of the gauge responses is (a) 3.8 and (b) 4.0, which indicates that the 0.66-mm effusion hole in WHG No. 1 is too large. P = 590 mtorr and t = 20 sec/small div (right to left). (April 1, 1965).

Although the signal from the 10-hole WHG produced by an arbitrary amount of hydrogen atoms was always greater than the one from the split-membrane WHG, the large reading of the latter unit at total pressures below 100 mtorr was surprising. The ratio of the two readings decreased at lower pressures until it was 1.2 at 17 mtorr. In view of the possibility of atom recombination on the nickel catalytic surface of the WHG with the split membrane, this ratio was very reasonable. As the pressure was increased toward 1 torr, both WHG's continued to respond measurably, but the ratio increased rapidly to a value of 6.0 at 0.97 torr. This increase was easily explainable by the circumstance that the diameter of the hole in the split-membrane WHG was 13 times the diameter of the effusion holes, and thus failed to satisfy the molecular-flow requirements at higher pressures. What was surprising was that this ratio wasn't any larger than 6.0. The significance of these observations is discussed in Sec. III.F.

Figures 42 to 44 show other characteristics of the WHG.

F. Discussion

The Wrede-Harteck gauge has always been assumed to be absolute, but no thorough set of experiments has ever proved this assumption. This is somewhat understandable since it is difficult to prove that the WHG is absolute by a comparison with nonabsolute methods of atom measurement and detection. The only reasonable approach is either for one to compare it to the change in total pressure in a small closed system, or else to thoroughly investigate each variable associated with its function as an absolute measurement device.

This was an ambitious assignment and incidental to the main direction of my research. The WHG seemed to function well at least as a relative atom-concentration measurement device, and was adequate for my kinetic experiments with atomic hydrogen.

However, one of my two tests checking the absolute accuracy of the WHG gave a disturbing result. The fact that the split-membrane

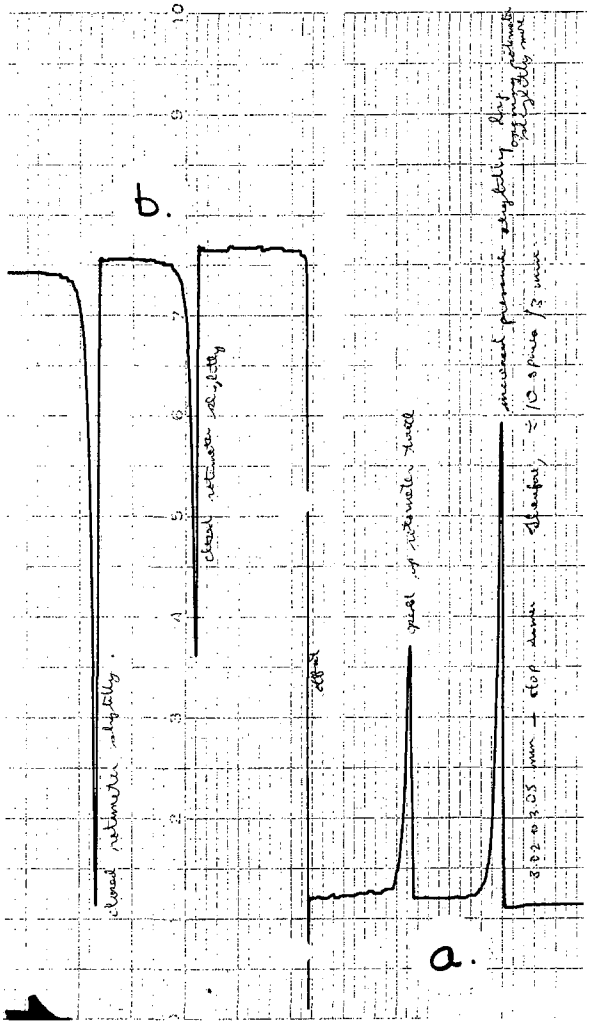

MU-35466

Fig. 42. Response of non-water-cooled WHG (about 100 holes, about 2.5 mtorr full scale) to (a) increased flow of hydrogen gas and (b) decreased flow of hydrogen gas. P = about 75 mtorr and t = 20 sec/small div (right to left). (November 26, 1964).

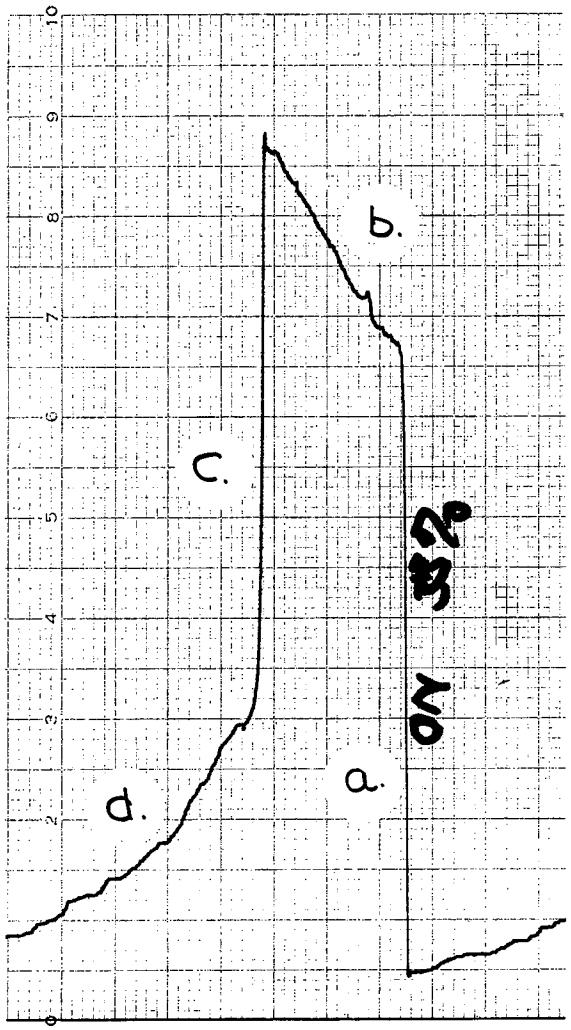

Fig. 43. Response of non-water-cooled WHG (about 100 holes) to the actions of (a) starting the microwave discharge, (b) heating the surrounding gas by the discharge, (c) stopping the discharge, and (d) allowing the surrounding gas to cool to room temperature. This curve illustrates why it is preferable to use low discharge powers and to locate the discharge far away from the WHG. P = about 75 mtorr and t = 20 sec/small div (right to left). (September 10, 1964).

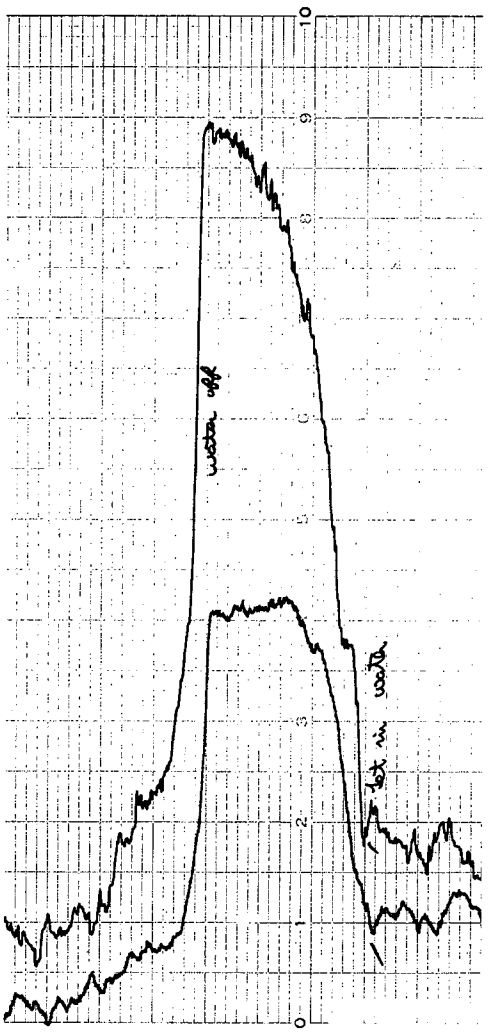

Fig. 44. Response of water-cooled WHG No. 1 (split diaphragm, 0.53 mtorr full scale) and WHG No. 2 (10 holes, 0.63 mtorr full scale) to identical changes (assumed) in the concentration of water added to the low-pressure hydrogen system. These curves suggest that water alters the effusion equilibrium within the WHG. P = 340 mtorr and t = 20 sec/small div (right to left). (April 1, 1965)

WHG produced a measurable signal at a pressure as high as 0.97 torr indicates that perhaps the main reason why a WHG might deviate from being an absolute gauge is that both sides act as concentration-to-pressure transducers. This is possible if the side that is supposed to measure the total pressure has constrictions in the glass or metal tubing that recombine atoms and act as a pseudo-WHG. The effect of this process is to decrease the overall differential pressure and thus to make the measured atom concentration lower than the actual one. Further tests should be made on the WHG to clear up this point.

G. Conclusions

a. A differential micromanometer and a WHG fitting have been constructed and are easily capable of detecting 0.06% hydrogen atom concentrations at a pressure of 75 mtorr.

b. The fitting is water cooled, located external to the pressure transducer, has easily replaceable effusion membranes, and can be quickly interchanged among several reaction tubes.

c. As a relative atom-concentration measurement device, the WHG works well.

d. A test involving two WHG's with different hole sizes has cast suspicion on the WHG as an absolute atom-concentration-measurement device.

e. At higher pressures, fluctuations in the total pressure level make it difficult for one to measure very small atom concentrations accurately.

f. The use of a laser may provide a convenient method for producing very small effusion holes in plastic films.

g. A needed study of the WHG would show if it is an absolute device.

IV. MATHEMATICAL THEORY OF FLOW AND DIFFUSION TUBES

A. Introduction

The mathematical theory of flow and diffusion tubes has been given by different authors.[1-8,22,29-42] As most of the derivations have been made for the specific experimental stiuation encountered, there have been no attempts, except the notable one by Dickens, Schofield, and Walsh,[22] to accumulate and systematize the various equations.

Since I also am adding to the already large number of equations, it is certainly appropriate at this time for me to repeat some of the derivations previously applied to a diffusion tube operated in the absence of three-body recombination reactions.

I have gone into considerable detail with the derivations and solutions in order that they may serve as reference calculations for future investigators. Cases C, D, E, F, F1, F2, G, J, L, and M are all new to the literature. The others have been derived by some of the various authors mentioned above.

Cases C, D, E, F, F1, F2, and G are essentially extensions of the calculations of Tsu and Boudart,[30] who made a definite improvement in the description of diffusion- and flow-tube systems by treating the discharge and reactor zones separately. These cases remove the divergence in the concentration in the limit of inactive discharge-zone walls, describe the situation when the recombination coefficients for the walls in the discharge and reactor zones are not the same, describe the case when the discharge zone is of finite length, and finally, give the explicit mathematical statement for their observation that the magnitude of the atom sink is proportional to the area of the end plate. Equation (IV-69) is the boundary condition accidentally omitted from their paper.

Case L, the more general solution of Morgan and Schiff, is for when the atom flux to the catalytic probe is dependent on its catalytic efficiency.[39] Case J is a result for a similar but simpler situation.

I have used the dimensionless-group terminology and symbols developed by Dickens et al.[22] with only a few minor changes, principally in the definitions of δ and δ', which have been changed to ξ and ξ' solely on the basis of typewriter convenience. The terms δ and δ' still refer to the recombination of atoms on a surface, but are defined differently in this report.

B. Principal Equations

The basic equations governing the operation of an isothermal cylindrical reactor operated in the viscous-flow region are the conservation equations of mass and momentum:[107]

$$\frac{\partial \rho}{\partial t} + \nabla \cdot \rho \vec{v} = 0 \qquad \text{(IV-1)}$$

$$\frac{\partial \rho_i}{\partial t} = -\nabla \cdot \vec{n}_i + \vec{r}_i \qquad (i = 1, 2, 3, \ldots n) \qquad \text{(IV-2)}$$

$$\frac{\partial \rho \vec{v}}{\partial t} = -[\nabla \cdot \underset{\sim}{\Phi}] + \sum_{i=1}^{n} \rho_i \vec{g} \qquad \text{(IV-3)}$$

The terms $\underset{\sim}{\Phi}$ and $\vec{n}_i$ are the momentum and mass fluxes with respect to a coordinate system fixed in space,

$$\vec{n}_i = \rho_i \vec{v} + \vec{j}_i \qquad (i = 1, 2, 3, \ldots n) \qquad \text{(IV-4)}$$

$$\underset{\sim}{\Phi} = \rho \vec{v}\,\vec{v} + \underset{\sim}{\tau} + p\,\underset{\sim}{\delta} \qquad \text{(IV-5)}$$

$$\underset{\sim}{\tau} = -\mu\,[\nabla \vec{v} + (\nabla \vec{v})] + \left[\frac{2}{3}\mu - \kappa\right][\nabla \cdot \vec{v}]\,\underset{\sim}{\delta}$$

These equations, given above in their general vector ($\rightarrow$) and tensor ($\underset{\sim}{\ }$) forms, can be simplified with the following set of assumptions for an isothermal cylindrical reactor:

a. No mass flow in directions perpendicular to the z axis,

b. Symmetry in planes perpendicular to the axis,

c. No pressure gradients in directions perpendicular to the z axis,

d. Steady-state operation,

e. Negligible gravitational or other external forces.

Under the above five assumptions, the generalized mass, species, and momentum-conservation equations reduce to

$$\frac{\partial \rho v_z}{\partial z} + \frac{1}{r}\frac{\partial \rho r v_r}{\partial r} = 0 \qquad \text{(IV-7)}$$

$$\nabla \cdot \vec{j}_i + v_z \cdot \nabla \rho_i = r_i \qquad (i = 1, 2, 3, \ldots n) \qquad \text{(IV-8)}$$

$$\mu \nabla^2 v_z = \frac{\partial p}{\partial z} \quad . \qquad \text{(IV-9)}$$

The isothermal cylindrical reactor is typically operated in one of two ways: as a flow tube, [in which case Eqs. (IV-7) to (IV-9) all apply], or as a diffusion tube with no axial mass velocity $v_z = 0$ (in which case only the following species continuity equation is relevant),

$$\nabla \cdot \vec{j}_i = r_i \qquad (i = 1, 2, 3, \ldots n) \qquad \text{(IV-10)}$$

Since there is no creation of mass in a diffusion tube and since the pressure is constant,

$$\sum^{n} \vec{j}_i = 0 \qquad \text{(IV-11)}$$

$$\sum c_i = c = \text{constant} \qquad \text{(IV-12)}$$

$$\sum_i \nabla c_i = 0 \quad . \qquad \text{(IV-13)}$$

In Eq. (IV-7) each term can be separately set equal to zero and then integrated under the conditions that $v_z = 0$ at $z = L$ (end plate) and

$v_r = 0$ at $r = R$ for a diffusion tube, or $v_r = 0$ at $r = R$ and $\rho v_z = \rho_o v_{zo}$ (entering gas) at an arbitrary z for a flow tube. The results are

$$v_z = 0 \qquad \text{(diffusion tube)} \qquad \text{(IV-14)}$$

$$\rho v_z = \rho_o v_{zo} \qquad \text{(flow tube)} \qquad \text{(IV-15)}$$

where $\rho = \rho(z)$ and $v_z = v_z(z)$ for the flow tube.

For an ideal gas mixture, which is an excellent approximation for the gases and pressures used, the mass flux $\vec{j}_i$ becomes[107]

$$\vec{j}_i = \frac{c^2}{\rho} \sum_{j=1}^{n} M_i M_j D_{ij} \nabla x_j \qquad (i = 1, 2, 3, \ldots n) \qquad \text{(IV-16)}$$

where D_{ij} are the multicomponent diffusion coefficients for a n-component mixture, with $D_{ii} = 0$ by definition. For a two-component ideal gas mixture, D_{12} is identical to the binary diffusion coefficient $\mathcal{S}_{12}$

$$D_{12} = \mathcal{S}_{12} = D_{21} = \mathcal{S}_{21} \qquad \text{(IV-17)}$$

with the mass flux of components 1 and 2 given by

$$\vec{j}_1 = \frac{c^2}{\rho} M_1 M_2 \mathcal{S}_{12} \nabla x_2 \qquad \text{(IV-18)}$$

$$\vec{j}_2 = \frac{c^2}{\rho} M_1 M_2 \mathcal{S}_{12} \nabla x_1 \; . \qquad \text{(IV-19)}$$

For a ternary system, a binary diffusivity $\mathcal{S}_{im}$ defined by

$$\vec{n}_i = - cM_i \mathcal{S}_{im} \nabla x_i + \rho_i \vec{v} \qquad \text{(IV-20)}$$

reduces for trace components 1 and 2 in nearly pure 3 to the binary diffusion coefficients

$$\mathcal{D}_{1m} = \mathcal{D}_{13} \tag{IV-21}$$

$$\mathcal{D}_{2m} = \mathcal{D}_{23} \tag{IV-22}$$

so that

$$\vec{j}_1 = -cM_1\mathcal{D}_{13}\nabla x_1 \tag{IV-23}$$

$$\vec{j}_2 = -cM_2\mathcal{D}_{23}\nabla x_2 \quad . \tag{IV-24}$$

For a binary system consisting only of atoms and diatomic molecules, $2M_1 = M_2$, $-\nabla c_1 = \nabla c_2$, and the steady-state continuity equations for the diffusion tube reduce to the following equations (there is no mass flow, $\vec{j}_1 + \vec{j}_2 = 0$),

$$-\nabla \cdot \frac{2c\mathcal{D}_{12}\nabla c_1}{2c - c_1} = R_1 \tag{IV-25}$$

$$-\nabla \cdot \frac{c\mathcal{D}_{12}\nabla c_2}{c - c_2} = R_2 \quad , \tag{IV-26}$$

where R_1 and R_2 are the molar rates of production of species 1 and 2 per unit volume—$R_1 = r_1/M_1$.

For a ternary system consisting of atoms and diatomic molecules in nearly pure component 3, the continuity equations for species 1 and 2 are

$$-\nabla \cdot \mathcal{D}_{13}\nabla c_1 = R_1 \tag{IV-27}$$

$$-\nabla \cdot \mathcal{D}_{23}\nabla c_2 = R_2 \tag{IV-28}$$

The term R_1 represents the molar rate of atom loss in the cylindrical reactor due to chemical reactions that are not included as boundary conditions. In a complicated system such as a gaseous mixture containing atomic hydrogen, molecular hydrogen, water, nitric oxide, and atomic oxygen, the gas-phase reaction kinetics must be represented by a complicated equation involving zero-, first-, second-, and third-order rate expressions,

$$R_1 = \frac{-d\{H\}}{dt} = f(\{H\},\{H_2\},\{O\},\{O_2\},\{OH\},\{H_2O\},\{N\}, \text{ etc.}) \quad \text{(IV-29)}$$

If not already considered in the boundary conditions, the rate expressions for the loss of atoms due to recombination on the surfaces present must be also included in this equation.

Reaction expressions with zero-, first-, second-, and third-order rate terms simultaneously present are possible. Thus, if good kinetic data are desired, the cylindrical reactor must be operated under precisely known and controlled conditions in which all complicating features are minimized.

For the case of a binary system consisting of atomic and molecular hydrogen, the only reactions that contribute to the term R_1 are (a) second- or third-order three-body recombination reactions in the gas phase; (b) zero-, first-, or second-order recombination reactions on the surfaces present; and (c) a zero-order atom-production term

$$R_1 = k_{0g}\{H_2\} - k_{2g}\{H_2\}\{H\}^2 - k_{3g}\{H\}^3 - f(k_{0s}, k_{1s}\{H\}, k_{2s}\{H\}^2) \quad , \quad \text{(IV-30)}$$

where k is a reaction-rate constant and the subscripts 0, 1, 2, and 3 represent the order of the reaction term and g and s represent the gas and surface phases, respectively.

If the three-dimensional species-continuity equation for the cylindrical reactor is used, then the rate expressions involving surface recombination on the walls, end plate, or other surfaces are part of the boundary conditions and do not appear in R_1. Otherwise, if the one-dimensional equation is used, the recombination-rate expressions for the cylinder walls at least must be included in R_1.

C. Derivation of Boundary Conditions for a Catalytic Surface

The boundary conditions describing the flux and atom concentration at a catalytic surface can be derived from elementary kinetic theory. In a gaseous system, the molar flux per unit area of atoms crossing an arbitrarily chosen plane in the positive and negative directions is given by the formulas[5]

$$J_1^+ = 1/4\ c_1\bar{v}_1 + 1/2\ J_1 \qquad \text{(IV-31)}$$

$$J_1^- = 1/4\ c_1\bar{v}_1 - 1/2\ J_1\ , \qquad \text{(IV-32)}$$

where $\bar{v}_1$ is the mean random velocity and J_1 is the net molar flux of atoms per unit area

$$J_1 = J_1^+ - J_1^-\ . \qquad \text{(IV-33)}$$

For a binary system consisting of only atoms and diatomic molecules in a diffusion tube where there is no mass flux $\vec{j}_1$, the molar flux $\vec{J}_1 = \vec{j}_1/M_1$ has already been shown to be equal to

$$J_1 = \frac{2cD_{12}\nabla c_1}{2c - c_1}\ . \qquad \text{(IV-34)}$$

At a catalytic surface, a fraction γ of the atoms recombine. The net flux at the surface is therefore

$$J_1 = J_1^+ - (1-\gamma)J_1^+ = \gamma J_1^+ \qquad \text{(IV-35)}$$

and can be considered the definition of the recombination coefficient γ. Manipulation of the above formulas leads to the following result for the surface flux of atoms at a catalytic surface—

$$J_{1s} = -\frac{2cD_{12}}{2c-c_1}\ \nabla_s c_1 = \frac{\gamma}{1 - 1/2}\ 1/4\ c_1\bar{v}_1\ , \qquad \text{(IV-36)}$$

where s designates the surface. If $2c \gg c_1$ and $\gamma \ll 2$, this equation reduces to the commonly used linear form of the boundary condition,

$$J_{1s} \approx - D_{12} \nabla_s c_1 \approx 1/4 \gamma c_1 \bar{v}_1 \quad . \qquad \text{(IV-37)}$$

This equation holds only under the conditions of low atom concentration and a very noncatalytic surface. Another definition of the recombination coefficient γ is

$$\gamma = \frac{\frac{-d\{H\}}{dt} V}{1/4\, c_1 \bar{v}_1 S} = \frac{R_{1s} V}{1/4\, c_1 \bar{v}_1 S} \, , \qquad \text{(IV-38)}$$

where R_{1s} is the molar recombination rate for atoms on the catalytic surface and S/V is the surface-to-volume ratio of the reactor. This rate was given before as some function of zero-, first-, and second-order elementary reaction steps,

$$R_{1s} = f(k_{0s}, k_{1s}\{H\}, k_{2s}\{H\}^2) \quad . \qquad \text{(IV-39)}$$

For simple zero-, first-, and second-order recombination rates, the recombination coefficient takes the following forms:

$$\frac{S}{V} \gamma = \frac{k_{0s}}{1/4\, \bar{v}_1 \{H\}} = \frac{k_{0s}}{1/4\, \bar{v}_1 c_1} \qquad \text{(zero order)} \quad \text{(IV-40)}$$

$$\frac{S}{V} \gamma = \frac{k_{1s}}{1/4\, \bar{v}_1} \qquad \text{(first order)} \quad \text{(IV-41)}$$

$$\frac{S}{V} \gamma = \frac{k_{2s}\{H\}}{1/4\, \bar{v}_1} = \frac{k_{2s} c_1}{1/4\, \bar{v}_1} \qquad \text{(second order)} \quad \text{(IV-42)}$$

For a cylinder of circular cross section, S/V = 2/R. If the cylinder has a square cross section of sides 2a, the area-to-volume ratio is 2/a. Thus, the recombination coefficient for a first-order surface reaction taking place inside a cylinder of circular cross-section is, according to the above analysis,

$$\gamma = \frac{2k_{1s}R}{\bar{v}_1} \quad . \qquad \text{(IV-43)}$$

With reference to this formula, Shuler and Laidler have said:[180]

> "It may be noted that the appearance of R in this equation is due to the fact that k as ordinarily defined for a surface reaction
>
> $$\frac{-d\{H\}}{dt} = k\{H\}$$
>
> is not a true constant but is inversely proportional to R; the true heterogeneous first-order rate constant is k' = k V/S; γ on the other hand is a true constant."

D. Solutions

The continuity equation in the cylindrical reactor for atomic hydrogen can be solved for a wide variety of different boundary conditions, rate expressions R_1, and assumptions (Figs. 45 to 47). These are now considered starting with the simplest cases.

Case A. 1. One-dimensional case;

2. Binary system consisting of atomic hydrogen c_1 and molecular hydrogen c_2 with a binary diffusion coefficient D_{12};

3. Cylindrical reactor of circular cross section, radius R, and axial coordinate z;

4. Constant temperature throughout reactor;

5. Constant pressure throughout reactor;

6. No second- or third-order three-body recombination reactions in the gas phase;

7. Diffusion tube ($v_z = 0$);

8. Perfectly reflecting walls, i.e., walls with no catalytic activity;

9. Distance to end plate is L;

10. $c_1 = c_{1o}$ at $z = 0$;

11. Steady state;

12. Linear diffusion equation, i.e., $2c > c_1$ where $c_1 = \{H\}$ and $c = c_1 + c_2 = \{H\} + \{H_2\}$;

13. Circular end plate of radius R and first-order recombination coefficient γ';

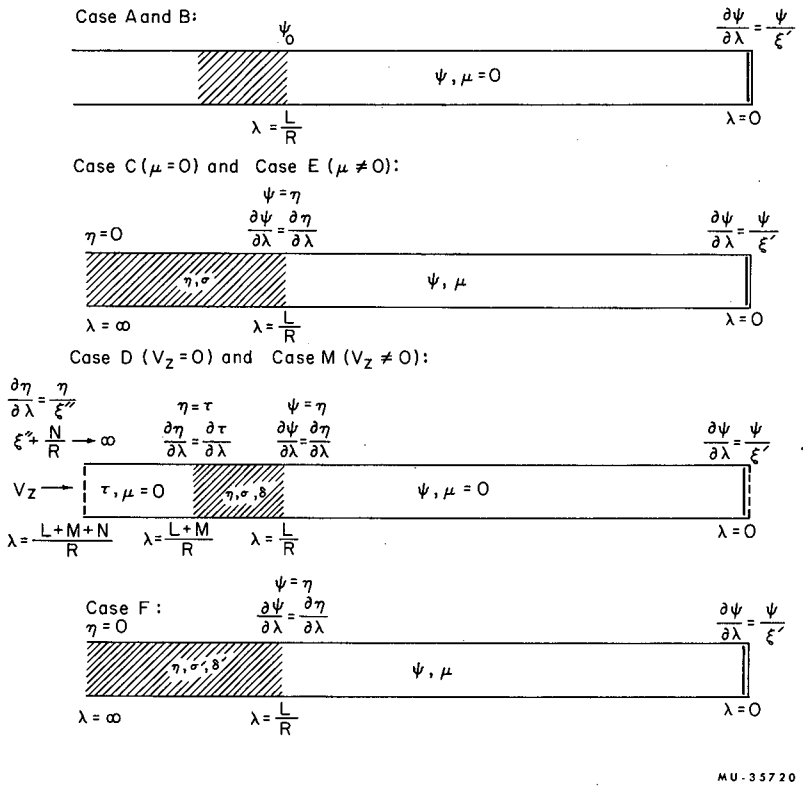

Fig. 45. Schematic drawing showing dimensionless groups and boundary conditions for Cases A to F and M.

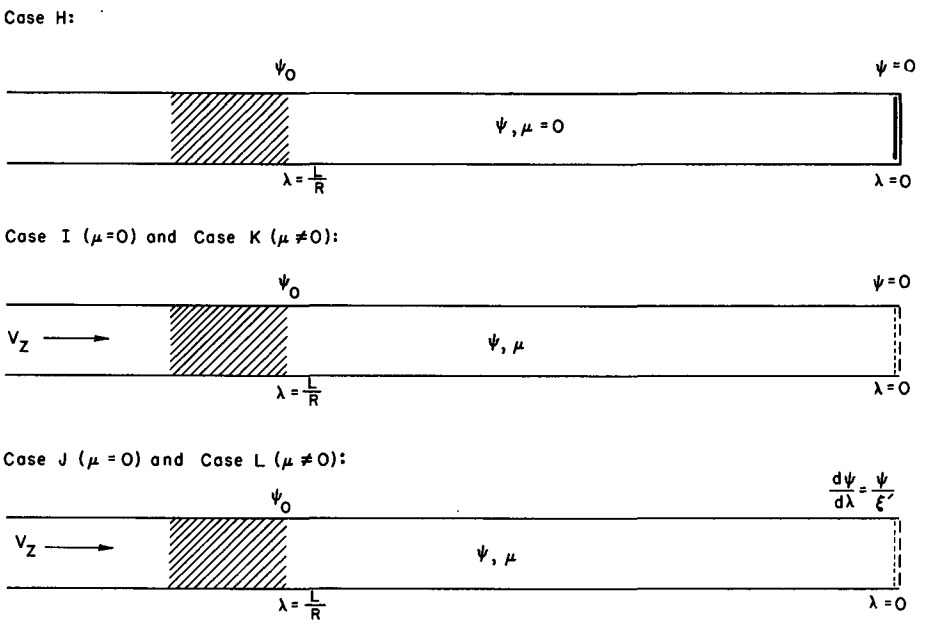

Fig. 46. Schematic drawing showing dimensionless groups and boundary conditions for Cases H to L.

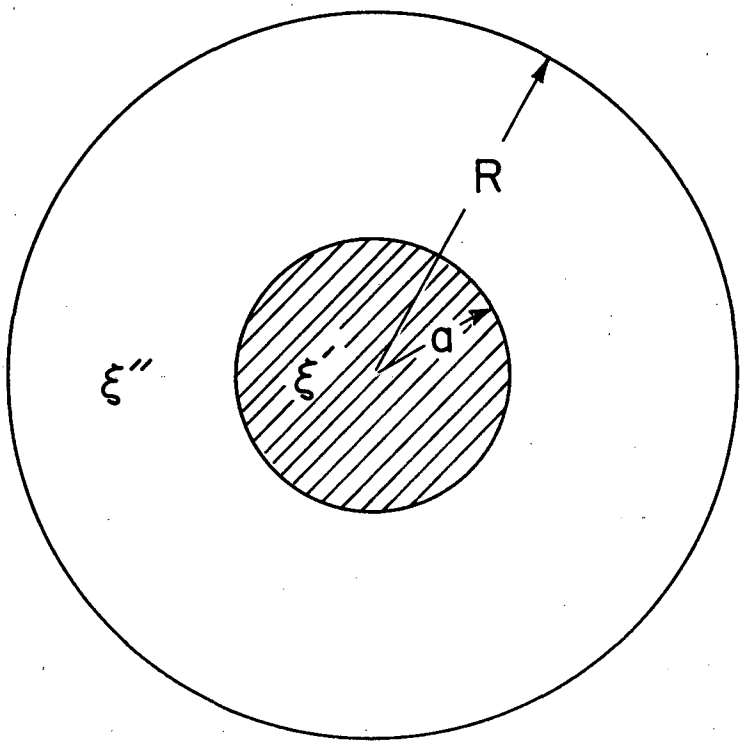

MU-35722

Fig. 47. Schematic drawing of the composite catalytic end plate. The inner disk is the more reactive of the two materials.

14. Flux per unit area to end plate at $z = L$ is $J_{1s} \approx -D_{12} \frac{\partial c_1}{\partial z} \approx 1/4\, \gamma'\, c_1 \bar{v}_1$;

15. The binary diffusion coefficient is constant throughout the tube.

In solving this problem, we can define the following dimensionless quantities:

$$\psi = \frac{c_1}{c} \tag{IV-44}$$

$$\lambda = \frac{L-z}{R} \tag{IV-45}$$

$$\xi' = \frac{4D_{12}}{\gamma' \bar{v}_1 R} (1 - 1/2\, \gamma) \quad . \tag{IV-46}$$

Thus the equation and boundary conditions for Case A are

$$\frac{d^2\psi}{d\lambda^2} = 0 \tag{IV-47}$$

$$\psi = \psi_o \qquad (\text{at } \lambda = \frac{L}{R}) \tag{IV-48}$$

$$\frac{d\psi}{d\lambda} = \frac{\psi}{\xi'}, \qquad (\text{at } \lambda = 0) \quad . \tag{IV-49}$$

The solution of Eq. (IV-47) is of the form $\psi = A\lambda + B$, which leads to the following result

$$\frac{\psi}{\psi_o} = \frac{\lambda + \xi'}{L/R + \xi'}, \tag{IV-50}$$

$$\frac{d\psi}{d\lambda} = \frac{\psi_o}{L/R + \xi'}, \tag{IV-51}$$

If $L/R \gg \xi'$, kinetic data cannot be obtained by measurement of the mass flux at the end plate [Eq. (IV-51)]. If $\lambda \approx \xi'$, it is still possible for one to obtain the value of ξ' by measuring ψ while varying

λ and then extrapolating the linear function to $\lambda = 0$. Under the conditions of the derivation of the above equations, the end plate must be fixed at $z = L$ and the distance $L - z$ between the end plate and the device measuring the atom concentration varied.

If $L/R \approx \xi'$, we can obtain the value of ξ' by varying the binary diffusion coefficient D_{12}. Since D_{12} is inversely proportional to pressure, the simple experimental procedure of taking data at different pressures provides the way of determining ξ'.

If $\xi' \gg L/R$, kinetic data cannot be obtained by measuring ψ because it is essentially constant throughout the tube. Since the end plate is very inactive, it is likewise useless for one to measure the mass flux.

Case B. Items 1 to 11 are the same as for Case A;

12. Nonlinear diffusion equation and end-plate boundary condition;

13. Same as Case A;

14. Flux per unit area to end plate at $z = L$ is

$$J_{1s} = - \frac{2cD_{12}}{2c-c_1} \frac{dc_1}{dz} \approx 1/4 \, \gamma' \, c_1 \bar{v}_1 ;$$

15. The binary diffusion coefficient is constant throughout the reactor.

On the basis of the same dimensionless quantities as were used for Case A, the diffusion equation and associated boundary conditions can be written

$$\frac{d}{d\lambda} \frac{d\psi/d\lambda}{2 - \psi} = 0 \qquad \text{(IV-52)}$$

$$\psi = \psi_o \qquad (\text{at } \lambda = L/R) \qquad \text{(IV-53)}$$

$$\frac{d\psi}{d\lambda} = \frac{\psi(2-\psi)}{2\xi'} \quad (\text{at } \lambda = 0) \quad . \qquad \text{(IV-54)}$$

The diffusion equation can be transformed to a linear form

$$\frac{d^2\phi}{d\lambda^2} = 0 \qquad \text{(IV-55)}$$

by the transformation

$$\frac{d\phi}{d\lambda} = \frac{d\psi/d\lambda}{2 - \psi} \qquad \text{(IV-56)}$$

or its equivalent representation

$$\phi = - \ln \left(1 - \frac{\psi}{2}\right) \quad . \qquad \text{(IV-57)}$$

According to Dickens et al.,[22] the solution of the above equation is

$$\psi = 2 - Ae^{\alpha z/R} \quad , \qquad \text{(IV-58)}$$

where

$$\alpha = \frac{2 - Ae^{\alpha L/R}}{2\xi'} \qquad \text{(IV-59)}$$

and

$$A = 2 - \psi_o \quad . \qquad \text{(IV-60)}$$

Case C. Items 1 to 7 are the same as for Case A;

8. Not applicable to discharge zone;

9. Same as Case A;

10. Not applicable;

11 to 15 are the same as for Case A;

16. Two distinct regions are considered mathematically: the discharge zone $z \leq 0$, and the reactor zone $z \geq 0$;

17. The boundary conditions at $z = 0$ are

$$c_1 \text{ (reactor zone)} = c_1' \text{ (discharge zone)}$$

$$-D_{12} \frac{dc_1}{dz} \text{ (reactor zone)} = -D_{12} \frac{dc_1'}{dz} \text{ (discharge zone)};$$

18. Number of moles of atoms generated uniformly per unit time per unit volume in the discharge zone is Q';

19. At $z = -\infty$, $c_1' = 0$;

20. Rate of loss of moles of atoms in discharge zone is given by a first-order rate expression $k_1'c_1'$.

The diffusion equations in the two zones subject to the above limitations are given by

$$D_{12}\frac{d^2c_1'}{dz^2} + Q' - k_1'c_1' = 0 \qquad \text{(discharge zone)} \quad \text{(IV-61)}$$

and

$$D_{12}\frac{d^2c_1}{dz^2} = 0 \qquad \text{(reactor zone)} \quad \text{(IV-62)}$$

where $R_1' = Q' - k_1'c_1'$ for the discharge zone and $R_1 = 0$ for the reactor zone. In addition to the dimensionless quantities defined for Case A, the following dimensionless groups are also useful:

$$\eta = \frac{c_1'}{c} \qquad \text{(IV-63)}$$

$$\frac{1}{\delta^2} = \frac{k_1'R^2}{D_{12}} \qquad \text{(gas-phase reaction)} \quad \text{(IV-64)}$$

$$\frac{1}{\delta^2} = \frac{R\gamma\bar{v}_1}{2D_{12}(1 - \gamma/2)} \approx \frac{R\gamma\bar{v}_1}{2D_{12}} \qquad \text{(surface reaction)} \quad \text{(IV-65)}$$

$$\sigma = \frac{Q'R^2}{cD_{12}} \quad . \qquad \text{(IV-66)}$$

Thus the diffusion equations and boundary conditions for Case C are

$$\frac{d^2\eta}{d\lambda^2} + \sigma - \frac{\eta}{\delta^2} = 0 \qquad \text{(discharge zone)} \quad \text{(IV-67)}$$

$$\frac{d^2\psi}{d\lambda^2} = 0 \qquad \text{(reactor zone)} \quad \text{(IV-68)}$$

$$\eta = 0 \qquad (\text{at } \lambda = \infty) \quad \text{(IV-69)}$$

$$\psi = \eta \qquad (\text{at } \lambda = L/R) \quad \text{(IV-70)}$$

$$\frac{d\psi}{d\lambda} = \frac{d\eta}{d\lambda} \qquad (\text{at } \lambda = L/R) \qquad \text{(IV-71)}$$

$$\frac{d\psi}{d\lambda} = \frac{\psi}{\xi'} \qquad (\text{at } \lambda = 0) \quad . \qquad \text{(IV-72)}$$

The solutions of these equations are of the form

$$\eta = Ae^{\lambda/\delta} + Be^{-\lambda/\delta} + \sigma\delta^2 \qquad \text{(IV-73)}$$

$$\psi = C\lambda + D \quad , \qquad \text{(IV-74)}$$

which, when the boundary conditions are applied, lead to the following results:

$$\eta = \sigma\delta^2 \left[1 - \frac{\delta e^{z/\delta R}}{\delta + \xi' + L/R}\right] \qquad (z \leqq 0) \qquad \text{(IV-75)}$$

$$\psi = \sigma\delta^2 \frac{\lambda + \xi'}{\delta + \xi' + L/R} \qquad (z \geqq 0) \qquad \text{(IV-76)}$$

$$\frac{d\psi}{d\lambda} = \sigma\delta^2 \frac{1}{\delta + \xi' + L/R} \qquad (z \geqq 0) \qquad \text{(IV-77)}$$

$$\psi_o = \sigma\delta^2 \frac{\xi' + L/R}{\delta + \xi' + L/R} \qquad (\lambda = L/R) \quad . \qquad \text{(IV-78)}$$

In these formulas, the terms σ, δ, and ξ' are unknown but L/R and λ can be measured independently. On the basis of these equations, the following experiments can be performed:

a. Two metals are compared at a fixed L/R: variation of ξ';
b. The pressure is changed: variation of ξ';
c. The discharge power is changed: variation of σ;
d. With fixed z/R, the metal is moved: variation of L/R;
e. With fixed L/R, the gauge is moved: variation of z/R;
f. The discharge-zone surface is changed: variation of δ.

Therefore it seems possible in principle to determine all or selected kinetic parameters in this system with carefully planned and

executed experiments. The condition that the discharge zone is very long must be met if these equations are to be used.

At this point it is useful for us to extimate the magnitudes of the quantities ξ', δ, and L/R. The first two dimensionless numbers have been given as

$$\xi' = \frac{4D_{12}}{\gamma' \bar{v}_1 R}(1 - 1/2\,\gamma') \qquad \text{(IV-46)}$$

$$\delta^2 = \frac{2D_{12}}{\gamma \bar{v}_1 R}(1 - 1/2\,\gamma) \quad . \qquad \text{(IV-65)}$$

A useful set of parametric values can be obtained from the work of Tsu and Boudart,[30] who gave

$$D_{12} = 2.3 \times 10^4 \text{ cm}^2/\text{sec}$$

$$\bar{v}_1 = 2.6 \times 10^5 \text{ cm/sec}$$

$$R = 1.9 \text{ cm}$$

$$\gamma' = 1 \text{ to } 10^{-6} \quad \text{(end plate)}$$

$$\gamma = 10^{-1} \text{ to } 10^{-6} \quad \text{(wall)} \quad .$$

An important assumption here is that the major loss of atoms in the discharge zone is due to first-order recombination on the relatively inactive walls. At low pressures and in the absence of impurities such as water, this may be a useful assumption. The numerical results for the dimensionless groups are

$\delta = 300$	if $\gamma = 10^{-6}$
$\delta = 100$	if $\gamma = 10^{-5}$
$\delta = 30$	if $\gamma = 10^{-4}$

$$\delta = 10 \quad \text{if } \gamma = 10^{-3}$$
$$\delta = 3 \quad \text{if } \gamma = 10^{-2}$$
$$\delta = 1 \quad \text{if } \gamma = 10^{-1}$$

$$\xi' = 1.9 \cdot 10^{5} \quad \text{if } \gamma' = 10^{-6}$$
$$\xi' = 1.9 \cdot 10^{4} \quad \text{if } \gamma' = 10^{-5}$$
$$\xi' = 1.9 \cdot 10^{3} \quad \text{if } \gamma' = 10^{-4}$$
$$\xi' = 190 \quad \text{if } \gamma' = 10^{-3}$$
$$\xi' = 19 \quad \text{if } \gamma' = 10^{-2}$$
$$\xi' = 1.8 \quad \text{if } \gamma' = 10^{-1}$$
$$\xi' = 0.093 \quad \text{if } \gamma' = 1$$

$$L/R = 5 \quad \text{for most reaction tubes}$$

$$\delta^2 = \frac{\xi'}{2} \quad \text{if } \gamma = \gamma' \qquad \text{(IV-79)}$$

$$\frac{4D_{12}}{\bar{v}_1 R} = 0.186$$

Case D. Items 1 to 15 are the same as for Case C;

16. Three distinct regions are considered mathematically: the reactor zone $0 \leqq \lambda \leqq L/R$; the discharge zone $L/R \leqq \lambda \leqq (L+M)/R$; and the buffer zone $(L+M)/R \leqq \lambda \leqq (L+M+N)/R$;

17. Same as for Case C;

18. Same as for Case C;

19. At $z = -N$, $-\frac{dc_1''}{d\lambda} = \frac{c_1''}{\xi''}$;

20. Same as for Case C;

21. The boundary conditions at $z = -M$ are similar in form to those given in Item 17 above.

Only two new dimensionless groups need to be defined—ξ'' is similar in form to ξ', with γ'' substituted for γ', and the other quantity τ is defined as

$$\tau = \frac{c_1''}{c} \quad . \qquad \text{(IV-80)}$$

The dimensionless equations and boundary conditions are the same as those given for Case C with the exception for Eq (IV-69). Three more boundary conditions must be given in addition to the three already listed:

$$\frac{d^2\tau}{d\lambda^2} = 0 \qquad \text{(auxiliary zone)} \qquad \text{(IV-81)}$$

$$\tau = \eta \qquad (\text{at } \lambda = (L+M)/R) \qquad \text{(IV-82)}$$

$$\frac{d\tau}{d\lambda} = \frac{d\eta}{d\lambda} \qquad (\text{at } \lambda = (L+M)/R) \qquad \text{(IV-83)}$$

$$-\frac{d\tau}{d\lambda} = \frac{\tau}{\xi''} \qquad (\text{at } \lambda = (L+M+N)/R) \quad . \qquad \text{(IV-84)}$$

The solutions of the reactor- and discharge-zone diffusion equations are of the same form as those given for Case C. The form for the solution of the auxiliary-zone diffusion equation is

$$\tau = E\lambda + F \quad . \qquad \text{(IV-85)}$$

With the boundary conditions applied, the solutions take the following form

$$\frac{\psi}{\sigma\delta^2} = \frac{\left[\lambda + \xi'\right]\left[\left(\xi'' + \frac{N}{R}\right)\sinh\left(\frac{M}{\delta R}\right) + \delta\cosh\left(\frac{M}{\delta R}\right) - \delta\right]}{H} \qquad \text{(IV-86)}$$

$$\frac{\eta}{\sigma\delta^2} = 1 - \frac{\delta\left(\xi'' + \frac{N}{R}\right)\cosh\left[\left(\lambda - \frac{L}{R} - \frac{M}{R}\right)/\delta\right] - \delta^2\sinh\left[\left(\lambda - \frac{L}{R} - \frac{M}{R}\right)/\delta\right]}{H}$$

$$+ \frac{\delta\left(\xi' + \frac{L}{R}\right)\left[\cosh\left(\lambda - \frac{L}{R}\right)/\delta\right] + \delta^2\sinh\left[\left(\lambda - \frac{L}{R}\right)/\delta\right]}{H} \qquad \text{(IV-87)}$$

$$\frac{\tau}{\sigma\delta^2} = \frac{\left[\lambda - \xi'' - \frac{L+M+N}{R}\right]\left[\delta - \left(\xi' + \frac{L}{R}\right)\sinh\frac{M}{\delta R} - \delta\cosh\frac{M}{\delta R}\right]}{H} \quad \text{(IV-88)}$$

where

$$H = \left[\left(\xi' + \frac{L}{R}\right)\left(\xi'' + \frac{N}{R}\right) + \delta^2\right]\sinh\frac{M}{\delta R} + \delta\left(\xi' + \xi'' + \frac{L}{R} + \frac{N}{R}\right)\cosh\frac{M}{\delta R} \quad . \quad \text{(IV-89)}$$

These equations can be easily simplified with the assumption that N/R is very large and that the catalytic surface at $\lambda = (L+M+N)/R$ is extremely inactive—$\xi'' + N/R \to \infty$. Therefore, Eq. (IV-86), the only one of interest, reduces to

$$\psi = \sigma\delta^2 \frac{\lambda + \xi'}{\xi' + \frac{L}{R} + \delta\coth\frac{M}{\delta R}} \quad , \quad \text{(IV-90)}$$

which can be further reduced, with the assumption that $M/\delta R$ is small, to

$$\psi = \sigma\delta^2 \frac{\lambda + \xi'}{\xi' + \frac{L}{R} + \frac{\delta^2 R}{M}} \quad . \quad \text{(IV-91)}$$

Case E. Items 1 to 20 are the same as for Case C;

21. Molar rate of atom loss to walls in reactor zone is given by the first-order expression, $k_1 c_1$.

The diffusion equation in the discharge zone is the same as for Case C. For the reactor zone, the diffusion equation is

$$D_{12}\frac{d^2 c_1}{dz^2} - k_1 c_1 = 0 \quad . \quad \text{(IV-82)}$$

The following new dimensionless group must be defined as

$$\frac{1}{\mu^2} = \frac{R\bar{v}_1}{2D_{12}}\frac{\gamma}{1 - \gamma/2} \approx \frac{\gamma R\bar{v}_1}{2D_{12}} \quad \text{(IV-93)}$$

and the dimensionless equations become

$$\frac{d^2\eta}{d\lambda^2} + \sigma - \frac{\eta}{\delta^2} = 0 \quad \text{(discharge zone)} \quad \text{(IV-94)}$$

$$\frac{d^2\psi}{d\lambda^2} - \frac{\psi}{\mu^2} = 0 \quad \text{(reactor zone)} \quad \text{(IV-95)}$$

with the boundary conditions the same as for Case C. The solutions are

$$\psi = \sigma\delta^2 \frac{(\xi'+\mu)e^{\lambda/\mu} + (\xi'-\mu)e^{-\lambda/\mu}}{(1+\delta/\mu)(\xi'+\mu)e^{L/\mu R} + (1-\delta/\mu)(\xi'-\mu)e^{-1/\mu R}} \quad \text{(IV-96)}$$

$$\frac{\eta}{\sigma\delta^2} = 1 - \frac{\delta(\xi'+\mu)e^{\lambda/\delta} - \delta(\xi'-\mu)e^{-\lambda/\delta}}{(\mu+\delta)(\xi'+\mu)e^{L/\mu R} + (\mu-\delta)(\xi'-\mu)e^{-L/\mu R}} \quad \text{(IV-97)}$$

If $\delta = \mu$, Case E reduces to the equation obtained by Tsu and Boudart,[C1]

$$\psi = \sigma\mu^2 \frac{(\xi'+\mu)e^{\lambda/\mu} + (\xi'-\mu)e^{-\lambda/\mu}}{2(\xi'+\mu)e^{L/\mu R}} \quad . \quad \text{(IV-98)}$$

IF λ/μ and $L/\mu R$ are small enough, a linear approximation to the exponentials can be made—

$$e^{\pm\lambda/\mu} \approx 1 \pm \frac{\lambda}{\mu} \qquad e^{\pm L/\mu R} \approx 1 \pm \frac{L}{\mu R} \quad \text{(IV-99)}$$

Other useful results are

$$\psi_o = \sigma\delta^2 \frac{(\xi'+\mu)e^{L/\mu R} + (\xi'-\mu)e^{-L/\mu R}}{(1+\delta/\mu)(\xi'+\mu)e^{L/\mu R} + (1-\delta/\mu)(\xi'-\mu)e^{-L/\mu R}} \quad \text{(IV-100)}$$

$$\psi_o = \sigma\mu^2 \frac{(\xi'+\mu)e^{L/\mu R} + (\xi'-\mu)e^{-L/\mu R}}{2(\xi'+\mu)e^{L/\mu R}} \qquad (\delta = \mu) \quad \text{(IV-101)}$$

$$\frac{\psi}{\psi_o} = \frac{(\xi'+\mu)e^{\lambda/\mu} + (\xi'-\mu)e^{-\lambda/\mu}}{(\xi'+\mu)e^{L/\mu R} + (\xi'-\mu)e^{-L/\mu R}} \quad \text{(IV-102)}$$

$$\left.\frac{d\psi}{d\lambda}\right|_{\lambda=0} = \frac{2\sigma\delta^2}{(1+\delta/\mu)(\xi'+\mu)e^{L/\mu R} + (1-\delta/\mu)(\xi'-\mu)e^{-L/\mu R}} \quad \text{(IV-103)}$$

$$\left.\frac{d\psi}{d\lambda}\right|_{\lambda=0} = \frac{\sigma\mu^2}{(\xi'+\mu)} \; e^{-L/\mu R} \quad (\delta = \mu) \quad . \tag{IV-104}$$

Equations (IV-96, 98, and 103) can be linearized to

$$\psi = \sigma\delta^2 \; \frac{\xi' + \lambda}{\xi' + \frac{L}{R} + \delta + \frac{\delta\xi' L}{\mu^2 R}} \tag{IV-105}$$

$$\psi = \sigma\mu^2 \; \frac{\xi' + \lambda}{\xi' + \mu} \; e^{-L/\mu R} \quad (\delta = \mu) \tag{IV-106}$$

$$\left.\frac{d\psi}{d\lambda}\right|_{\lambda=0} = \frac{\sigma\delta^2}{\xi' + \frac{L}{R} + \delta + \frac{\delta\xi' L}{\mu^2 R}} \; . \tag{IV-107}$$

Case F. Items 1 to 17 are the same as for Case C;

18. Number of moles of atoms generated uniformly per unit time per unit volume in the discharge zone is proportional to the molecular hydrogen concentration $k_o'(c - c_1')$;

19. Same as for Case C;

20. Same as for Case C.

The diffusion equation for the discharge zone in this case is somewhat different than that for Case C, as

$$D_{12} \frac{d^2 c_1'}{dz^2} + k_o'(c - c_1') - k_1' c_1' = 0 \text{ (discharge zone)} \tag{IV-108}$$

This equation can be put in dimensionless form by the definition of two more dimensionless parameters

$$\sigma'^2 = \frac{k_o' R^2}{D_{12}} \tag{IV-109}$$

$$\frac{1}{\delta'^2} = \sigma'^2 + \frac{1}{\delta^2} \; , \tag{IV-110}$$

which leads to the following dimensionless diffusion equation

$$\frac{d^2\eta}{d\lambda^2} + \sigma'^2 - \frac{\eta}{\delta'^2} = 0 \quad . \qquad \text{(IV-111)}$$

By inspection it can be seen that the final results for Case C can be casily modified to apply to Case F by substitution of σ'^2 for σ and δ' for δ in Eqs. (IV-75) to (IV-78). Similarly, the results for Cases D and E can be modified with the same substitutions. More formally, the cases consisting of these two other modifications are called Case F1 (D) and Case F2 (E) respectively. They need not be re-derived.

For Case F, the mole fraction of atoms ψ is

$$\psi = \frac{\sigma'^2 \delta^2}{1+\sigma'^2\delta^2} \frac{\lambda + \xi'}{L/R + \xi' + \delta/(1+\sigma'^2 \delta^2)^{1/2}} \quad . \qquad \text{(IV-112)}$$

When the walls are very noncatalytic, δ becomes very large and ψ becomes

$$\psi \approx \frac{\lambda + \xi'}{L/R + \xi' + 1/\sigma'} \quad . \qquad \text{(IV-113)}$$

If the end plate is extremely noncatalytic, $\xi' \gg L/R + 1/\sigma'$, and the equation for ψ reduces to

$$\psi = \frac{1}{1 + 1/\sigma'^2 \delta^2} \quad . \qquad \text{(IV-114)}$$

Thus, the use of a non-catalytic end plate provides a simple way for us to obtain the value of $\sigma'^2 \delta^2$. Generally, the discharge power will be regulated so that the mole fraction of atoms is about 10%. Under these conditions, the value of $\sigma'^2 \delta^2$ is

$$0.10 = \frac{1}{1 + 1/\sigma'^2 \delta^2}$$

$$\sigma'^2 \delta^2 = 1/9$$

$$\frac{\delta}{(1 + 1/9)^{1/2}} = 0.95 \approx \delta \quad .$$

Consequently, the formulas for ψ given for Case C are satisfactory. For mole fractions less than 10%, the approximation of Case C becomes even better. If now a highly catalytic metal end plate is inserted at L/R = 30 so that $0.95\delta + L/R \gg \xi'$, and ψ is measured at $\lambda = L/R$ and found to be 0.060, the actual values of σ' and δ can be computed, providing that σ' remains the same:

$$0.06 = 0.10 \frac{30}{30 + 0.95\delta}$$

$$\delta = 21$$

$$\sigma' = 0.016 \quad .$$

Case G. 1. Two-dimensional case;

Items 2 to 7 are the same as for Case A;

8. Catalytic walls with first-order recombination coefficient γ;

Items 9 to 12 are the same as for Case A;

13. Composite end plate consisting of a disk of radius a and recombination coefficient γ', and an annular ring of radii a and R and recombination coefficient γ'';

14. Flux to each part of the composite end plate is of the same form as in Case A;

15. Same as for Case A.

Two new necessary dimensionless groups are (Fig. 47)

$$\rho = r/R \qquad \text{(IV-115)}$$

and

$$\kappa = a/R \quad . \qquad \text{(IV-116)}$$

The diffusion equation and boundary conditions can be written as

$$\frac{d^2\psi}{d\lambda^2} + \frac{1}{\rho}\frac{\partial\psi}{\partial\rho} + \frac{\partial^2\psi}{\partial\rho^2} = 0 \qquad \text{(IV-117)}$$

$$\frac{\partial\psi}{\partial\rho} = 0 \qquad (\text{at } \rho = 0) \qquad \text{(IV-118)}$$

$$\frac{\partial\psi}{\partial\rho} = -\frac{\psi}{\xi} \qquad (\text{at } \rho = 1) \qquad \text{(IV-119)}$$

$$\psi = \psi_o \qquad (\text{at } \lambda = L/R) \qquad \text{(IV-120)}$$

$$\frac{\partial\psi}{\partial\lambda} = \frac{\psi}{\xi'}, \qquad (\text{at } \lambda=0,\ 0 \leqq \rho \leqq \kappa) \qquad \text{(IV-121)}$$

$$\frac{\partial\psi}{\partial\lambda} = \frac{\psi}{\xi''} \qquad (\text{at } \lambda = 0,\ \kappa \leqq \rho \leqq 1) \quad . \qquad \text{(IV-122)}$$

The solution of the diffusion equation is in the form of a of a Bessel-exponential series in which the variables are separated—

$$\psi = \sum_{i=1}^{\infty} [A_i e^{\alpha_i \lambda} + B_i e^{-\alpha_i \lambda}][J_o(\alpha_i \rho) + C_i Y_o(\alpha_i \rho)]. \qquad \text{(IV-123)}$$

From the first boundary condition, $C_i = 0$. From the second,

$$J_o(\alpha) = \alpha_i \xi\ J_1(\alpha_i) \quad . \qquad \text{(IV-124)}$$

The third boundary condition is used after multiplying by $\rho\ J_o(\alpha_n \rho)$ both sides of the equation for ψ at $\lambda = L/R$ and integrating over ρ,

$$\int_0^1 \rho\,\psi_o\ J_o(\alpha_n \rho)\,d\rho = \sum_{i=1}^{\infty} \left[A_i e^{\alpha_i L/R} + B_i e^{-\alpha_i L/R} \right] \int_0^1 \rho\ J_o(\alpha_n \rho) J_o(\alpha_i \rho)\,d\rho \quad . \qquad \text{(IV-125)}$$

Advantage is taken of the orthogonality properties of the integral on the right side, which equals 0 if $n \neq i$ and equals $1/2(1 + \xi^2\alpha_i^2)J_i^2(\alpha_i)$ if $i = n$. The value of the integral on the left is $J_1(\alpha_i)/\alpha_i$. Thus,

$$\psi_o = \left[A_i e^{\alpha_i L/R} + B_i e^{-\alpha_i L/R}\right]\left[1/2\ \alpha_i\ (1 + \xi^2\alpha_i^2)J_1(\alpha_i)\right]. \tag{IV-126}$$

The final boundary condition creates the most difficulties. This time, the integration involves the size of the central catalytic disk.

$$\sum_{i=1}^{\infty} \alpha_i(A_i - B_i) \int_0^1 \rho J_o(\alpha_n\rho)J_o(\alpha_i\rho)d\rho =$$

$$= \left(\frac{1}{\xi'} - \frac{1}{\xi''}\right) \sum_{i=1}^{\infty} (A_i + B_i) \int_0^K \rho J_o(\alpha_n\rho)J_o(\alpha_i\rho)d\rho$$

$$+ \frac{1}{\xi''} \sum_{i=1}^{\infty} (A_i + B_i) \int_0^1 \rho J_o(\alpha_n\rho)J_o(\alpha_i\rho)d\rho \quad . \tag{IV-127}$$

This equation under ordinary circumstances is useless, since the integral involving κ as a limit is not over an orthogonal interval. If $\xi \gg 1$, the first term, i=1, in the series predominates and the following <u>important</u> approximation can be made:

$$\int_0^K \rho J_o(\alpha_n\rho)J_o(\alpha_i\rho)d\rho \approx \kappa^2 \int_0^1 \rho J_o(\alpha_n\rho)J_o(\alpha_i\rho)d\rho \tag{IV-128}$$

$$(i = n = 1) \quad .$$

Thus

$$\alpha_i(A_i - B_i) = \left(\frac{\kappa^2}{\xi'} + \frac{1-\kappa^2}{\xi''}\right)(A_i + B_i) \quad . \tag{IV-129}$$

The final solution for ψ under the above four boundary conditions is

$$\frac{\psi}{\psi_o} = \sum_{i=1}^{\infty} \frac{2J_o(\alpha_i \rho)}{\alpha_i(1+\xi^2\alpha_i^2)J_1(\alpha_i)}$$

$$\cdot \frac{(\alpha_i + \frac{\kappa^2}{\xi'} + \frac{1-\kappa^2}{\xi''})\, e^{\alpha_i \lambda} + (\alpha_i - \frac{\kappa^2}{\xi'} - \frac{1-\kappa^2}{\xi''})\, e^{-\alpha_i \lambda}}{(\alpha_i + \frac{\kappa^2}{\xi'} + \frac{1-\kappa^2}{\xi''})\, e^{\alpha_i L/R} + (\alpha_i - \frac{\kappa^2}{\xi'} - \frac{1-\kappa^2}{\xi''})\, e^{-\alpha_i L/R}} \qquad \text{(IV-130)}$$

where the first term, i = 1, is the predominant term in the series.

Since $\xi \gg 1$, the following relations also hold:

$$\alpha_1 \approx (2/\xi)^{1/2} \qquad \text{(IV-131)}$$

$$J_1(\alpha_1) \approx \frac{\alpha_1}{2} . \qquad \text{(IV-132)}$$

If α_1 is so small that the exponentials can be approximated by

$$e^{\alpha_1 \lambda} \approx 1 + \alpha_1 \lambda \qquad \text{and} \qquad e^{\alpha_1 L/R} \approx 1 + \alpha_1 L/R , \qquad \text{(IV-133)}$$

the equation for ψ simplifies to

$$\frac{\psi}{\psi_o} = \frac{\frac{\xi'}{\kappa^2 + (1-\kappa^2)\frac{\xi'}{\xi''}} + \lambda}{\frac{\xi'}{\kappa^2 + (1-\kappa^2)\frac{\xi'}{\xi''}} + \frac{L}{R}} . \qquad \text{(IV-134)}$$

If $\frac{(1-\kappa^2)\xi'}{\xi''} \ll \kappa^2$,

$$\frac{\psi}{\psi_o} = \frac{(\xi'/\kappa^2) + \lambda}{(\xi'/\kappa^2) + L/R} . \qquad \text{(IV-135)}$$

If $\frac{(1-\kappa^2)\xi'}{\xi''} \gg \kappa^2$,

$$\frac{\psi}{\psi_o} = \frac{[\xi''/(1-\kappa^2)] + \lambda}{[\xi''/(1-\kappa^2)] + L/R} . \qquad \text{(IV-136)}$$

If $\xi' = \xi''$,

$$\frac{\psi}{\psi_o} = \frac{\xi' + \lambda}{\xi' + L/R} \quad . \tag{IV-137}$$

These simplified results (for $\alpha_1 L/R$ small) correspond exactly to Case A, with the exception of the boundary condition at $\lambda = 0$, which is now

$$- \frac{d\psi}{d\lambda} = \left(\frac{\kappa^2}{\xi'} + \frac{1-\kappa^2}{\xi''} \right) \psi \qquad \text{at } \lambda = 0 \quad . \tag{IV-138}$$

Consequently, Cases B, C, D, E, F, F_1, and F_2 can all be modified accordingly to satisfy this revised boundary condition.

From a comparison of the definitions for ξ and μ,

$$\frac{2}{\xi} = \frac{1}{\mu^2} = \alpha_1^2 \quad . \tag{IV-139}$$

This result clearly demonstrates how the solutions for ψ compare for Cases E and G.

Case H. Items 1 to 12 are the same as for Case A;

13. $c_1 = 0$ at $z = L$;

14. Same as for Case A.15.

Use of the boundary condition

$$\psi = 0 \qquad \text{at } \lambda = 0 \tag{IV-140}$$

instead of Eq. (IV-49) changes Eqs. (IV-50) and IV-51, respectively, t

$$\frac{\psi}{\psi_o} = \frac{\lambda}{L/R} \tag{IV-141}$$

$$\frac{d\psi}{d\lambda} = \frac{\psi_o}{L/R} \quad . \tag{IV-142}$$

Case I. Items 1 to 6 are the same as for Case H;

7. Flow tube, $v_z \neq 0$.

Items 8 to 14 are the same as for Case H;

15. v_z = constant;

16. p = constant.

Only one new dimensionless group is needed for this and most other flow-tube situations—

$$\beta = \frac{v_z R}{D_{12}} \quad . \tag{IV-143}$$

The atom-conservation equation for this case is

$$D_{12} \frac{\partial^2 c_1}{\partial z^2} - v_z \frac{\partial c_1}{\partial z} = 0 \quad , \tag{IV-144}$$

which converts to the dimensionless equation

$$\frac{d^2\psi}{d\lambda^2} + \beta \frac{d\psi}{d\lambda} = 0 \tag{IV-145}$$

with the simple boundary conditions

$$\psi = \psi_o \qquad (\text{at } \lambda = L/R) \tag{IV-146}$$

$$\psi = 0 \qquad (\text{at } \lambda = 0) \quad . \tag{IV-147}$$

The solution is in the form $\psi = Ae^{-\beta\lambda} + B$, which leads to

$$\frac{\psi}{\psi_o} = \frac{e^{-\beta\lambda} - 1}{e^{-\beta L/R} - 1} \tag{IV-148}$$

$$\left.\frac{d\psi}{d\lambda}\right|_{\lambda=0} = \frac{\beta\psi_o}{1 - e^{-\beta L/R}} \quad . \tag{IV-149}$$

Case J. Items 1 to 12 are the same as for Case I;

13. The boundary condition at $z = L$ is $-D_{12} \frac{\partial c_1}{\partial z} + v_z c_1 = 1/4\, \gamma'\, c_1 v_1 + v_z c_1$;

Items 14 to 16 are the same as for Case I.

The boundary condition in Item 13 (Case J) may seem strange, but it is correct and has a physically understandable result. The terms on the left of the equal sign are the normal ones for the molar flux of atoms by convection and diffusion. The terms on the right correspond to the loss of atoms to the end plate and to the flux of atoms that continues traveling with the gas stream.

The dimensionless diffusion equation is the same as Eq. (IV-145), but one boundary condition has changed

$$\frac{d\psi}{d\lambda} = \frac{\psi}{\xi'} \qquad (\text{at } \lambda = 0) \quad . \qquad \text{(IV-150)}$$

The solutions are

$$\frac{\psi}{\psi_o} = \frac{(\beta\xi' + 1) - e^{-\beta\lambda}}{(\beta\xi' + 1) - e^{-\beta L/R}} \qquad \text{(IV-151)}$$

$$\left.\frac{d\psi}{d\lambda}\right|_{\lambda=0} = \frac{\beta\psi_o}{(\beta\xi' + 1) - e^{-\beta L/R}} \quad . \qquad \text{(IV-152)}$$

Case K. Items 1 to 7 are the same as for Case I;

8. Catalytic walls with first-order recombination coefficient γ;

Items 9 to 16 are the same as for Case I.

The dimensionless conservation equation is a composite of Eqs. (IV-95) and (IV-145),

$$\frac{d^2\psi}{d\lambda^2} + \beta \frac{d\psi}{d\lambda} - \frac{\psi}{\mu^2} = 0 \ , \qquad \text{(IV-153)}$$

and is subject to the same boundary conditions as in Case I. In writing the solution, I found it useful to redefine a special combination of dimensionless groups

$$\frac{\Omega}{2} = \left[\frac{\beta^2}{4} + \frac{1}{\mu^2}\right]^{1/2} , \qquad \text{(IV-154)}$$

so that

$$\frac{\psi}{\psi_o} = \frac{e^{(\Omega-\beta)\lambda/2} - e^{-(\Omega+\beta)\lambda/2}}{e^{(\Omega-\beta)L/2R} - e^{-(\Omega+\beta)L/2R}} \qquad \text{(IV-155)}$$

$$\left.\frac{d\psi}{d\lambda}\right|_{\lambda=0} = \frac{\Omega\,\psi_o}{e^{(\Omega-\beta)L/2R} + e^{-(\Omega+\beta)L/2R}} . \qquad \text{(IV-156)}$$

Case L. Items 1 to 12 are the same as for Case K.

Items 13 to 16 are the same as for Case J.

The dimensionless equation and boundary conditions are Eq. (IV-153), and Eqs. (IV-146 and IV-150), respectively. The solutions are

$$\frac{\psi}{\psi_o} = \frac{T\,e^{(\Omega-\beta)\lambda/2} + e^{-(\Omega+\beta)\lambda/2}}{T\,e^{(\Omega-\beta)L/2R} + e^{-(\Omega+\beta)L/2R}} \qquad \text{(IV-157)}$$

$$\left.\frac{d\psi}{d\lambda}\right|_{\lambda=0} = \frac{2\Omega/(\Omega\xi' - \beta\xi' - 2)}{T\,e^{(\Omega-\beta)L/2R} + e^{-(\Omega+\beta)L/2R}}\cdot\psi_o \qquad \text{(IV-158)}$$

where

$$T = \frac{\Omega\xi' + \beta\xi' + 2}{\Omega\xi' - \beta\xi' - 2} . \qquad \text{(IV-159)}$$

Case M. Items 1 to 12 are the same as for Case I;

13. Same as for Case J;

14. v_z = constant;

15. p = constant;

Items 16 to 20 are the same as for Case F;

21. Same as Case A.15.

The dimensionless equations for the two zones are

$$\frac{d^2\eta}{d\lambda^2} + \beta\frac{d\eta}{d\lambda} - \frac{\eta}{\delta'^2} + \sigma'^2 = 0 \qquad \text{(discharge zone)} \qquad \text{(IV-160)}$$

$$\frac{d^2\psi}{d\lambda^2} + \beta \frac{d\psi}{d\lambda} = 0 \qquad \text{(reactor zone)} \qquad \text{(IV-161)}$$

and the boundary conditions are Eqs. (IV-69) to (IV-72). The solution to Eq. (IV-161) is

$$\psi = \sigma'^2 \delta'^2 \frac{(\beta\xi' + 1) - e^{-\beta\lambda}}{(\beta\xi' + 1) - \left(\frac{\chi-\beta}{\chi+\beta}\right) e^{-\beta L/R}} \qquad \text{(IV-162)}$$

where

$$\frac{\chi}{2} = \left[\frac{\beta^2}{4} + \frac{1}{\delta'^2}\right]^{1/2} \qquad \text{(IV-163)}$$

E. Meaning of Dimensionless Groups

The dimensionless groups given in this section and in Secs. V and VI are (a) normalized length or concentration parameters or else are (b) the ratio of two rate processes occurring within the diffusion or flow tube. Given below are the verbal descriptions of these groups:

$$\psi = \frac{\text{atom concentration in reaction zone}}{\text{total concentration of atoms and molecules}}$$

$$\psi_o = \frac{\text{atom concentration at discharge-reactor-zone boundary}}{\text{total concentration of atoms and molecules}}$$

$$\eta = \frac{\text{atom concentration in discharge zone}}{\text{total concentration of atoms and molecules}}$$

$$\tau = \frac{\text{atom concentration in buffer zone}}{\text{total concentration of atoms and molecules}}$$

$$\lambda = \frac{\text{distance from end plate to point in reactor, discharge, or buffer zone}}{\text{radius of reaction tube}}$$

$$\rho = \frac{\text{radial distance from axis of reaction tube to point between axis and wall}}{\text{radius of reaction tube}}$$

$$\kappa = \frac{\text{smaller radius of annular end plate}}{\text{radius of reaction tube}}$$

$$\frac{L}{R} = \frac{\text{rate of radial diffusion}}{\text{rate of axial diffusion through reactor zone}}$$

$$\xi' = \frac{\text{rate of radial diffusion}}{\text{rate of atom recombination on end plate}}$$

$$\frac{L}{\xi' R} = \frac{\text{rate of atom recombination on end plate}}{\text{rate of axial diffusion through reactor zone}}$$

$$\mu^2 = \frac{\text{rate of radial diffusion}}{\text{rate of atom recombination on reactor-zone walls}}$$

$$\delta^2 = \frac{\text{rate of radial diffusion}}{\text{rate of atom recombination on discharge-zone walls}}$$

$$\sigma'^2 = \frac{\text{rate of atom production in discharge zone}}{\text{rate of radial diffusion}}$$

$$\beta = \frac{\text{rate of axial convection}}{\text{rate of radial diffusion}}$$

$$\frac{\beta L}{R} = \frac{\text{rate of axial convection through reactor zone}}{\text{rate of axial diffusion through reactor zone}}$$

$$\frac{\delta^2 R}{M} = \frac{\text{rate of axial diffusion through discharge zone}}{\text{rate of atom recombination on discharge-zone walls}}$$

$$\frac{\sigma'^2 M}{R} = \frac{\text{rate of atom production in discharge zone}}{\text{rate of axial diffusion through discharge zone}}$$

V. THE EFFECT OF GASEOUS IMPURITIES ON THE PRODUCTION OF ATOMIC HYDROGEN IN A LOW-PRESSURE DISCHARGE

A. Introduction

One of the most interesting and persistent observations associated with the use of low-pressure electrical discharges for producing atoms from diatomic molecules has been that small quantities of impurities (such as water) greatly increase the atom yield.

Wood,[53] Bichowsky and Copeland,[57] and Lord Rayleigh (R. J. Strutt)[59] were the first to study the effect of such impurities in discharges in hydrogen, oxygen, and nitrogen, respectively. A complete listing of all investigators who have subsequently used this phenomenon in their experiments is unnecessary since the number is very large. Surprisingly, not too many of them have actually studied it.[52-73,76-81] Despite their best efforts, there still is no real agreement on the role of the gaseous impurities in the various molecular-gas discharge systems. The most recent papers tend only to confirm this viewpoint, as well as the fact that the entire problem is open for reinvestigation and clarification.[8,78,79,81]

The increase in atom yield may be an actual increase, or only an apparent one caused by an impurity that affects only the measurement device and thereby simulates an increased atom concentration. A good example of the latter situation occurs if an ESR spectrometer is operated at power saturation. The addition or production of any paramagnetic species within the gas stream increases the spectrometer signal, and thus falsely indicates the presence of more atoms to the unwary observer. An apparent increase in atom concentration or apparent high atom-concentration levels may also occur if an incorrect mathematical description is applied to the measurement device or to the system as a whole.

If the increase in atom concentration is real, then it is attributable to a change in some rate process. This process must be associated only with a specific region within the vacuum system: the discharge zone or the reactor zone. Other parts of the system may also be important, but their role must be to affect directly the gas, the

surfaces, the measurement device, or the plasma in the discharge and reactor zones. Oil or mercury from the pumps can conceivably have such a widespread effect.

The impurity gas either increases the rate of atom production or decreases the rate of atom loss somewhere in the two zones, either in the gas or the surface phases. When the existence of two zones is assumed, the effect of water and other impurities in discharges can be immediately explained:

Discharge zone, gas phase:

Catalytic effect: impurity species act catalytically within the discharge to produce more atoms;

Stoichiometric effect: impurity species are dissociated and then react to produce atoms directly;

Inhibition of a loss process: impurity species counteract the effect of another plasma contaminant or species, which acts to reduce the rate of atom production;

Discharge zone, surface phase:

Catalytic effect: impurity species act catalytically at the charged surface where electron-ion recombination takes place;

Inhibition of a loss process: impurity species counteract the effect of a surface which either recombines atoms or else abstracts intermediate species important in the production of atoms;

Reactor zone, gas phase:

Stoichiometric effect: dissociated or altered impurity species coming from the discharge zone react to produce atoms directly;

Inhibition of a loss process: dissociated or altered impurity species coming from the discharge zone counteract the effect of another gas-phase species which acts to reduce the atom concentration or rate of atom production by the stoichiometric effect;

Reactor zone, surface phase:

Inhibition of a loss process: impurity species counteract the effect of the surface, which recombines atoms.

Diverse as these explanations may seem, almost all of them have been applied at one time or another to explain the effect of impurities in the low-pressure discharge production of atomic hydrogen, oxygen, or nitrogen.

With two sensitive, stable, and perhaps absolute WHG's in my possession, I decided to prove definitively whether the action of water in increasing the yield of hydrogen atoms from a low-pressure discharge was either a gas-phase or a surface-phase effect. The surprising experimental results and their implications are the most important segment of this report.

B. Plan of the Experiments

The concept of the experiments (to determine whether the action of water in increasing the yield of atomic hydrogen from a low-pressure discharge was either a gas-phase or a surface-phase effect) was simple (Fig. 48):

a. Verify the phenomenon in a simple glass flow-tube system first with very pure hydrogen and with hydrogen containing several percent H_2O;

b. Coat the walls of the glass flow tube with a thin film of Teflon, then repeat the above experiment at low discharge power levels, first with very pure hydrogen, and then hydrogen containing a small amount of H_2O;

c. If it is a gas-phase effect, determine quantitatively the amount or atomic hydrogen produced per molecule of oxygen, nitrogen, water, and other impurity gases added in small quantities to an initially pure hydrogen gas stream;

d. If it is a surface-phase effect, measure the recombination coefficient of atomic hydrogen on various metals and glass; perform the experiments both with pure hydrogen and with hydrogen containing several percent H_2O.

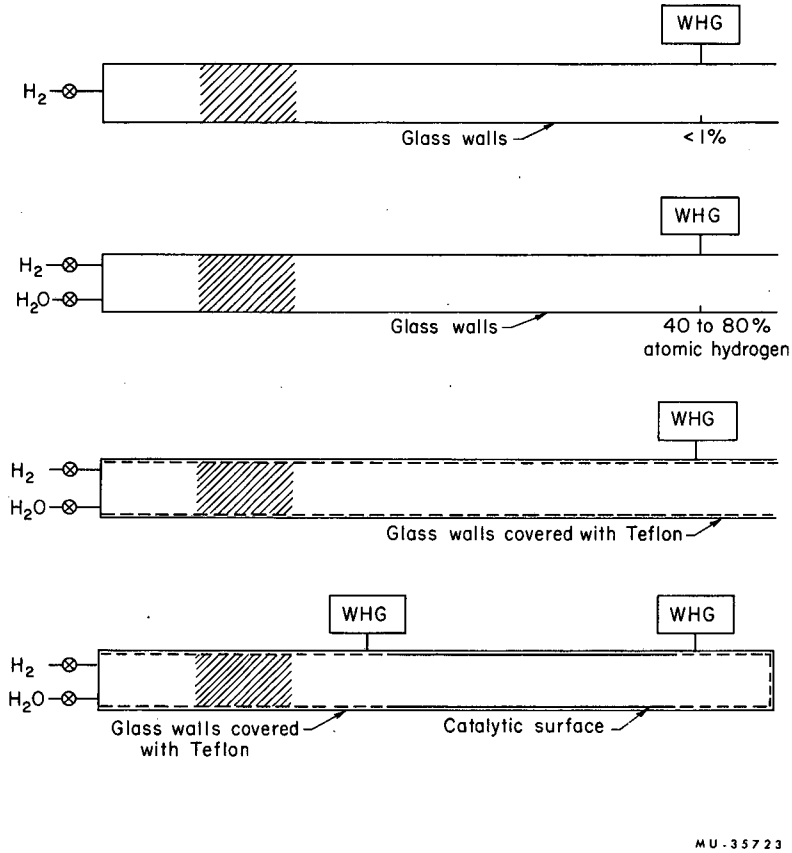

Fig. 48. Schematic drawing showing the four stages of the planned experiments: (a) verify that a discharge in pure hydrogen produces few atoms, (b) verify that the addition of water to the hydrogen increases the atom yield, (c) determine if the addition of water is a gas- or surface-phase effect, and (d) study the catalytic properties of surfaces in the presence and absence of water (if it is a surface-phase effect).

This group of proposed experiments was based on the observation by Berg and Kleppner than the recombination coefficient for atomic hydrogen on a film of Teflon (DuPont Teflon Clear Finish 852-201) was less than $1.3 \cdot 10^{-5}$.[88] Thus if water still increased the yield of atoms in the Teflon-coated tube, then its mode of action was in the gas phase. On the other hand, if the Teflon-poisoning of the glass walls completely eliminated the effect of water, the water acted as a poison for reactive glass-wall surfaces.

No information on the exact mechanism of the water effect in either phase was anticipated. The main experiments by virtue of their simplicity and decisiveness, were sufficiently valuable by themselves.

The experiments determining the role of water in hydrogen discharges usually required a measurement determining the presence or absence or some predicted effect or behavior. In this respect, they resembled the types of experiments performed by molecular biologists, biochemists, and virologists to determine the role of DNA, RNA, transfer RNA, enzymes, and special chemical agents in viruses, bacteria, and cells. Accordingly, the results of the discharge experiments are presented in the very appealing Scientific American format—numerous schematic diagrams, simplified data curves, extensive use of logic and reasoning, and step-by-step presentation of experimental observations.

C. Experimental Observations

1. Survey of the Experiments

The experiments determining the effect of water on the production of atomic hydrogen in a low-pressure discharge were performed in three distinct groups. In the first group (primarily flow-tube experiments), purified hydrogen, reaction tube No. 1, the non-water-cooled Wrede-Harteck gauge (WHG) fitting with 125 effusion holes, the water bubbler, the diathermy machine and large-diameter microwave cavity, the 50 MHz power source, and cylinder hydrogen were used. Air, oxygen, or water were the impurity gases.

The numerous measurements tested the effect of: the location of the 50-MHz and microwave discharges; source of the hydrogen gas; use of the water bubbler; water, air, or oxygen on the atom concentration produced by the discharge and measured by the WHG. Unfortunately, the recombination of the hydrogen atoms on the WHG catalytic surface produced thermal effusion effects that caused the WHG signal to decay while the discharge was still on. This made all quantitative and some qualitative measurements suspect.

To circumvent this decay, a second group of measurements was made with a water-cooled WHG fitting containing approximately 200 effusion holes. The previous tests were carefully repeated and essentially the same conclusions were reached. Several additional definitive experiments were also performed to further test the opposing roles of oxygen and water in the low-pressure hydrogen-discharge system.

Finally, reaction tube No. 3 was set up with two water-cooled WHG's and a thermocouple probe soldered to a small square of silver foil. The third group of experiments tested the relative behavior of the WHG compared to that of a thermocouple probe.

In order to avoid repetition, the three groups of experiments are treated as one unit. Only those recorder-chart tracings or quantitative measurements that most dramatically illustrate the various observations are shown. Since all of the experimental observations were consistent and generally reproducible, each recorder tracing represents the best result of a large number of similar curves.

2. Effect of H_2O

The apparatus is described and pictured in Sec. II.C.3 and also in Fig. 49. The Decker micromanometer was not very useful because condensation of the water on the glass or the pressure-transducer surfaces produced a reading that drifted erratically.

The entire vacuum system was evacuated overnight with the diffusion pump. In the morning, pure hydrogen from the Engelhard hydrogen purifier flowed through the system at a pressure of approximately 75 mtorr.

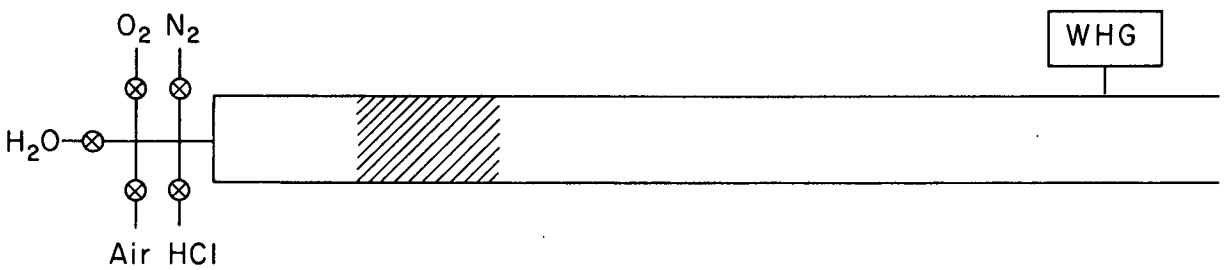

Fig. 49. Schematic drawing for the experiments to determine the effect of O_2, N_2, H_2O, HCl, and air on the yield of atomic hydrogen from a low-pressure discharge (Sec. V.C.2 to 5).

After a period of 20 to 30 minutes for pressure equilibration, the discharge was repeatedly pulsed for 1 minute at 3-minute intervals to check the clean-up of air and other contaminants from the walls. The progress of the clean-up was observed by the steady decrease in pulse heights with time. Most of the weakly adsorbed impurities appeared to be eliminated on the very first pulse (Fig. 50).

After several pulses, the pulse heights remained at a steady level, approximately 0.1% atomic-hydrogen concentration. Prolonged operation of the reaction tube thereafter did not reduce this value, which was taken as the atom concentration characteristic of my "pure" hydrogen. The general level of this value (0.1%) agreed with previous measurements.

The first experiments on the effect of H_2O employed the large-diameter microwave cavity located as near as 3 cm to the WHG port hole or as far as 20 to 25 cm away. With the fast-flow system (v_z = 75 cm/sec), the distance between the discharge and the WHG port hole didn't make much difference. Subsequent experiments performed with the small microwave cavity or with the 50 Mc/sec oscillator are described in Sec. V.C.8.

The effect of water addition is shown in the samples of the recorder readings (Figs. 44 and 51). The results were surprising. First of all, the water alone, in the absence of a discharge, had a definite effect on the signal level of the WHG—the water caused the WHG to move in the same direction as when it measured atoms. The steady-state WHG signal was proportional to the concentration of the water, although the shape of the proportionality curve was never determined owing to the problems in measuring the water flow rate.

I have had no success in pinning down the reasons for this effect experimentally. I first thought that it might be some type of adsorption phenomenon on the electrodes or the diaphragm of the WHG micromanometer. This was not correct, since the change in WHG signal reading predicted by this cause was opposite to that actually observed.

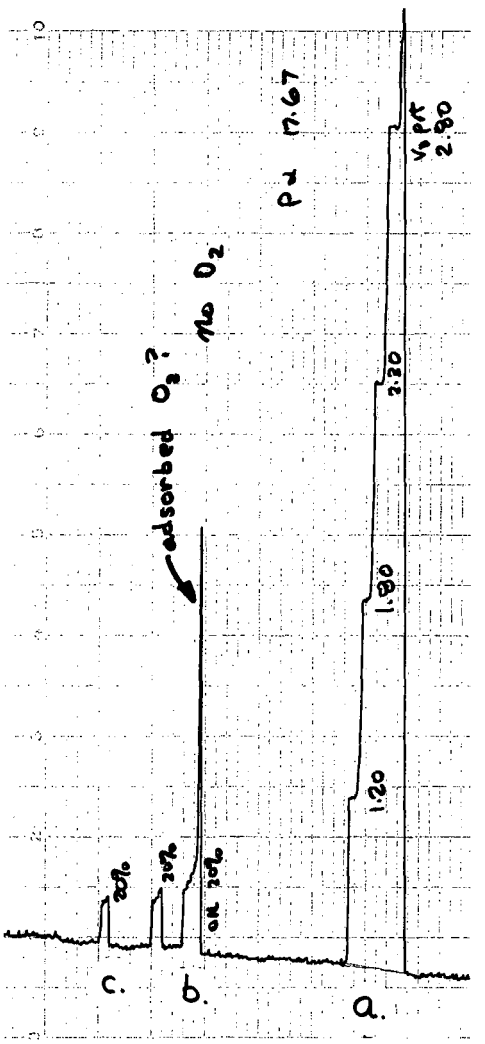

MU-35473

Fig. 50. Response of water-cooled WHG No. 1 (125 holes, 0.59 mtorr full scale) to (a) an electrostatic calibration, (b) the rapid outgassing of impurities adsorbed on the reaction-tube walls by the 50-MHz discharge, and (c) the production of small quantities of atoms (0.1%) by a 20% dial setting on the 50-MHz oscillator. P = 78 mtorr and t = 20 sec/small div (right to left). (February 2, 1965).

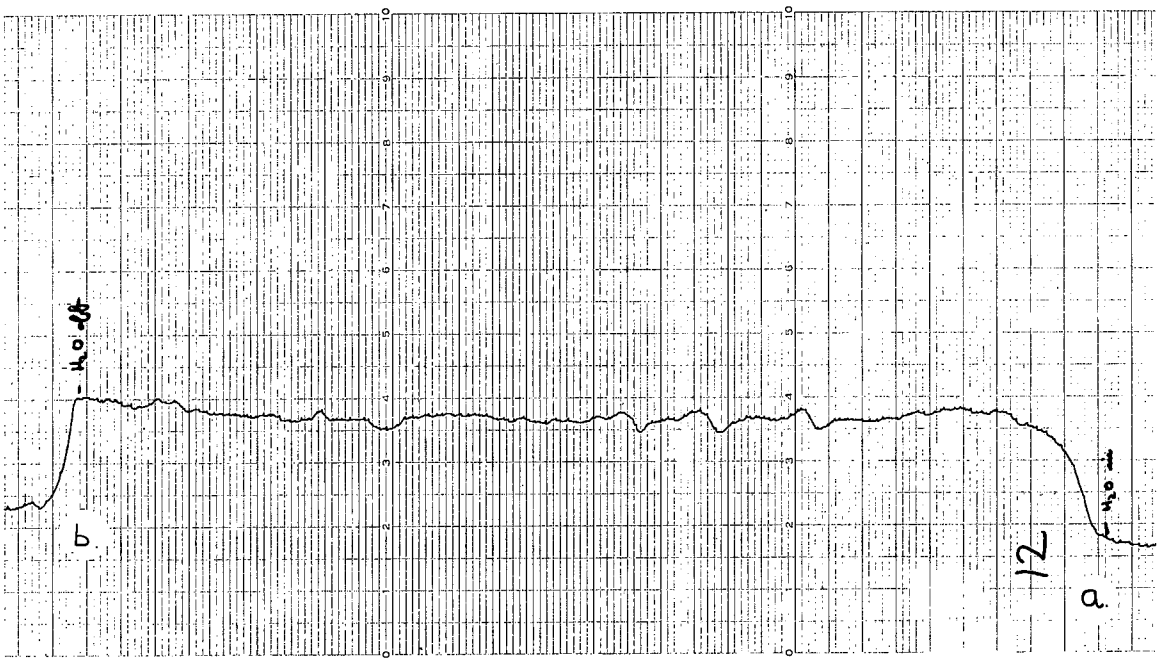

Fig. 51. Response of water-cooled WHG No. 1 (125 holes, 0.7 mtorr full scale) to the actions of (a) adding a small amount of water to the hydrogen gas, and (b) stopping the addition of water. The effect persisted for 50 minutes and showed no tendency to decay. This curve strongly suggests that the presence of water alters the effusion equilibrium within the WHG, although other explanations are also possible. P = about 75 mtorr and t = 20 sec/small div (right to left). (February 2, 1965).

Another possibility was that the water participating in some effusion process across the effusion diaphragm, thus produced a detectable signal. Because the process conserved neither mass no momentum, a theoretical description was impossible in the absence of mass or molar flux data. I have not proved this hypothesis but feel that it is probably the most likely one.

The second and more important observation was that, under my set of experimental conditions, water had no effect on the yield of atomic hydrogen from the microwave discharge (Figs. 52-55). This result disagreed completely with the practice of bubbling hydrogen gas through water prior to passing the gas through a low-pressure discharge, and also with the observations of a majority of investigators who had previously studied or had passively used but not studied the effect.

I thought that the peculiar effect on the operation of the WHG in the absence of a discharge also manifested itself by eliminating the signal due to atoms in the presence of the discharge. Experiments performed to check this point are described in detail in Sec. V.C.10.

The color of the discharge in a small-diameter glass tube, used by many investigators as a qualitative indication of the rate of atomic hydrogen production, remained the same before and after the addition of small quantities of water (estimated to be less than 5%)—a whitish-pink or pinkish white. This color was the same as that mentioned by Shaw,[70] but distinctly different from the beautiful and characteristic crimson observed when appreciable quantities of oxygen were added to the hydrogen gas prior to the discharge.

With the large-diameter microwave cavity, the discharge color was a whitish purple for pure hydrogen or hydrogen containing water, and red for hydrogen containing several percent oxygen. With the 50-MHz discharge, the color varied from pink to deep red.

3. Effect of HCl

The apparatus and experimental procedure were the same as those used for H_2O. The HCl caused the Decker micromanometer to behave somewhat less erratically, but did cause the strange increase in signal

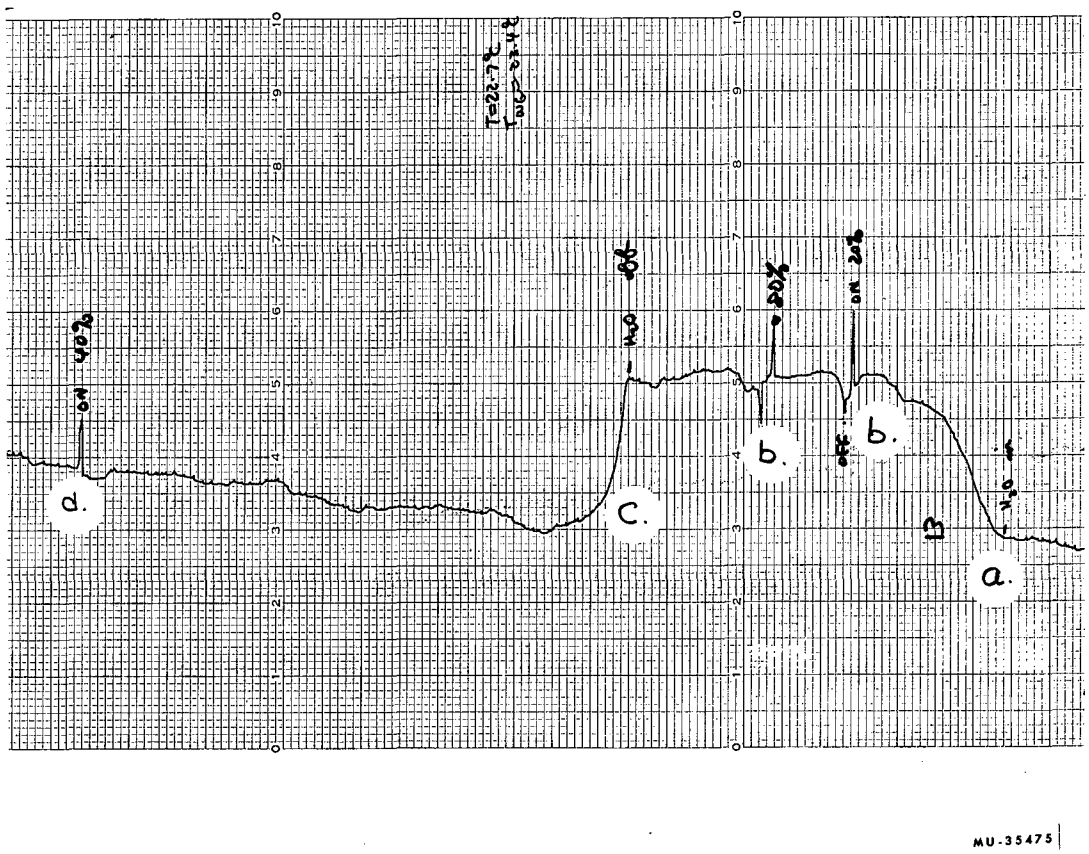

Fig. 52. Response of water-cooled WHG No. 1 (125 holes, 0.7 mtorr full scale) to the actions of (a) adding a small amount of water to the hydrogen gas, (b) operating the 50-MHz discharge at a 20% or 80% dial setting for 30 sec, (c) stopping the addition of water, and (d) operating the discharge at a 40% dial setting in pure hydrogen (yield of atoms = 0.19%). The curve shows that water has no effect on the yield of atoms from the discharge. P = about 75 mtorr and t = 20 sec/small div (right to left). (February 2, 1965).

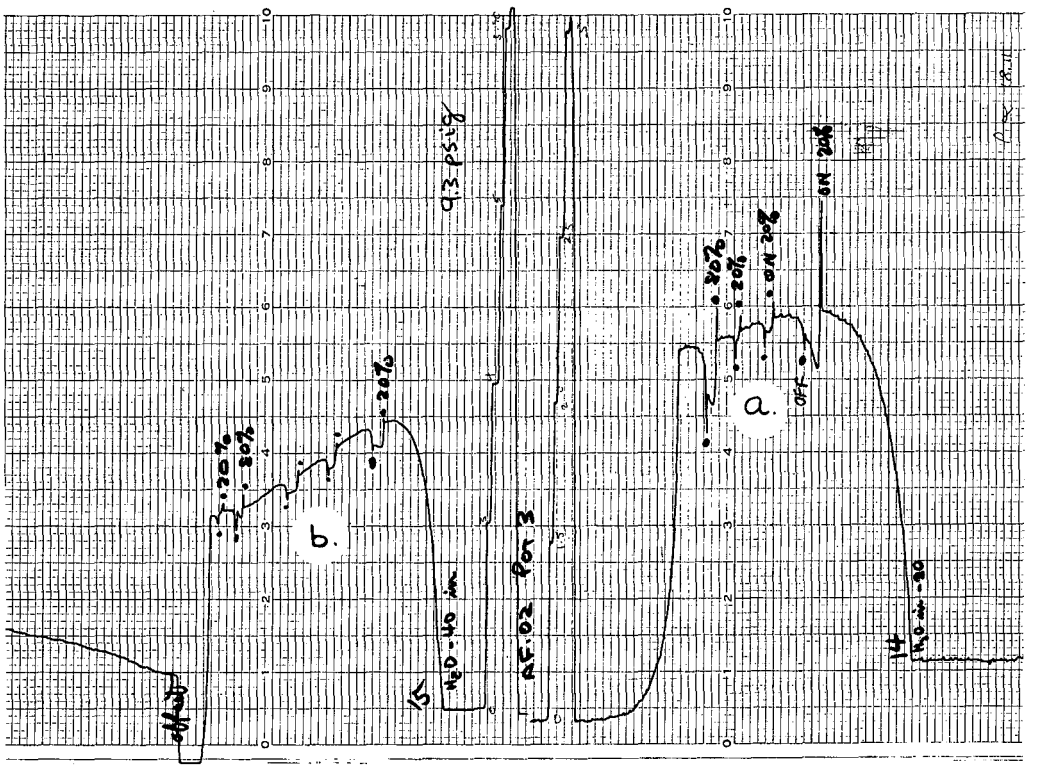

MU-35476

Fig. 53. Response of water-cooled WHG No. 1 [125 holes, (a) 0.73 mtorr and (b) 2.40 mtorr full scale] to the actions of operating the 50-MHz oscillator at 20% and 80% dial settings after adding > 0.5% water to the hydrogen gas. These curves show that water has no effect on the yield of atoms from the discharge. P = 82 mtorr and t = 20 sec/small div (right to left). (February 3, 1965).

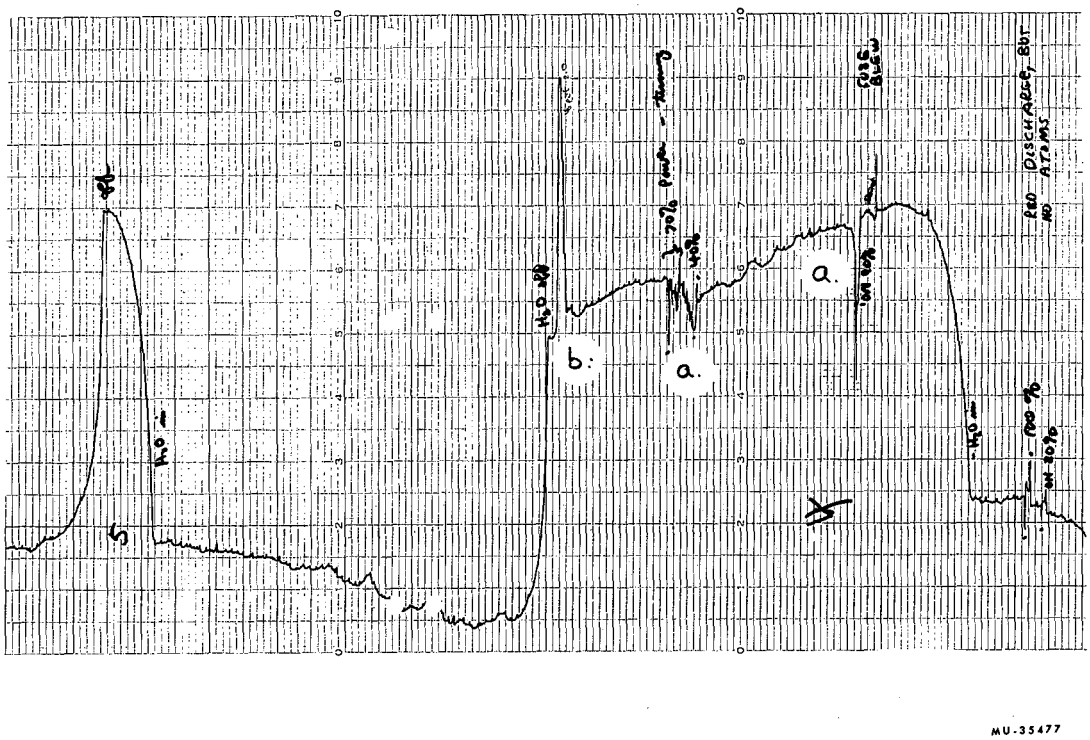

Fig. 54. Response of water-cooled WHG No. 1 (125 holes, about 0.5 mtorr full scale) to the actions of (a) operating the 50-MHz oscillator at 40%, 70%, and 90% dial settings after adding > 0.16% water to the hydrogen gas, and (b) electrostatically applying a 0.25 mtorr "pressure" pulse. The curve shows that water has no effect on the yield of atoms from the discharge. P = 78 mtorr and t = 20 sec/small div (right to left). (February 1, 1965).

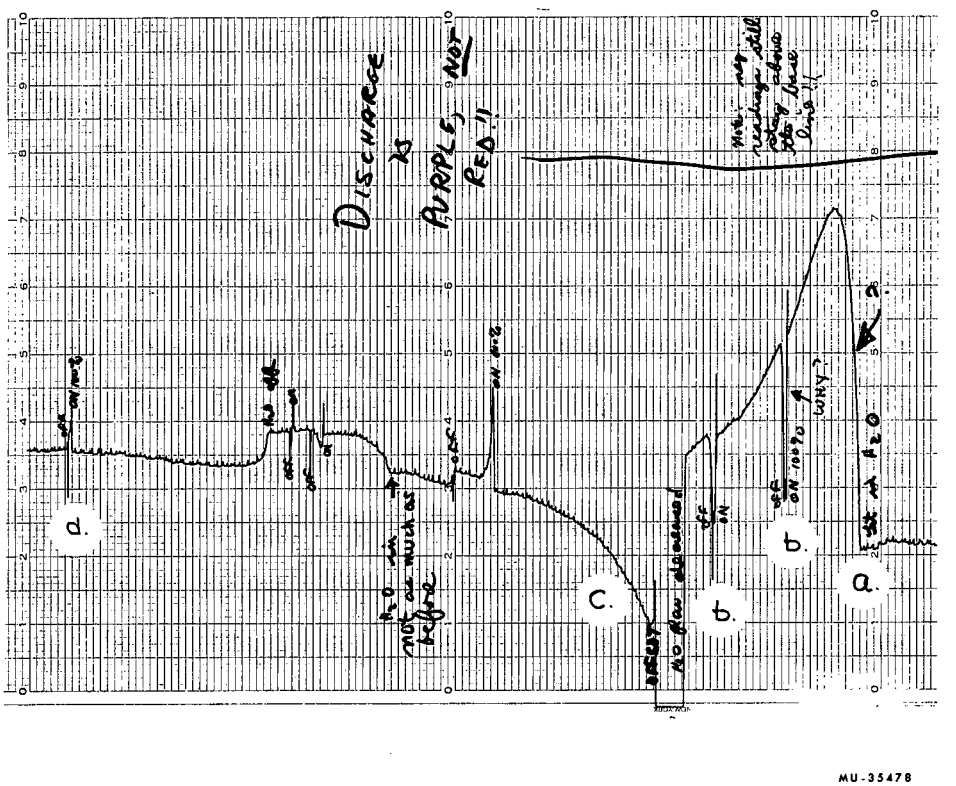

Fig. 55. Response of non-water-cooled WHG (125 holes, about 0.5 mtorr full scale) to the actions of (a) adding water to the hydrogen gas, (b) operating the 50-MHz discharge at a 100% dial setting, (c) allowing the drifting baseline to stabilize, and (d) operating the discharge at 100% in pure hydrogen. Though the behavior at points (b) is strange, these curves still show that water has little effect on the yield of atoms from the discharge. P = approx 100 mtorr and t = 20 sec/small div (right to left). (January 25, 1965).

level of the WHG when it was added in small quantities to the hydrogen gas in the flow-tube system in the absence of a discharge. This observation led to the untested hypothesis that all molecules having an appreciable dipole moment will give the same effect as for H_2O and HCl. As with H_2O, the addition of HCl failed to affect hydrogen-atom yield from the discharge (Fig. 56).

4. Effect of O_2

The apparatus and experimental procedure were the same as for H_2O and HCl with the important exception that the Decker micromanometer was successfully used to monitor the oxygen flow rate from a bulb of known volume.

The addition of molecular oxygen to the initially pure hydrogen gas did not produce the strange effect in the absence of a discharge characteristic of water and also HCl. Instead, the WHG reading decayed immediately back to the zero base line after a pulse characteristic of the addition of H_2 gas to the system (Fig. 42).

The quantitative effect of oxygen on the yield of hydrogen atoms was measured by the same procedure used to clean the system initially. The discharge was successively pulsed for 1 minute durations at 3 minute intervals. This procedure was repeated several times for each oxygen-concentration level ranging between the values

$$0.00 \leq \frac{c_{O_2}}{c_{H_2}} \leq 0.16 \quad .$$

Samples of the recorder readings are given in Figs. 57 to 60 and the results plotted in Figs. 61 to 63. All concentration values, whether of the oxygen or of the atomic hydrogen, are given as a fraction of the total concentration of molecular hydrogen present in the entering gas.

In these experiments I had no way to prove that the atoms measured by the WHG were exclusively of hydrogen. Unlike an electron-spin resonance or a mass spectrometer, the WHG cannot distinguish between types of atoms.

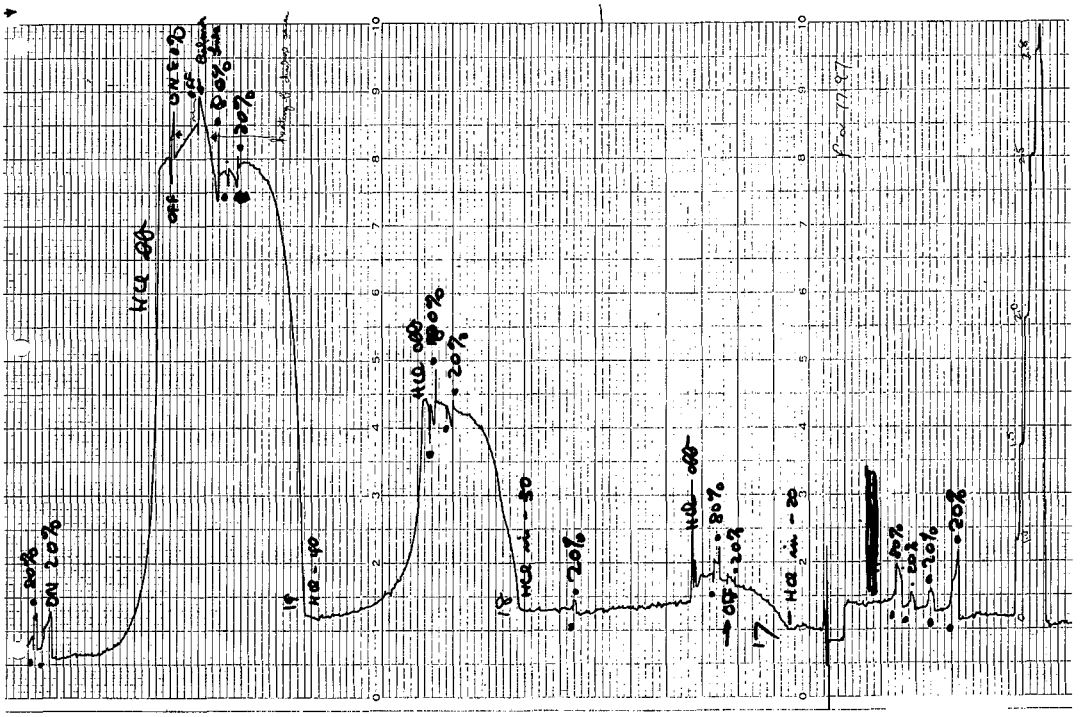

Fig. 56. Response of water-cooled WHG No. 1 (125 holes, 0.59 mtorr full scale) to the actions of adding progressively larger amounts of HCl gas and trying to produce atomic hydrogen with a 50-MHz discharge. The curves demonstrate that the HCl has no effect on the yield of atoms and that the percent dissociation in pure hydrogen is small (0.1%). P = 81 mtorr and t = 20 sec/small div (right to left). (February 2, 1965).

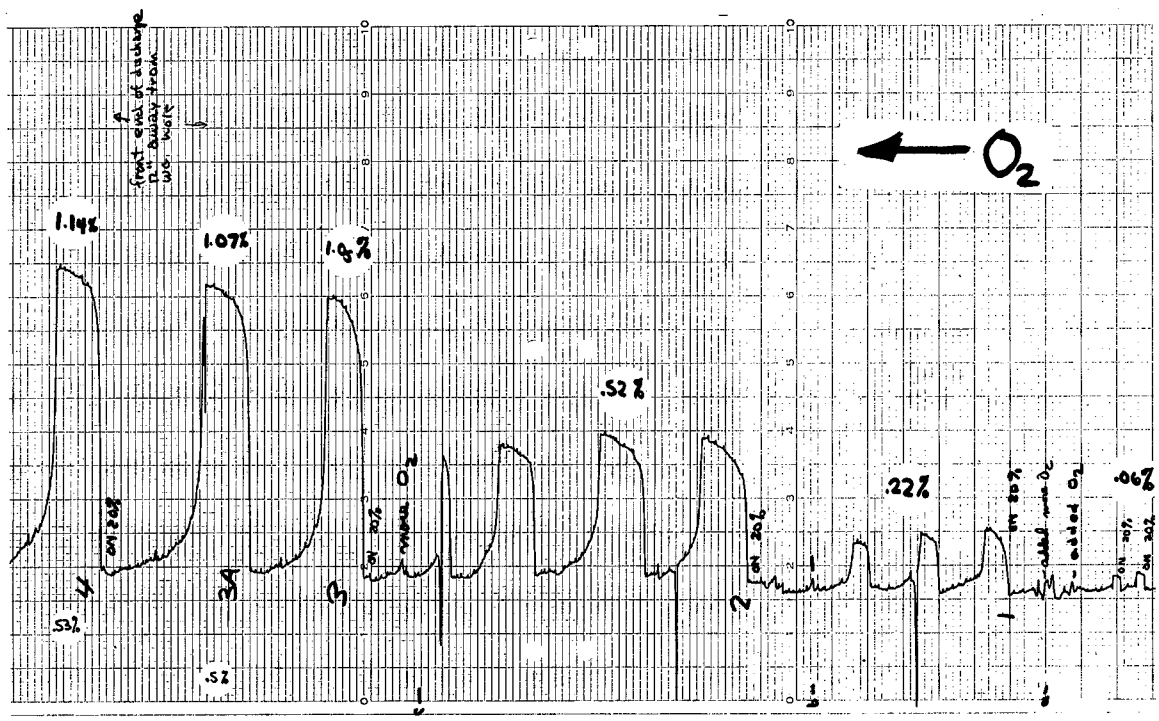

Fig. 57. Response of water-cooled WHG No. 1 (125 holes, 0.58 mtorr full scale) to 50-MHz discharge pulses (20% dial setting) with successively increasing quantities of O_2 added to the hydrogen gas. The top and bottom figures show the measured atom concentration and the amount of O_2 added, respectively. The yield of atoms in pure hydrogen is very low (0.06%). P=79 mtorr, $v_z \approx 72$ cm/sec, and t = 20 sec/small div (right to left). (January 31, 1965).

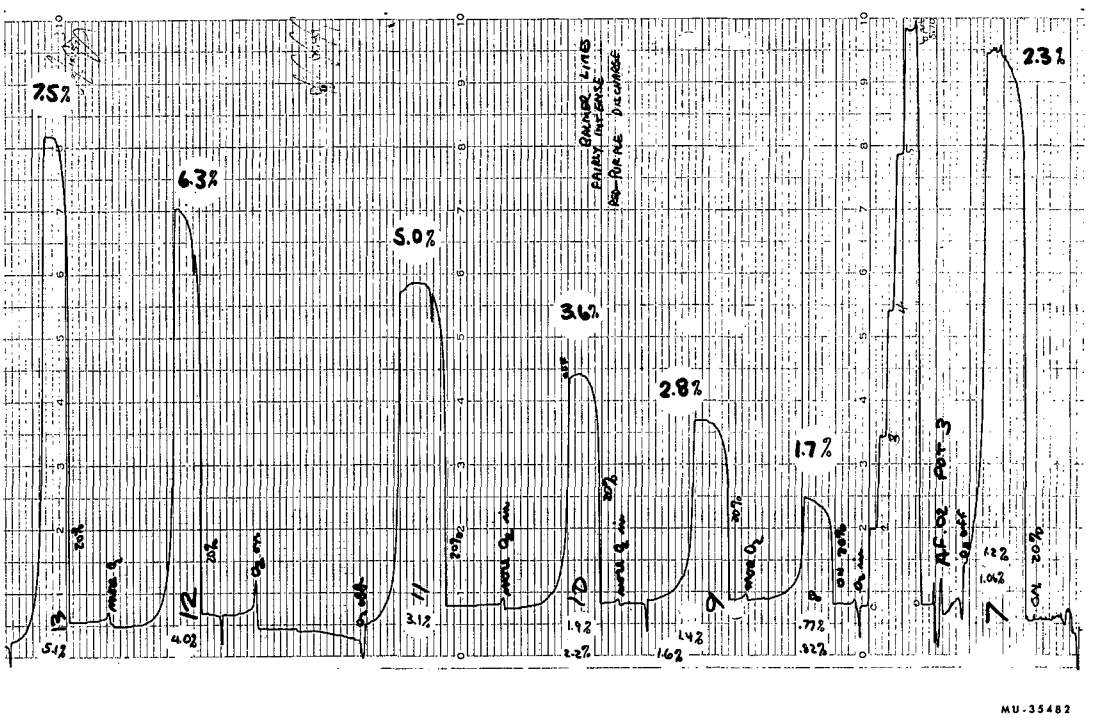

Fig. 58. Response of water-cooled WHG No. 1 (125 holes, 2.30 mtorr full scale) to 50-MHz discharge pulses (20% dial setting) with successively increasing quantities of O_2 added to the hydrogen gas. The top and bottom figures show the measured atom concentration and the amount of O_2 added, respectively. The step-like curve between peaks Nos. 7 and 8 is an electrostatic calibration curve for the pressure transducer. P = 79 mtorr H_2, $v_z \approx 72$ cm/sec, and t = 20 sec/small div (right to left). (January 31, 1965).

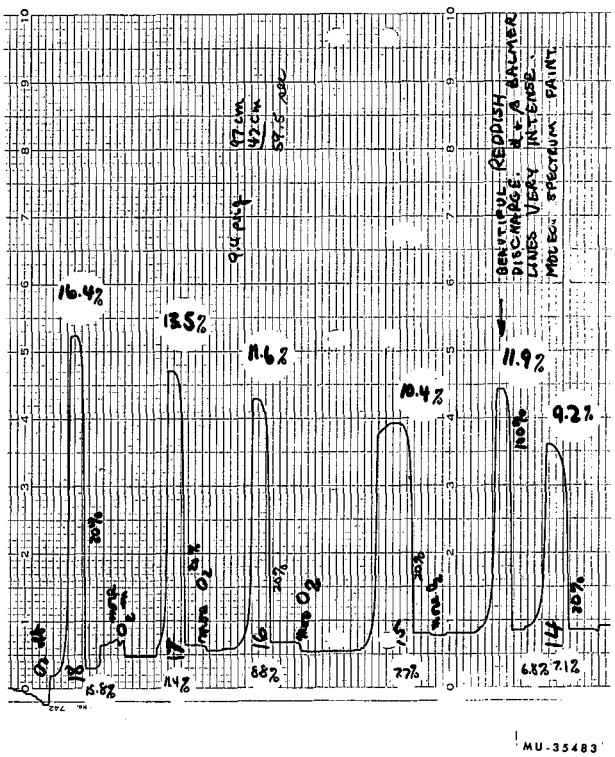

Fig. 59. Response of water-cooled WHG No. 1 (125 holes, 7.70 mtorr full scale) to 50-MHz discharge pulses (20% dial setting) with successively increasing quantities of O_2 added to the hydrogen gas. The top and bottom figures show the measured atom concentration and the amount of O_2 added, respectively. The discharge was an intense and beautiful crimson and the yield of atoms (16.4%) was the highest of all the experiments with low-pressure atomic hydrogen. P = 79 mtorr H_2, $v_z \approx 72$ cm/sec, and t = 20 sec/small div (right to left). (January 31, 1965).

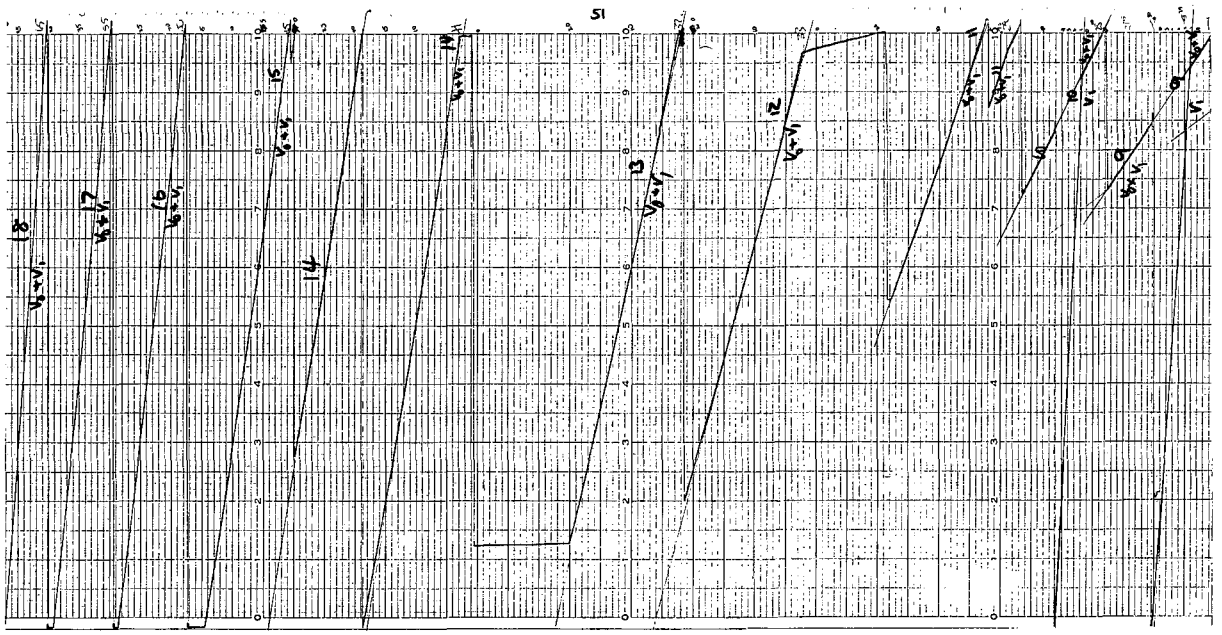

MU-35480

Fig. 60. Typical response of Decker micromanometer (2300 mtorr full scale) to the loss of O_2 from a bulb of known volume (V_1 = 44 cm^3 and $V_o + V_1$ = 537 cm^3). These curves show the O_2 flow rate into the vacuum system and consequently the mole fraction of O_2 in the hydrogen gas. Slopes Nos. 9 to 18 correspond to the discharge peaks Nos. 9 to 18 (2.8% to 16.4% atom yield) in Figs. 58 and 59. t = 20 sec/small div (right to left). (January 31, 1965).

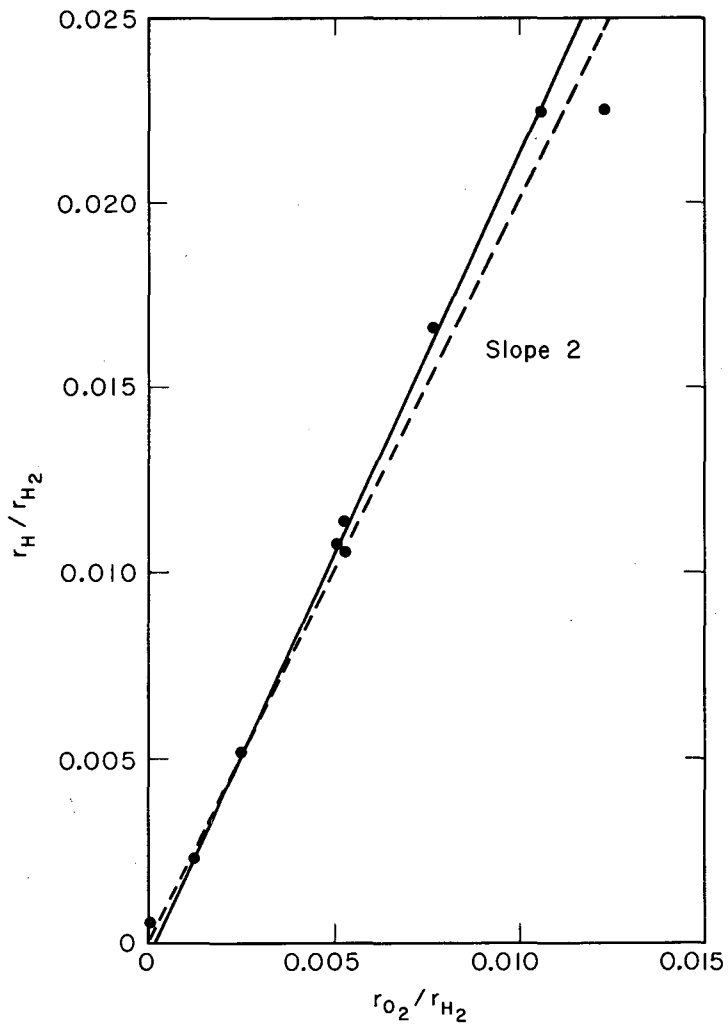

Fig. 61. The effect of low O_2 flow rates on the yield of atoms from a low-pressure (80 mtorr H_2) 50-MHz discharge (20% dial setting). At least two atoms are produced per molecule of O_2 added. The concentrations of H and O_2 are plotted relative to the amount of H_2 in the entering gas stream. (January 31, 1965).

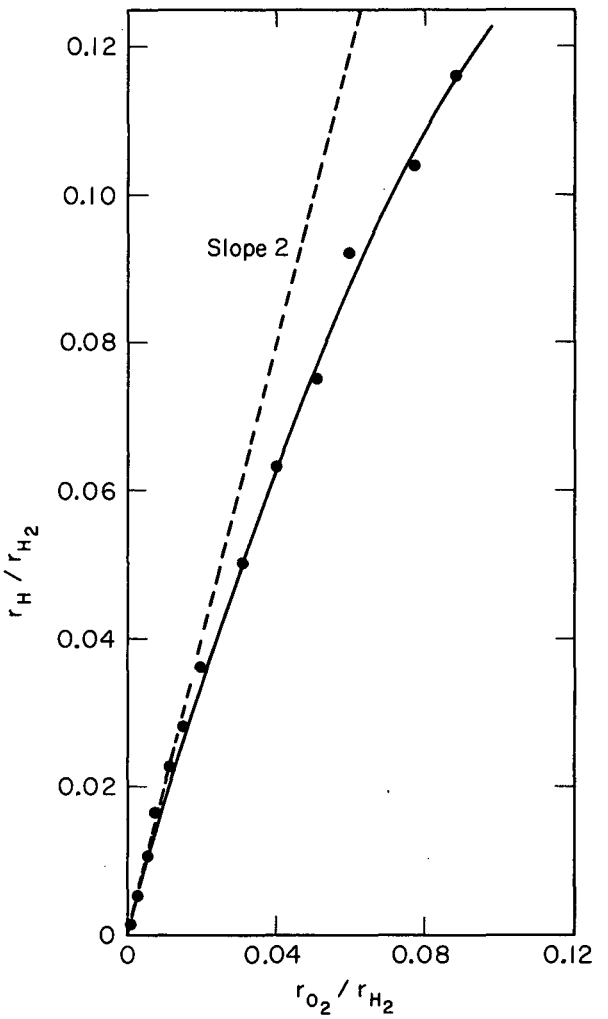

Fig. 62. The effect of high O_2 flow rates on the yield of atoms from a low-pressure (80 mtorr H_2) 50-MHz discharge (20% dial setting). Partial saturation occurs at higher O_2 flow rates. The concentrations of H and O_2 are plotted relative to the amount of H_2 in the entering gas stream. (January 31, 1965).

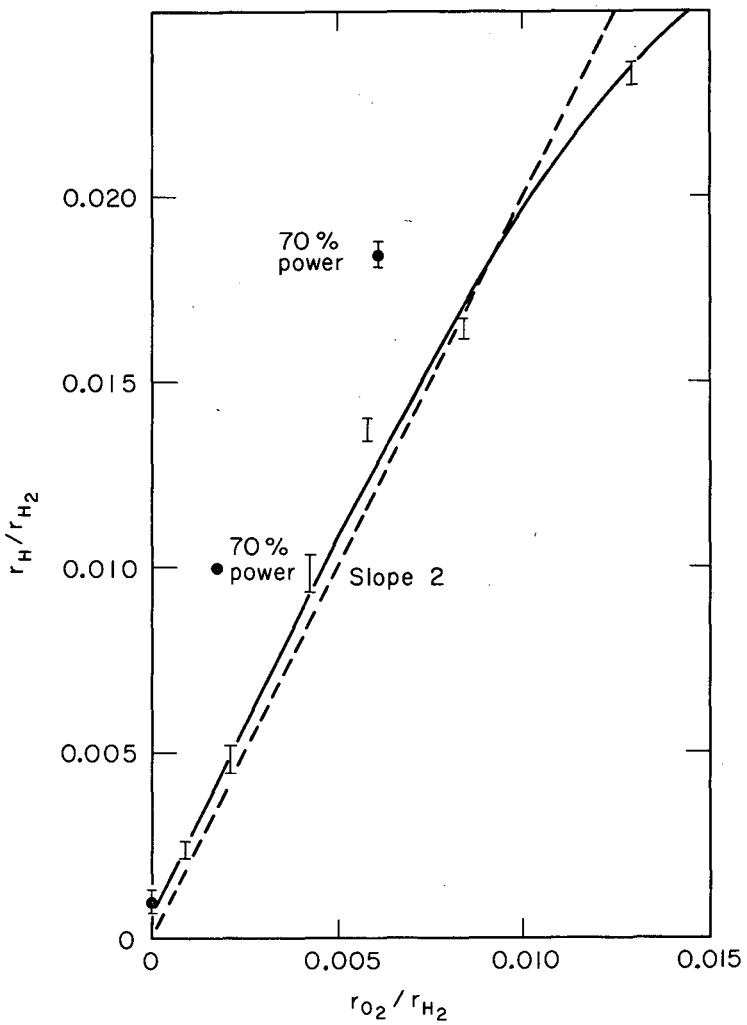

Fig. 63. The effect of low O_2 flow rates on the yield of atoms from a low-pressure (80 mtorr H_2) 50-MHz discharge (20% dial setting). The points corresponding to a 70% dial setting on the 50-MHz oscillator indicate that the stoichiometric ratio of two atoms per O_2 molecule is only a lower limit. The concentration of H and O_2 are plotted relative to the amount of H_2 in the entering gas stream. (February 7, 1965).

5. Effect of N_2

The apparatus and experimental procedure for quantitatively determining the effect of nitrogen on the hydrogen yield from the discharge were identical to the ones described in Sec. V.C.4. In fact, the experiments for oxygen and nitrogen were preformed successively on the same day. The results are similarly given as a group of figures and a graph (Figs. 64-66). Again, I did not prove that hydrogen atoms exclusively were being measured.

6. Project Reorientation

Disagreeing with current practice as well as with a majority of investigators who had previously studied the subject was very disconcerting to me. I had no reason to doubt the reliability of the Wrede-Harteck gauge as a relative atom-concentration measurement device, the purity of the hydrogen gas, the inactivity of the glass walls, the efficiency of the hydrogen discharge, the purity of the water, or any other features of my gas-handling or vacuum system.

Nevertheless, since I was in complete disagreement and probably wrong, I decided to undertake a step-by-step study of every facet of the system until the subtle effect causing the apparent unreactivity of the water was isolated. In making this decision, I implicitly made a value judgement between (a) the original purpose of this research work—to determine the recombination coefficient of atomic hydrogen on various metals—and (b) my strange result for the effect of water in a hydrogen discharge. Considering the widespread use of electrical discharges to produce atoms, I felt that it was much more timely and important to pinpoint that part of the experimental equipment responsible for my seemingly incorrect result.

7. Comparison of Different Hydrogen-Gas Sources

I considered many parts of the experiment as natural starting points for isolating the subtle effect: the gas source, the discharge, the method of adding water, or the measurement device. As the easiest to try was the gas source, it was investigated first.

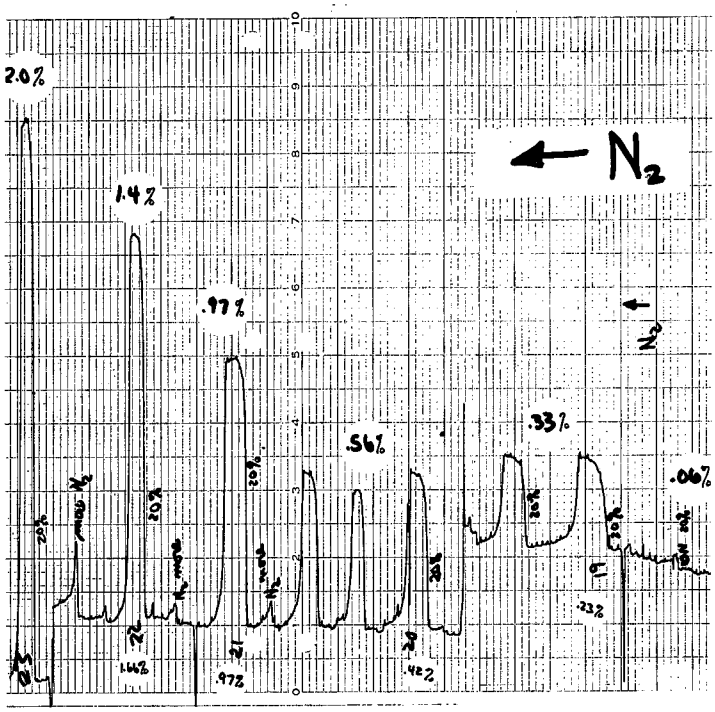

Fig. 64. Response of water-cooled WHG No. 1 (125 holes, 0.57 mtorr full scale) to 50-MHz discharge pulses (20% dial setting) with successively increasing quantities of N_2 added to the hydrogen gas. The top and bottom figures show the measured atom concentration and the amount of N_2 added, respectively. The addition of N_2 had a much smaller effect on the atom concentration than the addition of O_2. P = 79 mtorr H_2, $v_z \approx 72$ cm/sec, and t = 20 sec/small div (right to left). (January 31, 1965).

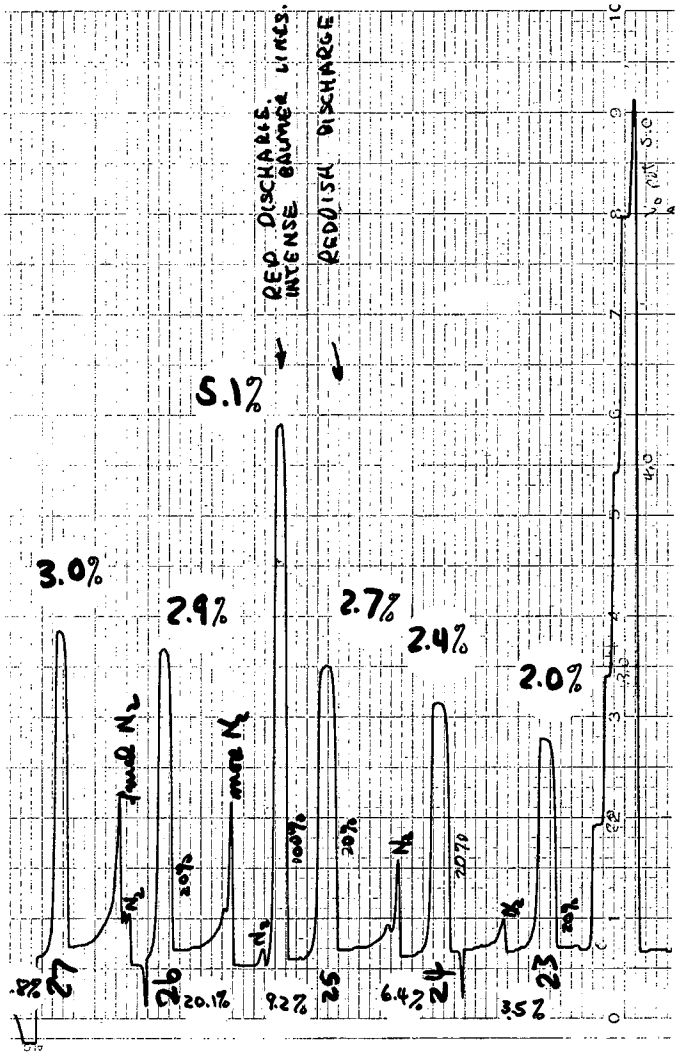

Fig. 65. Response of water-cooled WHG No. 1 (125 holes, 2.20 mtorr full scale) to 50-MHz discharge pulses (20% dial setting) with successively increasing quantities of N_2 added to the hydrogen gas. The top and bottom figures show the measured atom concentration and the amount of N_2 added, respectively. The step-like curve on the right is an electrostatic calibration curve for the pressure transducer. The highest peak corresponds to 9.2% N_2 added and 5.1% atoms. The nitrogen effect begins to saturate at low N_2 concentrations. P = 79 mtorr, $v_z \approx 72$ cm/sec, and t = 20 sec/small div (right to left). (January 31, 1965).

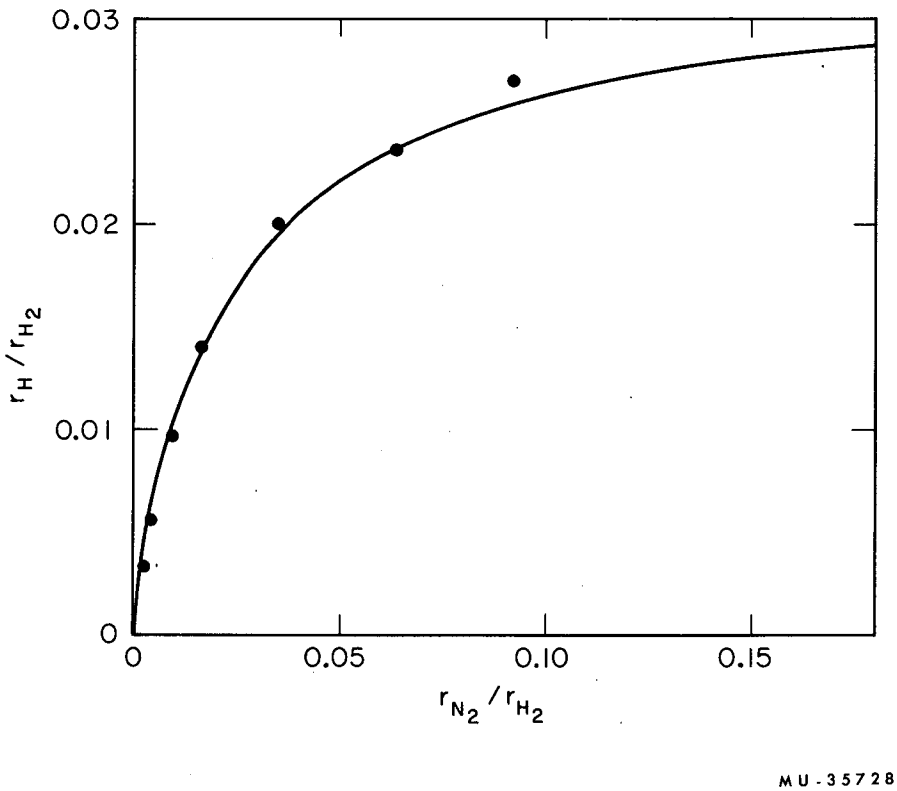

Fig. 66. The effect of high N_2 flow rates on the yield of atoms from a low-pressure (80 mtorr H_2) 50-MHz discharge (20% dial setting). The pronounced saturation and the low yield of atoms per N_2 molecule show that N_2 is much less effective than O_2. The concentrations of H and N_2 are plotted relative to the amount of H_2 in the entering gas stream. (January 31, 1965).

Cylinder hydrogen gas (Liquid Carbonic Company, rated at 99.99+ % with $N_+ < 3$ ppm, $O_2 < 1$ ppm, $H_2O < 1$ ppm, hydrocarbons < 0.5 ppm, dew point -105°F) was used as a substitute for the Englehard purified hydrogen gas. During these early experiments the Fischer and Porter flowmeter was thoroughly flushed with the cylinder hydrogen before the system was allowed to equilibrate at a pressure of about 75 mtorr. Except for this flushing, all other aspects of the system were exactly the same as mentioned above. Since the sapphire flowmeter ball was very low on the scale, no hydrogen flow-rate measurements were possible.

The result was exactly the same as before. Water had no effect other than the strange one of increasing the signal level in the absence of the discharge. The discharge color was the same—pinkish white. Oxygen had its usual effect of increasing the atom yield and changing the discharge color to a light crimson. No quantitative measurements were made on the oxygen-in-hydrogen system as there was nothing different about the qualitative results observed on the recorder charts. Nitrogen and HCl were presumed to have their usual effects and were not tried.

It was certainly important to thoroughly flush the F. and P. flowmeter prior to the experiments. The rotameter was leaky, and when I did not flush it well, I observed the startling and quite definitive results described in Sec. V.C.9.

8. Comparison of Different Discharge Methods

Since the gas was not responsible for the behavior difference of water in my system, I next decided to try two discharge methods simultaneously: the microwave discharge and an electrodeless discharge from an eight-turn copper coil and a 500-W 50-MHz oscillator. The experiments were performed with pure hydrogen, hydrogen containing oxygen as an impurity, and hydrogen containing water as an impurity [Fig. 76(a)]. The power transmitted to the discharge by these separate power supplies was never measured. Instead, the entire range of power settings was tried for each transmitter.

There was no difference between either discharge source for the yield of atomic hydrogen, as measured by the WHG. The 2.45-GHz (microwave) discharge was hotter, visually more intense, and more confined than the 50-MHz discharge (Fig. 68).

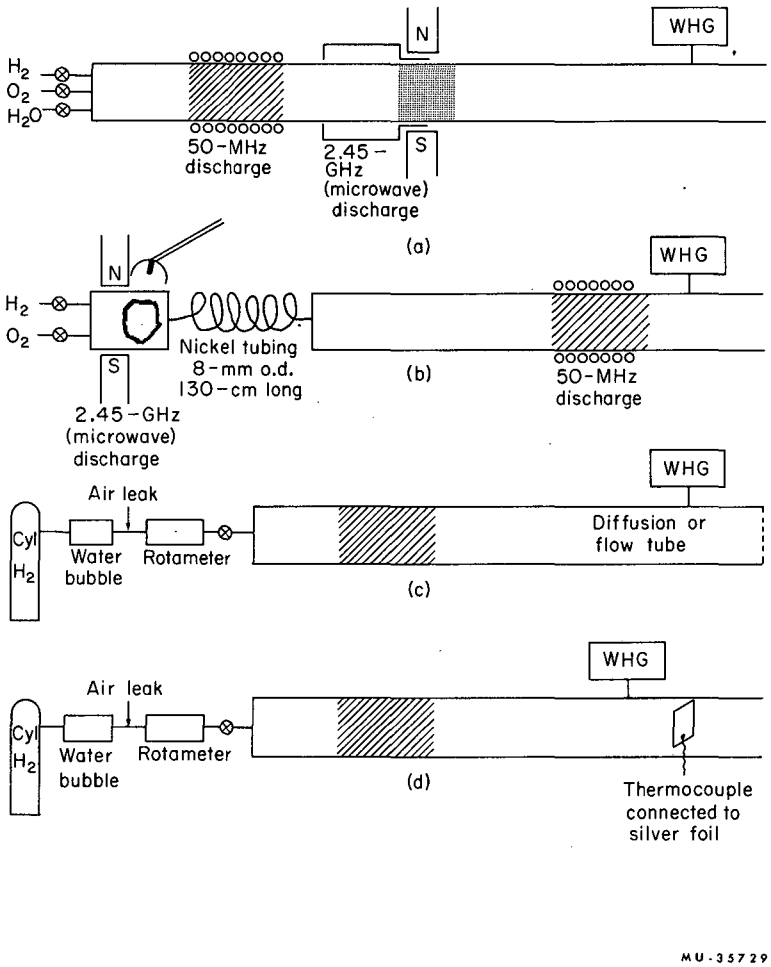

Fig. 67. Schematic drawing showing four critical experiments to determine the effect of water on the yield of atomic hydrogen from a low-pressure discharge: (a) the effect of different discharges; (b) the effect of the upstream conversion of oxygen to water; (c) the effects of cylinder hydrogen, a water bubbler, and an air leak in the rotameter; and (d) the response of different measurement devices to the effect of water.

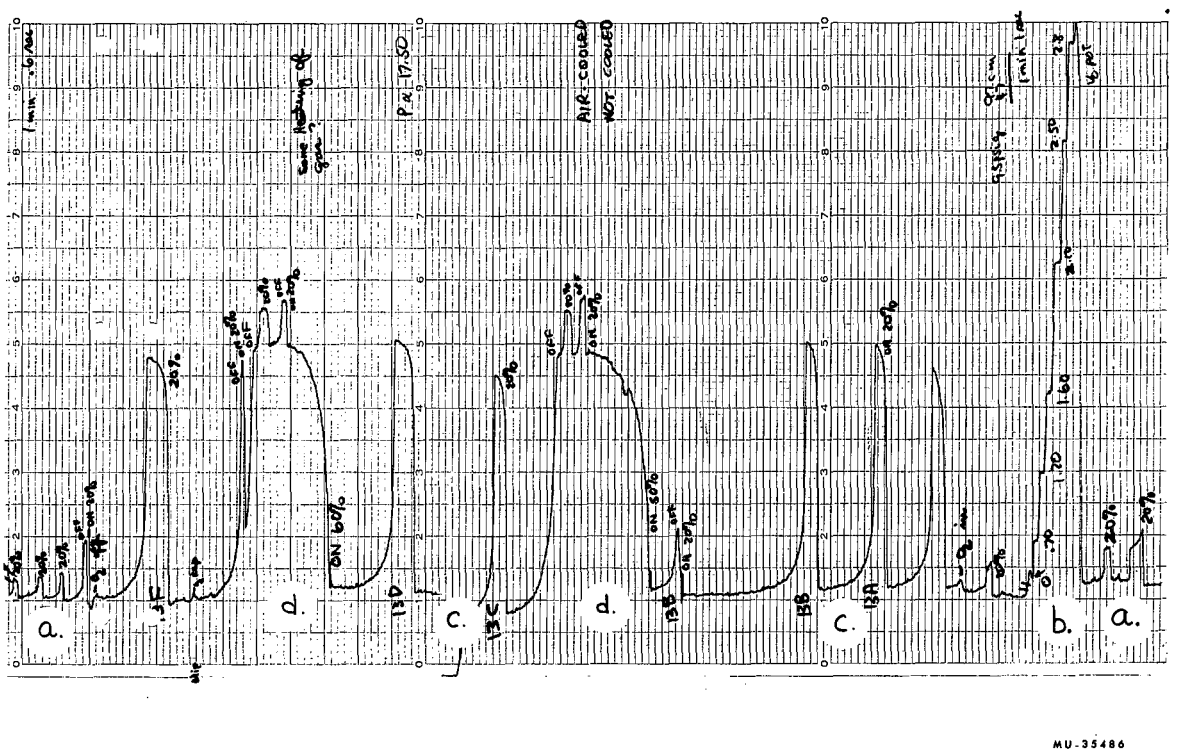

Fig. 68. Response of water-cooled WHG No. 1 (125 holes, 0.59 mtorr full scale) to (a) a downstream 50-MHz discharge (20% dial setting) in pure H_2, (b) an electrostatic calibration of the pressure transducer, (c) a downstream 50-MHz discharge in the presence of 0.50% O_2. The percent dissociation is (a) 0.13%; (c) 1.0%; and (d) 1.0% with only the microwave discharge or 1.2% with both discharges on simultaneously. The velocity in the 8-mm o.d. 45-foot long catalytic tube is so fast (1000 cm/sec) that it has little effect on the atom concentration produced by the upstream discharge. P = 73 mtorr and t = 20 sec/small div (right to left). (February 6, 1965).

Later, a small-diameter cavity was used to produce a very intense discharge in the 14-mm-o.d. quartz tube located 85-cm upstream from the WHG port hole. The results were identical with the ones mentioned in the two preceding paragraphs, despite the more efficient coupling of the microwave power to the discharge.

The color of this small-cavity discharge was an unreliable indication of the atom concentration measured by the WHG. With low oxygen impurity concentrations and high microwave power settings, the discharge color appeared to be about the same as for high oxygen concentration and and low microwave power settings. For either extreme—pure hydrogen and low microwave power settings or high oxygen impurity concentrations and high microwave power settings—the discharge colors were quite different: pinkish white and crimson, respectively. These results did not conflict with those of investigators who have passively used hydrogen discharges with or without water for the production of atomic hydrogen in low-pressure systems. For many of them, discharge color was their only indication for the amount of atomic hydrogen present.

Near the end of the experiments I borrowed a slotted line from Vincent J. Honey to measure the standing-wave ratios for the microwave energy transmitted and reflected from the small cavity. By means of careful tuning and adjustment, a standing-wave ratio of 1.6 could be obtained. In typical operation, this ratio was between 5 and 20, depending on the care exercised in the tuning procedure. Although I could easily have spent more time on this aspect and improved these figures, I didn't need to do so because I had power to spare.

All of these results indicated that the cyclotron-resonant microwave discharge did not differ from other discharges from the standpoint of the yield of atomic hydrogen.

I would like to stress the advantages of using such a discharge. The diathermy unit was inexpensive, portable, simple to operate and tune, quite reliable and rugged, and usually did not interfere electronically with other equipment. The use of a large magnetron magnet producing an inhomogeneous magnetic field instead of an electromagnet producing a

more uniform field eliminated unnecessary complexity and made the use of a Tesla coil to start the discharge unnecessary. By far, the biggest single advantage was that very low microwave power settings were used. With 75% reflected microwave power, stable discharges below-100 mtorr pressure were maintained with as little as 250 mW. Again with 75% reflected power, power levels exceeding 2.5 W in the discharge were rarely needed for the experiments. These properties should be important when cool operation of the discharge is required or when an ESR spectrometer is used to measure atom concentrations.

9. Effect of Water and Air: Use of a Water Bubbler

Because most previous investigators have used a water bubbler to add 2 to 3% water to hydrogen gas, I next decided to construct and operate such a bubbler [Figs. 11 and 67(c)]. Even though I had used distilled water in my previous experiments, I felt that there was a chance that while on the rack it had become contaminated in some strange and mysterious way.

When the bubbler was used, the WHG signal never showed the strange water effect in the absence of a discharge, because water was always present: during the flushing of the rotameter and bubbler, equilibration of the system, the experiments, and re-evacuation of the system. The large liquid-nitrogen trap in front of the Kinney KC-5 pump was kept full to minimize the contamination of the pump oil by water.

The ambient room temperature was typically 24°C and the hydrogen pressure within the water bubbler was usually about 830 torr. Thus, if the hydrogen gas was thoroughly equilibrated with the water, about 2.6% water would have been present. I made no measurements to determine if this were true.

Both the F. and P. rotameter and the water bubbler were first thoroughly flushed with hydrogen gas. The vacuum system was then allowed to equilibrate and the experiments were done in a manner similar to that described in Sec. V.C.2.

The results were exactly the same: water had a negligible effect on the atom yield from the microwave discharges, which were located between

3 and 8 inches upstream from the WHG port hole. This negligible effect was very disturbing, but at least it was consistent with my previous measurements with water.

A revealing series of experiments was next stimulated by my inability to repeat the water-bubbler experiments before an interested friend, Dr. Norman Edelstein.[36] After leaving the system alone over the weekend, I tried to quickly repeat the water-bubbler experiment and flushed the bubbler and rotameter only slightly. When I turned on the discharge the first time, he observed a high concentration of atoms as measured by the WHG, a beautiful crimson discharge, and a crimson-faced graduate student. Upon prolonged operation, the color of the discharge gradually changed to a whitish purple the WHG atom concentration decreased, and the color of the graduate-students' face returned to normal.

The next day, with reaction tube No. 1 set up as a diffusion tube (no flow of gasses through the tube), I successfully repeated the previous day's observations. By pulsing the microwave discharge for approximately one-minute at several-minute intervals, I was able to follow the gradual decline in the atom-concentration level at a constant power setting (Fig. 69).

Suspecting an air leak in either the bubbler or the rotameter, I opened a connecting fitting, let some air into the bubbler, closed the fitting again, and repeated the experiment. The result was the same: I observed the gradual flushing of the accumulated air in the rotameter and bubbler by watching the decrease in the atom-concentration level with time (Fig. 70). I repeated this procedure a third time, but this time I left the discharge on rather than pulse it. The results were again the same (Fig. 71). When the rotameter and bubbler were next completely flushed with hydrogen, the WHG signal decreased to a very low level.

This experiment was subsequently repeated many times, and understandably was favorite of mine for demonstrating changes in other parts of the system. The effects of (a) different discharges, (b) another measurement technique, (c) two WHG's operated simultaneously, (d) flow-tube and diffusion-tube operation, (e) and different reaction tubes

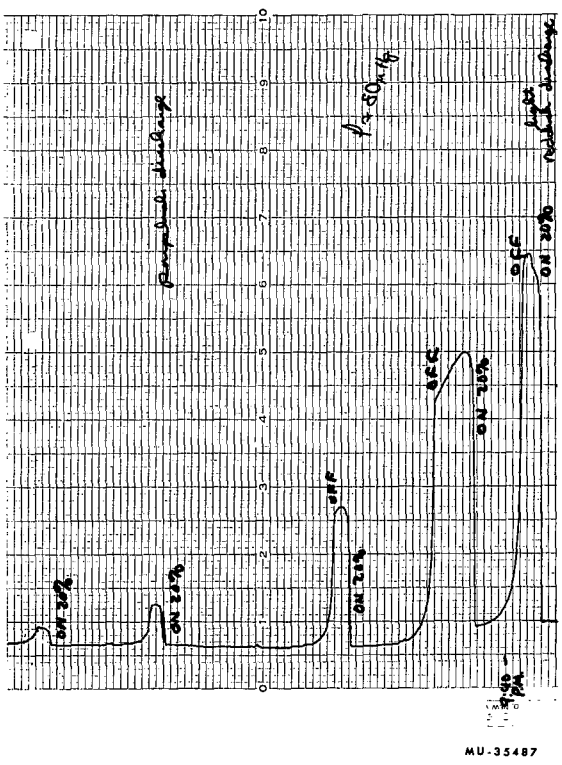

Fig. 69. Response of water-cooled WHG No. 1 (125 holes, 2.0 mtorr full scale) to cylinder hydrogen contaminated with air (due to an air leak in the rotameter). The process of gradually flushing the air from the rotameter and water bubbler decreases the atom yield (50-MHz discharge) and changes the discharge color from red to purplish white. This change shows that water has no effect on the yield of atoms from the low-pressure discharge. P = about 80 mtorr in the diffusion tube and t = 20 sec/small div (right to left). (January 29, 1965).

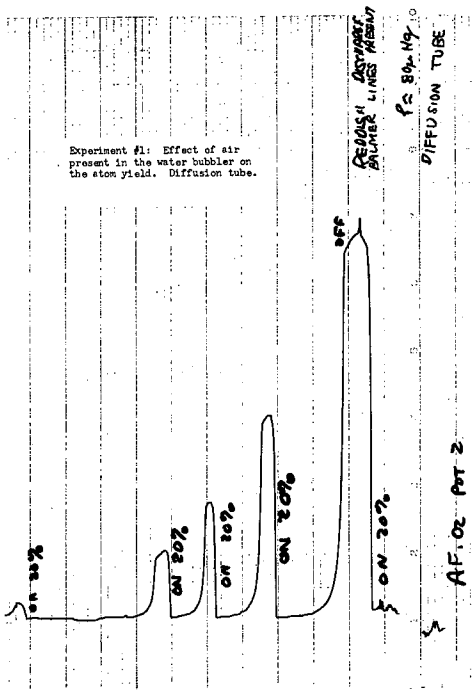

Fig. 70. Curve (similar to Fig. 69) resulting from the deliberate addition of air to the hydrogen in the water bubbler. The smallest peak corresponds to 0.17% atoms. In Figs. 69 and 70, the measured and theoretical time constants for flushing a gas from the water bubbler are both about 20 min. P = about 80 mtorr in the diffusion tube and t = 20 sec/small div (right to left). (January 29, 1965).

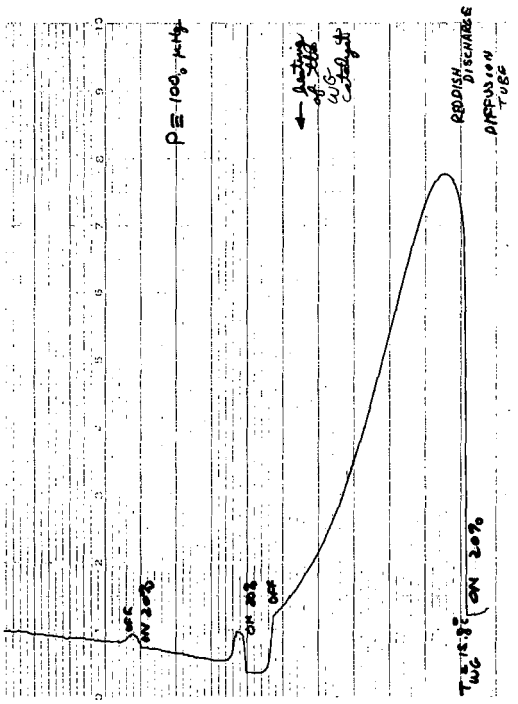

Fig. 71. Curve (similar to Figs. 69 and 70) resulting from the deliberate addition of air to the hydrogen in the water bubbler. The 50-MHz discharge (20% dial setting) was sustained rather than pulsed. The smallest peak corresponds to 0.1% atoms. P = 100 mtorr in the diffusion tube and t = 20 sec/small div (right to left). (January 29, 1965).

were all investigated with cylinder hydrogen, the leaky rotameter, and the water bubbler. In all cases, the result was exactly the same: the atom concentration decreased with time to a very low level as the air was flushed from the bubbler and rotameter (Figs. 72 and 73).

Because the water in the bubbler never seemed to have any effect on the atom yield from the discharges, I never tried to heat or cool it in order to vary the concentration of water in the entering hydrogen-gas stream.

This experiment—demonstrating the simultaneous and independent behavior of air and water in the entering hydrogen-gas stream—was very important because it refuted two arguments:

a. Water was somehow adversely affecting the WHG;
b. Although oxygen could oxidize and remove hydrocarbon impurities that influenced the atom yield from the discharge, water could not.

Further experiments to demonstrate that the effects of air and water on the atom yield from the discharges were completely superimposable are described in Sec. V.C.10.

10. Upstream Conversion of Oxygen to Water

By this time, my excitement and mystification over the course of the experiments was understandably pronounced. I had previously tried adding water (formed by the reaction of a stoichiometric low-pressure mixture of hydrogen and oxygen in a closed volume) to the pure hydrogen gas stream. The water produced in this fashion also had no effect on the atom yield. So, I was not able to show by any of three different methods that water had any effect on increasing the yield of atomic hydrogen from either a microwave or a 50-MHz discharge at a pressure level of about 75 mtorr.

The two different discharge methods that acted similarly made it possible for me to further examine the effect on the yield of atoms of varying ratios of oxygen and water. The concept of the experiment was simple: add pure oxygen to the hydrogen gas stream, convert the oxygen to water far upstream with one of the discharge methods, recombine the atoms produced, and finally, try to produce atoms with the

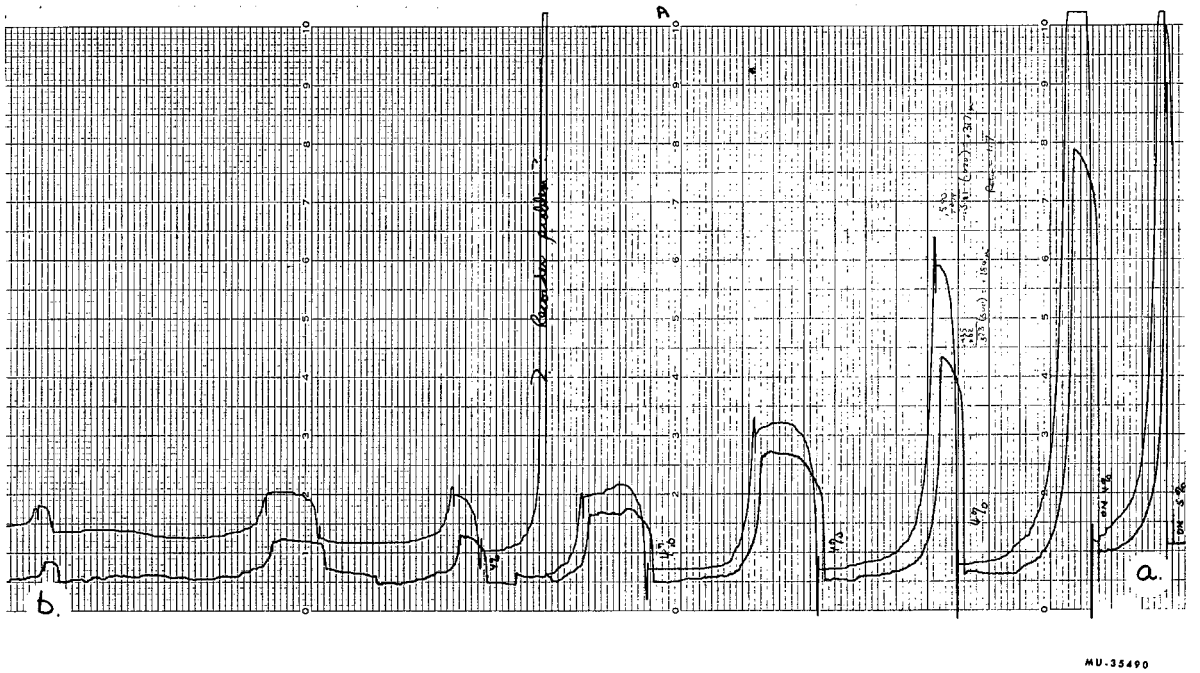

Fig. 72. Response of water-cooled WHG No. 1 (split diaphragm, 0.50 mtorr full scale) and WHG No. 2 (10 holes, 0.62 mtorr full scale) to repeated discharge pulses (small microwave-discharge cavity at 4% dial setting located 80 cm upstream from the WHG) and the action of flushing air from the rotameter and water bubbler with a hydrogen-gas stream. These curves confirm Figs. 69 to 71 and demonstrate that the phenomenon is independent of the type of discharge used. P = 55 mtorr and the time from (a) to (b) corresponds to exactly one hour (right to left). (April 2, 1965).

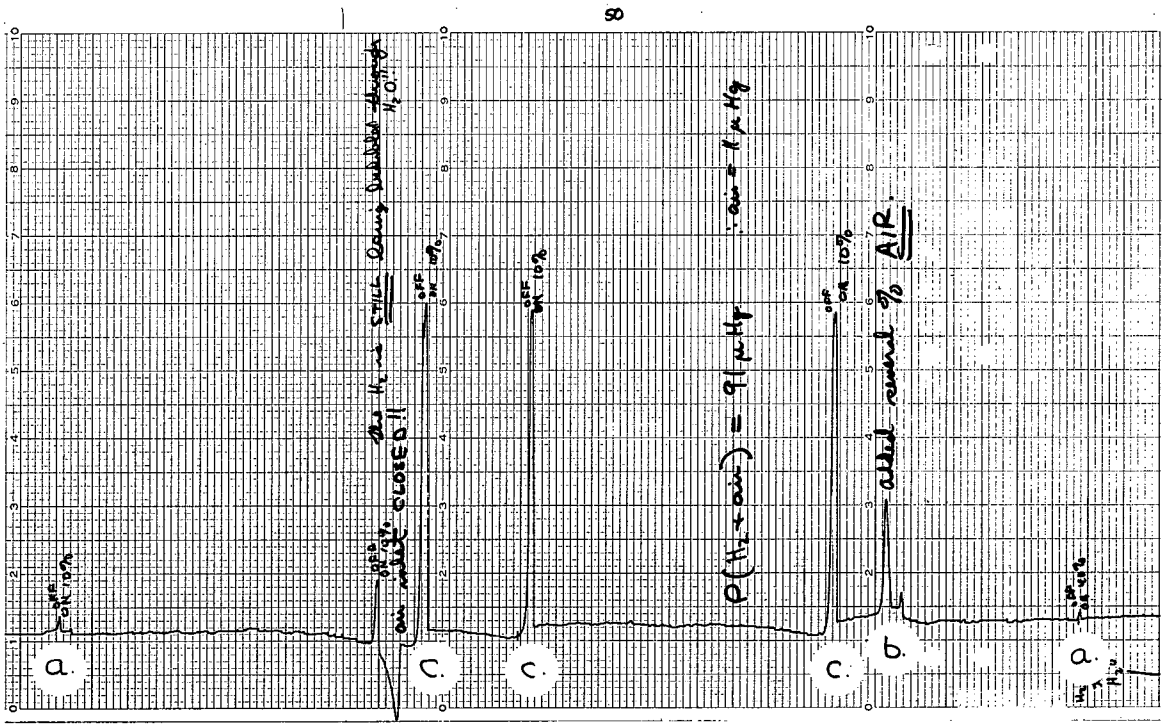

Fig. 73. Response of non-water-cooled WHG (about 100 holes, 0.86 mtorr full scale) to the actions of (a) operating a microwave discharge at a 40% dial setting in H_2 passed through a thoroughly flushed water bubbler, (b) adding some air to the H_2-H_2O gas stream, and (c) operating the discharge (10% dial setting) in the air-H_2-H_2O mixture. The percent dissociation is (a) 0.05% and (c) 1.7%. These curves again demonstrate that water has an effect on the yield of atoms from a low-pressure discharge. P = 80 to 90 mtorr H_2 and t = 20 sec/small div (right to left). (January 19, 1965).

downstream discharge located near the WHG port hole [Fig. 67(b)]. If my previous results on the effect of water and oxygen were valid, then the effect of turning on the far-upstream discharge would be to gradually decrease the yield of atoms coming from the downstream discharge. The initial rate of this process would depend simply on how fast the residual oxygen in the large reaction tube No. 1 would be flushed out. By then turning off the far-upstream discharge, the atom concentration level would gradually increase to its previous level, again at a rate characteristic of the residence time of the water in the large reaction tube.

At the same time, the ratio of the WHG response to water (in the absence of a discharge) and atoms (produced by a discharge) could be measured simply by turning the far-upstream discharge on and noting the change in the WHG signal while the downstream discharge was off. This test assumed that all of the atoms produced by the upstream discharge recombined by the time they reached the WHG.

The experimental apparatus, which was somewhat different than that previously used, consisted of (1) an upstream glass reaction tube and atom recombination tube consisting of copper tubing internally electroplated with nickel (Fig. 12), (2) the diathermy machine fitted with reflector "A" to produce the upstream discharge (Fig. 12), (3) the large magnetron magnet which operated in conjunction with the microwave discharge, (4) reaction tube No. 1, (5) pure hydrogen from the Englehard hydrogen purifier, (6) oxygen gas from a known-volume bulb, (7) the same WHG as used for previous experiments, (8) the same large liquid-nitrogen trap used previously, (9) the McLeod gauge, and (10) the Kinney KC-5 mechanical pump. The system was evacuated overnight and at all times when not in use with the portable diffusion-pump unit.

The experimental procedure was as follows: Equilibrate the vacuum system with pure hydrogen gas; determine the atom concentration produced by the downstream discharge at a fixed power-level setting P_D in the pure hydrogen gas; add the oxygen; redetermine the new atom concentration with the downstream discharge at the same power level setting, P_D; turn off the downstream discharge; turn on the far-upstream discharge

to a chosen power level, P_U; determine the decay in the atom concentration produced by the downstream discharge at power level setting P_D; when the atom concentration is low, turn off the upstream discharge and observe the rise in atom concentration produced by the downstream discharge.

In practice, the downstream discharge was pulsed for 1 minute at approximately 3 minute intervals. The upstream discharge was either off or on continuously, and was cooled with a forceful blast of air.

The experiment worked as planned. The conversion of oxygen to water by the upstream discharge reduced the yield of hydrogen atoms produced by the downstream discharge (Figs. 74 to 76). The results enabled me to demonstrate that the strange water effect on the operation of the WHG was small compared to the response of the WHG to atoms (Figs. 74 and 75).

I repeated the experiment with the modification that the downstream discharge was pulsed only twice, in order to minimize the conversion of oxygen by the discharge to water inside reaction tube No. 1. The results again showed that the upstream discharge was exerting a definite influence on the atom concentration produced by the downstream discharge (Fig. 75).

11. Decay of Atom Concentrations in Diffusion and Flow Tubes

By this time, I had shown that oxygen or nitrogen increased the yield of atoms from a discharge, verified in four different ways that water had little or no effect, and verified that the conversion of oxygen to water resulted in a continuously decreasing atom concentration. I had also demonstrated an air leak in the rotameter used for experiments to determine the effect of a catalytic probe on the atom-concentration distribution in a diffusion tube.

I thus decided to show (a) that the conversion of oxygen to water in a diffusion tube produced the same type of decay curves observed for the catalytic-probe experiments mentioned above and described in Sec. VI, and (b) that such a conversion produced a smaller decay in a fast-flow system typical of that used for determining quantitatively the effect of oxygen and nitrogen on the yield of atomic hydrogen from a discharge.

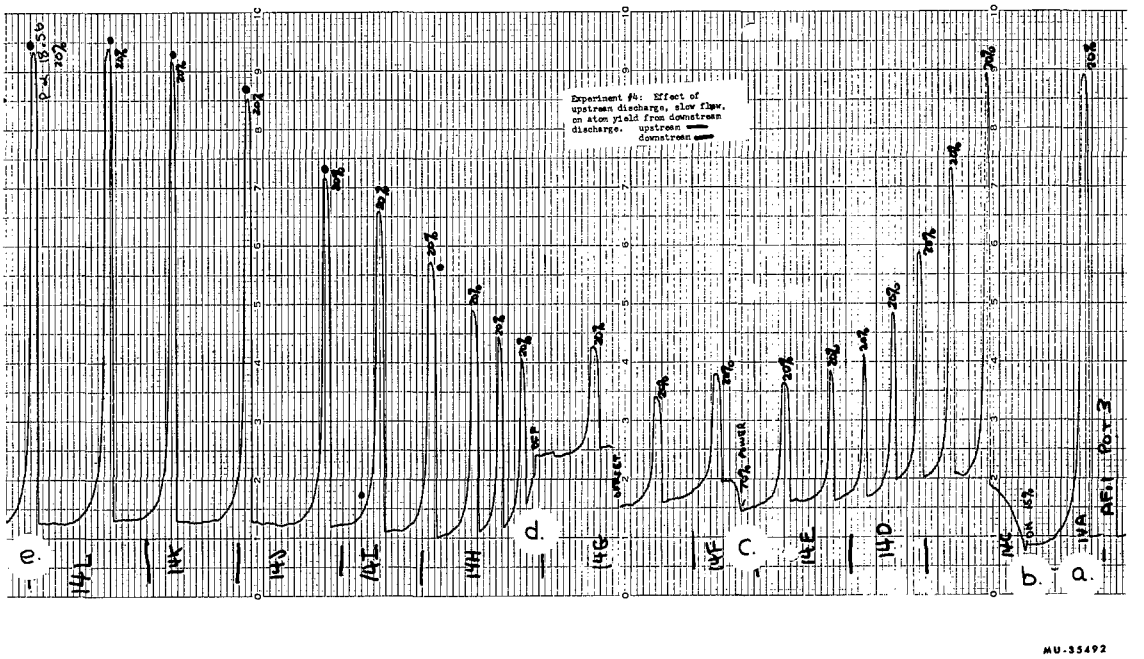

Fig. 74. Response of water-cooled WHG No. 1 (125 holes, 0.59 mtorr full scale) to the actions of (a) pulsing the downstream 50-MHz discharge (20% dial setting) in the presence of 0.9% O_2, (b) turning the upstream microwave discharge in the oxygen-to-water converter on (15% dial setting), (c) increasing the upstream power level to 70%, (d) shutting off the upstream discharge, and (e) demonstrating with a 50-MHz discharge pulse that the atom concentration has returned to its initial level at (a). The decrease in height of the 50-MHz discharge pulses between (a) and (d) demonstrates that the conversion of O_2 to H_2O far upstream gradually eliminates O_2 from the system and reduces the yield of atoms from the downstream discharge. When the upstream discharge is turned off, this effect is reversed between (d) and (e) and the atom yield increases as the entering O_2 displaces the accumulated H_2O from the reaction tube. P = 86 mtorr, v_z = 9 cm/sec, and t = 20 sec/small div (right to left). (February 6, 1965).

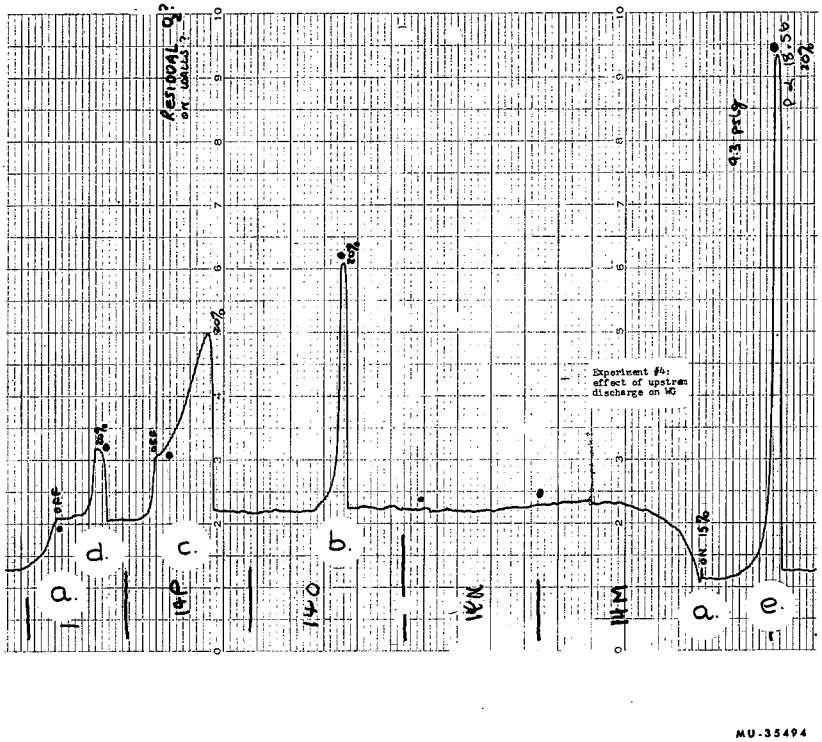

Fig. 75. An experiment similar to that shown in Fig. 74. Points of interest on the recorder tracing are: (e) the atom yield from the downstream 50-MHz discharge in the presence of only O_2, (a) the WHG response to the upstream microwave discharge in the O_2-to-H_2O converter, (b) the atom yield from the 50-MHz discharge after H_2O has displaced part of the O_2 in the reaction tube, (c) the conversion of O_2 to H_2O by the 50-MHz discharge, (d) the decreased yield of atoms, and (a') the action of turning off the upstream discharge. These curves demonstrate that the WHG measures atoms predominantly instead of H_2O and that water has little effect on a low-pressure hydrogen discharge. The measured time constant is 1.7 to 2.4 times the theoretical value for the overall vacuum system of 170 sec (assuming rapid diffusional equilibration of O_2 and H_2O throughout the entire volume, which is estimated to be 16 liters, of the system). P = 86 mtorr, v_z = 9 cm/sec, and t = 20 sec/small div (right to left). (February 6, 1965).

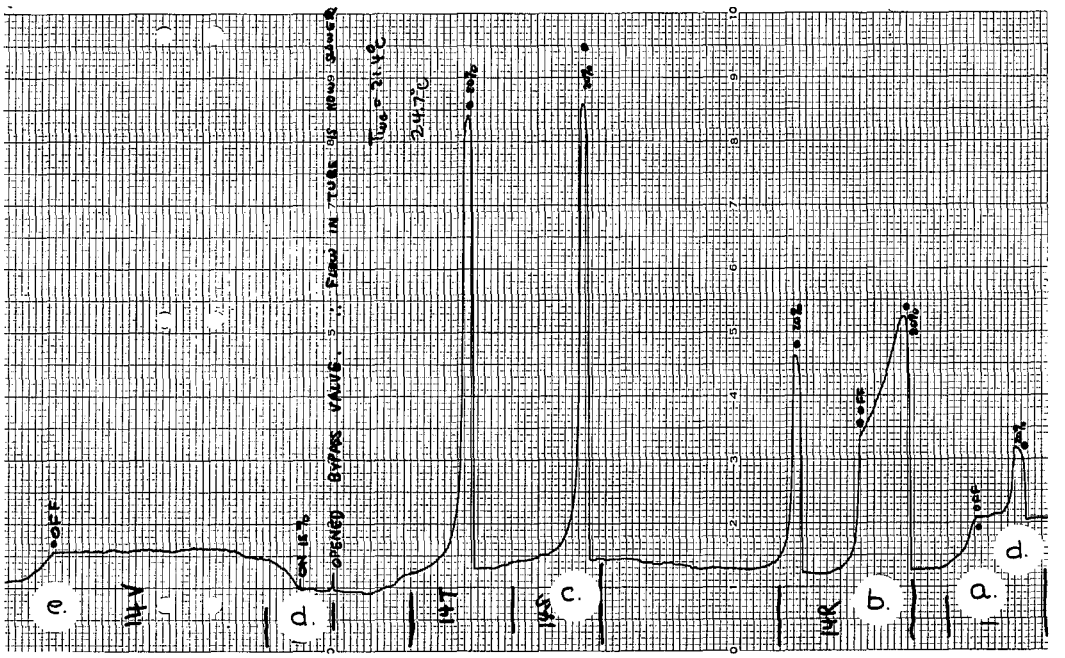

Fig. 76. A recorder-chart tracing continued from Fig. 75. After the upstream microwave discharge is turned off at point (a), the O_2 flushes the accumulated H_2O from the system until the atom concentration produced by the downstream 50-MHz discharge once again reaches its normal value [point (c)]. The small signal between points (d) and (e) shows the effect of the upstream discharge when v_z is decreased by an unknown amount below 9 cm/sec. The fact that this signal is smaller than that produced at point (a) indicates that both are due to atoms transported via convection and diffusion through the 45-foot long catalytic tubing. The measured time constant is larger than the theoretical time constant (170 sec) also. P = 86 mtorr, v_z = 9 cm/sec and less, and t = 20 sec/small div (right to left). (February 6, 1965).

The results for the cases of diffusion, slow flow, and fast flow are shown on recorder charts in Figs. 77 and 78. The curves conclusively show the cause of my troubles with the catalytic-probe measurements: the air leak in the rotameter.

These experiments demonstrated in another way the consistent and reproducible role of oxygen and water. This consistency and reproducibility was hard to explain in any other way. The contrary interpretation of these results based on some mysterious effect is somewhat improbable.

12. Comparison of Different Measurement Methods

As the final experiment in this long and interesting series to elucidate the roles of water and oxygen in a low-pressure hydrogen discharge, I decided to check whether the WHG was operating correctly. I constructed a glass water-cooled thermocouple-probe assembly, consisting of a small concenser with a iron-constantan thermocouple soldered to a piece of silver foil inside the vacuum system. The vacuum-to-atmosphere seal was made with epoxy and Glyptal (Fig. 1). Reaction tube No. 3, with two operating WHG's, was used for these experiments. The thermocouple assembly was attached between the two outer tubes with O-rings and clamps [Figs. 9, 26, and 67(d)]. Otherwise, the system was the same as before.

I checked the simultaneous response of both WHG's, or the response of the upstream WHG and the thermocouple probe, to the cylinder hydrogen passing through the leaky rotameter and water bubbler in order to get parallel atom-concentration decay curves similar to those mentioned and shown previously in Sec. V.C.9.

The results, shown as photographs of the recorder-chart readings, (Figs. 72 and 79 to 81) were interesting but essentially as expected: both WHG's, or the upstream WHG and the thermocouple probe, showed essentially the same decay curves, indicating that they were responding to the same quantity, despite the fact that in the latter case one device measured concentration and the other measured atom flux.

This experiment conclusively proved that, though not necessarily absolute, the WHG at least was totally reliable as a relative atom-concentration measurement device. The experiment also showed in what ways

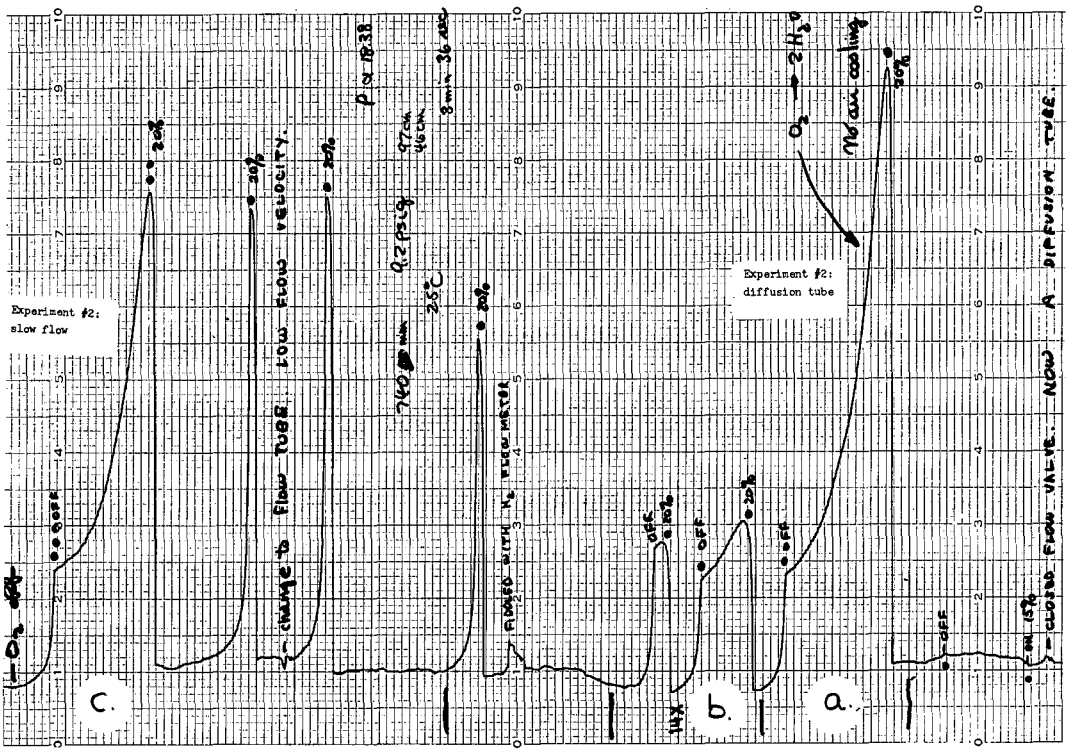

Fig. 77. Response of water-cooled WHG No. 1 (125 holes, 0.59 mtorr full scale) to (a) the conversion of O_2 to H_2O by the 50-MHz discharge when the reaction tube is used as a diffusion tube, and (c) the same conversion process for a low-gas-velocity flow tube. These curves simulate the effect of an air leak in the hydrogen-gas rotameter and explain what was wrong with the earlier catalytic probe experiments (shown in Figs. 85 to 87). This conversion process again indicates that water has little effect in a low-pressure hydrogen discharge. P = 85 mtorr and t = 20 sec/small div (right to left). (February 6, 1965).

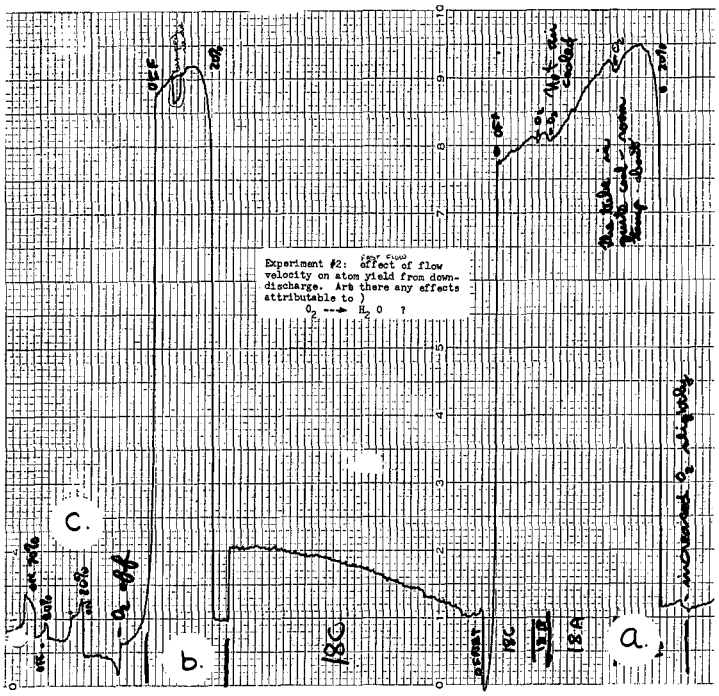

Fig. 78. Experiments similar to those in Fig. 77 showing the response of the water-cooled WHG to a higher velocity in the flow tube. Curves (a) and (b) no longer show the pronounced decay characteristic of curves (a) and (c) in Fig. 77, indicating that the entering O_2 quickly replaces the H_2O formed by the 50-MHz discharge. This accounts for the stability of the WHG signal in many of the recorder-chart tracings previously shown and also indicates that experiments to determine the recombination coefficient of atomic hydrogen on metals in a diffusion tube may be difficult to perform. P = 85 mtorr and t = 20 sec/small div (right to left). (February 6, 1965).

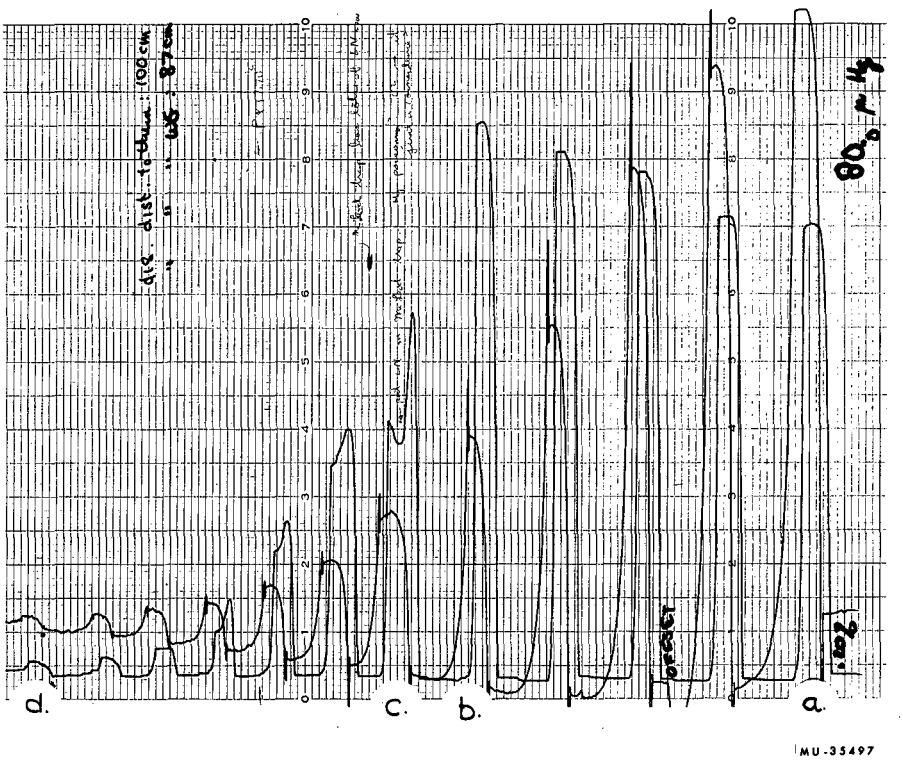

Fig. 79. Air-in-water-bubbler experiment showing the simultaneous response of water-cooled WHG No. 2 (10 holes, 2.40 mtorr full scale) and the silver thermocouple probe to pulsed microwave discharges while air is flushed from the bubbler and the leaky rotameter by hydrogen gas. These curves conclusively demonstrate that the WHG is reliable as a relative atom-concentration measurement device and also that water has little effect on a low-pressure hydrogen discharge. The response of the thermocouple probe increases from (a) to (b), shows a peculiar behavior at (c), and then decreases more normally to (d). Since the WHG signal shows a smooth exponential decline between (a) and (c), the strange behavior of the thermocouple probe can be attributed to changes in the recombination coefficient of the metal. These results emphasize the problems associated with the use of thermal detectors for measuring atom concentrations. P = 80 mtorr and t = 20 sec/small div (right to left). (March 6, 1965).

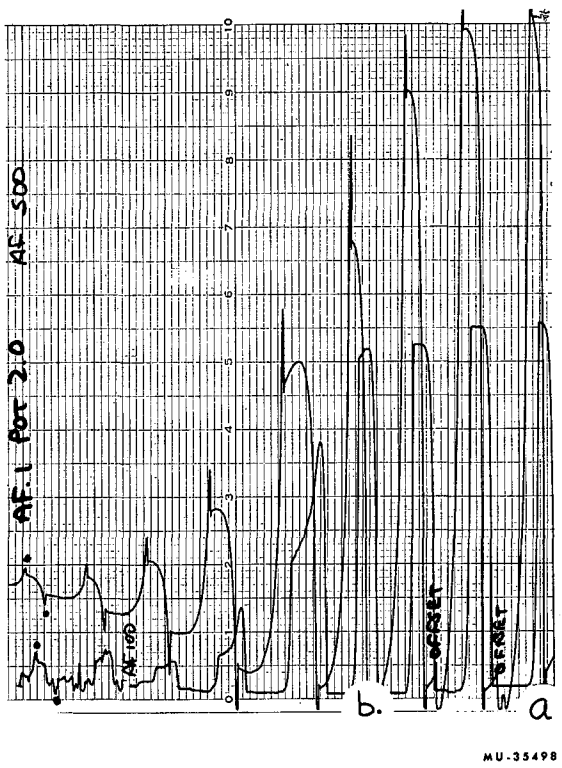

Fig. 80. Curves similar to those in Fig. 79 illustrating the consistent behavior of the WHG and the strange behavior of the thermocouple probe, which actually remains at a constant level between (a) and (b) while the WHG signal decreases by 35%. The fact that the signals from both measurement devices decline as the air is flushed from the bubbler and rotameter again demonstrates that water is ineffective in this system. P = 81 mtorr and t = 20 sec/small div (right to left). (March 6, 1965).

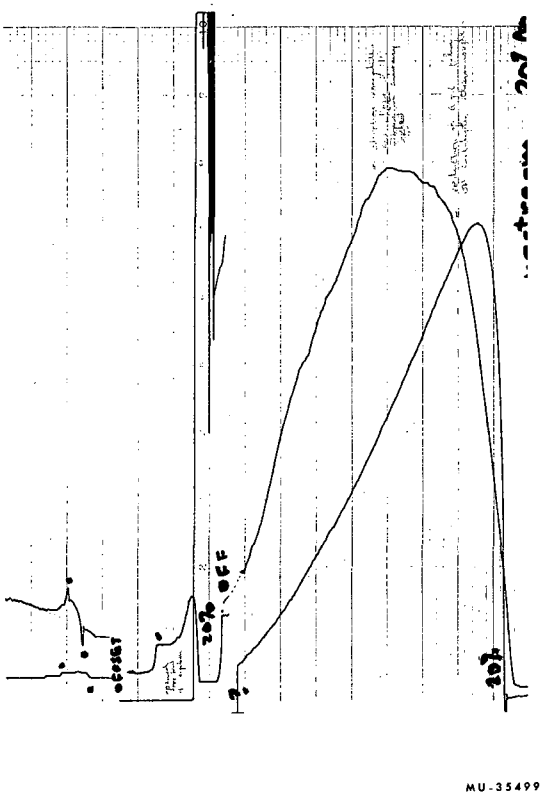

Fig. 81. Curves similar to those in Figs. 79 and 80 with the exception that the upstream small-diameter microwave cavity is operated continuously rather than being pulsed. The conversion of oxygen to water appears to be accelerated by this action. t = 20 sec/small div (right to left). (March 6, 1965).

the thermocouple probe was somewhat unreliable. For instance, in Fig. 79, while the WHG signal was steadily decreasing at the beginning, the thermocouple probe was actually increasing, with the changes indicating that the large amounts of oxygen and atomic hydrogen present in the system were having definite effects on the recombination coefficient of the silver. This was also shown halfway through the decay pulses by the unexpected but temporary increase in the thermocouple signal. Thus thermocouple probes and isothermal calorimeters should be operated under prolonged and aging conditions, although not so prolonged that poisoning of the metal occurs. A judicious choice of metal and perhaps operating temperature must be made.

13. Subtle Factors and Mysterious Effects

Having eliminated, at least in my opinion, the discharge, measurement device, source of hydrogen gas, source of water, and the reaction tube, from being responsible for the lack of effect of water in increasing the yield of atomic hydrogen from a low-pressure discharge, I stopped the experiments, began consolidating the recorder charts and data, and reread some of the more important technical papers on the subject.

Consultations with several people familiar with such kinetic studies failed to produce any compelling reasons for further experiments. The diffusion pump was mentioned as a source of silicone or hydrocarbon impurities and the use of atomic nitrogen at several torr pressure was suggested as a method to clean the vacuum system. This was tried, but it had no effect on any of the results.

Therefore, except for subtle factors and mysterious effects, I had tried to do almost all possible experiments to prove that my initial result—that water had no effect—was wrong, only to show in a variety of ways why it had to be correct. Any future work that contradicts these results must show explicitly what subtle factor or mysterious effect was operating in my system and in all of my seemingly consistent experiments.

D. Discussion

1. Use of Discharge Color as a Qualitative Indication of Atom Yield

The use of the intensity of the discharge color or the Balmer lines as a qualitative indication of the atomic-hydrogen yield depends on the assumption that

$$\{H\} = k\{H^*\} \quad ,$$

where $\{H\}$ represents the ground-state hydrogen atom concentration, $\{H^*\}$ represents the excited-state hydrogen-atom concentration, and k is some proportionality constant between the two.

This assumption is not generally true. If there are several different mechanisms for producing ground-state or excited-state atoms, the concentration of either the ground-state or excited-state atoms in the discharge may easily be independent of each other.

This can be demonstrated by the following five reactions (assumed for discussion purposes only), which are assumed to occur within the discharge zone:

$$H_3^+ + e \xrightarrow{k_1} H^* + H_2$$

$$H^* \xrightarrow{k_2} H$$

$$H + e \xrightarrow{k_3} H^* + e$$

$$OH + H_2 \xrightarrow{k_4} H_2O + H$$

$$H \xrightarrow[\text{wall}]{k_5} H_2 \quad .$$

At steady-state conditions, the concentrations of $\{H\}$ and $\{H^*\}$ are

$$\{H\} = \frac{k_2\{H^*\} + k_4\{OH\}\{H_2\}}{k_5 + k_3\{e\}}$$

$$\{H^*\} = \frac{k_3\{H\}\{e\} + k_1\{H_3^+\}\{e\}}{k_2} .$$

With the proper choice of values for the rate constants k_1, k_2, k_3, k_4, and k_5 and for the species concentrations $\{e\}$, $\{H_3^+\}$, $\{OH\}$, and $\{H_2\}$, the concentrations of ground- and excited-state hydrogen atoms can be made to be completely independent of each other.

Thus, discharge color cannot be used as basis for refutation of my observation that water has no effect on the atom yield from a low-pressure hydrogen discharge.

2. Effect of O_2

Several reaction mechanisms can be proposed for converting an impurity of O_2 in a low-pressure hydrogen discharge into atomic hydrogen:[109]

$$H_2^+ + O_2 \longrightarrow HO_2^+ + H$$
$$HO_2^+ + H_2 \longrightarrow OH^+ + H_2O$$
$$OH^+ + H_2 \longrightarrow H^+ + H_2O$$
$$H^+ \xrightarrow[\text{wall}]{} H$$

$$OH^+ + H_2 \longrightarrow H_2O^+ + H$$
$$H_2O^+ + H_2 \longrightarrow H_3O^+ + H$$
$$H_3O^+ \xrightarrow[\text{wall}]{} H_2O + H$$

$$H_2^+ + O_2 \longrightarrow H_2O^+ + O$$
$$H_2^+ + O \longrightarrow OH^+ + H$$

$$O + H_2 \longrightarrow OH + H$$
$$OH + H_2 \longrightarrow H_2O + H$$

From these predictions, it is easy to predict stoichiometrically values ranging from 2 to 6 for r_H/r_{O_2}, which is the ratio of the amount of atomic hydrogen produced to the amount of molecular oxygen initially added to the hydrogen-gas stream, complete conversion of O_2 to H_2O by the time it reaches the Wrede-Harteck gauge assumed.

My experiments at low O_2-impurity concentrations indicated a ratio of 2. This value may be low for several reasons: (a) The molecular oxygen may not have been completely converted to the equivalent amount of atomic hydrogen (Fig. 63), (b) the WHG was not proven to be absolute and may easily have been low (Sec. V.C.6), and (c) some of the atomic hydrogen may have recombined on the reactor-zone walls before reaching the WHG. However, the measurements did show that the effect of O_2 (and also N_2) was stoichiometric, and not catalytic!

My experimental apparatus was not equipped to determine which of the reaction mechanisms proposed was the correct one, so I made no attempts to do so. To determine the correct one, I need to answer several questions experimentally:

a. What is the state of the oxygen impurity after it has passed through the hydrogen discharge, i.e., is it in the form of OH or H_2O?
b. What are the principal ionic species containing oxygen within the steady-state electrical discharge?
c. What are the principal transient ionic species containing oxygen in a pulsed microwave or electrodeless discharge?

Only such studies, which would use a fast-response mass spectrometer, would give a definitive answer to the question of the mechanism. The techniques developed would be valuable for the study of other discharge systems as well, and generally would increase the scientific interest in plasma chemistry.

3. Use of an Isothermal Calorimeter to Measure Absolute Atom Concentrations

The isothermal calorimeter, or more generally the thermal calorimeter, is the most popular measurement device for determining the concentration of atomic hydrogen produced by low-pressure electrical discharges. The calorimeter has usually taken one of three forms: (a) a tungsten filament heated from 100°C to 1000°C above the ambient gas temperature,[70,77] (b) a long coil of resistance wire initially at the ambient gas temperature and heated only to about 100°C by the action of the recombining atoms,[48,81] and (c) a water calorimeter employing a catalytic cavity or section of tubing which is usually maintained within several degrees of the ambient gas temperature.[61]

The steady-state atom concentration with dc, ac, electrodeless, or microwave discharges measured by these calorimeters has been high. Shaw, and Bak and Rastrup-Andersen, using coiled tungsten filaments from light bulbs maintained at temperatures higher than 700°C, reported atom yields in a flow tube of 90% at 500 mtorr and 80% at 300 mtorr, respectively.[68,77] Bergh, in the most recent paper on the subject, mentioned that the atom concentration (measured by a tungsten-wire calorimeter at 150°C) produced by a rf discharge in a diffusion tube at 200 mtorr was high.[81] Other results typical of the 1930's, such as those of Amdur,[34] Poole,[61] Steiner,[110] and Smallwood,[111] fall in the 10 to 94% atom-concentration range.

With the notable exceptions of Jennings and Linnet,[64] Browning and Fox,[80] Hildebrandt et al,[112] and perhaps a few others, the above calorimeter results are the principal ones that tend to refute my experimental observations that water has no effect on the atom yield from an electrical discharge. Each one of the above investigators used a water bubbler to increase the atom yield.

If my results with water as an impurity are correct, then I must explain all high-atom-dissociation percentages previously obtained in 45 years of work with low-pressure atomic hydrogen as being due either to (a) the presence of oxygen or other gaseous impurities besides

water, (b) the faulty mathematical interpretation of the diffusion- or flow-tube system, or (c) the faulty mathematical interpretation of the measurement device. To do this, I have directed my main attention to the thermal calorimeter.

In order to use the frequently mentioned formula,[38,70]

$$F = \frac{R_w(i_o^2 - i_2)}{4.18\ \Delta H} \qquad \text{(IV-1)}$$

for the flow rate F of atomic hydrogen (R is the resistance of the heated wire, i_o and i are the measured currents in the absence and presence of H atoms, and ΔH = 52 kcal/mole), the following four conditions must be satisfied for the operation of the isothermal calorimeter:

a. The thermal accommodation coefficient of the recombination energy on the catalytic surface must be unity,[113]
b. The diffusive contribution to the mass flux from the discharge must be small;
c. The gas velocity must not be so large or the overall catalytic efficiency of the calorimeter (which depends both on the recombination coefficient and the surface area of the catalyst) so small that the calorimeter doesn't abstract all of the atoms;
d. The presence of atomic hydrogen instead of molecular hydrogen must not alter the heat-transfer properties between the hot wire and the gas (by heat conduction) or the surroundings (by radiation).

The fact that Eq. (V-1) has usually been used without qualification points to the fact that these four conditions have rarely been considered. This observation alone made me feel that my unusual results were not so wrong as I initially suspected.

For instance, consider the 80 and 90% dissociation values reported by Bak et al. and by Shaw. Conditions a and c, if not satisfied, would tend only to increase this value, as would d if the effect

of atomic hydrogen would be to lower the emissivity of the tungsten wire or lower the effective heat conductivity between the wire and the gas. Only condition b, if not properly satisfied, would lower the above percentage figures. Such a situation "would result in impossible values of D, the percent dissociation."[70]

The mathematics of the diffusion- and flow-tube systems relevant to conditions b and c have already been derived in Sec. IV., Cases A and H to J. In these cases, the concentration of atoms c_1 at the discharge-zone—reactor-zone boundary was assigned the value c_{1_o}, and the derivation was made under the assumption that there was no loss of atoms to the cylindrical walls (Fig. 82).

Reinterpreting Eqs. (IV-51, IV-142, IV-149, and IV-152) by substituting the correct physical quantities for the dimensionless groups ψ, ψ_o, ξ', and β [Eqs. (IV-44, IV-46, IV-48, and IV-143], we obtain the following results:

DIFFUSION TUBE with highly catalytic end-plate ($\psi = 0$ at $\lambda = 0$):

$$J_{1s} = \frac{D_{12}}{L} c_{1_o} = - D_{12} \frac{\partial c_1}{\partial z} \qquad \text{(V-2)}$$

DIFFUSION TUBE with end plate of recombination coefficient γ' ($2 \gg \gamma'$):

$$J_{1s} = \frac{D_{12}/L}{1 + \frac{4D_{12}}{\gamma' \bar{v}_1 L}} \, c_{1_o} \qquad \text{(V-3)}$$

FLOW TUBE with highly catalytic wire mesh ($\psi = 0$ at $\lambda = 0$):

$$J_{1s} = \frac{v_z}{1 - e^{-v_z L/D_{12}}} \, c_{1_o} \qquad \text{(V-4)}$$

FLOW TUBE with wire mesh of recombination coefficient γ' ($2 \gg \gamma'$):

$$J_{1s} = \frac{v_z}{\left[\frac{4v_z}{\gamma' \bar{v}_1} + 1\right] - e^{-v_z L/D_{12}}} \, c_{1_o} , \qquad \text{(V-5)}$$

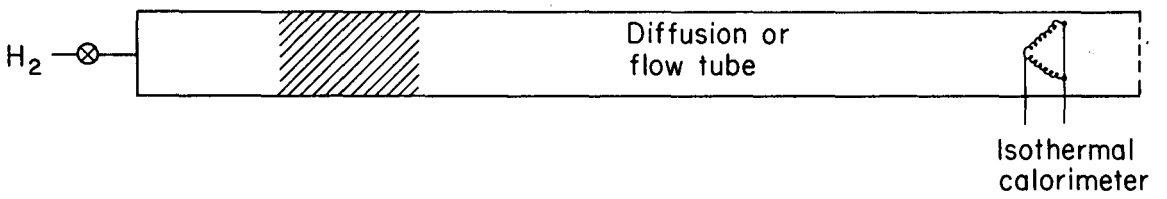

Fig. 82. Schematic drawing showing an isothermal calorimeter located in a low-pressure reaction-tube system.

where J_{1s} is the molar flux of atoms to the catalytic surface (in atoms/cm^2-sec), D_{12} is the binary diffusion coefficient for atomic hydrogen in molecular hydrogen, $\bar{v}_1$ is the average velocity of the hydrogen atoms, L is the distance from the discharge to the end plate or wire mesh, and v_z is the gas flow velocity in the flow tube. Equations (V-4) and (V-5) correctly simplify to Eqs. (V-2) and (V-3), respectively, in the limit of small $v_z L/D_{12}$. The quantity $v_z L/D_{12}$ is particularly significant since it is the ratio of two important rates,

$$\frac{v_z L}{D_{12}} = \frac{\begin{array}{l}\text{rate or atom convection from the discharge zone}\\ \text{to the catalytic surface}\end{array}}{\begin{array}{l}\text{rate of atom diffusion from the discharge zone}\\ \text{to the catalytic surface}\end{array}} \qquad \text{(V-6)}$$

In practice, $\int J_{1s} dA'$, the rate of atom recombination on the thermal calorimeter, is the quantity measured, and $100\, c_{1o}/c$, the percent dissociation, is the quantity calculated. Therefore, for a diffusion tube with a highly catalytic end plate,

$$\% \text{ dissociation} = 100\,\frac{c_{1o}}{c} = 100\,\frac{\int J_{1s} dA'}{c\int \frac{D_{12}}{L}\, dA}$$

$$= 100\,\frac{\begin{array}{l}\text{rate of atom recombination}\\ \text{on the thermal calorimeter}\end{array}}{\pi R^2 (D_{12})/L}\,. \qquad \text{(V-7)}$$

With v_z substituted for D_{12}/L, Eq. (V-7) corresponds exactly to Eq. (E1). The term A' is the area of the catalytic surface, and A is the cross-sectional area of the diffusion or flow tube. Schulz and LeRoy made a similar type of derivation for a flow tube in which atoms were lost by a first-order reaction in the gas phase.[41]

Therefore, Eqs. (V-2) to (V-5), modified to appear like Eq. (V-7) are the generalized equations for the operation of thermal calorimeters in the absence of atom recombination on the reactor-zone walls. The equation commonly used to compute atom dissociation percentages [Eq. (V-1)] is oversimplified and is useful only when the flow velocity v_z is much

greater than the diffusional velocity D_{12}/L, and the flow velocity is sufficiently slow or the calorimeter sufficiently active so that the quantity $4v_z/\gamma'\bar{v}_1$ is much less than 1.

As an example of the use of these equations, consider the system of Bak and Rastrup-Andersen and assume that $c_1 = 0$ at their calorimeter. On the basis of the values $v_z = 150$ cm/sec and $L = 18$ cm given by these authors and 3300 cm^2/sec as the diffusion coefficient,[31]

$$\frac{v_z L}{D_{12}} = 0.82$$

This immediately indicates that their system was intermediate between a diffusion tube and a flow tube. The more correct atom concentration, calculated from Equation (V-4) is 45% instead of the value of 80% calculated from Eq. (V-1). The calculated concentration actually is higher, since the value of $v_z = 150$ cm/sec was calculated with the assumption of no atom dissociation. Bak and Rastrup-Andersen also noted that when $L = 25$ cm, the percent dissociation was 65%. The ratio of their two percentage values, $65/80 = 0.81$, is close to the ratio computed for the two values of L with Eq. (V-4), 0.82. If the tungsten calorimeter were situated 6 cm from the discharge, the calculated percent dissociation from either Eq. (V-1) or (V-4) would exceed the absurd value of 100%.

In the case of Shaw's experiments, the dimensionless group $v_z L/D_{12}$ was much greater than one, so his use of Eq. (V-1) was justified on the basis that his triple-filament calorimeter abstracted all of the atoms.

In summary, it is clear that the inclusion of mass transfer from the discharge to the calorimeter by diffusion fails to explain the high-atom-concentration values of the two cases considered. Since it is easy to make either of the percentage figures absurd, the whole measurement technique must be suspect.

Wise attempted to measure the energy-accommodation coefficient for the recombination of hydrogen atoms on various metal filaments at elevated temperatures.[113] He observed a value of approximately 0.8 for tungsten between 443 and 773°K. Although I will not vouch for the validity of his results, the point he made is pertinent to this discussion. The application of the factor of 0.8 would only increase the absurdity of many of the isothermal calorimeter results of Shaw, Bak and Rastrup-Andersen, and others.

Condition d, given several pages previously, is the most difficult for me to estimate quantitatively. According to Eq. (1.140) in Dushman, the free-molecule heat conductivities of atomic and molecular hydrogen are about the same.[102] Therefore the presence of atomic hydrogen can lower the effective thermal conductivity from the wire to the gas only if the accommodation coefficient for atomic hydrogen is less than that for molecular hydrogen. By comparing the accommodation coefficients for helium and molecular hydrogen, we can easily see that atomic hydrogen probably does have a lower thermal accommodation coefficient.[114] The action of atomic hydrogen on the tungsten calorimeter may also be to clean the surface and lower the emissivity.

These arguments point to one conclusion: The hotter the tungsten wire is, the more power is involved in sustaining its temperature, and the easier it is for small changes in the state of the metal or the local environment to simulate large atom concentrations. Only at low wire temperatures can this problem be minimized.

With the assumption of an idealized flow tube, my order of preference of thermal calorimeters for the measurement of atom concentrations is: (a) a water calorimeter maintained near the ambient gas temperature, and (b) a long resistance wire initially maintained at the ambient gas temperature, but heated above it in the presence of atoms. A hot tungsten filament maintained at a high temperature is not applicable for this measurement.

Finally, the mathematics developed earlier can also be applied to the recent publication of Bergh.[81] With L = 10 cm, D_{12} = 5000 cm^2/sec at 200 mtorr, a cross-sectional area of 3.14 cm^2, and the loss of atoms to the Teflon-coated glass walls assumed negligible, the atom concentration c_{1_o} at the discharge-zone boundary of his diffusion tube is only 2.1% [from Eq. (V-2)].

Bergh showed experimentally that water had no poisoning effect on phosphorous-coated Pyrex, Teflon-coated Pyrex, quartz rinsed with HNO_3, Pyrex rinsed with HNO_3, Pyrex rinsed with HF, or Pyrex coated with dry film. The feature of these experiments which is significant for my own results is the low atom concentration produced by such a high expenditure of energy—typically 500 W.[115]

4. Effect of the Glass Walls

One of the boundary conditions in Case K of Sec. II must be altered before Eq. (IV-153) can be used to describe my apparatus. Instead of a thermal calorimeter, I used a Wrede-Harteck gauge, so the boundary condition must be

$$\psi = 0 \qquad \text{at } \lambda = -\infty \quad . \tag{V-8}$$

With this boundary condition, the solution of (II-153) changes from (II-155) to

$$\frac{\psi}{\psi_o} = e^{-(\Omega-\beta)z/2R} \quad . \tag{V-9}$$

The following parameters were typical of my experiments:

v_z = 75 cm/sec $\qquad$ $D_{12} = 2.3 \cdot 10^4$ cm^2/sec

R = 1.9 cm $\qquad$ $\gamma = 10^{-3}$ to 10^{-6}

$\bar{v}_1 = 2.6 \cdot 10^5$ cm/sec $\qquad$ z/R = 10

and are the same values suggested for such calculations by Tsu and Boudart. With these quantities, $\beta = 0.0062$ and $\mu = 10$, 30, 100, and 300 for $\gamma = 10^{-3}$, 10^{-4}, 10^{-5}, and 10^{-6}, respectively. Since $1/\mu \gg \beta$ for most of the values of γ, Eq. (V-9) simplifies to

$$\frac{\psi}{\psi_o} = e^{-z/\mu R} \quad . \tag{V-10}$$

This ratio has values of 0.37, 0.72, and 0.91 for $\mu = 10$, 30, and 100, respectively.

5. Effect of H_2O

My experiments led to the unmistakable conclusion that water, in my apparatus and under my experimental conditions, did not influence the yield of atomic hydrogen from a low-pressure discharge. I tried hard in several different ways to demonstrate such an effect, but never succeeded. The interesting question that arises is: Is this result general?

The low yield of hydrogen atoms appears to be a kinetic problem associated with the low rate of production of atomic hydrogen in the discharge zone, and not a problem determined by the location and magnitude of the sinks in the diffusion or flow tube. This can be demonstrated mathematically.

Consider Eq. (V-100) for the atom concentration at the discharge-zone—reactor-zone boundary. This equation can be simplified by the experimental use of a Teflon end plate (ξ' is very large) located several tube radii from the discharge zone ($L/\mu R$ is small). The walls throughout the reaction tube are made of Pyrex or quartz glass, and δ is assumed to be equal to μ, the dimensionless group associated with the recombination of atomic hydrogen on glass. Equation (IV-100) simplifies first to

$$\psi_o = \frac{\sigma'^2\mu^2}{1 + \sigma'^2\mu^2} \; \frac{\cosh L/\mu R}{\cosh L/\mu R + \dfrac{1}{(1 + \sigma'^2\mu^2)^{1/2}} \sinh L/\mu R} \tag{V-11}$$

and then to

$$\psi_o = \frac{\sigma'^2\mu^2}{1 + \sigma'^2\mu^2} \quad , \tag{V-12}$$

which is similar to Eq. (IV-114). Since the steady-state atom concentration is small ($\psi_o = 0.001$), Eq. (V-12) reduces further to

$$\psi_o = \sigma'^2\mu^2 = \frac{2R}{\gamma\bar{v}_1} k'_o \quad , \tag{V-13}$$

where R is the radius of the reaction tube, γ is the recombination coefficient for atomic hydrogen on glass, $\bar{v}_1$ is the average velocity for an atom of hydrogen, and k'_o is the first-order rate constant for the production of atomic hydrogen in the discharge (with units of sec^{-1}). By means of Eq. (IV-43) and $\psi_o \approx \{H\}/\{H_2\}$, Eq. (V-13) can be converted entirely to the kinetic notation

$$\{H\} = \frac{k'_o}{k_{1s}} \{H_2\} \quad , \tag{V-14}$$

where k_{1s} is the first-order rate constant, in sec^{-1}, for the recombination of atomic hydrogen on glass. Equation (V-14) corresponds to the reaction mechanism

$$H_2 + M \xrightarrow{k_{0g}} H + MH$$

$$H \xrightarrow[wall]{k_{1s}} H_2$$

where

$$k'_o = k_{0g} \{M\} \quad , \tag{V-15}$$

and M is some atomic, ionic, or molecular species.

One surprising observation about an electrical discharge in <u>pure</u> hydrogen was that no more than 0.1% atomic hydrogen was produced with at least 25 W (and maybe more) of absorbed rf or microwave power. The ionic species H_3^+ is commonly found in such discharge plasmas and, when created and destroyed, must form a minimum of two atoms of hydrogen per molecule of H_3^+. The rate constant for the reaction

$$H_2^+ + H_2 \longrightarrow H_3^+ + H$$

is between 2.1 and 2.9 · 10^{-9} cm^3/molecule-sec.[116-118]

In my experiments, the mole fraction of atomic hydrogen from a discharge in pure hydrogen was 0.001, the reaction-tube radius was about 1.9 cm, the average velocity of the hydrogen atoms was about 2.6 · 10^5 cm/sec, and the recombination coefficient for the atomic hydrogen on the Pyrex surfaces was probably 2.8 · 10^{-3}.[8] From Eq. (V-13), k'_o is calculated to be 0.19 sec^{-1}. With the assumption that $\{M\} = \{H_3^+\} = 10^8$ ions/cm^3, Eq. (V-15) indicates that $k_{0g} = 1.9 \cdot 10^{-9}$ cm^3/molecule-sec, a result close to the rate constant for the ion-molecule reaction given above. This close agreement between the two values is fortuitous, in view of the simplifications made to Eqs. (IV-100) and (V-11) and the uncertainty in the values of $\{H_3^+\}$ and $\{H\}/\{H_2\}$ chosen for the calculations. These results are suggestive, though, and make the low yield of atomic hydrogen from a discharge in pure molecular hydrogen appear more understandable and reasonable.

Equations (V-13) and (V-14) help to explain the difficulty of previous investigators in trying to distinguish between gas- or surface-phase effects when H_2O to O_2 was added. If only the increase in the steady-state atom concentration by the impurity gas is measured, the two effects cannot be separated, except perhaps by the time constant of the change in atom concentration. Other experimental evidence, however, indicates that water does not poison the glass walls of a low-pressure reaction tube.

Equations (V-13) and (V-14) also indicate that if the reaction-tube walls are inactive and if a nonperturbing measurement device is used (this eliminates thermal detectors)—i.e., if all atom sinks in the system are eliminated or minimized—the steady-state atom concentration in a diffusion or low-velocity flow tube would be considerably higher than 0.1%. Therefore, the results of investigators who have measured high percent dissociation figures for hydrogen discharges in the presence of water cannot be immediately used to refute my observations that water has no effect. Many of them have not shown definitively that water was the cause of their high measured atom yields.

As an example, Shaw showed that "saturating" commercial tank hydrogen with water vapor increased the yield of atomic hydrogen measured with an isothermal tungsten calorimeter from $34 \cdot 10^{-6}$ moles/sec to only $41 \cdot 10^{-6}$ moles/sec. Research-grade hydrogen containing a maximum impurity content of 0.15% N_2 and 0.002% O_2 gave a yield of $12 \cdot 10^{-6}$ moles/sec, which decreased during the course of the experiment and indicated "a possible clean-up of impurities in the system." The commercial tank hydrogen passed through a "Deoxo" unit and a liquid nitrogen trap gave a yield of $1 \cdot 10^{-6}$ moles/sec. Shaw also indicated that oxygen might have influenced the rate of production of hydrogen atoms directly, since it was not removed in the line by a silica-gel tower which removed water from the commercial-tank-hydrogen gas stream.[70]

The different behavior of O_2 and H_2O in my hydrogen discharges is difficult to "explain" kinetically (in fact, it is much more difficult to explain that the similar behavior of the two compounds). The rate constants for the following comparative pairs of reactions are in each case similar, so I cannot use them as a basis for any explanation:

$$\begin{cases} O_2 + e \longrightarrow O_2^+ + 2e & \text{I.P.} = 12.5 \text{ eV}; \quad Q_i = 2.5 \cdot 10^{-16} \text{ cm}^2 \text{ at } 75 \text{ eV}^{119} \\ H_2O + e \longrightarrow H_2O^+ + 2e & \text{I.P.} = 12.6 \text{ eV}; \quad Q_i = 2.9 \cdot 10^{-16} \text{ cm}^2 \text{ at } 75 \text{ eV}^{119} \end{cases}$$

$$\begin{cases} H_2^+ + O_2 \longrightarrow HO_2^+ + H & k = 7.6 \text{ or } 9.6 \cdot 10^{-9} \dfrac{\text{cm}^3}{\text{molecule-sec}}^{118} \\ H_2^+ + H_2O \longrightarrow H_3O^+ + H & k \approx 3 \cdot 10^{-9} \text{ cm}^3/\text{molecule-sec}^{118} \end{cases}$$

$$\begin{cases} O_2^+ + e \longrightarrow O^* + O^* & k \approx 3 \cdot 10^{-7} \text{ cm}^3/\text{molecule-sec}^{120} \\ H_2O^+ + e \longrightarrow H^* + OH^* & k \approx 10^{-5} \text{ cm}^3/\text{molecule-sec}^{120} \end{cases}$$

$$\begin{cases} O_2 + e \longrightarrow O^- + O & Q_i = 1.3 \cdot 10^{-18} \text{ cm}^2 \text{ at } 6.7 \text{ eV}^{121} \\ H_2O + e \longrightarrow H^- + OH & Q_i = 7.0 \cdot 10^{-18} \text{ cm}^2 \text{ at } 6.5 \text{ eV}^{121} \end{cases}$$

These comparative pairs seem to eliminate most of the simpler reaction mechanisms I have previously proposed. They illustrate the danger of speculation about a complex system such as a low-pressure electrical discharge.

The conversion of the oxygen impurity to atomic hydrogen and water in the hydrogen discharge proceeds according to the formula

$$\frac{\{O_2\}}{\{O_2\}_o} = e^{-k\{N\}t} , \qquad \text{(V-16)}$$

where k is the slow-step second-order rate constant of O_2 reacting with N, and may be an atom, molecule, ion, electron, or excited species,

$$O_2 + N \xrightarrow[H_2 \text{ discharge}]{k(\text{slow step})} n\,H + 2\,H_2O$$

where n is an integer (probably between 2 and 6) characteristic of the stoichiometry of the reaction mechanism. In my large-diameter Pyrex reaction tubes, this conversion process may have occurred entirely in the 2- or 3-cm discharge zone or, after formation of excited but not ionic species in the discharge, in the reactor zone. For the latter process, the reaction may have even taken place downstream from the WHG to produce atomic hydrogen, which then diffused back and was measured.

One pitfall in describing such processes is that the use of v_z and a chosen length does not characterize the residence time in the chosen region in low-pressure flow tubes. The flow velocity v_z is usually much smaller than the effective diffusional velocity D_{12}/L. The mathematics of such a situation, which is analogous to Cases C to F in Sec. III, will be derived at a later date.

If 5000 cm^2/sec is chosen as the binary-diffusion coefficient typical of atomic or molecular oxygen or some other nonionic but perhaps excited species at 75 mtorr of hydrogen, the effective residence time in a 2.5-cm discharge zone or a 50-cm reactor zone is 1.25 and

500 msec, respectively. The effective diffusional velocity for the discharge zone is dependent on its length but independent of the cross-sectional area of the tube.

With the assumption that 50% of the O_2 is converted to atomic hydrogen and water, Eq. (V-16) simplifies to

$$k\{N\}\ t = \ln \frac{\{O_2\}}{\{O_2\}_o} = \ln 0.5 = 0.693 \qquad \text{(V-17)}$$

or

$$\{N\} = \frac{0.693}{kt} \qquad \text{(V-18)}$$

where $\{N\}$ is calculated from the residence time t and the assumed slow-step second-order rate constant k. Table IV shows the result of these calculations.

For Case A, in which the reaction is entirely in the discharge zone, it is unlikely that there are so many electrons or ions reacting with a rate constant of 10^{-8} cm^3/molecule-sec. It is remotely possible that excited species are present with a concentration of $5.5 \cdot 10^{12}$ species/cm^3 (0.23%) and react with a rate constant of 10^{-10} cm^3/molecule-sec.

For Case B, in which the reaction is primarily in the reactor zone, it is very possible that excited species, present in concentrations between $1.4 \cdot 10^{10}$ species/cm^3 (0.00058%) and $1.4 \cdot 10^{12}$ species/cm^3 (0.058%) have rate constants between 10^{-10} and 10^{-12} cm^3/molecule-sec. Thus the suggestion of Wise, Ablow, and Sancier may be applicable for this case, though probably for a different species.[8] A likely reaction is

$$O^*(^1D) + H_2 \longrightarrow OH + H \ ,$$

which is exothermic by 44.6 kcal/mole and has been observed to occur, by Neuimin and Popov, at pressures of 100 mtorr with an activation energy of less than 1.4 kcal/mole.

Table IV. Actual and predicted species concentrations in a hydrogen-discharge system at 75 mtorr.

Assumed k (slow step) (cm^3/molecule-sec)	Calculated {N} (species/cm^3)
A. Reaction to convert O_2 to atomic hydrogen and H_2O only in discharge zone	
10^{-8}	$5.5 \cdot 10^{10}$
10^{-9}	$5.5 \cdot 10^{11}$
10^{-10}	$5.5 \cdot 10^{12}$
10^{-11}	$5.5 \cdot 10^{13}$
B. Reaction of O_2 in discharge zone to produce excited species, which then react slowly over a long distance in reactor zone	
10^{-9}	$1.4 \cdot 10^{9}$
10^{-10}	$1.4 \cdot 10^{10}$
10^{-11}	$1.4 \cdot 10^{11}$
10^{-12}	$1.4 \cdot 10^{12}$
10^{-13}	$1.4 \cdot 10^{13}$
C. Typical concentrations of atomic, molecular, and ionic species at 75 mtorr	
H_2	$2.43 \cdot 10^{15}$
1% O_2	$2.43 \cdot 10^{13}$
2% H	$4.86 \cdot 10^{13}$
Electrons	10^{8} to 10^{10}
Ions	10^{8} to 10^{10}

From the tenuous arguments given here, it does seem that the action of O_2 in increasing the yield of hydrogen atoms from a low-pressure discharge is primarily gas kinetic rather than ionic. The use of a fast-response mass spectrometer, as suggested previously, may do a lot to solve this problem.

To conclude this part, I will not say that water has no effect in all low-pressure hydrogen-discharge systems, since I may have missed a very subtle but extremely important factor. However, I have made every reasonable effort to find this factor—without any success. I have checked the measurement technique, gas source, impurity source, type of discharge, and discharge power level, and have operated at pressures near those at which results for the effect of water have been previously found. Perhaps the only two remaining items are the state of the glass surface, which I didn't change often, or the presence of hydrocarbon impurities from the pumps. I have not been able to stretch my imagination to account for how either of these two items could influence the behavior of water but not of oxygen, both gases being present at the same time.

I suggest that these experiments be carefully repeated, perhaps with modifications as individual tastes or budgets require, to again show whether water does or does not have an effect on the hydrogen-atom yield. Despite the wealth of conflicting evidence, I will stick to my results—at least for my experimental system—until proven wrong. If this never happens—and the results are shown to be correct—I would like to know why so many people have been led astray during 45 years of work with atomic hydrogen in low-pressure systems. Just like the recent demonstration of noble-gas compounds, it would indicate that old taboos and practices can still be occasionally overturned.

E. Conclusions

1. The presence of small amounts of H_2O in a hydrogen discharge at 75-mtorr pressure did not influence the yield of atoms.
2. The presence of small amounts of O_2 in a hydrogen discharge at 75-mtorr pressure produced a minimum of two atoms of atomic hydrogen per molecule of O_2. At higher O_2 concentrations, saturation occurred and the atom yield per molecule decreased.
3. The presence of small amounts of N_2 in a hydrogen discharge at 75-mtorr pressure produced a minimum of 3 atoms of atomic hydrogen per two molecules of N_2 concentrations, saturation occurred and the atomic-hydrogen percentage never increased beyond 3%.
4. The behavior of H_2O and O_2 in these experiments was independent of the atom-measurement technique, the source of hydrogen, the source of O_2 or H_2O, and the discharge-production method or power.
5. Molecular oxygen may increase the yield of atoms from a low-pressure hydrogen discharge by a slow-gas-kinetic rather than a fast ion-molecule reaction.
6. The intensity of the Balmer lines or the discharge color is not a reliable qualitative indication of the atomic hydrogen yield.
7. A cyclotron-resonant microwave discharge, employing a diathermy unit, microwave cavity, and a large magnetron magnet, is a convenient device for producing an electrical discharge in a low-pressure system with microwave powers as low as 250 mW.
8. At low pressures, the residence time of an atom or molecule in a given length L is usually characterized by the effective diffusional velocity D_{12}/L rather than the convective velocity v_z.
9. For an isothermal calorimeter to be used in the measurement of absolute atom concentrations in a low-pressure system, both the diffusive and convective flux of atoms must be known, the presence of the atoms must not alter the rate of heat loss from the calorimeter, most of the atoms produced must recombine on the calorimeter, and the thermal-accommodation coefficient of the recombination energy must be equal to unity.

VI. EFFECT OF A CATALYTIC PROBE ON THE ATOM-CONCENTRATION DISTRIBUTION IN A DIFFUSION TUBE

A. Introduction

In 1961 Tsu and Boudart raised some questions concerning the results and experimental technique used by Wood and Wise to measure the recombination coefficients of atomic hydrogen on various metals.[30] In their preliminary report, these latter authors listed the value of the recombination coefficient (which averaged about 0.16 within 100°C of room temperature) for 13 different metals: Ti, V, Cr, Mn, Fe, Co, Ni, Cu, Pd, Pt, Ag, Au, and Al.[4] To obtain these results, they moved a Pyrex-covered thermocouple coated with the catalytically active metal along the axis of a diffusion tube, measured the change in temperature of the thermocouple as a function of its distance from a source of atoms, and then computed the recombination coefficient of atoms on the probe with the help of a theoretical model which assumed that (a) the atom concentration at the atom source (the discharge boundary) remained constant throughout the experiment, and (b) the thermocouple probe simulated a disk-shaped end plate which occupied the entire cross-sectional area of the tube. Their apparatus consisted of a cylindrical water-jacketed Pyrex side arm closed at one end and at the other joined perpendicularly to a discharge tube (in which hydrogen gas was dissociated into atoms by a 17-MHz radio transmitter).

Tsu and Boudart questioned both assumptions and explored the possibility that the lack of catalytic specificity was the result of the experimental technique used in the determination of the recombination coefficients. They definitely improved the theoretical description of diffusion and flow tubes by treating the discharge and reactor zones separately. As a consequence, they demonstrated that the atom concentration at the discharge-zone boundary (which Wood and Wise had assumed to be constant irrespective of the location of their probe) was dependent on (a) the volume rate of production of atoms in the discharge zone (which they assumed to be of infinite length), (b) the surface-phase

atom-recombination rates (which they assumed to be identical) on the discharge- and reactor-zone walls, and (c) the catalytic-probe recombination rate (which was determined by the probe's distance from the atom source, its recombination coefficient, its surface area, and its geometry).

In two subsequent papers on the kinetics of hydrogen-atom recombination on metal surfaces, Wood and Wise gave the results of several experiments that they felt demonstrated that "the atom density of an atom source remains essentially constant during the course of an experiment:"[12,14]

a. A tenfold increase in the absolute atom concentration did not affect the relative atom density profile in the diffusion tube,
b. Changes in the radius of the diffusion tube affected the measured value of ξ' according to their theoretical predictions,
c. Changes in the total pressure affected the value of ξ' according to their theoretical prediction,
d. A filament traverse of the region near the atom source in the flow tube indicated a uniform atom concentration up to the juncture of the side arm of the discharge,
e. The measured activity of the Pyrex walls at small values of L/R agreed well with the measured activity at large values of L/R,
f. The reading of one probe located in a side arm was not affected by the movement of a second probe located in another side arm and separated from the first by the discharge zone,
g. The use of two probes—one a tungsten wire located very near the atom source and the other a movable nickel wire located further away from the discharge—demonstrated that movement of the latter didn't affect the reading of the former,
h. The relative hydrogen-atom concentration at a given distance from the atom source—measured by ESR as a function of the position of a tungsten probe—was in "excellent agreement... [with] theoretical data."[14]

Tsu discounted items a, b, c, and e on the basis that (a) there were always three unknowns in the above experiments (μ^2, ξ', and $d\psi/d\lambda\big|_{\lambda=0}$), (b) a large range of parameters could fit the nonlinear theoretical model, and (c) Figs. 4, 5, 6, and 7 were "not compatible with the scatter of the data as shown in Fig. 8" of Ref. 32.

Tsu also made calculations on item f to show that the perturbation from one probe does not usually reach beyond a distance greater than several tube radii, and finally stated that in item d it would be difficult for one to measure a discharge perturbation with a device that might have caused the perturbation itself.[32]

Westenberg indicated that crude experiments in which a nickel screen was used in the presence of atomic oxygen did show some sort of perturbing effect when the nickel was closer than 20 tube radii to the discharge, but he did not take a definite stand on the subject.[14]

Schofield, using a method similar to that developed by Smith,[1] measured hydrogen-atom recombination coefficients (at room temperature) of $3 \cdot 10^{-2}$ for vapor-plated gold, silver, and copper; $1 \cdot 10^{-3}$ for vapor-plated aluminum; and $5 \cdot 10^{-4}$ for aluminum foil (Wood and Wise obtained values of 0.10, 0.13, 0.19, and about 0.3 for the recombination coefficient of atomic hydrogen on Au, Ag, Cu, and Al, respectively).[29] Schofield noted the discrepancy between his results and those of Wood and Wise (thermocouple probes) and stated that (a) an end plate closing the cross section of the tube was not a realistic model for a thermocouple probe, and (b) he did not see how observed values of ξ' could be related to the recombination coefficient γ' for the metal surface coating the probe.

In the same laboratory four years later, Dickens, Linnett, and Palczewska reported values of 10^{-2} and $6 \cdot 10^{-4}$ for the hydrogen-atom recombination coefficients (at room temperature) on Pd and Au foils, respectively. They extrapolated Wood and Wise's (W and W) high-temperature data for Pd-Au alloys to room temperature (obtaining a value of $8 \cdot 10^{-2}$ for either metal), ignored W and W's thermocouple-probe data for the pure metals at room temperature (0.20 for Pd and 0.10 for Au), and attributed the discrepancy between their data and W and W's

high temperature values to the different physical conditioning and annealing treatment of the alloys and to hydrogen saturation of W and W's metals.[25]

Only Bergh has treated the recombination-coefficient data cautiously.[81]

B. Theory

As a consequence of studies of atomic hydrogen at low pressures, an opportunity occurred to rederive and refine the derivations for the atom kinetics within a diffusion tube and to test one of their implications experimentally. From the calculations, Tsu and Boudart's results for the concentration at the discharge boundary ψ_o were changed from

$$\psi_o = \frac{\sigma\mu^2}{2} \frac{(\xi' + \mu)\, e^{L/\mu R} + (\xi' - \mu)\, e^{-L/\mu R}}{(\xi' + \mu)\, e^{L/\mu R}} \qquad \text{(IV-98)}$$

to a more complicated expression with (a) the assumption that the rates of atom recombination on the discharge- and reactor-zone walls were different (mathematical consequences: $\sigma\mu^2$ changes to $\sigma\delta^2$ and the denominator becomes more complex); (b) the statement that the rate of atom production in the discharge is proportional to the mole fraction of the molecular hydrogen present [mathematical consequences: $\sigma\delta^2$ changes to $\sigma'^2\,\delta'^2$ and $\delta'^2 = \delta^2/(1 + \sigma'^2\delta^2)$]; (c) the assumption that the discharge zone has a finite length M (mathematical consequence: δ' changes to δ' coth $M/\delta'R$); and (d) the assumption that the end plate is an annular-ring composite catalyst consisting of an inner disk of recombination coefficient γ' and reduced radius κ and an outer annular ring of negligible catalytic activity (mathematical consequence: ξ' changes to ξ'/κ^2).

These results agree with previous ones,[30] i.e., a change occurring in the discharge zone affects only the absolute but not the relative atom concentrations, but a change in the end plate affects both the absolute and the relative atom concentrations. The previous arguments

thus are better restated in the following way: the steady-state atom concentration at a particular point within a diffusion tube is not fundamentally constant, but instead assumes a value determined by the magnitude and location of all the sources and sinks present within the system.

If a catalytic probe is highly active ($\gamma' > 0.1$), the derivations unequivocally state that the probe's size and location affect the atom concentration at the discharge boundary. Even if the end plate is extremely inactive ($\xi' \gg \mu$), moving the plate closer to the discharge as much as doubles the atom concentration at the discharge boundary.

All previous derivations, including the present one, do not account for the fact that an isothermal calorimeter or thermocouple probe does not completely close the cross-sectional area. A proper theoretical derivation would probably show that the atom concentration at the discharge boundary and the relative atom concentration profile are both dependent on this "closure" factor.

C. Experimental Results

In order to answer the questions raised by Tsu and Boudart, I performed the following experiment: place an atom-concentration-measurement device (a Wrede-Harteck gauge) at the discharge boundary and determine if the location of a hot-wire calorimeter or thermocouple probe of the same size used by Wood and Wise perturbs the measured atom concentration (Figs. 82 and 83). Figure 84 shows schematically the difference in behavior predicted by Wood and Wise (no change) by Tsu and Boudart (a straight line), or by the present results (a curved line). Since Wood and Wise performed their experiments close to the discharge zone ($L/R \gg 12$)—a region where the deviation between the three theories is quite pronounced—this experiment was certainly critical.

The apparatus consisted of a 142-cm diffusion tube (37-mm i.d.) with a discharge zone and a reactor zone, a microwave discharge produced

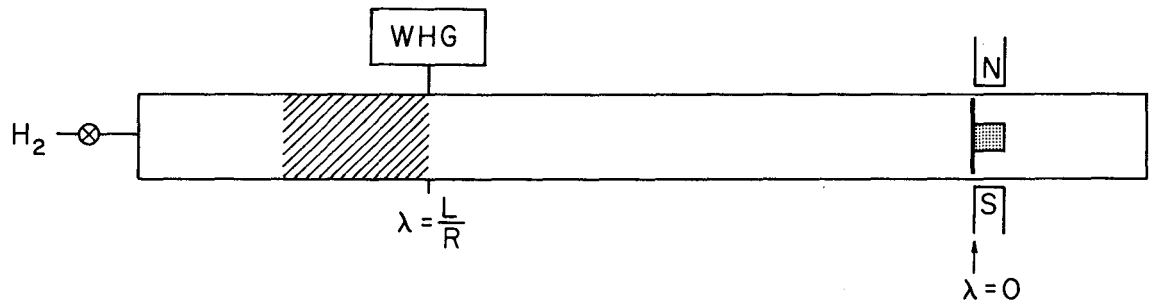

Fig. 83. Schematic drawing showing a movable probe located in a diffusion tube.

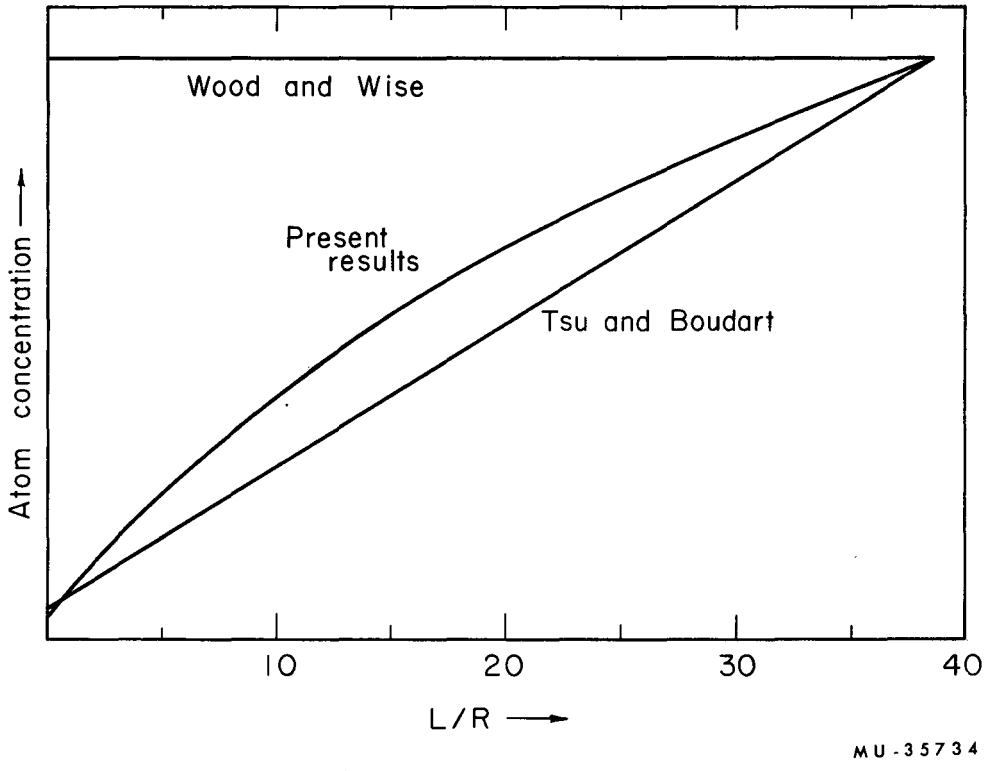

Fig. 84. Schematic drawing illustrating the concept of experiments performed to demonstrate the effect of a catalytic probe on the atom concentration at the discharge boundary. According to present theories on the subject, movement of a highly catalytic probe would have either no effect (Wood and Wise), a linear effect (Tsu and Boudart), or a non-linear effect (present results).

by a 100-W Burdick diathermy unit, a Wrede-Harteck gauge capable of measuring an atom mole fraction of 0.02 (at 75-mtorr total pressure) to 2% accuracy, a highly catalytic movable probe consisting of platinum mesh and nickel-plated copper mesh, and other movable probes such as a copper disk, a Teflon plug, a nickel-plated copper plug, a tungsten filament, and a thermometer containing an electroplated-nickel or $AgNO_3$ bulb. An Englehard palladium unit purified cylinder hydrogen for the experiments, but unfortunately a leak in a rotameter contaminated the "purified" hydrogen with air and made all of the catalytic-probe experiments somewhat erratic and difficult to perform (the leak was discovered only after the experiments were stopped).

The highly active platinum-and-nickel-mesh probe unequivocally lowered the measured atom concentration when it was close to the discharge boundary and to the Wrede-Harteck gauge (Figs. 85 to 90). The two quantitative curves obtained (Figs. 90 and 91) suggest that the present results are valid. The probe became poisoned during the experiments, a behavior probably due to the air present within the hydrogen gas.

The nickel-plated copper plug, the non-flashed tungsten filament, and the thermometer containing electroplated nickel or $AgNO_3$ on the bulb all showed either small or else no effects, a result which was possibly due to the poisoning of the above metal surfaces. On the other hand, the copper disk (Fig. 92) and the Teflon plug (not shown) both increased the measured atom concentration when brought close to the gauge and the discharge zone. This observation indicated that both surfaces were quite inactive but did not give any values for the recombination coefficients for the two surfaces.

The results for the active platinum-and-nickel-mesh probe and the inactive copper disk and Teflon plug are schematically compared in Fig. 93. Since poisoning occurred during the entire series of experiments, the results obtained for all of the probes tested may not necessarily be typical of their behavior in a purer hydrogen-discharge system. Nevertheless, the experiments demonstrated that Tsu and Boudart's analysis was valid and that the position of the SRI group was incorrect. The refined mathematical derivations, the experimental results, and this conclusion are my only contributions to this subject.

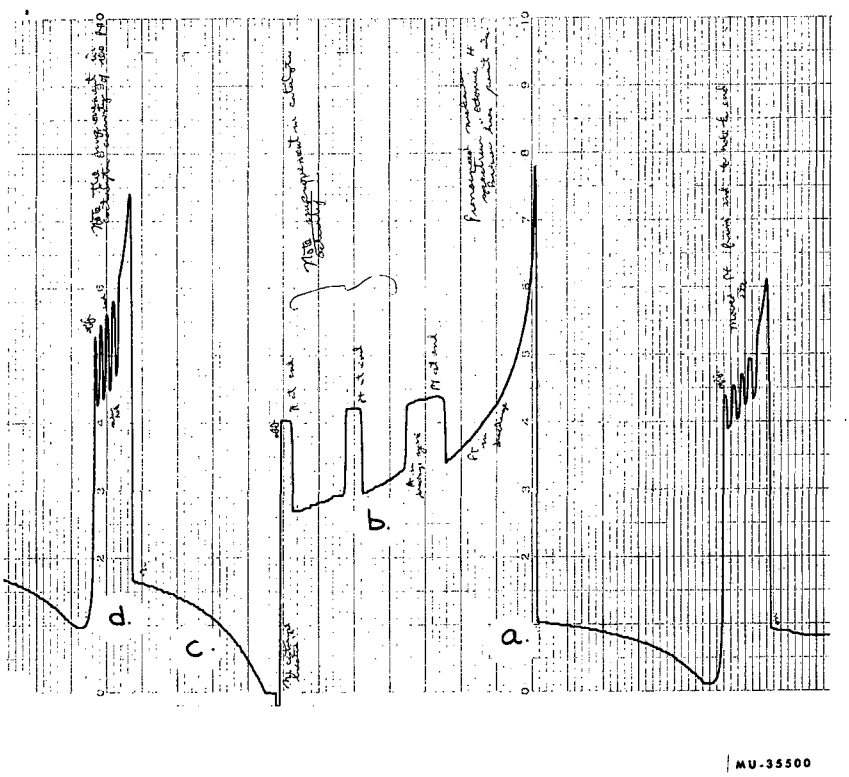

Fig. 85. Response of non-water-cooled WHG (100 holes, 2.6 mtorr full scale) to a microwave discharge in hydrogen containing air as a contaminant. The curve shows the effect of a movable platinum-mesh probe on the atom concentration near the discharge boundary. After the discharge is turned on [point (a)], the atom concentration decays to point (b) due to the conversion of O_2 to H_2O by the discharge. Point (c) shows the drift in the baseline after the discharge has been shut off, an observation which indicates that water has been formed and is adversely affecting the WHG. The plateaus at (b) and the spikes at (d) represent the difference in atom concentration when the Pt probe is alternately far away and close to the discharge, and demonstrate conclusively the perturbing effect of the probe on the concentration profile within the diffusion tube. P = about 90 mtorr and t = 20 sec/small div (right to left). (November 29, 1964).

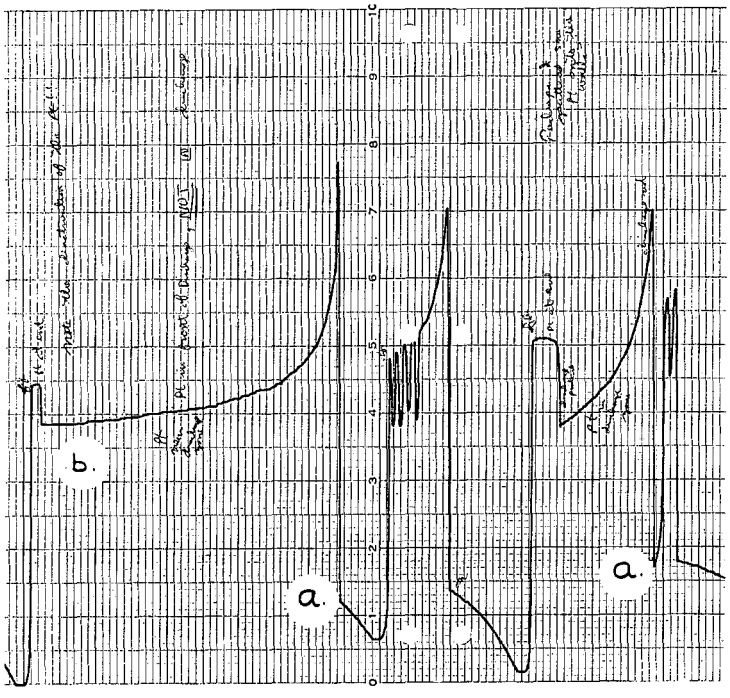

Fig. 86. Curves similar to those shown in Fig. 85, demonstrating the effect of a movable Pt probe on the atom concentration near a microwave discharge, and also the effect of the presence of small amounts of air on the yield of atomic hydrogen from the discharge. The discharge was turned on continuously until at point (b) it was turned off. This action poisoned the Pt probe, as is shown by the smaller height of the spikes in Fig. 87. t = 20 sec/small div (right to left). (November 29, 1964).

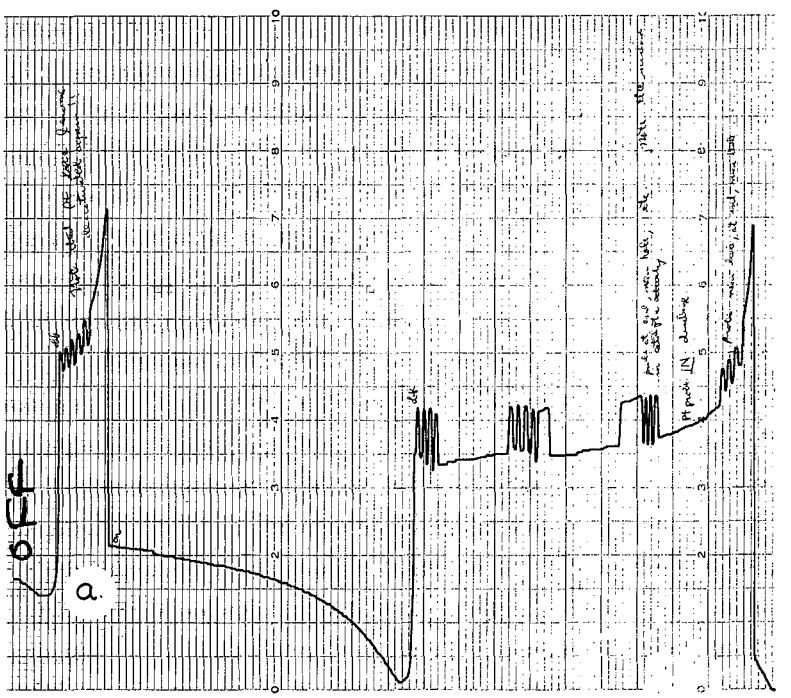

Fig. 87. Curves similar to those shown in Figs. 85 and 86, demonstrating the effect of a movable Pt probe on the atom concentration near a microwave discharge, and also the effect of the presence of small amounts of air on the yield of atomic hydrogen from the discharge. The height of the spikes at point (a) is much smaller than at point (d) in Fig. 85, an observation which indicates that the Pt probe has been poisoned by the products from the discharge. t = 20 sec/small div (right to left). (November 29, 1964).

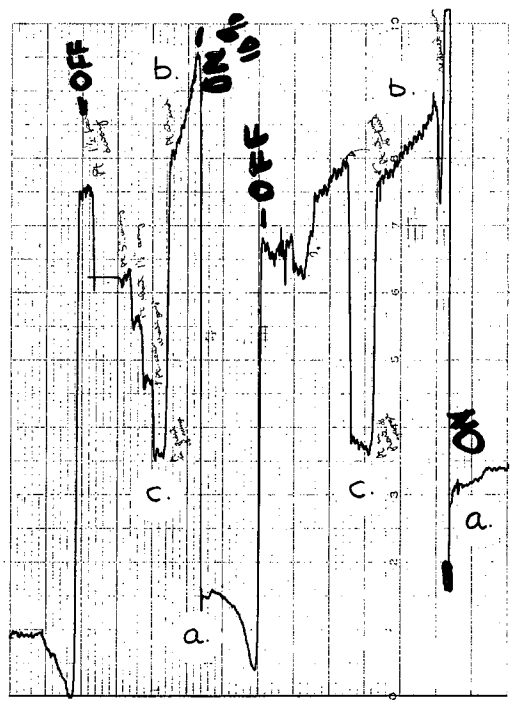

Fig. 88. Response of non-water-cooled WHG (100 holes), located at the discharge boundary, to a low-pressure microwave discharge in hydrogen and the movement of a platinum-mesh catalytic probe. After the discharge is started [point (a)], the platinum probe is moved from the end of the tube [point (b)] to the discharge [point (c)]. This process is repeated at points (a'), (b'), and (c'). The change in the atom concentration at the discharge zone between points (b) and (c) and points (b') and (c') demonstrate that the Pt catalytic probe perturbs the atom-concentration profile within the diffusion tube. P = 73 mtorr and t = 20 sec/small div (right to left). (September 1, 1964).

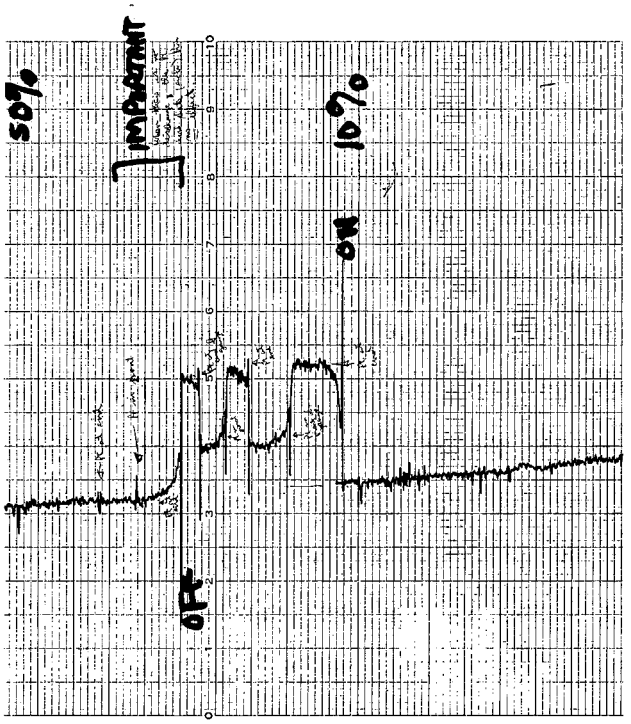

Fig. 89. Response of non-water-cooled WHG (100 holes), located at the discharge boundary, to a low-pressure microwave discharge in hydrogen and the movement of a platinum-mesh probe. The highest atom-concentration peaks are produced when the Pt probe is at the end of the diffusion tube, and the lowest peaks occur when the probe is near the WHG. These curves indicate that the position of the probe influences the atom-concentration profile throughout the diffusion tube. P = 80 mtorr and t = 20 sec/small div (right to left). (August 11, 1964).

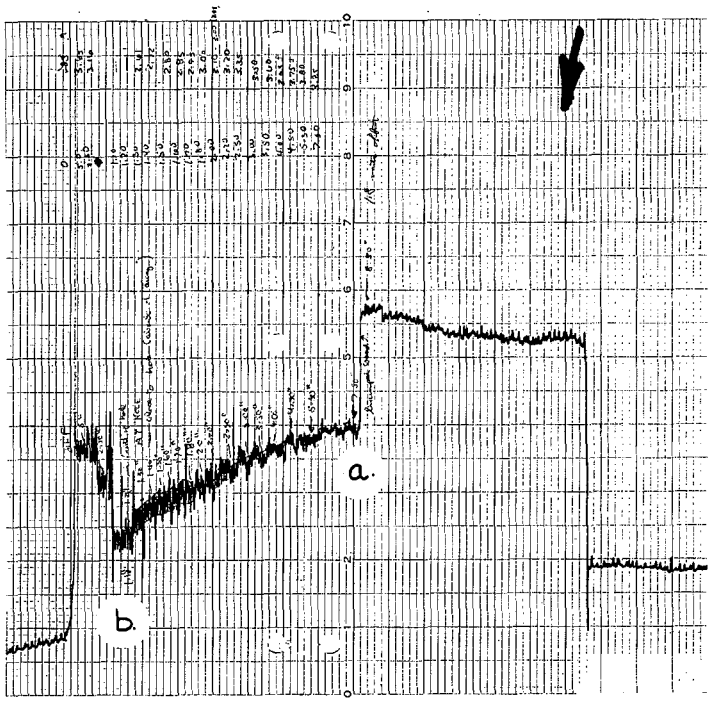

Fig. 90. Recorder-chart tracing showing the effect of moving the platinum-mesh and nickel-plated copper-mesh probe on the atom concentration at the discharge boundary in a diffusion tube. At point (a), the probe is 7.50 in. away from the discharge, and at point (b) the probe is only 1.10 in. away. The results of this quantitative run are shown in Fig. 91, and demonstrate that the location of the probe effects the concentration profile throughout the diffusion tube. Full-scale WHG signal = about 1.5 mtorr, P = about 80 mtorr, and t = 20 sec/small div (right to left). (December 8, 1964).

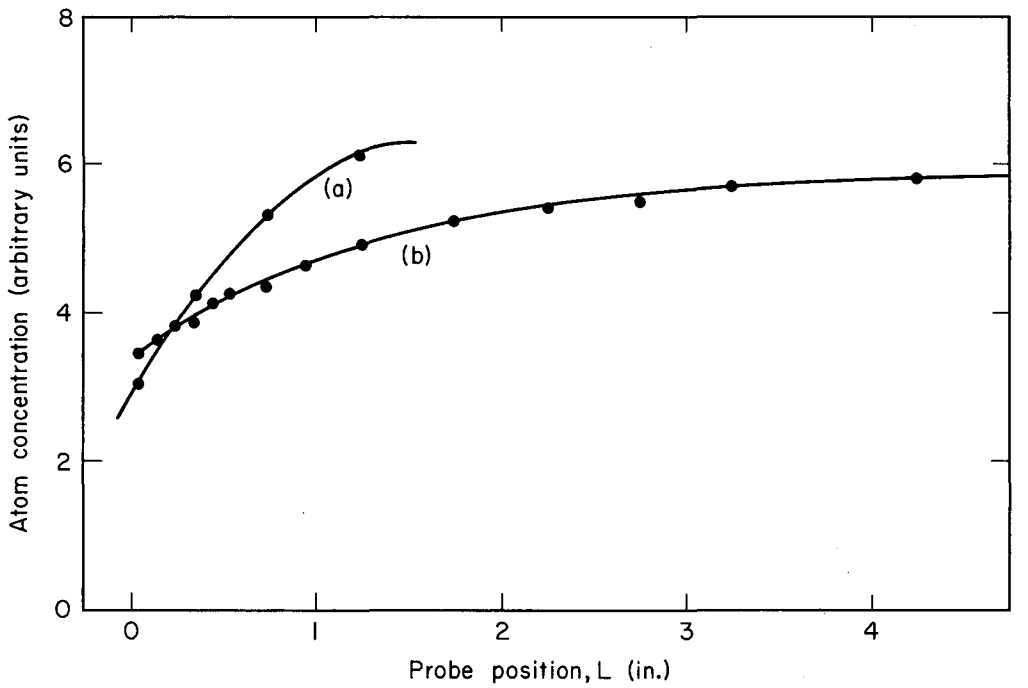

Fig. 91. The effect of a movable catalytic probe (composed of platinum mesh and nickel-plated copper mesh) on the atom concentration measured near a microwave discharge in a 37-mm i.d. Pyrex diffusion tube. The experiments yielding these curves were done on two separate occasions: at a time when (a) the probe was not poisoned (December 10, 1964), and (b) the probe was poisoned (December 8, 1964). The curved shape is in good agreement with theoretical predictions in the present paper. The average atom concentration during these experiments was about 0.7%.

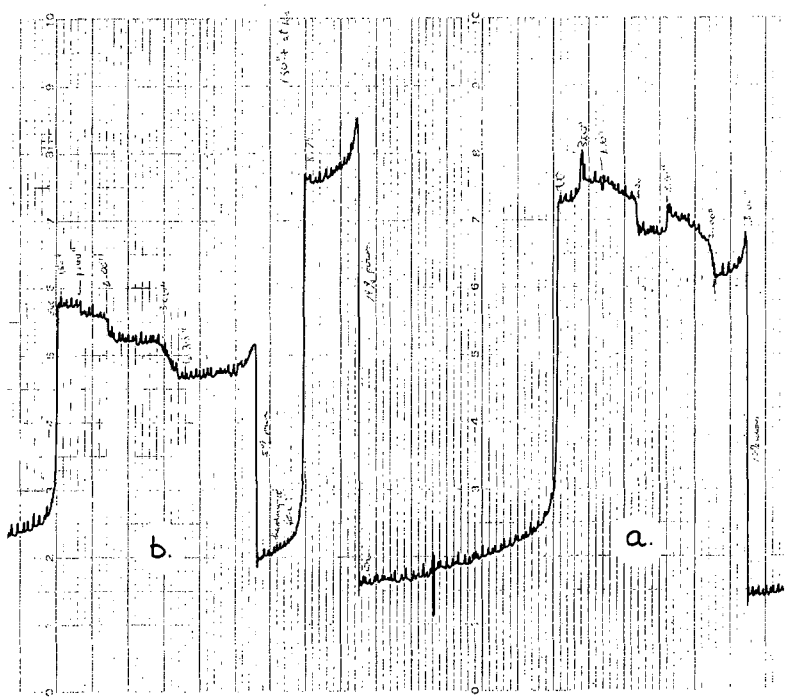

MU-35506

Fig. 92. Response of non-water-cooled WHG (100 holes, about 0.75 mtorr full scale) to a microwave discharge in hydrogen, showing the effect of a movable copper-disk catalytic probe on the atom concentration near the discharge. Peaks (a) and (b) demonstrate that the action of moving the copper disk closer to the discharge increases the measured atom concentration. This result occurs because the copper disk occupies the entire cross-sectional area of the diffusion tube and thus minimizes the influence of the catalytic glass walls behind the probe. This observation, which has also occurred with a Teflon plug occupying the entire cross-sectional area, is compared schematically to the effect of the platinum-mesh probe in Fig. 93. P = about 80 mtorr and t = 20 sec/small div (right to left). (December 15, 1964).

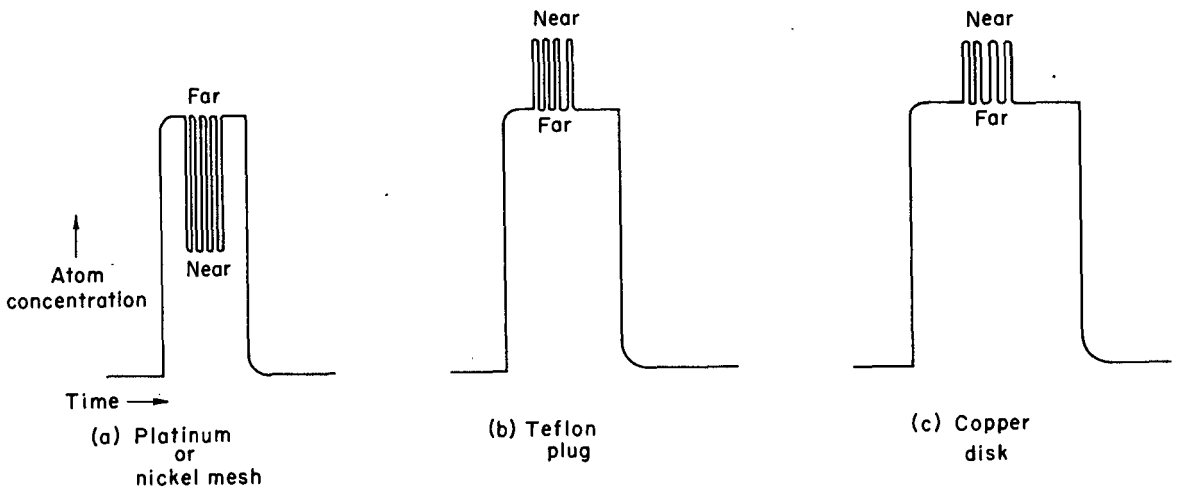

Fig. 93. Schematic drawing showing the results of experiments with the (a) platinum-mesh and nickel-plated copper-mesh probe, (b) Teflon plug, and (c) copper disk. The words near and far refer to the distance between the probes and the discharge boundary.

VII. NOTATION

A. Notation for Section III

γ	Recombination coefficient of catalytic surface in Wrede-Harteck gauge
π	3.1416
τ	Response time
A	Area of catalytic surface in Wrede-Harteck gauge
c, c_1, c_2	Molar Concentration
d	Diameter of effusion holes
k	Boltzmann constant
m, m_1, m_2	Mass
N	Number of effusion holes
$P, P_1, P_{1L}, P_2, P_{2L}, P_{2R}, P_H, P_{H_2}$, etc.	Pressure or partial pressure
R	Molar rate of collision of species on a surface
t	Time
T, T_L, T_R	Temperature (absolute)
$\bar{v}$, $\bar{v}_1$, $\bar{v}_2$	Average velocity
V_o	Residual volume of the catalytic chamber

Subscripts

1	Atoms
2	Molecules
H	Atomic hydrogen
H_2	Molecular hydrogen
H_2O	Water
O	Oxygen
L	Left-hand side
R	Right-hand side

B. Notation for Sections IV to VI

α	Defined by Eq. (IV-59)
α_i, α_n	Arguments of Bessel functions
α_1	Argument of Bessel functions, defined by Eq. (IV-139)
β	Dimensionless group defined by Eq. (IV-143)
γ	Recombination coefficient of atoms on reactor- or discharge-zone walls
γ'	Recombination coefficient of atoms on end plate
γ''	Recombination coefficient of atoms on part of annular-ring end plate
$\underset{\sim}{\delta}$	Unit tensor (dimensionless)
δ^2	Dimensionless group defined by Eq. (IV-65)
δ'^2	Dimensionless group defined by Eq. (IV-110)
η	Reduced atom concentration in discharge zone defined by Eq. (IV-63)
κ	Reduced smaller radius of annular-ring end plate defined by Eq. (IV-116)
λ	Reduced length defined by Eq. (IV-45)
μ^2	Dimensionless group defined by Eq. (IV-93)
ξ	Dimensionless group defined by Eq. (IV-46) corresponding to use of γ
ξ'	Dimensionless group defined by Eq. (IV-46) corresponding to use of γ'
ξ''	Dimensionless group defined by Eq. (IV-46) corresponding to use of γ''
ρ	Gas density
ρ	Dimensionless group defined by Eq. (IV-115)
ρ_i	Mass concentration of species i
ρ_o	Mass concentration of atoms in entering gas
σ^2	Dimensionless group defined by Eq. (IV-66)
σ'^2	Dimensionless group defined by Eq. (IV-109)
$\underset{\sim}{\Sigma}$	Shear-stress tensor

τ	Reduced atom concentrationin buffer zone defined by Eq. (IV-80)
ϕ	Function defined by Eq. (IV-57)
$\underset{\sim}{\Phi}$	Total momentum flux relative to stationary coordinates (tensor)
χ	Function defined by Eq. (IV-163)
ψ	Reduced atom concentration in reactor zone defined by Eq. (IV-44)
ψ_o	Reduced atom concentration at discharge-reactor-zone boundary
ω_i	Mass fraction of component i
Ω	Dimensionless function defined by Eq. (IV-154)
$\mathfrak{D}_{12}$, $\mathfrak{D}_{21}$	Binary diffusion coefficient
∇	Del operator (vector)
∞	Infinity
{ }	Braces indicating molar concentration of enclosed species
A	Cross-sectional area of reaction tube
A	Function defined by Eq. (IV-60)
A'	Surface area of thermal calorimeter
A,B,C,D,E,F,A_i, B_i,C_i	Integration constants
b	Side of square
c	Total molar concentration
c_1	Molar concentration of atoms in reactor zone
c'_1	Molar concentration of atoms in discharge zone
c''_1	Molar concentration of atoms in buffer zone
c_2	Molar concentration of molecules
D_{12}	Binary diffusion coefficient for atom-molecule system
D_{ij}	Binary diffusion coefficient for i-j system
e	Exponential
F	Flow rate
g	Gravitational acceleration

H	Dimensionless function defined by Eq. (IV-89)
ΔH	52 kcal/mole for atomic hydrogen
i	Current measured in presence of atoms
i_o	Current measured in absence of atoms
j_i	Mass flux of i relative to average velocity of mass
j_1	Mass flux of atoms relative to average velocity of mass
j_2	Mass flux of molecules relative to average velocity of mass
$J_o(\alpha_i)$	Bessel function of argument α_i
$J_1(\alpha_i)$	Another Bessel function of argument α_i
J_1^+, J_1^-	Molar atom fluxes defined by Eqs. (IV-31) and (IV-32)
J_1	Molar flux of atoms relative to the molar average velocity
J_{1s}	Molar flux of atoms to a surface
k	General reaction-rate constant (used where no specificity is needed)
$k_{0G}, k_{2g}, k_{3g}, k_{0s}, k_{1s}, k_{2s}$	Reaction-rate constants for gas and surface phases defined by Eq. (IV-30)
k_1	First-order reaction rate constant for atoms recombining on reactor-zone walls
k'_1	First-order reaction-rate constant for atoms recombining on discharge-zone walls
k'_o	First-order reaction-rate constant for the production of atoms in discharge zone
L	Length of reactor zone
L_f	Length (probe far away)
L_n	Length (probe near)
M	Length of discharge zone
M_1	Molecular weight of atoms
M_i, M_j	Molecular weight of components i and j
n_i	Mass flux of i with respect to stationary coordinates
N	Length of buffer zone

p	Pressure
Q'	Volume rate of generation of atoms in discharge zone
r_i	Mass rate of production of species i
r_1	Mass rate of production of atoms
R	Radius of reaction tube
R_i	Molar rate of production of species i
R_w	Resistance of isothermal calorimeter wire
R_1	Molar rate of atoms' production
R'_1	Molar rate of atoms' production in discharge zone
R_{1s}	Molar rate of atoms' loss on a catalytic surface
R_2	Molar rate of molecules' production
S/V	Surface-to-volume ratio of reaction tube
v	Mass average velocity
v_z	Mass average velocity in z direction (axial direction)
v_{zo}	Mass average velocity in z direction of entering gas
v_r	Mass average velocity in radial direction
$\bar{v}_1$	Velocity of an atom
t	Time
T	Dimensionless function defined by Eq. (IV-159)
x_i, x_j	Mole fractions of species i and j
x_1	Mole fraction of atoms
$Y_o(\alpha_i)$	Bessel function of argument α_i
z	Distance from discharge-reactor-zone boundary to end plate (+ direction) or to buffer zone (- direction)

ACKNOWLEDGMENTS

I would like to thank Professor D. N. Hanson and Professor M. Boudart for their frequent questions, penetrating comments, and timely suggestions; the glass-shop group—H. S. Powell, Dane H. Andenberg, Don J. Rogers, Ione G. Maxwell, and Norman E. Phillips—whose skill in constructing the glassware added greatly to the success of the experimental research work; G. G. Young and the mechanical-shop group for valuable assistance with the mechanical aspects of the experiments; and those individuals throughout the Laboratory who were so kind to loan me several key components of my apparatus.

This work was performed under the auspices of the U. S. Atomic Energy Commission.

REFERENCES

1. W. V. Smith, The Surface Recombination of H Atoms and OH Radicals, J. Chem. Phys. 11, 110 (1943).
2. Henry Wise and Clarence M. Ablow, Diffusion and Heterogeneous Reaction, I. The Dynamics of Radical Reactions, J. Chem. Phys. 29, 634 (1958).
3. B. J. Wood and Henry Wise, Diffusion and Heterogeneous Reaction, II. Catalytic Activity of Solids for Hydrogen Atom Recombination, J. Chem. Phys. 29. 1416 (1958).
4. B. J. Wood and Henry Wise, Errata: Diffusion and Heterogeneous Reaction. II., J. Chem. Phys. 30, 1104 (1959).
5. H. Motz and Henry Wise, Diffusion and Heterogeneous Reaction. III. Atom Recombination at a Catalytic Boundary, J. Chem. Phys. 32, 1893 (1960).
6. Henry Wise and Clarence M. Ablow, Diffusion and Heterogeneous Reaction. IV. Effects of Gas-Phase Reaction and Convective Flow, J. Chem. Phys. 35, 10 (1963).
7. Henry Wise, Clarence M. Ablow, and Dan J. Schott, Diffusion and Heterogeneous Reaction. V. Transition from a Surface-to a Diffusion-Controlled Process during Atom Recombination, J. Chem. Phys. 39, 2063 (1963).
8. Henry Wise, Clarence M. Ablow, and Kenneth M. Sancier, Diffusion and Heterogeneous Reaction. VI. Surface Recombination in the Presence of Distributed Atom Sources, J. Chem. Phys. 41, 3569 (1964).
9. Henry Wise, Diffusion Coefficient of Atomic Hydrogen through Multicomponent Mixtures, J. Chem. Phys. 31, 1414 (1959).
10. Henry Wise, Diffusional Transport of Atomic Hydrogen through Molecular Hydrogen at Elevated Temperatures, J. Chem. Phys. 34, 2139 (1961).
11. B. J. Wood and Henry Wise, Catalytic Activity of Solids for Hydrogen Atom Recombination, J. Chem. Phys. 31, 265 (1959).
12. B. J. Wood and Henry Wise, Kinetics of Hydrogen Atom Recombination on Surfaces, J. Phys. Chem. 65, 1976 (1961).
13. Bernard J. Wood and Henry Wise, The Kinetics of Hydrogen Atom Recombination on Pyrex Glass and Fused Quartz, J. Phys. Chem. 66, 1049, (1962).

14. H. Wise, and W. A. Rosser, Homogeneous and Heterogeneous Reactions of Flame Intermediates, Ninth Combusion Symposium, Cornell University, (August, 1962), page 733.

15. J. W. Linnett and D. G. H. Marsden, The Kinetics of the Recombination of Oxygen Atoms at a Glass Surface, Proc. Roy. Soc. (London) 234A, 489 (1956).

16. J. W. Linnett and D. G. H. Marsden, The Recombination of Oxygen at Salt and Oxide Surfaces, Proc. Roy. Soc. (London) 234A, 504 (1956).

17. J. C. Greaves and J. W. Linnett, The Recombination of Oxygen at Surfaces, Trans. Far. Soc. 54. 1323 (1958).

18. J. C. Greaves and J. W. Linnett, Recombination of Atoms at Surfaces. 4. Theory of Method and Measurement of Atom Concentrations, Trans. Far. Soc. 55, 1338 (1959).

19. J. C. Greaves and J. W. Linnett, Recombination of Atoms at Surfaces. 5. Oxygen Atoms at Oxide Surfaces, Trans. Far. Soc. 55, 1346 (1959).

20. J. C. Greaves and J. W. Linnett, Recombination of Atoms at Surfaces. 6. Recombination of Oxygen Atoms on Silica from 20°C to 600°C, Trans. Far. Soc. 55, 1355 (1959).

21. M. Green, K. R. Jennings, J. W. Linnett, and D. Schofield, Recombination of Atoms at Surfaces. 7. Hydrogen Atoms at Silica and Other Similar Surfaces, Trans. Far. Soc. 55, 2152 (1959).

22. P. G. Dickens, D. Schofield, and J. Walsh, Recombination of Atoms at Surfaces. 8. The Three-Dimensional Diffusion Equation, Trans. Far. Soc. 56, 225 (1960).

23. P. G. Dickens, R. D. Gould, J. W. Linnett, and A. Richmond, Recombination of Oxygen Atoms in the Gas Phase, Nature 187, 686 (1960).

24. P. G. Dickens and M. B. Sutcliffe, Recombination of Oxygen Atoms on Oxide Surfaces. 1. Activation Energies of Recombination. Trans. Far. Soc. 60, 1272 (1964).

25. P. G. Dickens, J. W. Linnett, and W. Palczewska, The Recombination of Atoms on Pd-Au Alloys, J. Catalysis 4, 140 (1965).

26. D. G. H. Marsden, A study of Some Atomic and Free Radical Reactions (Ph.D. Thesis), Queen's College, Oxford, 1954.

27. J. C. Greaves, Investigations of Some Atomic Reactions (Ph.D. Thesis), Queen's College, Oxford, 1957.

28. K. R. Jennings, A study of Some Atomic Reactions (Ph.D. Thesis), Queen's College, Oxford, 1958.

29. D. Schofield, Studies of Some Atomic Reactions (Ph.D. Thesis), Queen's College, Oxford, 1960.

30. Kin Tsu and M. Boudart, Recombination of Atoms at the Surface of Thermocouple Probes, Can. J. Chem. 39, 1239 (1961).

31. Kin Tsu, Recombination of Hydrogen Atoms on Glass (Ph.D. Thesis), Princeton University, 1960.

32. Kin Tsu, Experimental Techniques in Surface Atom Recombination Studies, American Cyanamid Company, Stamford, Connecticut, 1962 (unpublished).

33. Kin Tsu and M. Boudart, Surface Diffusion and Recombination of Hydrogen Atoms on Glass, Paper No. 23, Actes 2eme Congr. Int. Catalyse 593 (1961).

34. I. Amdur, Recombination of Hydrogen Atoms, III. J. Am. chem. Soc. 60, 2347 (1938).

35. S. Krongelb and M. W. P. Strandberg, Use of Paramagnetic-Resonance Techniques in the Study of Atomic Oxygen Recombinations, J. Chem. Phys. 31, 1196 (1959).

36. Norman Marvin Edelstein, A Study of the Kinetics of the Reaction $H + O_2$ by Paramagnetic Resonance (Ph.D. Thesis). UCRL-10108, 1962.

37. Thomas C. Marshall, Studies of Atomic Recombination of Nitrogen, Hydrogen, and Oxygen by Paramagnetic Resonance, Phys. Fluids 5, 743 (1962).

38. Frederick Kaufman, Reactions of Oxygen Atoms, in Progress in Reaction Kinetics, (Pergamon Press, New YOrk, 1961), Vol. 12.

39. J. E. Morgan and H. I. Schiff, Use of Catalytic Probes to Determine Atom Concentrations and Atom Diffusion Coefficients, J. Chem. Phys. 38, 2631 (1963).

40. J. E. Morgan and H. I. Schiff, Diffusion Coefficients of O and N Atoms in Inert Gases, Can. J. Chem. 42, 2300 (1964).

41. W. R. Schulz and D. J. Leroy, Kinetics of the Reactions of Atomic Hydrogen. Effect of Diffusion on the Determination of H Atom Concentration, Can. J. Chem. 40, 2413 (1962).

42. G. K. Lavroskaya and V. V. Voevodskii, Reactions of Hydrogen and Oxygen Atoms on Solid Surfaces, Ah. Fiz. Khim. 25, 1050 (1951); Chem. Abs. 2893c (1952).

43. E. Wrede, Konzentration des automaren Wasserstoffs in der Glimmentladung, Z. Instrumentenk, 48, 201 (1928).

44. E. Wrede, Method of Measuring Atomic Hydrogen, Oxygen, and Nitrogen Concentration, Z. Physik 54, 53 (1929).

45. P. Harteck, Concentration Measurement of Monatomic Hydrogen, Oxygen, and Nitrogen, Z. Physik 54, 881 (1929).

46. H. D. Beckey and P. Warneck, Anreicherung isotoper Molekule in der Gleichstrom-Glimmentladung 10a, 62 (1955).

47. W. Groth and P. Warneck, Bestimmung und Bildungsmechanismus von Atomkonzentrationen in Strickstoff-und Strickstoff-Edelgas-Glimmentladungen, Z. Physik. Chem. 10, 323 (1957).

48. L. Elias, E. A. Ogryzlo, and H. I. Schiff, The Study of Electrically Discharged O_2 by Means of an Isothermal Calorimetric Detector, Can. J. Chem. 37, 1680 (1959).

50. Robert Leonard Sharpless, A Fast Diffusion Gauge for Measurement of Atom Concentrations in Afterglows (M.S. Thesis), University of Washington, 1959.

51. R. L. Sharpless, K. C. Clark, and R. A. Young, Improved Wrede Gauge, Rev. Sci. Instr. 32, 532 (1961).

52. T. R. Merton, On the Structure of the Balmer Series of Hydrogen Lines, Proc. Roy. Soc. (London) 97A, 307 (1920).

53. R. W. Wood, Spectroscopic Phenomena of Very Long Vacuum Tubes, Proc. Roy, Soc. (London), 97A, 455 (1920).

54. R. W. Wood, Hydrogen Spectra from Long Vacuum Tubes, Phil. Mag. 42, 729 (1921).

55. R. W. Wood, Spontaneous Incandescence of Substances in Atomic Hydrogen Gas, Proc. Roy. Soc. (London), 102A, 1 (1922).

56. R. W. Wood, Atomic Hydrogen and the Balmer Series Spectra, Phil. Mag. 44, 538 (1922).

57. F. R. Bichowsky and L. C. Copeland, An Active Form of Oxygen, Nature 120, 729 (1927).

58. L. C. Copeland, The Heat of Formation of Molecular Oxygen, Phys. Rev. 36, 1221 (1930).

59. Lord Rayleigh (R. J. Strutt), A Chemically Active Modification of Nitrogen Produced by the Electric Discharge, Proc. Roy. Soc. 91A, 303 (1915).

60. Lord Rayleigh (R. J. Strutt), Further Studies on Active Nitrogen. III. Experiments to Show that Traces of Oxygen or Other Impurity Affect Primarily the Walls of the Vessel and Not the Phenomena in the Gas Space, Proc. Roy. Soc. (London), 180A, 123 (1942).

61. H. G. Poole, Atomic Hydrogen. II. Surface Effects in the Discharge Tube, Proc. Roy. Soc. (London), 163A, 415 (1937).

62. G. I. Finch, Steam in the Ring Discharge, Proc. Phys. Soc. (London), 62A, 465 (1949).

63. B. J. Fontana, Magnetic Study of the Frozen Products from the Nitrogen Microwave Discharge, J. Chem. Phys. 31, 148 (1959).

64. K. R. Jennings and J. W. Linnett, Production of High Concentrations of Hydrogen Atoms, Nature 182, 597 (1958).

65. J. C. Greaves, K. R. Jennings, and J. W. Linnett, Production of Atoms Using Electric Discharges, Inorganic Chemistry Laboratory, Oxford University, England, 1959, (Unpublished).

66. F. Kaufman and J. R. Kelso, Catalytic Effects in the Dissociation of Oxygen in Microwave Discharges, J. Chem. Phys. 32, 301 (1960).

67. F. Kaufman and J. R. Kelso, Catalytic Dissociative Reactions in Electrical Discharges, Paper No. 18, Eighth Combustion Symposium, California Institute of Technology (August, 1960), p. 230.

68. T. M. Shaw, Dissociation of Hydrogen in a Microwave Discharge, J. Chem. Phys. 30, 1366 (1959).

69. T. M. Shaw, Effect of Water Vapor on the Dissociation of Hydrogen in an Electrical Discharge, J. Chem. Phys. 31, 1142 (1959).

70. T. M. Shaw, Studies of Microwave Gas Discharges, Report No. TIS-R58ELM115, General Electric Microwave Laboratory, Palo Alto, California, 1958, (Unpublished).

71. T. M. Shaw, Techniques of Electrical Discharge for Radical Production, in Formation and Trapping of Free Radicals (Academic Press, New York, 1960).

72. De. E. Carr, Chemical Utilization of Trapped Radicals, in Formation and Trapping of Free Radicals (Academic Press, New York, 1960).

73. Frances Dunkle Coffin, Production of Atoms by a Glow Discharge in Dry Hydrogen, J. Chem. Phys. 30, 593 (1959).

74. E. J. Nowak, S. Nurzius, J. Deckers, and M. Boudart, Surface Recombination of Hydrogen Atoms in the Presence of Water, Report No. AD247-517, Armed Services Technical Information Agency, 1960 (unpublished).

75. R. C. Collins and J. W. Kutchins, Diffusion and Heterogeneous Recombination of H Atoms, Bull. Am. Phys. Soc. 7, 114, (1962).

76. P. F. Knewstubb and A. W. Tickner, Mass Spectrometry of Ions in Glow Discharges. II. Negative Glow in Rare Gases, J. Chem. Phys. 36, 684 (1962).

77. Borge Bak and John Rastrup-Andersen, Microwave Discharge Production of Hydrogen Atoms. Control of Hydrogen Atom Quantity Produced, Acta Chem. Scand. 16, 111. (1962).

78. Robert A. Young, Robert L. Sharpless, and Roger Stringham, Catalyzed Dissociation of N_2 in Microwave Discharges, I., J. Chem. Phys. 40, 117 (1964).

79. C. J. Ultee, Catalyzed Dissociation of N_2 in Microwave Discharges, J. Chem. Phys. 41, 281 (1964).

80. R. Browning and J. W. Fox, The Coefficient of Viscosity of Atomic Hydrogen and the Coefficient of Mutual Diffusion for Atomic and Molecular Hydrogen, Proc. Roy, Soc. (London), 278A, 274 (1964).

81. A. A. Bergh, Atomic Hydrogen as a Reducing Agent, Bell System Tech. Journal 44, 261 (1965).

82. Gerald P. Pfaff, Theory, Calibration, and Operation of a Mcleod Vacuum Gauge, Lawrence Radiation Laboratory UCID-2343, July 1964 (Unpublished).

83. Peter R. Rony, The Design, Construction, and Operation of a Differential Micromanometer. Part II. Theory and Operational Characteristics, UCRL-11218, Pt. II, April 1965 (Unpublished).

84. Monsanto Company, 800 No. Lindbergh Blvd., St. Louis, Missouri.

85. Arthur R. Von Hippel (editor), Dielectric Materials and Applications (the Technology Press of M.I.T. and John Wiley and Sons, Inc., New York, 1954), pp. 364-7.

86. K. W. Ehlers, Constant-Pressure Leak-Rate Gauge, Rev. Sci. Instr. 29, 72 (1958).

87. I. Chavet, Gas Flowmeter for Continuous Operation, J. Sci. Instr. 39, 530 (1962).

88. Howard C. Berg and Daniel Kleppner, Storage Technique for Atomic Hydrogen, Rev. Sci. Instr. 33, 248 (1962).

89. Murray Zelikof, Peter H. Wyckoff, Leonard M. Aschenbrand, and Robert S. Loomis, Electrodeless Discharge Lamps Containing Metallic Vapors, J. Opt. Soc. Am. 42, 818 (1952).

90. F. C. Fehsenfeld, K. M. Evenson, and H. P. Broida, Microwave Discharge Cavities Operating at 2450 MHz, Rev. Sci. Instr. 36 294 (1965).

91. S. J. Buchsbaum, E. I. Gordon, and S. C. Brown, Experimental Study of a Plasma Column in a Microwave Cavity, J. Nucl. Energy Part C. 2, 164 (1961).

92. Sanborn C. Brown, Plasma Physics Research at M.I.T., in Plasma Physics, James E. Drummond, editor (McGraw-Hill Book Company, Inc., New York, 1961), p. 354.

93. Magda Ericson, C. Seabury Ward, Sanborn C. Brown, and S. J. Buchsbaum, Containment of Plasmas by High-Frequency Electric Fields, J. Appl. Phys. 33, 2429 (1962).

94. Quarterly Progress Reports, M.I.T. Research Laboratory of Electronics, Cambridge Massachusetts, MIT-RLE-QPR-53 to 57, April 15, 1959 to April 15, 1960 (unpublished).

95. Nuclear Products Company, 15635 Saranac Road, Cleveland 10, Ohio.

96. Ali Bulent Cambel, Donald P. Duclos, and Thomas P. Anderson, Real Gases (Academic Press, New York, 1963) p. 119.

97. K. R. Jennings, The Production, Detection, and Estimation of Atoms in the Gaseous Phase, Quart. Rev. (London) 15, 237 (1961).

98. E. W. R. Steacie, Atomic and Free Radical Reactions (Reinhold Publishing Corporation, New York, 1954), Vol. I.

99. D. J. E. Ingram, Free Radicals as Studied by Electron Spin Resonance (Butterworths Scientific Publischations, London, 1958).

100. G. J. Minkoff, Frozen Free Radicals (Interscience Publishers, Inc., New York, 1960).

101. MKS Instruments, Inc., 45 Middlesex Turnpike, Burlington, Mass.

102. Saul Dushman, Scientific Foundations of Vacuum Technique (John Wiley and Sons, Inc., New York, 1962).

103. Sir Harry Melville and B. G. Gowenlock, Experimental Methods in Gas Reactions (Macmillan and Co., Ltd., New York, 1964).

104. Joseph O. Hirschfelder, Charles F. Curtiss, and R. Byron Bird, Molecular Theory of Gases and Liquids (John Wiley and Sons, Inc., New York, 1954).

105. Dielectrix Company, 211 48 Jamaica Avenue, Queen Village, New York,

106. H. G. Poole, Atomic Hydrogen. I. Proc. Roy. Soc. 163A, 404 (1937).

107. R. Byron Bird, Warren E. Stewart, and Edwin J. Lightfoot, Transport Phenomena (John Wiley and Sons, Inc., New York, 1960), p. 560.

108. K. E. Shuler and K. J. Laidler, The Kinetics of Heterogeneous Atom and Radical Reactions. I. The Recombination of Hydrogen Atoms on Surfaces, J. Chem. Phys. 17, 1212 (1949).

109. Peter R. Rony, Ion-Molecule Reactions in Gaseous Discharges (term paper), University of California, January 1962 (unpublished).

110. Hugh M. Smallwood, The Rate of Recombination of Atomic Hydrogen, J. Am. Chem. Soc. 51, 1985 (1929).

111. W. Steiner, The Recombination of Hydrogen Atoms, Trans. Faraday Soc. 31, 623 (1935).

112. A. F. Hildebrandt, C. A. Barth, and F. B. Booth, Atom Concentration Measurements Using Electron Paramagnetic Resonance, Planetary Space Science 3, 194 (1961).

113. Bernard J. Wood, James S. Mills, and Henry Wise, Energy Accommodation in Exothermic Heterogeneous Catalytic Reactions, J. Phys. Chem. 67, 1462 (1963).

114. J. P. Hartnett, A Survey of Thermal Accommodation Coefficients, in Rarefied Gas Dynamics (Academic Press, New York, 1961), p. 1.

115. A. A. Bergh (Bell Telephone Laboratories), private communication, 1965.

116. V. H. Gutbier, Massenspektrometrische untersuchung der reaction $X^+ + H_2 \rightarrow HX^+ + H$, Z. Naturforsch. 12a, 499 (1957).

117. F. W. Lampe, J. L. Franklin, and F. H. Field, Kinetics of the Reactions of Ions with Molecules, in Progress in Reaction Kinetics (Pergamon Press, New York, 1961), Vol. I.

118. Charles E. Merton, Ion-Molecule Reactions, in Mass Spectrometry of Organic Ions (Academic Press, New York, 1963).

119. F. W. Lampe, J. L. Franklin, and F. H. Field, Cross Sections for Ionization by Electrons, J. Am. Chem. Soc. 79, 6129 (1957).

120. H. F. Calcote, Relaxation Processes in Plasma, in Dynamics of Conducting Gases (Northwestern University Press, (Evanston, Illinois, 1960) p. 36.

121. Earl W. McDaniel, Collision Phenomena in Ionized Gases (John Wiley and Sons, Inc., New York, 1964), pp. 410, 417, 515, and 520.

122. V. N. Kondrat'ev, Chemical Kinetics of Gas Reactions (Pergamon Press, New York, 1964), p. 99.